Effects of Selenium Depletion and Selenoprotein Knockdown on Inflammatory Signalling in a Gut Epithelial Cell Line

By

Guanyu Gong

MSc University of Glasgow

BSc University of Qingdao

A thesis presented for the degree of

Doctor of Philosophy

At University of Newcastle-upon-tyne

2010

Declaration

I declare that this thesis was composed by myself, is a record of the original work of my own research and have not been presented in any other applications for a degree. All help kindly provided by others has been acknowledged and all sources of information are indicated in the text.

Guanyu Gong

July, 2010

Acknowledgements

As the record of my three years' PhD research work, this thesis, however, records far beyond the lab work itself, but also the generous helps and excellent guidance from my supervisors, brilliant collaboration from members in our lab team, and great support from my family. I particularly thank my supervisors, Prof. John Edward Hesketh and Dr. Judith Hall. Without their patient guidance, intelligent advices and considerate and constant support over the past four years --- especially when my research or life met difficulties, this thesis could not have been accomplished. I also greatly thank my supervisor Dr. Catherine Mėplan, who patiently taught and introduced me to the PhD research work with all her considerate help and advices.

Meanwhile, I would like to thank Mr. Brian Burtle and Dr. Hannah Gautrey for their kind helps of teaching me many techniques and all the members in the JEH, DF and JH labs for their friendly collaboration, generous support and harmonious working atmosphere.

I am grateful to Prof. Rune Blomhoff (University of Oslo, Norway) who had kindly donated the 3XκB-luciferase construct. I am grateful to Prof Dianne Ford (Newcastle University, UK) who had kindly donated the pBLUE-TOPO plasmid vector. I also thank Mr Guang Yang and Miss Yu Chen for their help with the cloning work.

I deeply appreciate my parents Naibin Gong and Zhenrong Liu for their selfless support over the past four years. It was their dream for their son being successful in career as a phD, but without their selfless help, I will not even have such a chance. Lastly, I will thank my girlfriend, Miss Jia Liu, for her support over my last difficult year and patient waiting me for two years.

Deep thanks are little present on a paperwork, but always born in mind!

July 2010

Abstract

Selenium is a micronutrient essential for human health. Low Se intake *versus* Se supplementation have been reported to elevate and lower mortality from colorectal cancer. Se is present in selenoproteins including glutathione peroxidases (GPx) 1-4. GPxs are antioxidant enzymes that protect cells from excessive oxidative stress and they may have a role in maintaining innate immunity homeostasis against inflammatory stimulation from exposure to luminal bacteria. This thesis describes studies of the regulatory effects of Se depletion and selenoprotein knockdown in the gastrointestinal cell line Caco-2 in relation to inflammatory responses. A luciferase reporter model was developed in which Caco-2 cells were stably transfected with gene constructs in which luciferase expression was under the control of regulatory elements that bind the Nuclear Factor-kappa B (NFκB), a transcription factor central to inflammatory signaling pathways (Chapter 3). As a control reporter luciferase coding sequences were linked to a TATA box. When Caco-2 cells expressing these constructs were grown in Se-deficient conditions, a 30% increase of reporter activity and a 50% increase in endogenous interleukin 8 mRNA levels were observed after stimulation with TNFα. In comparison, no changes in reporter activity were found in Se-deficient cells after stimulation with flagellin (Chapter 4). Small interfering RNA was used to knockdown expression of individual selenoproteins including GPx1, GPx4, SelW and SelH (Chapter 5). Knockdown of GPx1 expression by ~55% led to a 25% decrease of reporter activity and a 17% decrease of IL8 mRNA level after stimulation with TNFα. Knockdown of SelW or SelH expression had no observable effect on reporter activity. In addition, Se depletion elevated cellular ROS production as assessed by Carboxy-2'7'-dichlorodihydrofluorescein diacetate staining whereas GPx1 knockdown had no significant effect (Chapter 5). Knockdown of GPx4 by 85%,

as assessed by RT-PCR and Western blotting, had little effect on TNFα-driven luciferase activity. However, GPx4 knockdown lowered flagellin-induced reporter activity by 20% and interleukin 8 mRNA levels by 40% (Chapter 6). It is concluded that 1] low Se supply affects NFκB inflammatory response in Caco-2 cells, 2] the exact role of different selenoproteins in this effect remains to be elucidated, and 3] the endogenous and exogenous inflammatory responses in Caco-2 cells are differentially regulated by Se supply and by antioxidant selenoproteins.

List of abbreviations

AMP	Adenosine monophosphate
APS	Ammonium persulphate
ATP	Adenosine triphosphate
BCA	Bicinchoninic acid
BSA	Bovine serum albumin
BSC	Benzyl selenocyanate
Carboxy-H_2DCFDA	5-(and-6)-carboxy-2´7´-dichlorodihydrofluorescein diacetate
CDS	Coding sequence
cGPx4	cytosolic GPx4
CMV	Cytomegalovirus
COX	Cyclooxygenase
COX-1	Cyclooxygenase 1
COX-2	Cyclooxygenase 2
c-Rel	V-Rel avian reticuloendotheliosis viral oncogene homologue
Cu/Zn-SOD	Copper/Zinc superoxide dismutase
DEPC	Diethylpyrocarbonate
DD	Death domain
ddH_2O	double distilled water
ddNTP	Dideoxy nucleoside triphosphates
DIO	Deiodinase
EB	Ethidium bromide
EFsec	Selenocysteine-specific elongation factor
EMSA	Electrophoretic mobility shift assay
ER	Endoplasmic reticulum
FCS	Foetal calf serum
GAPDH	Glyceraldehyde-3-phosphate dehydrogenase
GI	Gastrointestinal
GPx1	Glutathione peroxidase 1
GPx2	Glutathione peroxidase 2
GPx3	Glutathione peroxidase 3
GPx4	Glutathione peroxidase 4
GSH	Glutathione
GSSG	Glutathione disulphide
HBSS	Hank's Buffered Salt Solution
H_2O_2	Hydrogen peroxide
5-HETE	5-Hydroxyeicosatetraenoic acid
HIV	Human immunodeficiency virus
5-HPETE	5-hydroperoxyeicosatetraenoic acid
H/R	Hypoxia/reoxygenation
HRP	Horseradish peroxidase

HUVEC	Human umbilical endothelial cells
I	Iodine
IκBs	Inhibitory κB proteins
IκBα	Inhibitory κB α
IκBβ	Inhibitory κB β
IκBγ	Inhibitory κB γ
IκBε	Inhibitory κB ε
IBD	Inflammatory bowel disease
IKK	IκB kinase
IL1β	Interleukin 1β
IL6	Interleukin 6
IL8	Interleukin 8
iNOS	inducible nitric oxide synthase
IRAK	IL-1 receptor associated kinase
IRAK1	IL-1 receptor associated kinase 1
IRAK4	IL-1 receptor associated kinase 4
JNK	c-Jun N-terminal kinases
LAR	Luciferase assay reagent
LB medium	Lysogeny broth medium
LOX	Lipoxygenase
5-LOX	5-Lipoxygenase
12-LOX	12- Lipoxygenase
15-LOX	15- Lipoxygenase
LPS	Lipopolysaccharide
LT	Leukotriene
LTB4	Leukotriene B4
LTC4	Leukotriene C4
MAP3Ks	MAP kinase kinase kinases
MAP3K1	MAP kinase kinase kinase 1
MAP3K3	MAP kinase kinase kinase 3
MAPK	Mitogen-activated protein kinase
MCS	Multiple cloning site
mGPx4	mitochondrial GPx4
MHC	Major histocompatibility complex
mRNA	Messenger RNA
MyD88	Myeloid differentiation primary response gene 88
NEAA	Non-essential amino acids
NFκB	Nuclear factor kappa B
NF• B1•	Nuclear factor kappa B 1
NF• B2•	Nuclear factor kappa B 2
NIK	NFκB-inducing kinase (**= MAP3K14** MAP kinase kinase kinase 14)
nGPx4	nuclear GPx4
NO	Nitric oxide
Nox	NADPH oxidase

Nox1	NADPH oxidase 1
Nox2	NADPH oxidase 2
PBS	Phosphate buffered saline
PCR	Polymerase chain reaction
PG	Prostaglandin
PGE2	Prostaglandin E2
PGI2	Prostaglandin I2
15d-PGJ2	15-deoxy-Delta 12, 14-prostaglandin J2
PPi	Pyrophosphate
p-XSC	1,4-phenylenebis (methylene) selenocyanate
Redox	Reduction-oxidation reaction
RelA	V-Rel avian reticul oendotheliosis viral oncogene homolog A
RelB	V-Rel avian reticul oendotheliosis viral oncogene homolog B
RHD	Rel homology domain
RIP	Receptor-interacting protein
RISC	RNA-induced silencing complex
RLA	Relative luciferase activity (luciferase activity per mg protein)
RLB	Reporter lysis buffer
ROOH	Lipid peroxides
ROS	Reactive oxygen species
RT-PCR	Reverse transcription-polymerase chain reaction
S	Sulphur
SBP2	SECIS-binding protein 2
SDS-PAGE	Sodium dodecyl sulphate-polyacrylamide gel electrophoresis
Se	Selenium
Se-	Selenium-depleted
Se+	Selenium-supplemented
SECIS	Selenocysteine insertion sequence
SeCys	Seleno-cysteine
Sel H	Selenoprotein H
Sel I	Selenoprotein I
Sel K	Selenoprotein K
Sel M	Selenoprotein M
Sel N	Selenoprotein N
Sel O	Selenoprotein O
Sel P	Selenoprotein P
Sel R	Selenoprotein R
Sel S	Selenoprotein S
Sel T	Selenoprotein T
Sel W	Selenoprotein W
Sep-15	Selenoprotein 15kDa
siRNA	small interfering RNA
SODD	Silencer of death domain
SPS2	Selenophosphate synthetase 2

TABs	TAK1 binding proteins
TAD	Transactivation domain
TAK1	TGF-beta activated kinase 1 (**= MAP3K7** MAP kinase kinase kinase 7)
tBOOH	tert-Butyl hydroperoxide
TGF	Transforming growth factor
TIR	Toll/IL-1 receptor
TIRAP	Toll-interleukin 1 receptor domain-containing adapter protein
TLR	Toll-like receptor
TLR2	Toll-like receptor 2
TLR4	Toll-like receptor 4
TLR5	Toll-like receptor 5
T-PBS	Tween-20-Phosphate buffered saline
TNFα	Tumor necrosis factor α
TNFR1	TNF receptor 1
TNFR2	TNF receptor 2
TRADD	TNFR1-associated death domain protein
TRAF2	TNFR-associated factor 2
TRAF6	TNFR-associated factor 6
TRAM	TRIF-related adaptor molecule
TRIF	TIR-domain-containing adapter-inducing interferon-β
TrxR	Thioredoxin reductase
TrxR1	Thioredoxin reductase 1
TrxR2	Thioredoxin reductase 2
TrxR3	Thioredoxin reductase 3
UTR	Untranslated region
VCAM	Vascular cell adhesion molecule

Index of Tables

Index of Figures

Table of Contents

1.Introduction:

1.1 Selenium, selenoproteins and human health

1.1a Micronutrient Selenium and its implications for human health from epidemiological studies and clinical trials

Selenium (Se) is contained in all foods with levels usually depending on available soil selenium in production area. The biological importance of Se was firstly highlighted when its low intake correlated with occurrence of several Se-responsive animal disorders in cattle and sheep, for example, white muscle disease (Brown and Arthur, 2001) and impaired immune defence to microbial challenges (Arthur and Boyne, 1985, Boyne and Arthur, 1979). Its relevance to human physiology was firstly highlighted when the severe cardiovascular defect Keshan Disease was found in the Keshan region of Heilongjiang province, China, where the soil is selenium-deficient (Combs, 2000). Although the aetiology of Keshan Disease is not completely understood, susceptibility to virus infection in human heart muscle together with insufficient Se intake has been widely suggested to be involved (Beck, 1999, Combs, 2000). This is supported by the fact that Se supplementation has almost completely prevented the high incidence of Keshan Disease in the region (Beck, 1999). However, since 1979, health implications of Se intake have been studied intensively and associated with additional aspects including protection against virus infection, bacterial infection and carcinogenesis, and is summarized below.

Se deficiency has been correlated with vulnerability to infections including Coxsackie virus (Beck, 1997, Beck et al., 1995), influenza virus (Beck et al., 2001, Jaspers et al., 2007) and human immunodeficiency virus (HIV) (Baum et al., 1997, Fawzi et al., 2005). Coxsackie B4 was among those viruses isolated from the cardiac muscle samples of Keshan disease (Beck, 1997). More recent studies, using a mouse model, found that under conditions of low Se intake, Coxsackie virus behaved more virulently that a benign strain Coxsackie B3 switched into a virulent type (Beck et al., 1995, Beck, 1999). In HIV infection, relatively low levels of plasma Se were associated with 10 fold, and 6 fold, higher risk of mortality from multiple infections in adults and children, respectively (Baum et al., 1997, Campa et al., 1999). Se supplementation (100-200μg/day) has been recommended in clinical trials for its beneficial effect in enhancing immunity (Fawzi et al., 2005). A recent finding has demonstrated that increased activity of selenoprotein Thioredoxin reductase 1 has inhibitory effects on HIV transactivation protein, which might partially explain Se's effects on HIV infection (Kalantari et al., 2008).

Se has been suggested to enhance resistance to bacterial infection and insufficient Se intake is associated with the progression of inflammatory bowel disease (IBD) (Karp and Koch, 2006, Halliwell et al., 2000). Inflammatory bowel disease is presumed to result from combined etiological events including genetic variations (Stoll et al., 2004, Hugot et al., 2001), microbial infections (Hisamatsu et al., 2008, Marteau et al., 2004) and possibly insufficient intake of nutrients including Se (Karp and Koch, 2006,

Geerling et al., 2000). As a result, the colon is often characterized by inflammation in response to stimulation by the activities and/or the presence of pathogenic or commensal micorbes (Wen and Fiocchi, 2004). Se supplementation was suggested to be helpful in the control of IBD symptoms (Halliwell et al., 2000, Tirosh et al., 2007), and to decrease the need for therapeutic steroids in clinical immunosuppression treatment (Karp and Koch, 2006). These observations suggest that there is a close association between Se intake and some bacterial infections.

Higher Se status has also been associated with lowered cancer risk. A low serum Se level was associated with increased mortality from multiple cancers, with gastrointestinal and prostate cancer showing the strongest association (Whanger, 2004, Willett et al., 1983, Russo et al., 1997). Se supplementation (200μg/d) in clinical trials was linked with lowered cancer risk in prostate, lung and gastrointestinal tract compared with placebo (Clark et al., 1996, Duffield-Lillico et al., 2002). In addition, Se's protective effects were suggested to be specific to some, but not all, types of cancers and no significant reduction was found, for example, in the risk of skin cancer following Se supplementation (Clark et al., 1996). Interestingly, the particular organs associated with lowered cancer risk followed Se supplementation are those frequently associated with inflammatory challenge, such as the gastrointestinal tract and lung.

To summarize, increased Se status has been suggested to improve the outcome of virus infection, bacterial infection and carcinogenesis. From these observations, it is reasonable to presume that Se has a more general biological role allowing it to participate in the maintenance of the host-defence system, such as in the gastrointestinal epithelium, where Se particularly exerts its protective effects. However, to date Se has been mainly studied as an antioxidant nutrient for its primary effect, mainly for the reason that Se is incorporated into the selenoproteins many of which are enzymes with antioxidant functions. As a result, a correlation between Se's antioxidant function and its role in the immune-defence system is central to the understanding of how Se exerts its biological functions.

1.1b The incorporation mechanism of Se into selenoproteins

Se is largely, although not exclusively, incorporated into proteins known as selenoproteins in the form of the amino acid Seleno-cysteine (SeCys) (Kryukov et al., 2003). The incorporation of SeCys into the selenoprotein sequence requires the interaction between two mRNA elements: the UGA triplet in the coding region and the Selenocysteine Insertion Sequence (SECIS) in the 3' untranslated region (UTR), which are present in all selenoprotein mRNAs (Kryukov et al., 2003, Brigelius-Flohe, 2008).

The triplicate nucleotide coding, UGA, is one of the stop signals (UAG, UAA, and UGA) and functions to stop polypeptide synthesis during translation. However, in the coding of selenoproteins, the biosynthesis of protein sequence is not terminated, but the UGA condon is translated into the specific amino acid SeCys (Meplan et al., 2006, Bellinger et al., 2009).

The SECIS is a stem-loop structure present in the 3'UTR of selenoprotein mRNAs that enables recognition of UGA as the codon of the SeCys, but not a stop signal (Kryukov et al., 2003). In all the selenoproteins, SECIS sequences show a low similarity in their sequence alignment, but all share a conserved stem-loop secondary structure (Berry, 2005). An example of SECIS secondary structure of human GPx4 (Villette et al., 2002) is given in Figure 1.

The interaction between UGA codon and SECIS recruits additional protein factors, including the SeCys-synthesizing $tRNA^{Sec}$ (Bosl et al., 1997), a specific elongation factor EFsec (Meplan et al., 2006) and binding proteins such as the SECIS-binding protein 2 (SBP2) (Copeland et al., 2000). The SeCys incorporation machinery is shown in Figure 1.

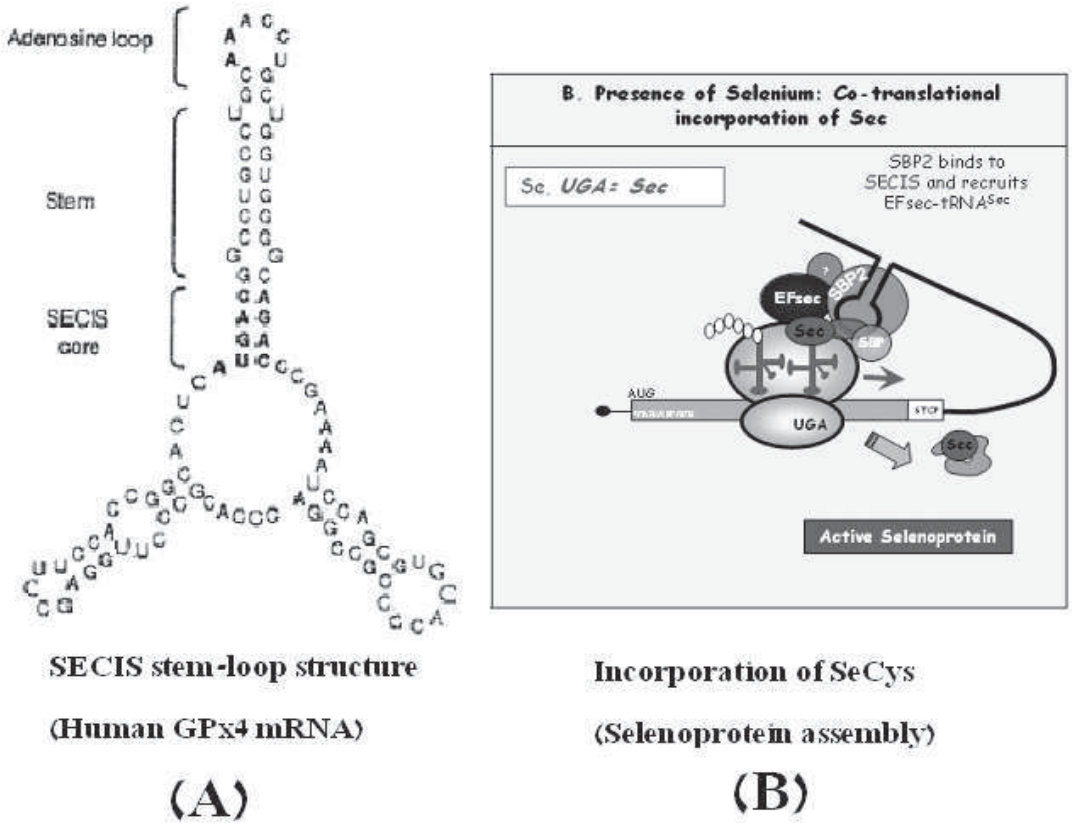

Figure 1: Stem-loop structure of SECIS and incorporation of SeCys in selenoprotein synthesis

Incorporation of Se into selenoproteins requires the interaction between UGA codon and SECIS, which is in a stem-loop structure conserved in the 3'UTR of all selenoprotein mRNAs (example, SECIS of human GPx4 mRNA, shown in (A)). Further, recognition of the UGA codon encoding SeCys by SECIS recruits additional factors of EFsec, SBP2 and $tRNA^{Sec}$ and allows insertion of the SeCys into the selenoprotein sequence (shown in (B)). (Taken from (Villette et al., 2002) (Meplan et al., 2006)).

The incorporation machinery is essential for the expression of selenoproteins and complete loss of Se incorporation causes severe effects. Such effects are shown by the $tRNA^{Sec}$ knock-out mouse model which exhibits a lethal phenotype of prenatal death (Bosl et al., 1997). In contrast, genetic polymorphisms in the 3'UTR of selenoprotein mRNAs result in functional selenoproteins but with altered biological activities (Berry,

2005, Pagmantidis et al., 2005). To date, polymorphisms with functional implications corresponding to the 3'UTR have been reported in selenoprotein genes: *GPX4*: 718T>C close to SECIS; *SELP*: r25191G>A; *SEP 15*: 811 C>T and 1125 G>A (Villette et al., 2002, Meplan et al., 2007, Jablonska et al., 2008, Kumaraswamy et al., 2000). The 718T>C polymorphism in GPx4 3'UTR has been associated with alterations in the 5-Lipoxygenase metabolism pathway (an inflammatory pathway described in Section 1.3a) (Villette et al., 2002), and the 1125 G>A polymorphism in Sep 15 3'UTR has been associated with an increased risk of lung cancer (Jablonska et al., 2008), presumably due to their effects on selenoprotein biosynthesis. In addition, mutations in *SEPN1* gene, which encodes selenoprotein N that regulates calcium homeostasis in muscle (Arbogast and Ferreiro, 2010), have been identified as responsible for early-onset myopathy (Maiti et al., 2009).

Despite the shared basic stem-loop structure, SECIS elements in individual selenoprotein mRNAs are variable in sequence and this influences their ability to incorporate Se (Berry, 2005, Kryukov et al., 2003). Partially as a result of such differences, selenoproteins respond differently to changes of Se supply and a hierarchy exists in the synthesis of selenoproteins, with some being synthesized in higher priority and others in relatively lower priority, especially when Se supply is limiting. For example, a known hierarchy in the GPx family is as follows (Brigelius-Flohe, 1999, Bermano et al., 1996a):

GPx2• GPx4• GPx1=GPx3

Owing to this effect, depletion in Se supply is known to lower dramatically the synthesis of a number of, but not all, selenoproteins, e.g. GPx1, SelW and SelH (Sunde et al., 2009, Pagmantidis et al., 2005).

1.1c selenoproteins and their antioxidant function

So far twenty-six selenoprotein genes have been identified in the human genome (Kryukov et al., 2003). Two groups of these selenoproteins, the Glutathione Peroxidase (GPx) family (GPx1-4 and GPx6) and the Thioredoxin Reductase (TrxR) family (TrxR1-3), are well-characterized antioxidants involved in metabolism of reactive oxygen species (ROS) (Lu and Holmgren, 2009, Arthur, 2000). Another group of selenoproteins, the deiodinase (DIO) family (DIO1-3), is specifically involved in the metabolism of Iodine (I) in thyroid hormones through oxidant-reductive activity (Kohrle, 2000, Brown and Arthur, 2001). Of the remaining selenoproteins, whereas some may have antioxidant ability, such as selenoprotein W (SelW) and selenoprotein H (SelH) (Dikiy et al., 2007), others are proposed to function in Se absorption and transportation (such as selenoprotein P, Sel P) (Kato et al., 1992), SeCys tRNA synthesis (such as selenophosphate synthetase 2, SPS2) (Xu et al., 2007), or their functions remain undefined. Seven selenoproteins, including Sep 15, DIO2, SelK, SelM, SelN, SelS and SelT, are localized in the endoplasmic reticulum (ER), and these selenoproteins may modulate protein folding in response to ER stress (Shchedrina et al., 2010, Labunskyy et al., 2009). The 26 selenoproteins

together with their respective tissue distributions, subcellular localizations and proposed functions are listed in Table 1.

selenoprotein	Tissue distribution	Subcellular Localization	Function
GPx1(c-GPx)	All tissues	Cytoplasm	Antioxidant
GPx2(GiGPx)	Gastrointestinal epithelium, liver	Cytoplasm	Antioxidant
GPx3(p-GPx)	Circulation plasma	Extracellular	Antioxidant
GPx4(phGPx)	All tissues	Cytoplasm Mitochondria	Antioxidant
GPx6	Unknown	Unknown	Antioxidant
TrxR1	All tissues	Cytoplasm; Mitochondria	Antioxidant
TrxR2	Liver, kidney, heart	Mitochondria	Antioxidant
TrxR3	Testis	Cytoplasm	Antioxidant
IOD1	Thyroid, liver, kidney	Plasma membrane	T3 T4 metabolism
IOD2	Thyroid	ER membrane	T3 T4 metabolism
IOD3	Brain, muscle, placenta	Plasma membrane	T3 T4 metabolism
SPS2	Wide	Cytoplasm	SeCys tRNA synthesis
SelS	Unknown	ER	Protein folding
SelP	Liver; and others?	Extracellular	Se transporation
Sep 15	Wide	ER	Protein folding
SelW	Muscle	Cytoplasm	Antioxidant?
SelN	Wide	ER membrane	Calcium homeostasis
SelR	Liver, kidney, pancreas	Cytoplasm?	Unknown
SelT	Prostate	Unknown	Protein folding?
SelH	Unknown	Cytoplasm?	Antioxidant?
SelI	Unknown	Cytoplasm?	Unknown
SelK	Unknown	Plasma membrane	Protein folding?
SelM	Unknown	Perinuclear?	Protein folding?
SelO	Unknown	Cytoplasm?	Unknown
SelV	Unknown	Cytoplasm	Unknown

Table 1: **Identified selenoproteins, their tissue distributions, subcellular localizations and possible functions**.

Taken from (Moghadaszadeh and Beggs, 2006) and modified according to (Dikiy et al., 2007, Brigelius-Flohe, 1999, Curran et al., 2005, Voudouri et al., 2003, Jablonska et al., 2008, Shchedrina et al., 2010, Labunskyy et al., 2009). (?=not confirmed)

More than half of the 26 selenoproteins have been found capable of reducing oxidative species, owing to the presence of SeCys in their core catalytic sequences (Table1). Se belongs to the same chemical family of Oxygen (O) and Sulphur (S), but is more active in its electron transferring ability. In SeCys where the S cofactor of cysteine is replaced by a Se cofactor, the catalytic ability to donate two electrons to unsaturated oxygen radicals results in a disulphide of glutathione and conversion of unsaturated oxygen radicals to saturated radicals, in the cases of selenoprotein glutathione peroxidases (GPxs) (Moghadaszadeh and Beggs, 2006, Brigelius-Flohe and Kipp, 2009). An example of the clearance of the free radical H_2O_2 by GPxs is presented in Figure 2 and it results in the following overall reaction:

$$2\ GSH + H_2O_2 \quad GSSG + 2H_2O$$

Afterwards, the glutathione disulphide (GSSG) is recycled to glutathione by Glutathione reductase at the expense of NADPH.

In addition to hydrogen peroxide, other free radicals can also be reduced by antioxidant selenoproteins. Removal of superoxides or lipid peroxides (ROOH) can be conducted by GPx4 (Imai and Nakagawa, 2003), and reduction of thioredoxin is through thioredoxin reductases (TrxRs) using NADPH as substrate (Ganther, 1999). However, it is worthwhile to emphasize that the reactive oxygen species (ROS) is continuously produced in the cells, and its clearance relies on the co-operation of many antioxidants, in which Se and antioxidant selenoproteins play an important part. The pathways of ROS production and clearance are given in Figure 2 (Droge, 2002).

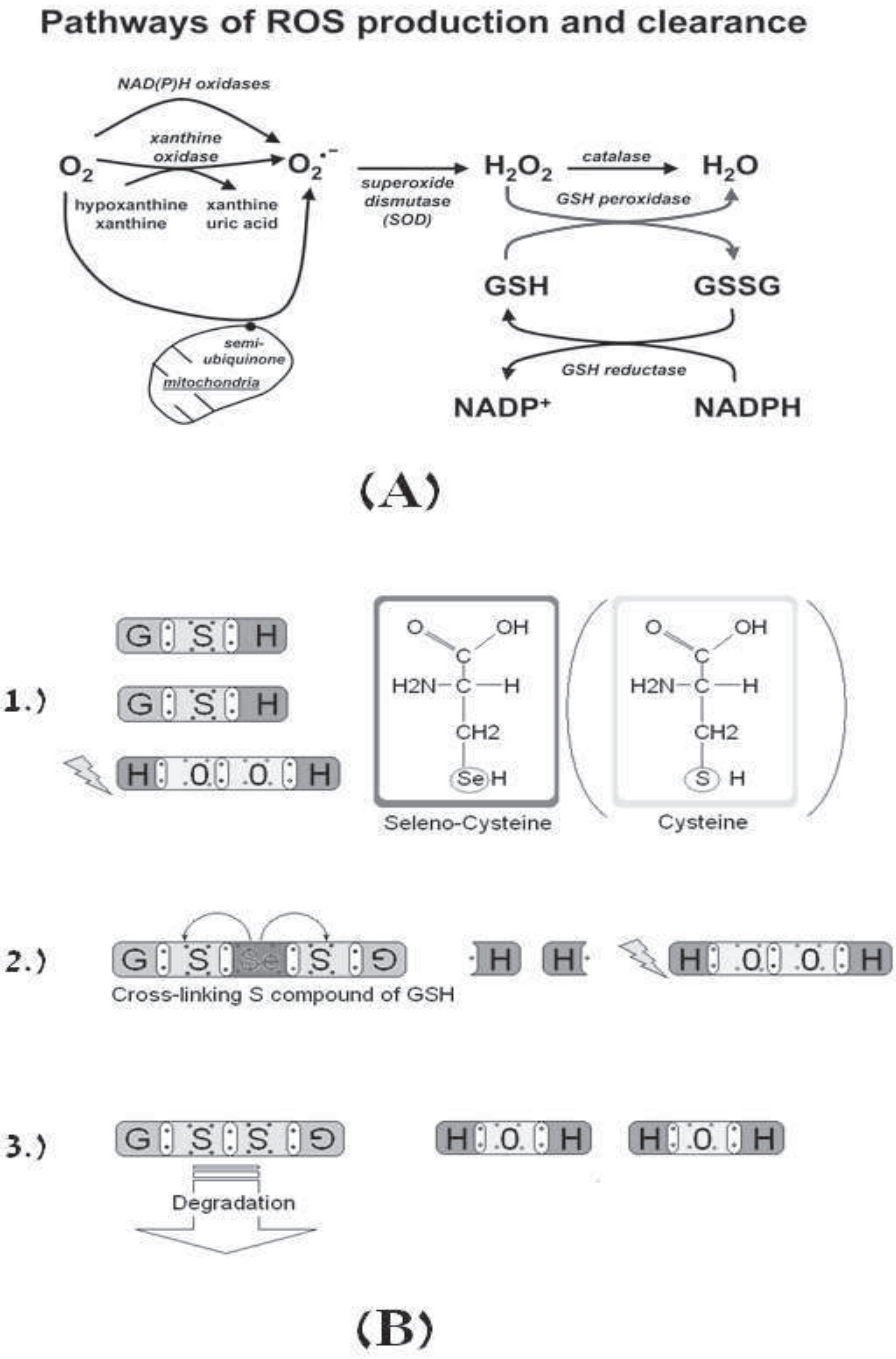

Figure 2: Pathways of ROS production and clearance in the cell environment & Reduction of hydrogen peroxide by GPx

ROS are produced and reduced constantly in the cell environment and a co-operative antioxidant system is required for the clearance of ROS (shown in (A), taken from (Droge, 2002)), in which antioxidant selenoproteins play an important part. SeCys uses Se as a substitute for S in cysteine and allows antioxidant selenoproteins such as GPxs to reduce free radicals. An example is given to show the reduction of H_2O_2 by GPx (shown in (B)), in which Se cross-links two GSH molecules and thereafter releases two hydrogen atoms to neutralize the unsaturated H_2O_2 into water.

1.1d Glutathione Peroxidases, SelW and SelH

The GPx family contains six members (GPx1 to GPx6), which exhibit considerable conservation of their catalytic sequences. Except for GPx5, which uses cysteine, GPx1-4 and GPx6 incorporate SeCys during translation and their syntheses are dependent on Se supply (Brigelius-Flohe, 1999). As shown in Figure 2, GPxs are characterized by their ability to metabolise ROS at the expense of glutathione (GSH). As a result, oxidative species are reduced and the reduction-oxidation reaction (redox) recovers the balance between ROS production and clearance. However, individual GPxs are variable in their tissue distribution, subcellular localization, ability to incorporate Se, i.e. Se incorporation hierarchy, and preference for different oxidative targets they metabolise (Brigelius-Flohe, 1999). The relatively well-studied peroxidases GPx1 to GPx4 are discussed below:

GPx1: GPx1, also known as cellular GPx, is expressed thoroughout in all tissues including the gastrointestinal tract (Moghadaszadeh and Beggs, 2006). GPx1 is located in the cell cytoplasm and is low in the Se incorporation hierarchy. Its mRNA expression decreased by >60% in cells grown in Se-deficient medium (Pagmantidis et al., 2005), or in rats and mice fed on Se-deficient diet (Sunde et al., 2009, Bermano et al., 1995). GPx1 catalyzes mainly the removal of water soluble hydroperoxides but is also able to reduce some fatty acid hydroperoxides after these oxidative species become disassociated from membranes by phospholipases (Grossmann and Wendel, 1983). The *GPX1* gene encodes 2 transcript variants, but no publications have

suggested that the two GPx1 isoforms are functionally different (Mullenbach et al., 1988).

GPx2: GPx2, also known as gastrointestinal GPx, is expressed only in the cytoplasm of gastrointestinal epithelium and liver (Chu et al., 1993). GPx2 is highest in the Se incorporation hierarchy in tissues where it is expressed, and therefore the synthesis of GPx2 is barely affected by Se depletion, as observed in mice fed on Se deficient diet (Sunde et al., 2009, Kipp et al., 2009). Consistent with this, GPx2 mRNA expression is slightly elevated in cells grown in Se deficient medium (Pagmantidis et al., 2005). GPx2 has similar substrate specificity to GPx1 (Brigelius-Flohe, 1999). The *GPX2* gene encodes one transcript.

GPx3: GPx3, also known as plasma GPx, is secreted from the kidney tubular cells and is present in the blood circulation (Avissar et al., 1994). Similar to GPx1, GPx3 is low in the incorporation hierarchy. GPx3 targets mainly the soluble hydroperoxides in the extracellular environment (Bjornstedt et al., 1994). The *GPX3* gene encodes one transcript.

GPx4: GPx4, also known as phospholipid hydroperoxide GPx, is expressed in almost all tissues including the gastrointestinal tract (Imai et al., 1995). GPx4 is located in cytoplasm and mitochondria, is particularly associated with cell membranes, and may be also transported into the nucleus in certain cell types (Imai and Nakagawa, 2003).

GPx4 is relatively high in the Se incorporation hierarchy and its expression has been found to be unaffected or mildly reduced (by ~20%) by Se depletion (Kipp et al., 2009, Pagmantidis et al., 2005, Bermano et al., 1996b). Compared with the other GPxs, GPx4 has a wider selection of oxidative substrates, which include phospholipid hydroperoxides (Ursini et al., 1985), lipid hydroperoxides (from cholesterol and cholesteryl esters) (Thomas et al., 1990), and thymine hydroperoxide (Bao et al., 1997). In addition, GPx4 is able to use reductants other than glutathione (GSH) in catalysis (Aumann et al., 1997).

Notably, the *GPX4* gene encodes 3 transcript variants, cytosolic GPx4 (cGPx4), mitochondrial GPx4 (mGPx4) and nuclear GPx4 (nGPx4). Whereas cGPx4 contains only the catalytic sequence and locates non-preferentially in the cytoplasm (Maiorino et al., 1991), mGPx4 and nGPx4 contain additional leader sequences for mitochondrial and nuclear translocation, respectively, and can be transported into mitochondria and the nucleus, respectively (Arai et al., 1996, Pfeifer et al., 2001). However, nGPx4 is highly specific and has been found to be present only in testis and associated with sperm maturation. Owing to the above features, GPx4 has been suggested to have evolved to repress oxidative radicals in lipid environments and are important in the protection of the mitochondria (Arai et al., 1996, Liang et al., 2007, Nomura et al., 1999).

The importance of GPxs has been supported by studies using several mouse knock-out models. In GPx1 knock-out (GPx1 -/-) mice, despite no apparent abnormalities being observed during embryonic development (Ho et al., 1997), increased susceptibility to coxsackievirus B3 infection has been identified (Beck et al., 1998). This mirrors the aetiology of Keshan disease where low Se intake results in an increased vulnerability to coxsackievirus infection. In addition, GPx1 -/- mice are more sensitive to secondary necrosis or neutrophil-induced cell injury in liver (Bajt et al., 2002), to ischemia-reperfusion injury in brain (Crack et al., 2006), to Doxorubicin-induced cyto-toxicity in heart (Gao et al., 2008) and to insulin and insulin-induced glucose uptake in muscle (Loh et al., 2009). In line with these observations, loss of GPx1 antioxidant protection has been associated with decreased cell tolerance to oxidative challenge and increased apoptosis. Moreover, in the studies of ischemia-reperfusion injury and insulin response, GPx1 deficiency has also been correlated with elevated responses of two signalling pathways, namely the NFκB inflammatory pathway (Crack et al., 2006) and the Akt signalling pathway (Loh et al., 2009).

Owing to its specific expression and function in gut, the importance of GPx2 has been limitedly revealed by the GPx2 knock-out model itself, owing to the lack of systematical phenotype. However, GPx2 -/- mice has been found to be sensitive to UV-irradation in skin and vulernable to develop keratinocytes-origined carcinomas, in which GPx2 has been suggested to control apoptosis as an stress-responsive gene

(Walshe et al., 2007). A recent study of the intestinal tissues of GPx2 -/- mice also found that GPx2 might be essential for intestinal mucosal homeostasis in a way that GPx2 is the main apoptosis regulator in gut (Florian et al., 2010). In the double knock-out model of both GPx1 and GPx2, GPx1 -/- and GPx2-/- mice exhibited increased sensitivity to microflora challenge and showed increased colonic inflammation (Esworthy et al., 2003). Moreover, the GPx1 and GPx2 double knock-out mice have also been found to have a higher risk of developing gastrointestinal cancer compared with the normal littermates, probably due to the effects of repeated occurrence of colitis (Lee et al., 2006). According to two recent findings, the increased carcinogenesis in the colon of GPx1 and GPx2 double knock-out mice has been associated with aberrant DNA methylation (Hahn et al., 2008) and COX-mediated malignant cell migration (Banning et al., 2008b). Therefore, a protective role of GPx2 has been suggested in the gut epithelium and combined, GPx1 and GPx2, deficiencies result in an elevated inflammatory response to intestinal stimuli.

Knock-out mice lacking GPx4 exhibit a severe phenotype and die at a prenatal stage with arrested embryonic development (Imai et al., 2003a). The inability to restructure the cavities during embryogenesis indicates an essential role of GPx4 in programmed cell death, i.e. apoptosis. Additional investigations have been performed on GPx4 haploid insufficient mice (GPx4 +/-), in which GPx4 mRNA, protein and activity were reduced to ~50% (Yant et al., 2003). The GPx4 +/- mice were more sensitive to

oxidative challenge by γ-irradiation and exhibited a lower survival rate than the normal littermates (Yant et al., 2003). In addition, the cultured embryonic fibroblasts from GPx4 +/- mice were more sensitive to oxidative attacks by t-butyl hydroperoxide, hydrogen peroxide or paraquat, and they displayed more abundant caspase-3-dependent apoptosis and lipid membrane peroxidation (Ran et al., 2003). In contrast, the livers of mice overexpressing GPx4 were resistant to oxidative challenge by diquat, and their fibroblast cells were resistant to challenges by t-butyl hydroperoxide and diquat (Ran et al., 2004). Taking these results together, GPx4 has a critical role in repressing oxidative stress in cells.

To summarize, GPxs are essential antioxidant selenoproteins and their primary function is to regulate ROS levels and neutralise the apoptotic lipid peroxidation effects of ROS. However, additional biological roles have also been correlated with the GPxs. For example, an association between GPx antioxidant protection and inflammatory response/inflammatory signalling has been found through the GPx1 knockout mouse model (Crack et al., 2006, de Haan et al., 2004) and the double GPx1 and GPx2 knockout model (Esworthy et al., 2003).

Considering the proposed importance of Se to the human immune response (described in section 1.1a), knowledge in this area remains limited and investigations to understand the mechanisms, through which Se and/or GPxs regulate inflammatory signalling, are necessary. A growing number of *in vitro* studies have been conducted

to investigate potential links between the control of redox-signalling and the activation of the NFκB inflammatory signalling pathway (Gloire et al., 2006). The NFκB signalling pathways and their regulation by reactive oxygen species (ROS) will be reviewed in Section 1.2, and the current knowledge on Se and/or GPxs' antioxidant function, and their possible interaction with NFκB responses will be reviewed in Section 1.3.

SelW and SelH: In addition to GPx1, SelW and SelH are two other selenoproteins that are highly sensitive to changes of Se supply (Sunde et al., 2009). However, their biochemical functions are far less well characterized than those of the GPxs. In humans, SelW has been detected in various tissues, with high expression in tissues including skeletal muscle, heart, brain, prostate, small intestine, and colon (Bellingham et al., 2003, Whanger, 2009). SelW has been associated with antioxidant protection against H_2O_2 and H_2O_2-induced apoptosis in neurons, myoblasts (by overexpression studies) and lung cancer cells (by ectopic expression of SelW) (Chung et al., 2009, Loflin et al., 2006, Jeong et al., 2002b). In addition, the catalytic ability of SelW has been suggested to be dependent on GSH (Kim et al., 2005, Jeong et al., 2002b). SelW expression in a gut epithelial cell line is highly sensitive to Se supply (Pagmantidis et al., 2005).

SelH has also been found in multiple tissues of humans and mice (Kryukov et al., 2003). Whereas studies overexpressing SelH in a murine neuron Ht22 cell line found

decreased cell death after UV irradiation together with decreased superoxide production (Ben Jilani et al., 2007, Mendelev et al., 2009), structural analysis suggests that SelH belongs to a family containing a conserved CxxC or CxxU motif (C: cysteine; x: unspecified amino acid; U: selenocysteine) and exerting a thioredoxin-like redox function (Dikiy et al., 2007). Subcellular localization of SelH has been suggested to be nuclear (Novoselov et al., 2007), and some authors additionally suggest that it binds DNA through its DNA-binding ability and regulates genes involved in glutathione synthesis and phase II detoxification (Panee et al., 2007). However, details in SelH's antioxidant function remain largely unknown. The other members of the CxxU family based on structural similarity include SelW and SelT (Dikiy et al., 2007).

The other essential selenoproteins: Clearly, all the selenoproteins are expected to have roles in the cell environment. However, so far not all of their functions have been clearly defined (Table 1). Of the remaining selenoproteins, the TrxR family members (TrxR1-3) are also essential antioxidants and their function has been associated with the control of inflammatory response (see below). TrxR1 is expressed ubiquitously in all tissues including the human gastrointestinal tract and is located mainly in the cytoplasm (Crosley et al., 2007, Lu and Holmgren, 2009). TrxR2 has been detected in various tissues including liver, kidney and heart and is located in the mitochondria (Crosley et al., 2007). TrxR3 is expressed at high levels in testis and is found in the cytoplasm (Lu and Holmgren, 2009).

At the expense of NADPH, TrxRs reduce thioredoxin (Turanov et al., 2010) and constitute another redox system co-operating with the GSH-reduction system (Figure 2(A)) (Lu et al., 2009, Mandal et al., 2010). Thioredoxin has been shown to repress the DNA-binding activity (and possibly the phosphorylation) of NFκB transcription factors by modifying the thiol groups (-SH) of cysteine residues of NFκB subunits (Hayashi et al., 1993, Glineur et al., 2000). Therefore, TrxR1 and TrxR2 may positively regulate the NFκB inflammatory response. Overexpression of thioredoxin has been shown to inhibit NFκB activation in Hela cells (Schenk et al., 1994, Hayashi et al., 1993) and overexpression of TrxR1 has been found to enhance the DNA-binding activity of NFκB and the expression of NFκB target genes in vascular endothelial cells (Sakurai et al., 2004). Furthermore, both of the knock-out mouse models of TrxR1 and TrxR2 resulted in embryonic death. This suggested that TrxR1 was important for cell proliferation and TrxR2 for mitochondria-related apoptosis regulation (Conrad, 2009).

TrxR1 and TrxR2 also respond to changes in Se supply. In a Caco-2 cell culture model, Se depletion resulted in 27% decrease of TrxR2 mRNA level compared with Se-supplemented cells (Pagmantidis et al., 2005). In the endothelial cell line EAhy926, neither TrxR2 protein expression nor activity was affected by 3 days of Se depletion but both decreased by ~33% after prolonged Se depletion (7 days) (Crane et al., 2009). In an *in vivo* mouse model, marginally low Se diet decreased TrxR1 mRNA expression by ~35% in the colon as assessed by microarray and real-time PCR (Kipp

et al., 2009). It appears that TrxR1 lies in the middle of Se incorporation hierarchy, whereas TrxR2 might be on a higher level of Se incorporation hierarchy.

Selenoprotein S (SelS) is located in the membrane of endoplasmic reticulum and is believed to regulate ER stress (Shchedrina et al., 2010). Notably, a polymorphism in the promoter of SelS (-105 G>A) has been associated with altered plasma levels of Tumor necrosis factor alpha (TNF-α) and Interleukin 1 beta (IL-1β), both as inflammatory biomarkers in human population (Curran et al., 2005). SelS has been found to interact with ER membrane proteins and participate in the transport of misfolded proteins into the cytosol (Ye et al., 2004, Bellinger et al., 2009). The SelS polymorphism has been associated with decreased SelS expression, increased ER stress and possibly elevated NFκB activation (Bellinger et al., 2009).

Selenoprotein P (SelP) functions extracellularly and is responsible for Se transporation from liver to blood circulation (Kato et al., 1992). SelP is sensitive to Se status and two functional polymorphisms, rs24731 and rs25191, have been suggested to affect sensitivity to Se supply (Meplan et al., 2007). SelP contains ten selenocysteines (SeCys), one in the N-terminal domain with redox activity and the other nine in the C-terminal domain, functioning in Se-storage and distribution (Burk and Hill, 2009). SelP is expressed in most tissues (Dreher et al., 1997). Targeted inactivation of SelP in mice (SelP -/-) has been found to decrease the expression of multiple selenoproteins, including GPx1 and TrxR1 (Hill et al., 2003), and cause

neurological dysfunction (serzures and ataxia), male infertility and premature death (Hill et al., 2003, Schomburg et al., 2003). Targeted expression of SelP in hepatic tissues rescued the Se transportation, infertility and neurological defects in SelP -/- mice (Renko et al., 2008). In addition, SelP -/- mice exhibited increased morbidity and mortality from *Trypanosoma congolense* infection (Bosschaerts et al., 2008).

1.2 NFκB inflammatory signalling pathway and its regulation by ROS

1.2a NFκB transcription factors, their inducers and target genes

NFκB is a group of transcription factors comprising five subunit members, including RelA (p65), RelB, c-Rel, NFκB1 (precursor p105 and p50) and NFκB2 (precursor p100 and p52). Importantly the N-terminus of all members contain a conserved Rel homology domain (RHD) with DNA binding affinity to regulate the expression of NFκB target genes (Hayden and Ghosh, 2008, Vallabhapurapu and Karin, 2009). In addition, the RHD domains have affinity with each other to form homo- or hetero-dimers and as a result NFκB is dimeric in structure. NFκB subunits and their structures are illustrated diagrammatically in Figure 3.

In RelA, RelB and c-Rel (Class II NFκB), the C-terminus contains a transactivation domain (TAD), whereas in NFκB1 and NFκB2 (Class I NFκB), the C-terminus lacks the TAD (Figure 3) (Hayden and Ghosh, 2008). The TAD has been suggested to be necessary for full activation of NFκB transcription activity and a homo-dimer, such as p50/p50, lacking this domain is unable to directly activate gene expression but requires disassociation and interaction with other subunits, most commonly p65 (Kang et al., 1992, Zhong et al., 2002). In addition, the molecules NFκB1 and NFκB2, i.e. p105 and p100, respectively, contain an ankyrin repeat region, which has an inhibitory effect against RHD transcriptional activity (Figure 3) (Liou et al., 1992, Dobrzanski et al., 1995). As a result, p105 and p100 precursors are not functionally active until being cleaved to form p50 and p52, respectively.

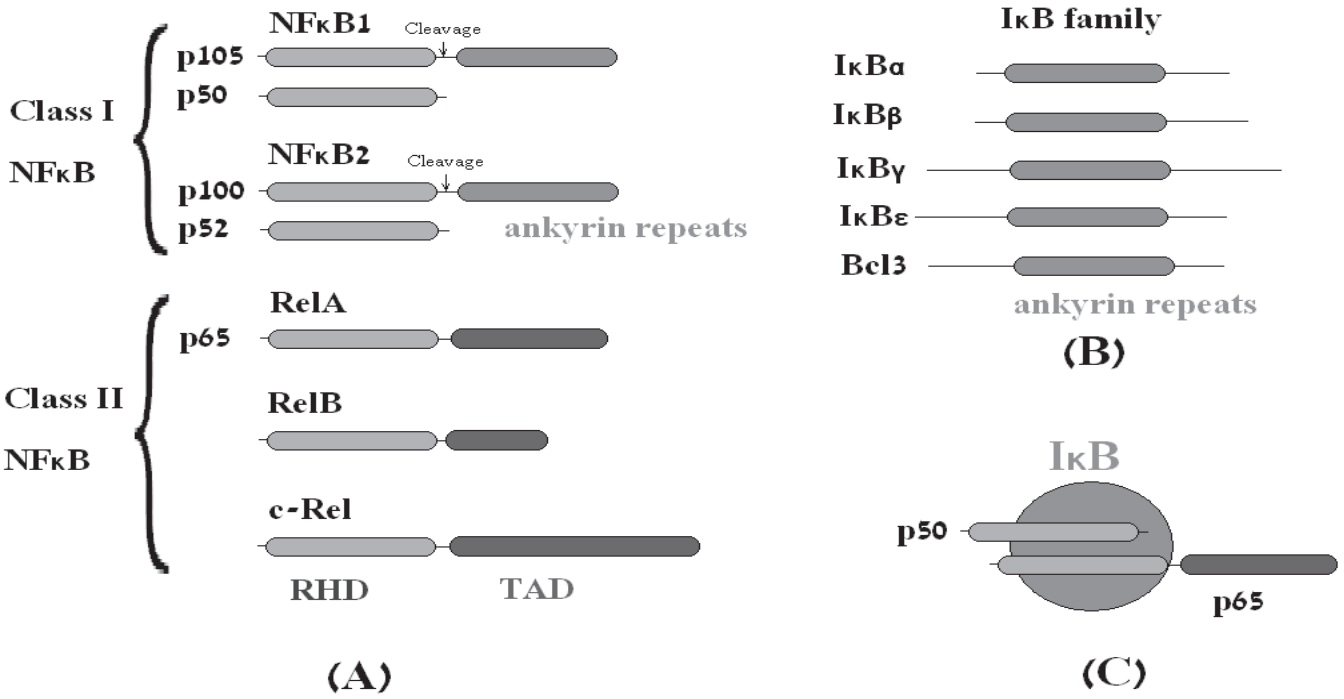

Figure 3: NFκB transcription factors, IκB family members and inactive state of NFκB bound to IκB

NFκB transcription factors comprise NFκB1 (precursor p105 and p50), NFκB2 (precursor p100 and p52), RelA, RelB and c-Rel, all conserving RHD with DNA binding affinity and dimeric ability at the N-terminus (shown in A). The precursors of Class I NFκB contain the ankyrin repeats with inhibitory effect against RHD, whereas Class II NFκB contains TAD responsible for full activation of NFκB activity. IκBs are inhibitory proteins inactivating NFκB in unstimulated cells and comprise IκBα, IκBβ, IκBγ, IκBε and Bcl3, which all conserve the ankyrin repeats (shown in B). As a result, NFκB transcription factors (example: the p50/p65 NFκB hetero-dimer) are silenced by IκB and retained in the cytoplasm (shown in C).

The NFκB transcription factor is normally in an inactive state in which the NFκB dimer is bound with, and silenced by, the inhibitory κB proteins (IκBs) (Karin and Ben-Neriah, 2000). The IκB family comprises mainly IκBα, IκBβ, IκBγ, IκBε and Bcl3, and all IκB members are characterised by an ankyrin repeat region which inactivates the RHD of NFκB (Figure 3). However, upon stimulation, the activation of the signalling cascade results in the disassociation of the IκB-NFκB complex and the release of NFκB, which translocates into the cell nucleus to promote gene expression (Vallabhapurapu and Karin, 2009, Hayden and Ghosh, 2008) (see Figures 4 and 5). The process of signal transduction from receptor activation to the activation of NFκB transcriptional activity is described as the NFκB inflammatory signalling pathway.

The downstream target genes controlled by NFκB comprise over 200 genes (Gilmore, 2008). Based on their biological roles, the NFκB target genes can be categorized as: cytokines/chemokines and their modulators, such as IL6 and IL8; immunoreceptors, such as CD40 (TNF-receptor family member) and TLR2 (Toll-like receptor member); proteins involved in antigen presentation, such as Tapasin (MHC class I presentation and assembly); stress response genes, such as 12-Lipoxygenase (an arachidonic acid metabolic enzyme) and Cu/Zn superoxide dismutase; regulators of apoptosis, such as Bcl-2 (pro-survival factor) and Fas-Ligand (apoptosis inducer) (Gilmore, 2008). The majority of these NFκB target genes are able to participate directly, or indirectly, in the development of inflammatory events in cells. As a consequence, NFκB has been widely studied as a key controlling factor in the expression of inflammatory cytokines, which influence the progression of inflammation and carcinogenesis in human tissues (Neurath et al., 1998, Karin and Greten, 2005, Kawai and Akira, 2006).

A combination of two out of five NFκB subunits generates various types of homo- or hetero- NFκB dimers, which can be used in different cells and induced by the activating signal (Karin and Ben-Neriah, 2000, Hoffmann et al., 2002a). One common type abundant in most cells is the NFκB1/RelA, i.e. P50/p65 hetero-dimer (shown in Figure 3) (Vallabhapurapu and Karin, 2009). The inducers of NFκB signalling pathways are broad in type and include the following: bacterial or fungal products, such as Lipopolysaccharide (LPS) and flagellin; inflammatory cytokines, such as Tumor necrosis factor α (TNFα) and interleukin 1β (IL1β); oxidative stress, such as H_2O_2, tert-Butyl hydroperoxide (tBOOH), reoxygenation; mitogens, growth factors and hormones, such as insulin and transforming growth factor (TGF) (Gilmore, 2008). As well as exogenous inducers of the NFκB signalling pathway, i.e. from bacteria, viruses, and fungi, many NFκB inducers are endogenously produced. These different NFκB activation mechanisms are essential for the efficient defence of the host during the innate and adaptive immunity.

However, a common feature of both the endogenously and exogenously originated NFκB signalling pathways is that, frequently, NFκB activation is subject to regulation by reactive oxygen species (ROS), and therefore, potentially, under the influence of antioxidant enzymes (Gloire et al., 2006, Li et al., 2009, Kim et al., 2008, Haddad, 2002). This is believed to be through ROS, acting as a secondary messenger during the signal transduction cascades that response to various inducers. The NFκB signalling pathways activated by TNFα (endogenous pathway) and by flagellin (exogenous pathway) are described in detail in the following two sub-sections.

1.2b TNFα-NFκB signalling pathway and its regulation by ROS

TNFα is an essential inflammatory cytokine that extracellularly binds to the TNF receptor 1 (TNFR1, also known as CD120a) and mediates two inflammatory signalling pathways including the NFκB pathway and the Mitogen-activated protein kinase (MAPK) pathway, as well as the apoptosis signalling pathway (Chen and Goeddel, 2002, Li and Lin, 2008). The other TNF receptor is TNF receptor 2 (TNFR2) the expression of which is mainly in cells of the immune system (Li and Lin, 2008). Signal transduction through TNFα-TNFR1 is generally described as the TNFR1 pathway and is present ubiquitously in tissues.

Once TNFR1 binds TNFα, a conformational change of its intracellular domain occurs and this leads to disassociation of the TNFR1 death domain (DD) from silencer of death domain (SODD), which normally binds to and inhibits TNFR1 activity (Jiang et al., 1999) (Figure 4, Step 1). Subsequently, the exposed DD recruits the adapter protein TNFR1-associated death domain protein (TRADD), which further recruits Receptor-interacting protein (RIP) and TNFR-associated factor 2 (TRAF2) for activation of the NFκB and MAPK signalling (Hsu et al., 1996, Ting et al., 1996) (Figure 4, Step 2). RIP and TRAF2, as targets of Ubiquitins, then undergo Lysine (K) 63-linked ubiquitiylnation and conformational change, which are required for the recruitment of the IκB kinases (IKKs) to the receptor complex (Ea et al., 2006, Devin et al., 2000, Wu et al., 2006) (Figure 4, Step 3).

After recruitment of the IKKs to the RIP-TRAF2 adaptor protein complex, the MAP kinase kinase kinases (MAP3Ks) are activated and initiate a phosphorylation cascade (Li and Lin, 2008). The MAP3Ks responsible for TNFα-NFκB signalling transduction

are variable according to the cell type and include TGF-beta activated kinase 1 (TAK1), NFκB-inducing kinase (NIK), MAP kinase kinase kinase 3 (MAP3K3) and MAP kinase kinase kinase 1 (MAP3K1) (Ling et al., 1998, Lee et al., 2008, Yang et al., 2001, Blonska et al., 2005). The mechanisms responsible for their activations remain not totally understood, but TAK1 and MAP3K3 have been associated with phosphorylation and activation by the RIP-TRAF2 complex (Blonska et al., 2005, Blonska et al., 2004).

To continue the phosphorylation cascade, TAK1/NIK/MAP3K3 phosphorylate IKKs (Shim et al., 2005, Li and Engelhardt, 2006, Ling et al., 1998, Blonska et al., 2004), and IKKs then phosphorylate the NFκB-binding protein IκBs (Li and Lin, 2008) (Figure 4, Step 4). The phosphorylated IκB undergoes degradation by proteasome lysis and eventually releases the NFκB transcription factors for nuclear translocation (Figure 4, Steps 5 and 6).

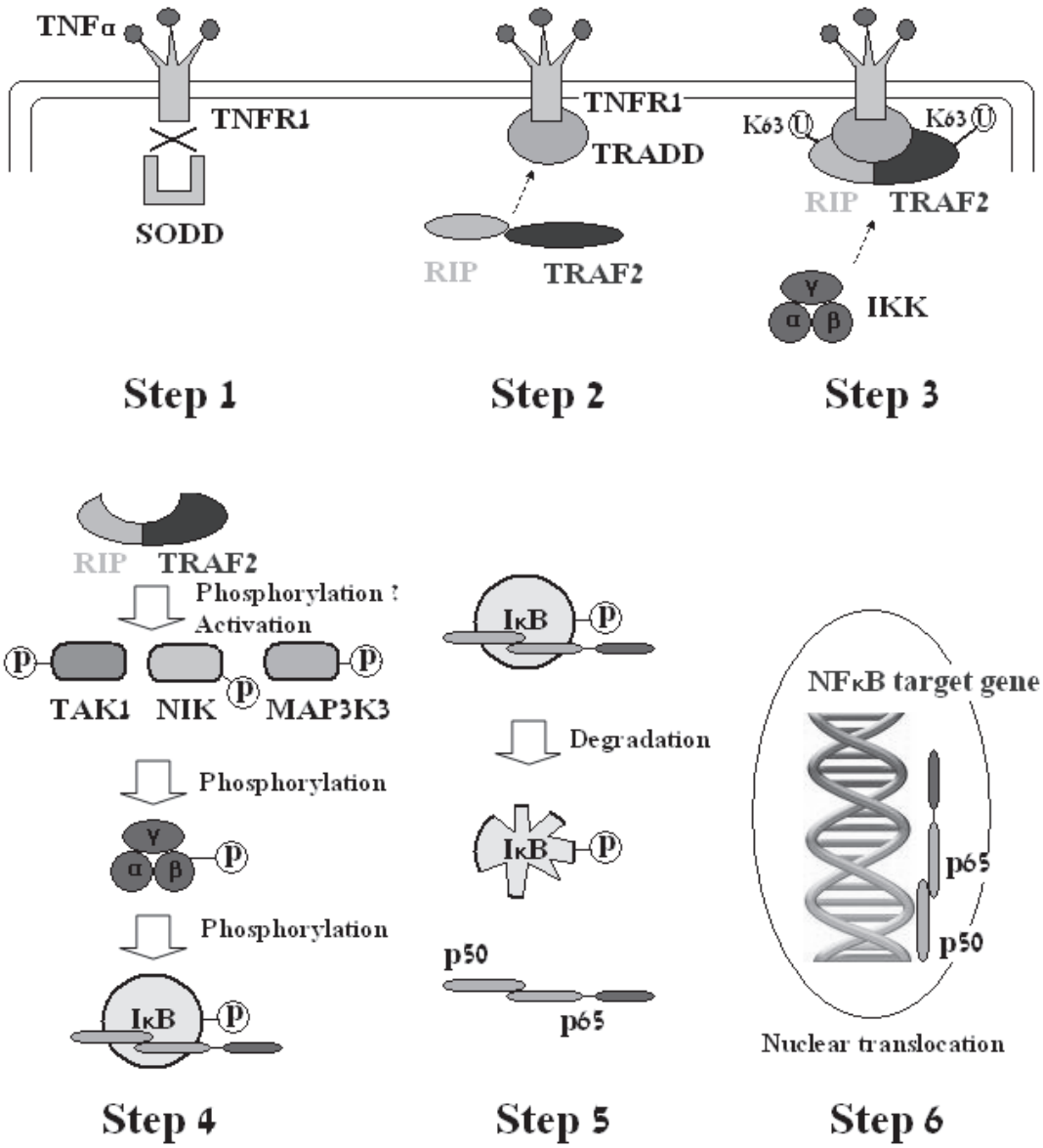

Figure 4: Signalling transduction in the TNFα-TNFR1 pathway leading to NFκB activation

Signalling transduction in the TNFα-TNFR1 pathway leads to activation of the NFκB transcription factors. Step1: TNFα binds to TNFR1 and the activated receptor disassociates from the inhibitory protein SODD. Step 2: The receptor complex binds to TRADD and further recruits RIP and TRAF2. Step 3: K63 ubiquitination of RIP and TRAF2 results in recruitment of the IKKs. Step 4: Phosphorylation cascade (RIP/TRAF2→TAK1/NIK/MAP3K1→IKK→IκB) results in NFκB inhibitory protein IκB being phosphorylated. Step 5: The phosphorylated IκB undergoes degradation by proteasome lysis and releases NFκB transcription factors. Step 6: The released NFκB tranlocates to cell nucleus and promotes the expression of NFκB target genes.

The participation of ROS during TNFα signalling is believed to regulate the activities of kinases which affect the phosphorylation cascade (Figure 4, Step 4). ROS have been suggested to activate the MAP3Ks, including NIK (Li and Engelhardt, 2006, Kim et al., 2008) and MAP3K1 (Lee and Koh, 2003, Lee et al., 2008). ROS have also been suggested to interact with TAK1 (Morioka et al., 2009, Omori et al., 2008, Sanchez-Duffhues et al., 2009), although the direct exposure of TAK1 to hydrogen peroxide failed to result in pathway activation (Cheung et al., 2003). In addition, ROS have also been suggested to be inactivators of MAPK phosphatases (Kamata et al., 2005, Chan et al., 2008, Hou et al., 2008), which degrade MAP3Ks and interfere with downstream MAPK or NFκB signalling (Figure 5) (Shen et al., 2001, King et al., 2009, Furst et al., 2007).

The origin of ROS production in the TNFR1 pathway is not fully understood. One possible source is from mitochondria during apoptosis. In addition to the NFκB signalling cascade, the TNFR1 death domain can alternatively activate MAPK signalling using the adaptor protein TRADD, and activate caspase-8 apoptotic signalling using another adaptor protein called Fas-Associated protein with Death Domain (FADD) (Figure 5) (Li and Lin, 2008). Both MAPK (mainly the stress-related c-Jun N-terminal kinases, a subgroup of MAPK, in terms of TNFR1 signalling) (Kamata et al., 2005) and caspase-8 cascades have apoptotic effects that might result in release of ROS from mitochondria (see Figure 2 (A)). However, it has been argued that the ROS production by apoptotic mitochondria is not rapid enough to influence NFκB signalling.

The other possible source of ROS is from the nicotinamide adenine dinucleotide phosphate (NADPH) oxidases (Noxs). Noxs are membrane-associated enzymatic complexes that generate superoxide and show fast responses to stimuli on the cell membrane. In macrophages and neutrophils, Nox2 is known to be activated by TNFα and results in superoxide production to destroy the phagotrophic microbes (Grandvaux et al., 2007). In non-phagocytic cells, Noxs are also expressed (Grandvaux et al., 2007) and their function has been associated with the signalling transduction in response to TNFα (Kim et al., 2007, Li et al., 2009). Nox2-derived H_2O_2 production was detected in fibroblast cells after TNFα stimulation, and has been suggested to play an important role in the recruitment of the TRAF2 adaptor to the TNFR1 complex and to activate the NFκB signalling cascade (Figure 5) (Li et al., 2009). In addition, the linkage between TNFR1 and Nox was identified to be the flavokinase, which binds both the TNFR1 death domain and a Nox subunit p22 (phox) (Yazdanpanah et al., 2009). The flavokinase phosphorylates Nox, then facilitates the assembly of Nox subunits and activates its oxidative activity (Figure 5). Comparatively, a similar role of flavokinase was not detected in the ROS generation by the Toll-like receptors (TLRs) (Yazdanpanah et al., 2009) (see Section 1.2c). Therefore, Nox could also be a critical candidate in the production of ROS for NFκB activation in the TNFR1 signalling pathway.

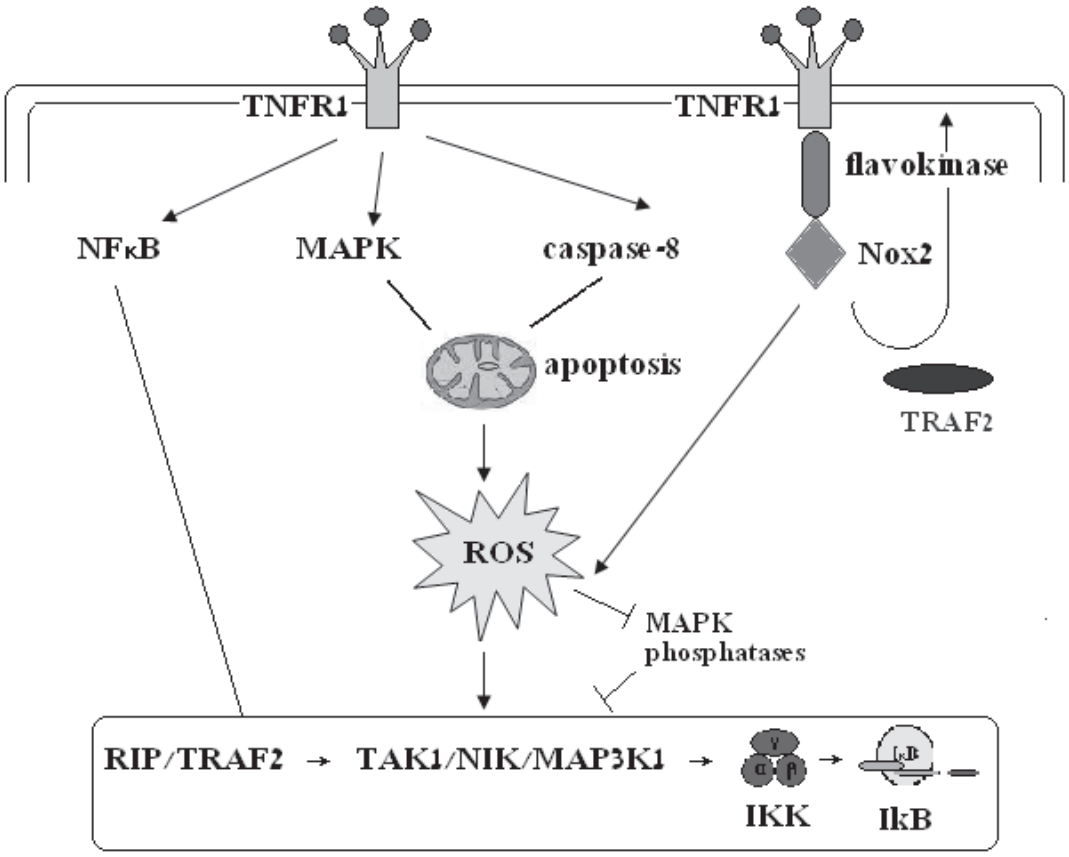

Figure 5: Scheme showing ROS production in the TNFR1 pathway and its possible role in mediation of NFκB activation

Signalling transduction in the TNFR1 pathways may result in the activation of NFκB transcription factors, MAPK kinases and caspase-8 apoptosis. Whereas NFκB activation relies on the phosphorylation cascade to activate the IκB kinases (IKKs), the MAPK and caspase-8 pathways have apoptotic effects and may result in release of ROS from mitochondria. In addition, ROS may also be produced from the NADPH oxidase 2 which is coupled by flavokinase with TNFR1 death domain. The mediation by ROS on the NFκB activation is to influence the phosphorylation cascade. ROS has been suggested to either activate the TAK1/NIK/MAP3K1 kinases, or inactivate the MAPK phosphatases which are negative regulators of the phosphorylation cascade. Moreover, the Nox2-derived H_2O_2 production has also been suggested to facilitate the binding between TNFR1 and TRAF2.

1.2c Flagellin-TLR5-NFκB signalling pathway and its regulation by ROS

Bacterial components such as flagellin are exogenous to cells and activate downstream signalling through their binding to Toll-like receptors (TLRs). There are 13 TLRs that differentiate various pathogen-associated molecular patterns (Arancibia et al., 2007). TLRs are widely expressed in the immune cells such as macrophages and dendritic cells (Carmody and Chen, 2007), whereas in non-immune gut epithelial cells, TLR5 is selectively expressed (Kawahara et al., 2004, Zeng et al., 2006). Importantly, TLR5 is reported to regulate inflammatory responses and apoptosis signalling in a model of colon cancer (Rhee et al., 2008). TLR5 recognizes and binds with flagellin using its extracellular domain (Andersen-Nissen et al., 2007).

The intracellular parts of all TLRs contain a conserved Toll/IL-1 receptor (TIR) domain with homology to the IL-1 receptor. After the formation of flagellin-TLR5 complex, the TIR domain recruits the essential adaptor protein Myeloid differentiation primary response gene 88 (MyD88) (Figure 6, Step 1) (Arancibia et al., 2007). The TLR5 signalling pathway has been suggested to be uniquely MyD88 dependent, since knockdown of other candidate adaptor proteins, e.g. TIR-domain-containing adapter-inducing interferon-β (TRIF), Toll-Interleukin 1 Receptor Domain-Containing Adapter Protein (TIRAP) and TRIF-related adaptor molecule (TRAM), appeared to have no effect on the TLR5 response (Yamamoto et al., 2003, Horng et al., 2002).

The C-terminus of MyD88 associates with TIR, and the N-terminus contains a death domain (DD) (Boldin et al., 1995) that interacts with the death domains of IL-1

receptor associated kinases (IRAKs) family member, IRAK4 and IRAK1 (Arancibia et al., 2007) (Figure 6, Step 2).

Initiation of the subsequent phosphorylation cascade has been suggested to be through IRAK4 auto-phosphorylation (Cheng et al., 2007), and the activated IRAK4 then phosphorylates IRAK1 (Suzuki et al., 2002, Kollewe et al., 2004). Meanwhile, the IRAK4-IRAK1 complex recruits TNFR-associated factor 6 (TRAF6) (Carmody and Chen, 2007, Li et al., 2002) (Figure 6, Step 3).

The phosphorylated IRAK4-IRAK1-TRAF6 complex disassociates from MyD88 (Kollewe et al., 2004), and TRAF6 undergoes K63-linked ubiquitylination and conformational change (Lamothe et al., 2007, Deng et al., 2000) (Figure 6, Step 4).

The release of TRAF6 allows it to recruit the TAK1 binding (TABs) proteins (Adhikari et al., 2007, Takaesu et al., 2001), to form a TRAF6-TAB-TAK1 complex that results in phosphorylation and activation of TAK1 (Carmody and Chen, 2007). In the remaining phosphorylation cascade, TAK1 phosphorylates IKK and IKK phosphorylates IκB (Sato et al., 2005, Adhikari et al., 2007) (Figure 6, Step 5). The phosphorylated IκB is degraded by the proteasome and the NFκB transcription factors are released for nuclear translocation (Figure 6, Step 6).

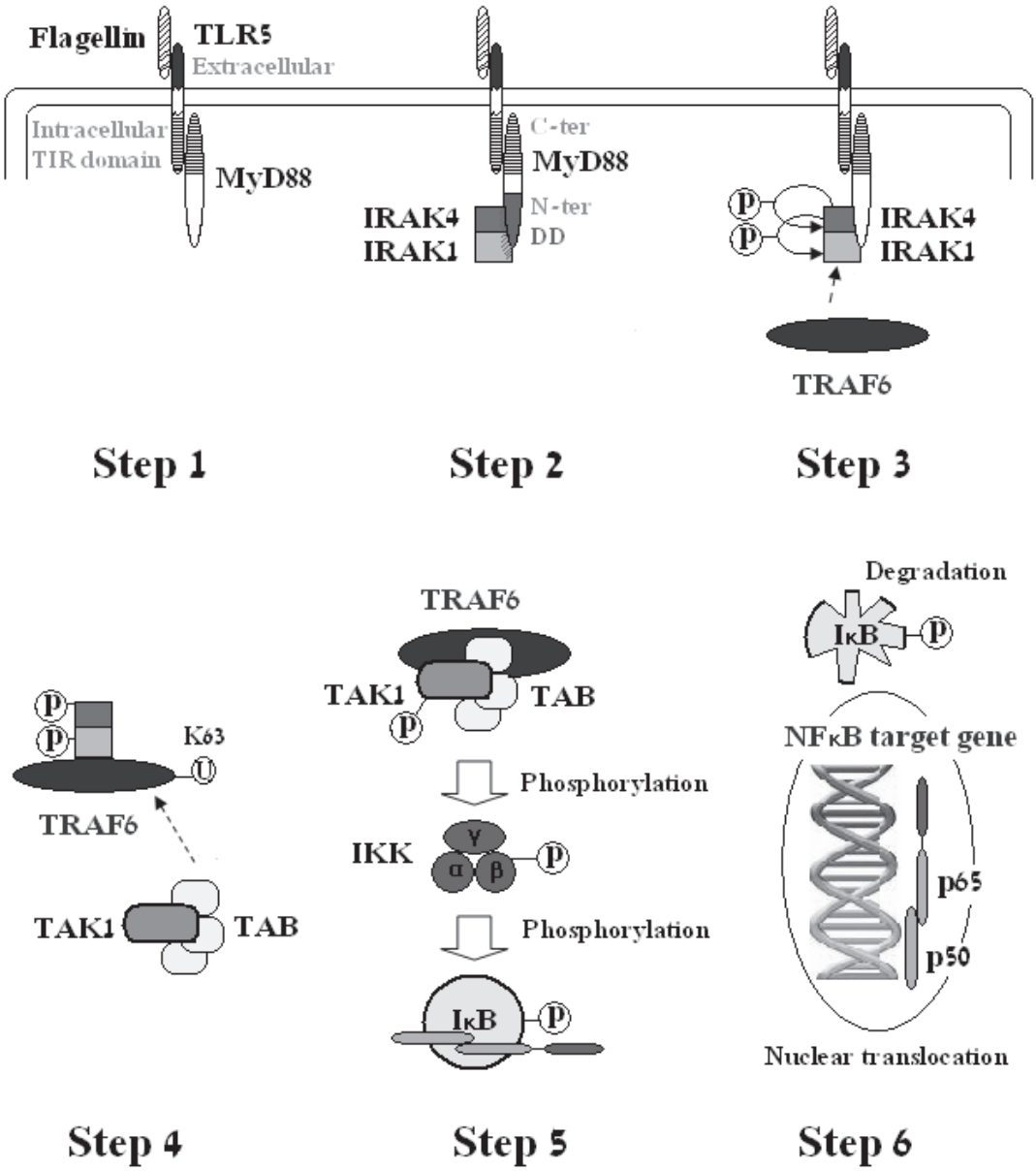

Figure 6: Signalling transduction in the flagellin-TLR5 pathway leading to NFκB activation

Signalling transduction in the flagellin-TLR5 pathway leads to activation of the NFκB transcription factors. Step1: Flagellin binds to TLR5 and the intracellular TLR5-TIR domain associates with adaptor protein MyD88. Step 2: The death domain of MyD88 N-terminus interacts with IRAK4 and IRAK1. Step 3: IRAK4 undergoes auto-phosphorylation and then IRAK4 phosphorylates IRAK1. The phosphorylated IRAKs recruit TRAF6. Step 4: The IRAK-TRAF6 complex disassociates with MyD88 and formation modification of TRAF6 by K63-linked ubiquitination results in recruitment of TAK1-TAB kinase complex. Step 5: The phosphorylation cascade (TAK1→IKK→IκB) results in the NFκB inhibitory protein IκB being phosphorylated. Step 6: IκB undergoes degradation by proteasome and the NFκB transcription factors tranlocate to cell nucleus and promote the expression of NFκB target genes.

The role of ROS during TLR5 signalling has been suggested to be a modulation of the kinase activities (such as TAK1) in the phosphorylation cascade (Kim et al., 2008). In addition, ROS appears to function downstream of the IRAK4-IRAK1 phosphorylation complex, since in the LPS-TLR4 signalling pathway, Nox1 has been identified as a phosphorylation target of IRAK4 and to be subject to IRAK4 regulation (Pacquelet et al., 2007). In IRAK4 overexpression, Nox activity increases in response to LPS (Pacquelet et al., 2007). Comparably, in the flagellin-TLR5 signalling pathway, Nox1-derived ROS production has been found and suggested to be responsible for the downstream TAK1 activation and IL8 expression (Kawahara et al., 2004). Considering the similarity between the TLR4 and TLR5 pathways in the MyD88-dependent signal transduction, ROS could also be regulated by IRAK4 in the flagellin-TLR5 cascade. Therefore, it is possible that ROS production by Nox1 functions between IRAK4 phosphorylation and TAK1 activation, and regulates the TLR5-NFκB signalling pathway by mediating the phosphorylation cascade (Figure 7).

In addition to IKK-NFκB signalling, TAK1 is also known to activate the MAPK pathway and the latter might serve as another source of ROS production through its apoptotic effect. Indeed, both the MAPK (p38 MAPK subgroup in the case of flagellin-TLR5 pathway) and NFκB signalling pathways respond to flagellin induction in human intestinal epithelial T84, HT29cl19A and Caco-2BBE cells and alveolar type II epithelial A549 cells (Im et al., 2009, Yu et al., 2003). However, the apoptotic effect of MAPK is frequently not apparent owing to the anti-apoptotic effect of NFκB (Kreuz et al., 2001, Catz and Johnson, 2001); when NFκB was inhibited, enhanced p38 activation resulted in increased cellular apoptosis (Zeng et al., 2006).

Therefore, ROS production from MAPK-derived apoptotic signalling might also occur and, in turn, regulate the NFκB signalling in response to flagellin (Figure 7).

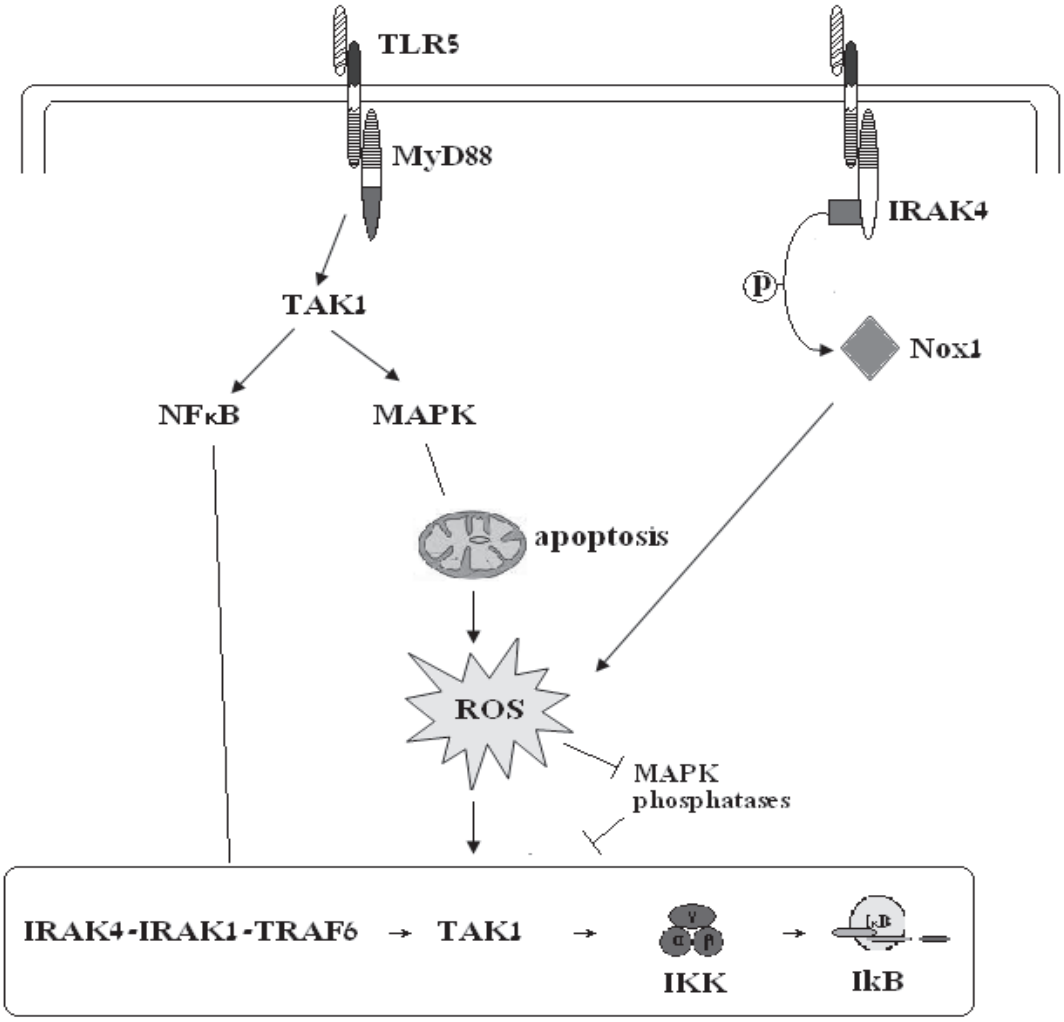

Figure 7: Scheme showing ROS production in the TLR5 pathway and its possible role in mediation of NFκB activation

Signalling transduction in the flagellin-TLR5 MyD88 dependent pathway may result in the activation of NFκB transcription factors and MAPK kinases. ROS production by flagellin could be generated through the apoptotic effect of MAPK on the mitochondria. In addition, a close association between IRAK4 and Nox1 has been identified, in which IRAK4 phosphorylates and activates Nox1 to produce ROS for downstream NFκB and MAPK signalling activation. The role of ROS in NFκB activation seems to regulate the TAK1 activity and therefore to influence the phosphorylation cascade.

1.2d Summary: the mediation of NFκB signalling activation by ROS

The described NFκB signalling pathways activated by TNFα and flagellin show how signals are transferred from receptor to the cytoplasmic NFκB-IκB complex. In summary, this involves multiple co-operative steps of ubiquitinylation (such as TRAF2 and TRAF6 K63 ubiquitnylation), phosphorylation (such as IKK phosphorylation by TAK1 and IκB phosphorylation by IKK) and proteolysis (such as IκB proteasome lysis). Importantly the regulatory effect of ROS is to enhance the phosphorylation cascade by either activation of the MAP3Ks or inactivation of the counteracting MAPK phosphatases (MKPs).

In addition, ROS also have regulatory effects on the IκB proteolysis. The oxidized IκB protein has been observed to be more sensitive to proteasome lysis, and undergoes more rapid degradation after exposure to micromolar concentration of H_2O_2 (Kretz-Remy et al., 1998, Schoonbroodt et al., 2000). This corresponds to the general observations of proteolysis, in which treatment with 20-400μM H_2O_2 increases proteolysis but treatment with high amount (>1mM) H_2O_2 causes accumulation of oxidized protein (Grune et al., 1997). In general, the physiological level of H_2O_2 production in cells is less than 100μM and therefore would be expected to mainly affect the process of IκB proteolysis (Droge, 2002, Gautam et al., 2006). Finally, ROS may further mediate the NFκB transcription activity in the nucleus by affecting chromatin remodeling, recruitment of co-activators, and DNA binding (Gloire and Piette, 2009).

1.3 Effects of Se and selenoproteins on NFκB signalling

1.3a Effects of Se/GPxs on eicosanoid synthesis

The repression of leukotriene (LT) and prostaglandin (PG) biosynthesis by GPx1 and GPx4 is thought to be through their mediation of lipoxygenase (LOX) and cyclooxygenase (COX)-catalyzed arachidonic acid metabolism pathways, which are also sensitive to redox-signalling, reviewed in (Brigelius-Flohe, 1999, Imai and Nakagawa, 2003). Leukotrienes are metabolites of 5-LOX (a subgroup of LOXs) and in this pathway, arachidonic acid is first oxidized by 5-LOX into 5-hydroperoxyeicosatetraenoic acids (5-HPETE) and then the 5-HPETE undergo further dehydration to form LTs (Hyde and Missailidis, 2009) (Figure 8). The intermediate product 5-HPETE can activate 5-LOX in an autonomous feedback cycle (Rouzer and Samuelsson, 1986). In the presence of GPx1 and GPx4, the antioxidant selenoproteins are thought to degrade 5-HPETE into 5-HETE and therefore impede the feedback activation of 5-LOX pathway (Imai et al., 1998, Straif et al., 2000) (Figure 8).

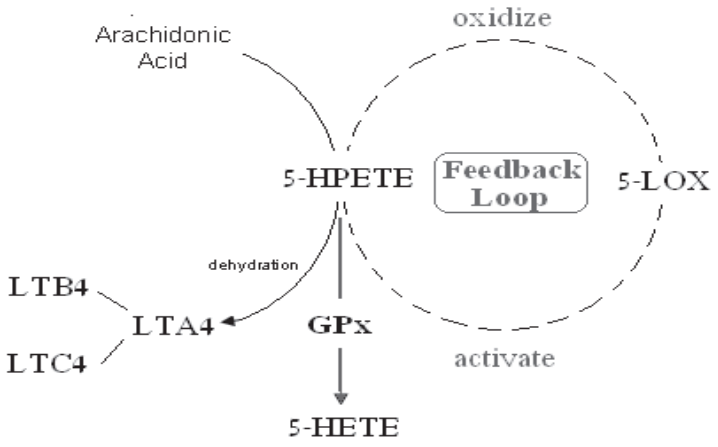

Figure 8: Inhibition of 5-LOX activation and LT production by GPx

The biosynthesis of leukotrienes is through the metabolism of arachidonic acid into 5-HPETE and catalyzed by 5-LOX. 5-LOX oxidizes arachidonic acid into 5-HPETE, which, in turn, activates 5-LOX in a positive feedback cycle. GPx1 and GPx4 are able to reduce 5-HPETE into 5-HETE and therefore break the 5-LOX feedback cycle and inhibit the LT production.

Similarly, GPx4 has also been observed to regulate the 12-LOX, 15-LOX (the other two subtypes of LOXs), and COX pathways by repressing their oxidized intermediary products and positive feedback (Sakamoto et al., 2000, Heirman et al., 2006, Chen et al., 2003), respectively. A number of investigations have identified these links and are listed in Table 2.

Cell Type	LOX/COX Pathway	Inhibitor	Enhancer	Key Indications	References
RBL-2H3	5-LOX	GPx4 ↑	5-HPETE; 12-HPETE; DEM(GPx4 inhibitor)	1. GPx4 represses 5-LOX activity by reducing 5-HPETE.	(Imai et al., 1998)
PMNs	5-LOX	GPx4 ↑	n.a.	1. GPx4 is up-regulated by Growth related oncogene but not TNFα or IL1β. 2. GPx4 represses 5-LOX	(Hattori et al., 2005)
A431	12-LOX; 5-LOX; COX;	GPx4	n.a.	1. GPx4 was identified to be the inhibitor of 12-LOX and was also found to inhibit 5-LOX and COX	(Huang et al., 1998)
A431	5-LOX; 12-LOX; 15-LOX; COX1and COX2	GPx4	Exogenous oxidative stress	1. 12- and 15-LOX and COX-2 are 10 times sensitive to GPx4 than 5-LOX and COX-1 2. High level of GPx4 was observed to inhibit 12-LOX.	(Huang et al., 1999)
A431	COX; 12-LOX	n.a.	GPx4 ↓ (antisense).	1. GPx4 inhibition increases the activity and metabolism of 12LOX and COX.	(Chen et al., 2000)
Monocyte	5-LOX	GPx1	n.a.	GPx1 but not GPx4 is involved in inhibition of 5-LOX in monocytes even at low thiol concentrations	(Straif et al., 2000)
	12-LOX	GPx4	n.a.	Hepoxilin A3 stimulates the expression of GPx4 and GPx4, in turn, represses 12-LOX to protect the cells.	(Zafiriou et al., 2007)
L929 B16BL6	COX-2	GPx4 ↑	n.a.	GPx4 inhibits COX-2 and PGE2 production, and this inhibition results in impediment of tumor growth and malignancy.	(Heirman et al., 2006)
HT29	COX-2	GPx2	GPx2 siRNA	GPx2 inhibits COX-2 and GPx2 knockdown results in enhance of tumor migration and invasion.	(Banning et al., 2008b)
HT29	COX-2	n.a.	GPx2 siRNA	GPx2 knockdown results in increased expression of COX-2 at baseline and after IL1 stimulation, and increased production of PGE2.	(Banning et al., 2008a)
Mice and mouse neurons	12-LOX; 15-LOX	GPx4 PD146176	GPx4 -/-	GPx4 inhibits 12/15-LOX and GPx4 -/- results in activation of 12/15-LOX and AIF-mediated apoptosis	(Seiler et al., 2008)
Human platelets	12-LOX	n.a.	Iodoacetate (GPx4 inhibitor)	1. GPx4 was found in platelets & megakaryocytes. 2. GPx4 inhibits the 12-LOX pathway and the generation of hepoxilins in platelets.	(Sutherland et al., 2001)
A431	12-LOX; COX	GPx4 ↑	n.a.	1. GPx4 represses the metabolism of 12-LOX and COX to form eicosanoids.	(Chen et al., 2002)

A431	12-LOX; COX1	n.a.	GPx4 ↓ (antisense).	1. GPx4 suppression by antisense increases the 12-HETE and COX1 activity.	(Chen et al., 2003)
In vitro	15-LOX	GPx4	n.a.	1. GPx4 represses 15-LOX metabolism on mitochondria membrane and lipoprotein.	(Schnurr et al., 1996)
RBL-2H3	COX2	GPx4 ↑	Exogenous oxidative stress	1. GPx4 represses COX2 to convert PGH2 to PGD2 in nucleus and endoplasmic reticulum.	(Sakamoto et al., 2000)
HT29 cl.19A	COX2	n.a.	GPx4 ↑	1. GPx4 increases COX2 metabolism and triggers COX2 mRNA expression.	(Barriere et al., 2004)

Table 2: Summary of observed effects of GPxs on eicosanoid biosynthesis through LOX/COX pathways.

Leukotriene and prostaglandin eicosanoids mediate inflammatory events such as leukocyte adhesion (LTB4), smooth muscle contraction (PGE2), pain sensing (PGE2) and vasodilation (PGI2) (Henderson, 1994), as well as carcinogenic events, such as cell differentiation and apoptosis (Shureiqi et al., 2005, Sordillo et al., 2008, Eisinger et al., 2007). In addition, LTB4, 12(S)-HETrE and platelet-type 12-LOX have been identified as NFκB inducers in human monocytes, endothelial cells and prostate cancer cells, respectively (Huang et al., 2004, Laniado-Schwartzman et al., 1994, Kandouz et al., 2003). Meanwhile, COX-2, 5-LOX and 12-LOX have been identified as NFκB target genes in human neuronal cells, guinea pig cells and human erythroleukemia cells, respectively (Kaltschmidt et al., 2002, Chopra et al., 1992, Arakawa et al., 1995). Overall, these studies suggest that the LOX and COX eicosanoid biosynthesis pathways are closely associated with inflammatory cytokine synthesis and partially associated with the inflammatory response driven by NFκB.

1.3b NFκB regulation by Se

The inflammatory cytokine TNFα induces the classical NFκB signalling pathway, described in Section 1.2b, and over the past decade, a few publications have reported the association between Se supplementation and TNFα-induced NFκB activation. In transformed prostate cells, supplementation of the growth medium with sodium selenite or organic Se-compound methylseleninic acid was found to inhibit the DNA-binding ability of NFκB in response to TNFα, together with reduced IKK kinase activity, IκB phosphorylation and IκB proteolysis (Gasparian et al., 2002). Similarly, in human airway epithelial cells, sodium selenite supplementation increased GPx1 expression and decreased H_2O_2 production and NFκB activation by TNFα (Jeong et al., 2002a). However, in human umbilical vein endothelial cells, the nuclear translocation of NFκB subunit p65 following TNFα induction was unaffected by Se supplementation (Zhang et al., 2002). Taken together these results suggested that Se regulates TNFα-activated NFκB signalling in a cell-type dependent manner.

Similar to flagellin, the bacterial component Lipopolysaccharide (LPS) is also capable of inducing the classical NFκB signalling pathway through a MyD88 dependent mechanism (described in Section 1.2c). In a prostate cell study, Se supplementation also inhibited NFκB activation by LPS (Gasparian et al., 2002). Conversely, in macrophage cells stimulated with LPS, Se depletion decreased GPx1 expression, increased cellular ROS production, and increased NFκB nuclear translocation and the expression of NFκB target gene COX-2 (Zamamiri-Davis et al., 2002). Interestingly,

the repressive effect of Se against LPS-induced NFκB activation in macrophage cells was associated with the generation of a prostaglandin product, 15-deoxy-Delta12,14-prostaglandin J2 (15d-PGJ2), which is produced through the COX-1 pathway (Vunta et al., 2007). Se supplementation was suggested to elevate the expression of 15d-PGJ2, which inhibits IKKβ (Vunta et al., 2007), a subunit of IKK that functions in the phosphorylation cascade of NFκB signalling transduction (Section 1.2b and c). As a result, Se may enhance IKKβ inhibition by 15d-PGJ2 and repress NFκB activation induced by LPS.

In addition to ROS production, in macrophage cells the LPS-induced NFκB signalling pathway has been associated with inducible nitric oxide (NO) production, and it has been suggested that Se supplementation inhibits the response of nitric oxide synthase (iNOS) together with NFκB activation by LPS (Prabhu et al., 2002, Kim et al., 2004). Moreover, this inhibitory effect of Se against NO production was specific to the MyD88-dependent NFκB signalling pathway, but not the other pathways upon LPS induction (Yun et al., 2007) and resulted in decreased IκB degradation and p65 nuclear translocation (Yun et al., 2007, Shin et al., 2009). Therefore, at least in certain cell-types such as macrophage cells, Se regulates NO production in addition to ROS, both of which might direct the NFκB response.

Finally, in unstimulated prostate cancer cells, a high concentration (7.6mM) of Se directly affected the DNA-binding ability of NFκB, but not affect the phosphorylation

cascade, IκB degradation and NFκB nuclear translocation, suggesting that Se might directly associate with NFκB subunits (Christensen et al., 2007). Interestingly, two organic Se-compounds, benzyl selenocyanate (BSC) and 1,4-phenylenebis (methylene) selenocyanate (p-XSC), were identified to catalyze Cys_{62} of NFκB subunit p50, a site within p50's DNA-binding domain (Chen et al., 2007). The Cys_{62} was suggested to be chemically modified and inhibited by Se-compounds (SeCys corss-linking) (also see Figure 2). Therefore, Se might also regulate the NFκB transcription activity in a non-specific manner.

In summary findings suggest that Se exerts a wide range of effects on the NFκB response in multiple cell types. However, its regulatory effect also depends on the cell-type and the specific transductional signalling used to activate NFκB transcription factors.

1.3c NFκB regulation by selenoprotein GPx1

The decreased tolerance of transgenic *GPX1* -/- mice (described in Section 1.1d) to oxidative stress appears not only to be due to the elevated apoptosis response, but has also been associated with elevated NFκB inflammatory response in various mouse tissues. For example, in a study of ischemia-reperfusion injury, a condition causing oxidative damage focussed in neuronal cells, *GPX1* -/- mice exhibited increased DNA-binding of p50/p65 NFκB dimer and p65 phosphorylation compared with normal littermates (Crack et al., 2006). Comparably, the fibroblast cells derived from

GPX1 -/- mice also displayed more abundant NFκB activation in response to H_2O_2 than control cells (de Haan et al., 2004). In contrast, transgenic mice overexpressing GPx1 were more resistant to ischemia-reperfusion in renal cells, and exhibited reduced NFκB activation and the reduced attraction of neutrophil cells (Ishibashi et al., 1999). Together these findings, from *in vivo* mouse model study, have identified GPx1 to be a potential NFκB modulator in response to oxidative stress.

The regulatory effects of GPx1 on NFκB activation have also been studied *in vitro*. In T47D breast cancer cells challenged with H_2O_2, GPx1 overexpression lowers cellular ROS production, inhibit IκBα degradation and decrease NFκB (p50) nuclear translocation (Kretz-Remy et al., 1996, Kretz-Remy and Arrigo, 2001). These effects were shown to be reversed by Se depletion, which limits GPx1 synthesis (Kretz-Remy et al., 1996). GPx1 overexpression also exerts a protective effect against the NFκB responses induced by TNFα, UV irradiation, IL1β and hypoxia/reoxygenation (H/R) in breast cancer and Hela cells (Kretz-Remy et al., 1996, Li et al., 2001, Fan et al., 2003, Li and Engelhardt, 2006). In fact, in T47D breast cancer cells, TNFα-induced NFκB activation was repressed by GPx1 overexpression, as shown by decreased ROS production and inhibition of IκBα phosphorylation (Kretz-Remy et al., 1996). In another breast cancer cell line, MCF7, GPx1-overexpressing cells showed reduced NFκB activation in response to TNFα (lowered by 25~30%), UV irradiation (by 25~30%) and H_2O_2 (by >50%), respectively, as assessed by the NFκB DNA-binding ability and reporter gene expression (Li et al., 2001).

The mechanism by which GPx1 regulates NFκB signalling is not fully known. The reduction in NFκB activation linked to GPx1 overexpression has been suggested to occur through inhibition of the IKKα Serine phosphorylation of IκB, which has been observed in the NFκB response to TNFα (Kretz-Remy et al., 1996, Li et al., 2001), to IL1β (Li and Engelhardt, 2006) and to H_2O_2 (Li et al., 2001). However, GPx1 overexpression in HeLa cells also inhibits NFκB activation through an IκB Tyrosine phosphorylation mechanism, where the NFκB signalling activated by H/R is IKK-independent (Fan et al., 2003). Together these findings, from *in vitro* experiments, suggest that GPx1 regulates NFκB activation by inhibiting IκB Serine or Tyrosine phosphorylation depending on the inducer. However, the current knowledge is from the breast cancer cells and the regulatory effects of GPx1 in alternative cell types remain to be explored.

In addition, in MCF7 cells stimulated with IL1 β, NFκB activation has been associated with Nox-driven H_2O_2 production, which was suggested to be necessary for the recruitment of NFκB-inducing kinase (NIK) to the adaptor protein TRAF6 (Li and Engelhardt, 2006). As a result, both GPx1 overexpression and siRNA knockdown of Nox subunit were found to inhibit this process and lead to a reduced NFκB response. Therefore GPx1 may regulate NFκB response by repressing the H_2O_2 production related to Nox acitivity. Moreover, GPx1 overexpression also inhibited the kinase activity of NIK, whereas the MAPK phosphatase- (described in Section 1.2d) inhibitor, okadaic acid, enhanced the kinase activity of NIK, suggesting that the role

of H_2O_2 is potentially to inhibit the MAPK phosphatase and then enhance NFκB activation (Li and Engelhardt, 2006). These results highlight the interaction between Nox-mediated redox signalling and antioxidant repression of NFκB response, indicating that different types of Nox also mediate NFκB induction by TNFα, flagellin (described in Section 1.2b and 1.2c, respectively) and LPS (Gloire et al., 2006).

1.3d NFκB regulation by selenoprotein GPx4

GPx4 is able to use a wider range of substrates than GPx1 and its essential function is to prevent lipid peroxidation in membrane (described in Section 1.1d). Nevertheless, to date little is known about its regulatory effect(s) on the NFκB signalling pathway. The limited number of relevant studies are described below.

In human ECV304 cells, GPx4 overexpression combined with selenophosphate synthetase overexpression, the latter to optimise selenoprotein incorporation, was adapted to enhance the GPx4 biosynthesis (Brigelius-Flohe et al., 1997). Under the conditions of Se depletion, GPx1 expression was reduced whereas GPx4 expression was selectively elevated. Using this model, it was found that IL1-induced NFκB activation, assessed by p65/p50 DNA-binding ability, was inhibited by GPx4 overexpression (Brigelius-Flohe et al., 1997). In rabbit abdominal smooth muscle cells, linoleic acid hydroperoxide was used to induce NFκB signalling, and GPx4 overexpressing cells exhibited a reduction in lipid peroxidation together with an inhibited NFκB response and apoptosis (Brigelius-Flohe et al., 2000). In addition, in

epidermal fibroblasts, NFκB activation following UV-irradiation was inhibited by GPx4 overexpression. GPx4 overexpression resulted in the decreased production of phosphatidylcholine hydroperoxides, p65 phosphorylation and nuclear translocation (Wenk et al., 2004). Finally, an NFκB target gene, vascular cell adhesion molecule-1 (VCAM), was also inhibited by GPx4 overexpression in rabbit smooth muscle cells stimulated by IL1 (Banning et al., 2004) but whether the regulatory effect is mediated through an NFκB-dependent mechanism remains to be elucidated (Banning et al., 2004, Zhang et al., 2002).

1.3e Summary

Whereas Se and selenoprotein GPxs exert important regulatory effects on apoptosis (Section 1.1d) and eicosanoid biosynthesis (Section 1.3a), investigations into their roles in the NFκB inflammatory responses suggest that Se and GPxs are potential mediators of NFκB signalling pathways in response to various endogenous and exogenous inducers. However, to-date the findings are limited, both in relation to the inducers and the tissues investigated, and NFκB signalling does appear to vary according to the cell-type and the inducer-type. The regulation of NFκB signalling pathways in many tissues, including the gastrointestinal tract, by Se and/or GPxs, is not understood. Therefore, the studies described in this thesis were undertaken to investigate whether, and how, Se and /or GPxs modulate NFκB signalling in a human gastrointestinal epithelial cell line.

1.4 Aim of the project

- **To develop a luciferase reporter model driven by NFκB transcription activity in the colonic epithelial cell line Caco-2 as a means to monitor the NFκB inflammatory response**
- **To study the regulatory effect of Se depletion on the NFκB response in Caco-2 cells to stimuli such as TNFα or bacteral flagellin**
- **To study the effects of knocking-down expression of selenoproteins GPx1, SelW and SelH on the NFκB response in Caco-2 cells**
- **To study the regulatory effect of selenoprotein GPx4 on the NFκB response in Caco-2 cells**

Previous research has used various methods to assess NFκB activation (briefly reviewed in Chapter 3 Section 3.1 introduction) and of them, one, a luciferase reporter system, has been developed by fusing a luciferase coding sequence with a promoter containing three NFκB binding sites (3X κB) (Carlsen et al., 2002, Kirillov et al., 1996) so as to monitor NFκB transcription activity. The first part of the work described in this thesis describes the generation of appropriate gene constructs to develop this luciferase reporter system (NFκB and control luciferase reporters) in stably transfected Caco-2 cells. These cells were then used to investigate the effects of Se depletion on the TNFα-induced and flagellin-induced NFκB response and such experiments are described in the second part of this thesis.

GPx1, SelW and SelH are selenoproteins sensitive to Se supply and their expression is reduced in Se depletion. GPx1 is a well-characterized antioxidant, and furthermore SelW and SelH may also have antioxidant effect (Dikiy et al., 2007). In addition, two existing publications have studied the effects of GPx1 overexpression on TNFα-NFκB response in breast cancer cells (Kretz-Remy et al., 1996, Li et al., 2001). The third part of the work described in this thesis was to knockdown the expression of GPx1 or SelW or SelH in Caco-2 cells using the siRNA technique and to assess the effects on the TNFα-NFκB response.

GPx4 catalyzes a wide selection of oxidative substrates and protects specifically against lipid peroxidation in membrane. Little previous work has explored its regulatory effect on NFκB responses, and only in fibroblasts (Wenk et al., 2004) or ECV304 cells (Brigelius-Flohe et al., 1997). The last part of the work described in this thesis was to knockdown GPx4 expression using siRNA and to assess its effect on the flagellin-NFκB response.

2. Materials and methods

All glassware and microcentrifuge tubes were sterilized by autoclaving at 121ºC for 20 minutes. All buffers and solutions were sterilized by autoclaving at 121ºC for 20 minutes or by filtration using a 0.2µm syringe filter (Whatman). All tissue culture and bacterial work was carried out in a sterile environment and with good microbial/cell culture practice. DEPC-treated water was prepared by adding 250µl Diethyl pyrocarbonate (DEPC) to 500ml distilled water, mixing thoroughly for 3 hours and autoclaving at 121ºC for 20 minutes. DEPC-treated water was used to dilute DNA (plasmids, primers, cDNAs and PCR products) and RNA and prepare buffers and solutions.

2.1 Routine techniques

2.1.1 Restriction enzyme digestion

Restriction enzyme digestion was carried out using *Apa* I, *BamH* I, *EcoR* V, *Hind* III, *Kpn* I and *Sal* I restriction enzymes (Promega) in reactions listed in Tables 4 and 5, according to instructions provided by the manufacturer. In each reaction of 20µl total volume, 1µg of substrate DNA (plasmid) was digested with 0.5µl of each restriction enzyme (concentration 10u/µl) together with 2µl of 10X buffer, 0.2µl of 10µg/µl acetylated bovine serum albumin (BSA) and DEPC water (added to fill the 20µl total volume). The respective buffers and enzymatic activities employed in different restriction digestions are as illustrated in Tables 4 and 5. In each case, the mixture was

mixed thoroughly by pipetting, briefly centrifuged and incubated at 37ºC for 4 hours for complete restriction digestion. Controls were carried out by adding no substrate DNA, no restriction enzymes (uncut) or adding single restriction enzyme (single cut) when the reaction required restriction digestion by double or triple enzymes. After digestion, products were checked by DNA electrophoresis.

2.1.2 Separation of DNA molecules by agarose gel electrophoresis

DNA molecules are normally negatively charged and migrate towards the positive electrode in agarose gel electrophoresis. DNA molecules large in size are more difficult to traverse the agarose gel than the small DNA molecules and therefore migrate in a slower speed. As a result, DNA molecules can be separated by agarose gel electrophoresis. The technique is frequently employed to separate the DNA fragments harvested from restriction digestion or polymerase chain reaction (PCR). Together with the DNA fragments to be tested, DNA molecules of known sizes (DNA markers) are generally co-electrophoresized and comparison between the two allows estimation of the actual sizes of the DNA products.

To separate the DNA fragments of restriction digestion products, 1% agarose gels were prepared by adding 1% agarose into 1X TAE buffer (Promega), heating gently in a microwave oven until thoroughly mixed, cooling down slowly until 50-60ºC, and adding, and mixing gently, with ethidium bromide (EB) (Promega) for DNA visualization. The mixture was then poured into a gel casting tray and left in room temperature until solid. A comb was also placed in the gel casting tray to generate

spaces for loading DNA samples. DNA samples were prepared by mixing with 5X loading buffers (Bioline) in a ratio of 4:1 (e.g. 8µl DNA sample and 2µl 5X loading buffer) and loaded into agarose gel. In addition, one or two extra lanes were used to load the DNA markers (Hyperladder I, Bioline) in parallel with the DNA samples. The agarose gel electrophoresis was carried out at <5 volts per cm gel until the dye front reached the bottom of the gel. Bands of DNA molecules were visualized on agarose gel after exposure under an UV light and the sizes of DNA molecules were estimated according to the lengths of Hyperladder I DNA markers. Examples of 1% agarose gel electrophoresis are shown in Figure 12 and 13.

To separate PCR products, 2% agarose gels were prepared following the same protocol as described above. DNA samples were prepared and co-electrophoresized with alternative DNA markers (Hyperladder IV or Hyperladder V, Bioline). Examples of 2% agarose gel electrophoresis are shown in Figures 18 and 19.

2.1.3 Extraction of DNA fragments from agarose gel

Following agarose gel electrophoresis, DNA fragments were extracted from the gel using the QIAquick Gel Extraction Kit™ (Qiagen) according to the protocol provided by the manufacturer. This was to harvest the DNA products from previous experiments (restriction digest and agarose gel electrophoresis) and the DNA fragments were subsequently purified to be used in further applications such as DNA ligation reactions.

Under an UV light, DNA fragments were visualized as bright bands on the agarose gel. The DNA fragments of correct estimated molecule sizes were excised from the agarose gel using a clean scalpel. Each sample was weighted and removed into a sterile microcentrifuge tube. Three volumes of Buffer QG, the gel solubilization and DNA-binding buffer (with pH indicator) (provided with kit), were added to one volume of excised gel slice (e.g. 300µl of Buffer QG and 100mg of gel). Buffer QG and gel were incubated at 50ºC for approximately 10 minutes until the gel slice was completely dissolved, at which point the mixture was transparent and a yellow colour (PH appropriate for the absorption of DNA molecules to the QIAquick spin column). Then the mixture was added to one volume of isopropanol (e.g. 100µl of isopropanol and 100mg of gel) and mixed thoroughly by vortexing. Each sample (mixture of dissolved gel slice, Buffer QG and isopropanol) was transferred into a QIAquick spin column and centrifuged at 13,000rpm for 1 minute. Any DNA molecules were absorbed on the column membrane and the flow-through was discarded. To remove the remaining trace agarose gel, 500µl Buffer QG was added to the spin column and centrifuged at 13,000rpm for 1 minute and the flow-through was discarded. To remove any remaining salt, 750µl Buffer PE was then added to each spin column, left at room temperature for 3 minutes and the column centrifuged at 13,000rpm for 1 minute, and the flow-through was discarded. To remove the remaining Buffer PE, each spin column was further centrifuged at 13,000rpm for 1 minute. Thereafter, each QIAquick spin column was placed into a sterile 1.5ml microcentrifuge tube and 50µl DEPC-treated water was applied gently to the centre of column membrane on which

the DNA molecules were absorbed. The spin column was centrifuged at 13,000rpm for 1 minute and the DNA sample, dissolved in approximately 50µl water, was collected in the microcentrifuge tube.

2.1.4 Spectrophotometric quantification of nucleic acids

The spectrophotometric quantification of nucleic acids (DNA and RNA) provides information of the concentration and purity (OD 260nm/280nm) of DNA/RNA solutions. The 260nm wavelength is the peak absorption wavelength of both DNA and RNA and a 260nm OD value of '1' equals to a concentration of 50µg/ml for DNA or 33µg/ml for RNA. Therefore, the concentrations of DNA/RNA samples can be derived from the measured 260nm OD values. Frequently when the DNA/RNA samples were highly concentrated (ranging from hundreds µg/ml to several thousand µg/ml), a dilution of 1/100, 1/70 or 1/50 with double distilled water (ddH_2O) was used.

The parameter of 260nm/280nm OD ratio is an indicator for the purity of DNA/RNA samples. For DNA samples a ratio of 1.6~1.8 or for RNA samples a ratio of 1.8~2.0 indicates that the sample is of good purity and can be used reliably in the further experiments such as PCR, ligation and reverse transcription (RT).

2.1.5 DNA ligation

Ligation of two DNA molecule ends takes advantage of DNA ligase which links the ends of two DNA molecules and generates the phosphate backbone at the ligation site. Commonly the two ligation ends are complementary with each other and each end comprises of one overhanging strand, which are called “sticky ends”. Sometimes the two ligation ends do not contain any overhanging strands, which are called “blunt ends”. Ligation of two DNA molecules either containing paired sticky ends or blunt ends can be achieved using DNA ligase. An example of ligation of two DNA molecules containing sticky ends resulting from *Hind* III restriction digestion is given below:

5'-A + A G C T T-3' 5'-A A G C T T-3'

3'-T T C G A-5’ A-5' 3'-T T C G A A-5'

In the works described in this thesis, DNA ligation was used to ligate the DNA fragments of plasmid vectors and inserts obtained from previous experiments (restriction digestion, agarose gel electrophoresis and gel extraction of DNA fragments) and the ligation products were plasmid constructs to be stably transfected into human colonic epithelial Caco-2 cells. Details of the plasmid vectors and inserts are described in Chapter 3.

DNA ligation was carried out using the T4 DNA ligase kit (Promega). DNA fragments of plasmid insert and vector were added in a molar ratio of 5:1, 3:1, 1:1, 1:3 or 1:5. In each reaction of 10µl total volume, 100ng of vector DNA was used and the amount of insert DNA was calculated according to the formula:

ng of insert = (100ng vector × kb size of insert/ kb size of vector) × molar ratio (of insert/vector)

According to their respective concentrations measured using spectrophotometric quantification, vector DNA and insert DNA were added into a sterile microcentrifuge tube. One microlitre of 10X DNA ligase buffer and 1µl of T4 DNA ligase were also added and nuclease free water (provided with the kit) was added to fill the 10µl total volume. The mixture (vector DNA, insert DNA, buffer, T4 DNA ligase and water) was mixed gently and ligation of insert and vector DNA molecules was achieved by incubating the mixture at room temperature for 3 hours, or alternatively at 4ºC overnight. After incubation was complete, the ligation product was transformed into chemically competent bacterial cells for amplification in further experiments.

2.1.6 Transformation of chemically competent bacterial cells

Transformation of chemically competent bacterial cells takes advantage of competent bacteria, which are capable of taking up and expressing (known as 'transform with') genetic material such as plasmid constructs. Selective growth of these transformed bacteria allows amplification of the plasmid constructs together with bacterial growth cycles. In the molecular cloning work described in this thesis, commercial competent bacteria, One Shot® TOP10 Chemically Competent E. Coli cells (Invitrogen), were used and the protocol followed the instructions provided by the manufacturer.

In each transformation, ~100ng of plasmid or 10µl of ligation product (containing putative plasmid construct produced from 100ng of vector DNA and various ng of insert DNA, see above) was mixed gently with one vial (50µl) TOP10 bacterial cells by flicking the bottom of the microcentrifuge tube. The mixture was incubated on ice for 1-2h, then heat-shocked at 42ºC for 30 seconds and then placed back on ice for 2 minutes. These steps enabled the uptake of DNA into TOP10 cells. Afterwards 250µl of pre-warmed (37ºC) S.O.C medium (Super Optimal broth with Catabolite repression medium, provided with the TOP10 kit) was added and incubated at 37°C and shaken at 225 rpm for 1 hour in a shaking incubator. Under these conditions, the TOP10 bacteria (containing the transformed bacteria) started to grow and after incubation, 10 to 100µl of transformation mix were spread on LB agar plates.

LB agar plates were prepared as follows. A dissolved agar gel solution containing 500ml water, 5g (1%) Tryptone (Sigma), 5g (1%) Sodium chloride (Sigma), 2.5g (0.5%) Yeast extract (Sigma) and 4g (0.8%) Agar (Sigma), was heated in a microwave oven until complete melting was achieved and then autoclaved at 121ºC for 20 minutes, cooled down until 50ºC and Ampicillin (100ug/ml) added. 25ml of agar gel solution was poured into a 100mm φ Petri-dish near the flame of a Bunsen burner, left at room temperature until the gel was solid, stored at 4ºC and pre-warmed at 37ºC before use. After being spread with the transformation mix, the LB agar plates were incubated at 37ºC overnight, which allowed the bacteria to grow under the selection of the antibiotic ampicillin. Any transformed bacteria that had acquired the plasmid that contains the ampicillin resistance gene are insensitive to ampicillin, whereas the non-transformed bacteria do not have the ampicillin resistance gene and are sensitive. As a result, those strains expressing the plasmid were selected to grow and after 16 hours, bacterial clones derived from each single transformed bacterium appeared on the surface of LB agar.

Single colonies were picked and incubated in 5ml LB medium at 37ºC overnight. The LB medium is a solution following the same recipe of LB agar (1% Tryptone, 1% sodium chloride and 0.5% Yeast extract) without agar being present. The LB medium was made following the same procedure of LB agar (heating, autoclaving and cooling) and contained 100ug/ml Ampicillin. When the incubation was finished, bacterial

suspension of each tube containing large number of cells split from the same transformed bacterial strain was used to harvest the plasmids.

2.1.7 Small scale plasmid preparation

Small scale plasmid preparation can be used to harvest and purify plasmid DNA from small scales (millilitres) of bacterial cultural suspension and yields approximately 10µg plasmid DNA per 1.5ml of bacterial suspension. In this study, the QIAprep® Miniprep kit (Qiagen) was used and the protocol followed the instructions provided by the manufacturer. The harvested plasmid DNA was ready to be used in various applications including PCR, sequencing, restriction digestion and transfection into mammalian cells in culture.

Each microcentrifuge tube containing 1.5ml of LB medium bacterial suspension was centrifuged at 13,000rpm for 3 minutes at room temperature, the supernatant discarded and the pelleted bacterial cells were resuspended in 250µl Buffer P1. The mixture was then transferred into a sterile microcentrifuge tube and 250µl Buffer P2 was added. The tube was gently inverted 4-6 times for thorough mixing, the mixture incubated at room temperature for 5 minutes and 350µl Buffer N3 added. The tube was gently inverted 4-6 times again, incubated at room temperature for 5 minutes and centrifuged at 13,000rpm for 10 minutes at room temperature. After centrifugation, the plasmid DNA was retained in the supernatant fluid whereas the waste was pelleted and discarded.

The supernatant fluid was removed to a QIAprep spin column and the column was centrifuged at 13,000rpm for 1 minute. The plasmid DNA was absorbed on the column membrane and flow-through was discarded. 500µl of Buffer PB was then added to the column and centrifuged at 13,000rpm for 1 minute. This step is to wash off the trace residual nuclease on the membrane. 750µl of Buffer PE was then added to the column and centrifuged at 13,000rpm for 1 minute. This step is to wash off the residual salts combining with the plasmid DNA. Additional centrifugation at 13,000rpm for 1 minute was then performed to remove the residual Buffer PE, which contains ethanol that might inhibit enzymatic activity in some experiments, such as PCR or restriction digestion. Finally, the column was moved to a new microcentrifuge tube and 50µl DEPC-treated water was gently added to the center of column membrane. The column was left for 1 minute and centrifuged at 13,000rpm for 1 minute, and the plasmid DNA, dissolved in approximately 50µl water, was collected in the tube.

2.1.8 DNA sequencing

The sequences of the NFκB-luciferase and TATA-luciferase reporter constructs (details in Chapter 3) were determined by DNA sequencing. Briefly, for each sample, >1µg of purified plasmid DNA was dried using a vacuum pump and then send for commercial sequencing (Eurofins). The primers used in sequencing were prepared in a 20µl solution at a concentration of 2pmol/µl. These primers were T7 primer (provided by Eurofins) for forward sequencing, short-reverse primer (binding to

luciferase coding sequence proximal to the NFκB sites) and long-reverse primer (binding to luciferase coding sequence distal to the NFκB sites) (for details, see Chapter 3, primer sequences in Table 3) for reverse sequencing.

2.1.9 Mammalian cell culture

The work described in this thesis used human colon adenocarcinoma Caco-2 cell line which is a model of differentiating colonic epithelial cells. Stocks of Caco-2 cells were routinely grown in DMEM + GlutaMAX-1 medium (4.5g/L D-Glucose and pyruvate, Gibco) supplemented with 10% (v/v) foetal calf serum (FCS) (Sigma) and 1% (v/v) penicillin-streptomycin (P/S)) and at 37°C in a 5% CO•• atmosphere. Cells were passaged when being 100% confluent. Cells were gently washed 2-3 times with 1X PBS, trypsinized at 37ºC for 10 minutes until being detached, resuspended in growth medium, pelleted by centrifugation at 1,500rpm for 5 minutes, resuspended in growth medium and sub-cultured at a concentration of 10-30% in a new flask. Alternative selections of cell growth medium were used in the experiments of stable transfection, siRNA transfection and Se depletion and supplementation, which are described in the following sections.

2.1.10 Stable transfection of human colonic epithelial Caco-2 cells with plasmid DNA

Transfection refers to selective delivery of genetic material such as plasmid DNA into eukaryotic cells and stable transfection, as opposed to transient transfection (such as

siRNA transfection, see Section 2.1.11), results in persistent expression of the target gene in the plasmid DNA. The uptake of the plasmid DNA into mammalian cells frequently takes advantage of an artificial cationic lipid agent which forms liposomes coating the plasmid, fuses with cell membrane so as to deliver the DNA into cells. In the work described in this study, the stable transfection experiments were carried out using Lipofectamine 2000™ (Invitrogen) following the procedure recommended by the manufacturer. The plasmids used were NFκB-luciferase and TATA-luciferase reporter constructs contained in PBLUE-TOPO (details in Chapter 3) and these two plasmids contain the Neomycin resistant gene. Therefore, persistent selection of successfully transfected cells was carried out using Neomycin (G418) (Invitrogen), and any untransfected cells were killed and screened out. This selection step generally takes several weeks. Four to six weeks were needed in this study.

To stably transfect the human colonic epithelial Caco-2 cells with the plasmid DNA, cells were seeded in a 6-well plate 24 hours before transfection, each well containing 2ml normal cell growth medium (DMEM + GlutaMAX-1 (4.5g/L D-Glucose and pyruvate, Gibco), supplemented with 10% (v/v) feotal calf serum and 1% (v/v) penicillin-streptomycin); cells were ~95% confluent. In each well, cell growth medium was changed to 2ml Optimem (Gibco). Five microlitres Lipofectamine 2000™ was mixed gently with 250µl Optimem in a universal tube by gently shaking and the mixture was incubated at room temperature for 5 minutes. At the same time, 2.0, 4.0 or 6.0µg DNA of each plasmid (the two plasmid constructs described above)

was mixed gently with 250µl Optimem in a second universal tube by gently shaking and the mixture was also incubated at room temperature for 5 minutes. Then the Lipofectamine mix and the DNA mix were added together, mixed gently and incubated at room temperature for 20 minutes. These steps allowed the coating of plasmid DNA with Lipofectamine. The 500µl transfection mix was dripped gently to wells each containing 2ml Optimem. The treated cells were grown in an ordinary cell culture environment at 37ºC with 5% CO•• for 24 hours in an incubator.

Twenty-four hours later, the uptake of plasmid DNA was complete (according to manufacturer's protocol) and the medium in each well was then replaced with 2ml normal cell growth medium. Cells were grown for another 24 hours and treated with 0.5ml trypsin to be detached from 6-well plate. Cells from each well were then moved into a 100mm petri-dish and grown in 10ml normal medium supplemented with 750µg/ml G418 to select the transfected cells. The culture medium was changed every 3-4 days. Cells were washed twice with 1X Phosphate buffered saline (PBS) to remove dead cells and fresh medium containing 750µg/ml G418 added. Cells were continuously cultured in such condition for 4-6 weeks until all the untransfected cells had been killed. The remaining cells transfected with each type of plasmid DNA were harvested in a mixed population.

2.1.11 Transient transfection of human colonic epithelial Caco-2 cells with small interfering RNA (siRNA)

Transient transfection delivers genetic material (such as plasmid DNA and siRNA) into eukaryotic cells so that the genetic material is expressed transiently in the cells for a few days. Selection using an antibiotic marker is not required. Transient transfection also uses cationic lipid transfection agent and the experiments described in this study used Lipofectamine 2000™ (Invitrogen).

Small interfering RNA (siRNA) is a small dimeric double-stranded RNA. Generally each strand contains 21nt, comprising 19nt complementary sequence together with 2nt AA overhang. siRNA are experimentally designed to be homologous with a 21nt sequence of a target mammalian transcript (mRNA target). After being delivered into cells, the siRNA double-strandeds dissociate from each other and recognize the mRNA target. The binding formation between an mRNA sequence and a siRNA strand results in the recruitment of an enzymatic complex, RNA-induced silencing complex (RISC), and degradation of mRNA by RISC (the process known as RNA interference). Therefore, transient transfection of mammalian cells with siRNA selectively degrades the target transcripts in the cells and is used to knockdown gene expression for a short period of approximately 2 days. siRNA has been suggested to decrease gene expression most efficiently on mRNA level 2 days after delivery and on protein level 3 days after delivery. In the present experiments, siRNAs were designed to knockdown the expressions of human *GPX1, SELW, SELH* and *GPX4*

genes, and commercially synthesized (20nmol siRNA annealed and with standard purity, AM16104, Ambion). In addition, a scrambledd control siRNA that is not homologous with any human mRNA transcripts was also designed and synthesized. Details of the siRNA and mRNA target sequences are given in Chapter 5 Section 5.2.1 and Chapter 6 Section 6.2.1.

To transiently transfect the human colonic epithelial Caco-2 cells with siRNA, $5X10^5$ cells were seeded in a 6-well plate and grown for 24 hours before transfection. Each well contained 2ml normal cell growth medium (DMEM + GlutaMAX-1 (4.5g/L D-Glucose and pyruvate, Gibco), supplemented with 10% (v/v) foetal calf serum (FCS) and 1% (v/v) penicillin-streptomycin (P/S)) and cells were 40-50% confluent. For transfection, each well was changed with 2ml of modified growth medium containing DMEM + GlutaMAX-1 (Gibco) supplemented with 5% (v/v) FCS and no P/S, as recommended in the manuals provided by the manufacturer (Ambion). Five microlitres Lipofectamine 2000™ was mixed gently with 250µl Optimem in a universal tube by gently shaking and the mixture was incubated at room temperature for 5 minutes. At the same time, 40, 80, or 120pmol siRNA or scrambledd control siRNA was mixed gently with 250µl Optimem in a second universal tube by gently shaking and the mixture was also incubated at room temperature for 5 minutes. Then the Lipofectamine mix and the siRNA mix were added together, mixed gently by gently shaking and incubated at room temperature for 20 minutes. The 500µl transfection mix was then dripped gently into one well containing 2ml reduced-serum

medium. After being added into the well and diluted in the total 2.5ml medium, the 40, 80 and 120pmol siRNA resulted in working concentrations of approximately 15, 30 and 45nM, respectively; the range of working concentration recommended by Ambion is 10-100nM.

Cells treated with the transfection mix were grown for 24 hours and then the medium was replaced with 2ml reduced-serum medium for a further 1-2 days until harvest. In general, to assess the effect of siRNA transfection on mRNA expression, cells were further grown for 24 hours and total RNA was harvested 2 days after transfection, whereas to assess the effect of siRNA transfection on protein expression, cells were further grown for 48 hours and total protein lysis was harvested 3 days after transfection.

2.1.12 Mammalian cell culture in Se-depleted and Se-supplemented medium

To assess the effect of Se depletion on selenoprotein expression and inflammatory response, a previously established protocol of mammalian cell culture in Se-depleted and Se-supplemented growth medium (Pagmantidis et al., 2005) was used. Briefly, 10^6 Caco-2 cells were seeded in each well of a 6-well plate and grown for 24 hours in normal cell growth medium (as described in Section 2.1.9) at 37°C in a 5% CO•• atmosphere. Cells were then grown in either Se-depleted or Se-supplemented culture medium for 3 days. Se-depleted medium was prepared from serum-free DMEM +

GlutaMAX-1 medium (4.5g/L D-Glucose and pyruvate, Gibco) supplemented with 0.1% (v/v) penicillin-streptomycin (P/S), 1% (v/v) non-essential amino acids (NEAA, Gibco), insulin (5μg/ml) and transferrin (5μg/ml). Se-supplemented medium was prepared from serum-free DMEM + GlutaMAX-1 medium (4.5g/L D-Glucose and pyruvate, Gibco) supplemented with 0.1% (v/v) penicillin-streptomycin (P/S), 1% (v/v) non-essential amino acids (NEAA, Gibco), insulin (5μg/ml), transferrin (5μg/ml) and selenium in the form of sodium selenite (7ng/ml).

Usually, Caco-2 cells seeded at 10^6 cells/well were 80~90% confluent after growing for 3 days in Se-depleted or Se-supplemented medium. Similarly, following siRNA transfection, Caco-2 cells seeded at $5X10^5$ cells/well were also 80~90% confluent after growing for 3 days in reduced-serum (5% (v/v) FCS) medium. Se depletion has been found (Pagmantidis et al., 2005) to lower the expressions of selenoproteins most efficiently at day 3 after changing into low Se medium (Chapter 4) and siRNA decreased the protein expression of a target gene (Chapter 6) at day 3 after transfection. Therefore, the comparable cell confluencies between the Se depletion and siRNA transfection experiments at day 3 were important for the comparison of their biological effects between experiments.

2.1.13 Extraction of total RNA from mammalian cells

Total RNA extraction from Caco-2 cells was carried out based on the method of (Chomczynski and Sacchi, 1987). For each sample, cells were washed twice with 1X PBS and then incubated with 0.5ml (in each well of a 6-well plate) or 1ml (in a 75mm flask) of TRIzol® (Invitrogen) at room temperature for 5 minutes. Cells were detached from 6-well plate or flask using a cell scraper. Each sample of cell suspension in TRIzol was transferred into a sterile 1.5ml microcentrifuge tube and then 200µl of chloroform (Sigma) added. The mixture was vertexed vigorously for 15 seconds and incubated at room temperature for 3 minutes. TRIzol is a mixture of guanidinium isothiocyanate and phenol. Whereas guanidinium isothiocyanate is used to lyse the cells and disassociate the nucleoprotein complexes, phenol and supplemented chloroform are used to dissolve protein, genomic DNA and RNA and separate these components in different phases after centrifugation. The sample was centrifuged at 12,000g for 15 minutes at 4ºC and total RNA was retained in the upper clear aqueous phase. The white-colour intermediate phase contained a mixture of cell debris and undissolved DNA and protein, and the pink lower organic phase contained the majority of DNA and protein. The upper aqueous phase was carefully transferred into another sterile 1.5ml microcentrifuge tube.

To participate the RNA, 500µl isopropanol (Sigma) was added into the upper aqueous phase solution (approximately 200-400µl), and the mixture was mixed by inverting the tube for 6-8 times and incubated at room temperature for 10 minutes. The sample

was centrifuged at 12,000g for 15 minutes at 4ºC and total RNA was participated in a pellet at the bottom of the tube. The supernatant was discarded and the RNA pellet was washed once with 1ml 75% ethanol by vortexing the tube for a few seconds. The sample was then centrifuged again at 7500g for 5 minutes at 4ºC, and the pelleted total RNA was briefly air dried and dissolved in 50µl of DEPC-treated water.

2.1.14 Reverse transcription to generate cDNA from RNA template

Reverse transcriptase, also known as RNA-dependent DNA polymerase, reversely transcribes single-stranded RNA into double-stranded DNA (cDNA) which can be used as a template for PCR amplification. Reverse transcription was carried out using Transcriptor Reverse Transcriptase® kit (Roche) following manufacturer's instructions.

Briefly, in each reaction of 20µl total volume, 1µg of total RNA was used as template and mixed with 4µl of 5X Transcription buffer (provided in kit), 2µl of ddNTP mix (Bioline) at a concentration of 10mM, 1µl of Oligo(dt)15 primer (100µM) (Roche), 0.5µl of RNAse inhibitor (40U/µl) (Roche). DEPC-treated water was added to make the total volume to 19.5µl and then 0.5µl of Transcriptor Reverse Transcriptase® (20U/µl) was added and mixed gently by pipetting. A programme for reverse transcription was set up on a PCR machine so as to incubate the sample at 55°C for 30 minutes and then cool down to 4°C. The cDNA produced was stored at -20°C before use.

2.1.15 Polymerase chain reaction (PCR) and semi-quantitative RT-PCR

Polymerase chain reaction takes advantage of the ability of a DNA polymerase, generally the thermostable Taq polymerase, to amplify a section of DNA sequence from very small number of copies to up to millions of copies. Combined with reverse transcription (RT-PCR), it is frequently used to detect gene expression. RT-PCR uses PCR amplification with the cDNA product from reverse transcription (Section 2.1.14). To disassociate the double-stranded DNA into single-stranded DNA, the initial step of PCR (Step 1: initial denaturation) is to denature DNA by heating at 94ºC for 5 minutes.

PCR amplification uses a pair of short (generally 20-30nt) single-stranded DNA oligonucleotides (known as the PCR primers, comprising a forward primer and a reverse primer), which are designed to be complementary to the template DNA, as initiation substrates to replicate the novel DNA strands from the template DNA. Following the initial denaturation, the template DNA and primer DNA are heated briefly at 94ºC for 30 seconds (Step 2a: denaturation) and then temperature lowered to 50-70ºC for 30 seconds. This allows the denatured single-stranded primer DNA to anneal to the template DNA (Step 2b: annealing). The annealing temperature is variable from one primer pair to another and is mainly dependent on the GC content of the primer oligonucleotides. The primer and template DNA are then heated to 72ºC for 1 minute and Taq polymerase synthesizes a novel DNA strand by elongating 3'end of the primer oligonucleotide in the presence of ddNTP mix (ddATP, ddTTP,

ddCTP and ddGTP) (Step 2c. elongation). Together, the three steps occurring in a series (denaturation, annealing and elongation) constitute a single cycle of PCR amplification. Theoretically, each PCR amplification cycle results in double number of copies of the amplified region (between the two primer binding sites) on the template DNA. To continuously increase the copy numbers, one PCR cycle is simply followed by another and generally 20-40 cycles are used in PCR amplification.

When the PCR amplification is finished, the final step is to heat the PCR sample at 72ºC for a few minutes (7 minutes in this study). This is to ensure that all single-stranded DNA finish the elongation (Step 3: final elongation). Together, the programme for PCR amplification is described as following:

Step 1 (initial denaturation):	94ºC	X	5 minutes
Step 2a (denaturation):	94ºC	X	30 seconds
Step 2b (annealing):	50-70ºC	X	30 seconds
Step 2c (elongation):	72ºC	X	1 minute

- Step 2 (PCR amplification) = (Step 2a + Step 2b +Step 2c) X cycle numbers

Step 3 (final elongation):	72ºC	X	7 minutes

PCR amplification in experiments described in this thesis used BIOTAQ polymerase (Bioline) following the protocol provided by manufacturer. In each reaction of 25µl total volume, 0.5µl of cDNA sample (RT product) was used as template DNA and

mixed with 2.5µl of 10X PCR buffer (provided in kit), 2.5µl of ddNTP mix (Bioline) at a concentration of 10mM, 2.5µl of forward primer and 2.5µl of reverse primer (each in solution at a concentration of 20pmol/µl) (custom synthesized, Eurofin) and 1µl of magnesium chloride (50mM). DEPC-treated water was added to make up the total volume to 20µl and then 0.15µl of BIOTAQ (Bioline) (5U/µl) was added to the sample.

The semi-quantitative RT-PCR is a variant technique of ordinary PCR amplification. When RT employs equal amount (1µg) of total RNA and PCR employs equal amount (0.5µl) of RT product for all the samples, the resulting copy numbers of the amplified DNA fragment following RT-PCR rely on the abundance of the template transcripts existing in the total RNA in different samples. Although a copy number cannot be quantified, the comparison of the intensities of PCR bands from different samples can be quantified and calculated as a percentage expression relative to one chosen as control (standardized as '1'). As a result, the abundance of template transcripts can be compared between one and another sample using a semi-quantitative method to calculate the relative percentages of the PCR band intensities. The method was adapted in this study to calculate the mRNA expression levels of *GPX1, SELW, SELH, GPX4, GPX2* and *IL8* genes (described in Chapter 4-6).

The semi-quantitative RT-PCR requires the PCR amplification to be at the linear stage before saturation. This is to ensure that the PCR amplification for all the

samples is effective for the reliability of the semi-quantification. For example, in the semi-quantitative RT-PCR experiments comparing GPx4 expression in normal Caco-2 cells and in cells treated with GPx4 siRNA, PCR amplification of GPx4 was performed at 25, 27, 29 and 31 cycles and results suggested that the 29 cycle PCR amplification for both samples was at the linear stage. Therefore, comparison of GPx4 expression between the normal and siRNA-treated samples was performed using 29-cycle PCR amplification and the GPx4 expression in the siRNA-treated cells was expressed in a percentage relative to the GPx4 level in the normal cells.

A list of PCR primers used in work described in this thesis is given in Table 3.

Primers	Sequences	Tm
***GPX4* for**	5'-CGA TAC GCT GAG TGT GGT TTG C-3'	66ºC
***GPX4* rev**	5'-CAT TTC CCA GGA TGC CCT TG-3'	
***GPX4* m-for**	5'-CAT TGG TCG GCT GGA CGA G-3'	65 ºC
***GAPDH* for**	5'-TGA AGG TCG GAG TCA ACG GAT TTG-3'	55 ºC
***GAPDH* rev**	5'-CAT GTA AAC CAT GTA GTT GAG GTC-3'	
***GPX1* for**	5'-CAG TCG GTG TAT GCC TTC TCG-3'	56 ºC
***GPX1* rev**	5'-TGT CAG GCT CGA TGT CAA TG-3'	
***GPX2* for**	5'-GGC TTT CAT TGC CAA GTC CTT C-3'	60ºC
***GPX2* rev**	5'-CTA TAT GGC AAC TTT AAG GAG GCG C-3'	
***SELW* for**	5'-GTT TAT TGT GGC GCT TGA GGC-3'	60 ºC
***SELW* rev**	5'-GAA CAT CAG GGA AAG ACC ACC-3'	
***SELH* for**	5'-GCT TCC AGT AAA GGT GAA CCC G-3'	62 ºC
***SELH* rev**	5'-ACC CAA ATC TCC CTA CGA CAG G-3'	
***IL8* for**	5'-ATG ACT TCC AAG CTG GCC GTG GCT-3'	60 ºC
***IL8* rev**	5'-TCT CAG CCC TCT TCA AAA ACT TCT C-3'	
NFκB for	5'-CAG GGG ACT TTC CGA AGG CTC-3'	60 ºC
TATA for	5'-CCG ATC TGG GGC AGA GCA TAT AAG-3'	60 ºC
Short rev	5'-CGT ACG TGA TGT TCA CCT CGA TAT GTG-3'	61 ºC
Long rev	5'-CGA CTT CTT TCG AAA GAG GTG CG-3'	60 ºC

Table 3: Primers for generating products from mRNA transcripts by PCR amplification and semi-quantitative RT-PCR

2.1.16 Preparation of cell lysate from mammalian cells using a sonication method

Cell lysates were prepared from Caco-2 cells by disruption using sonication and GPx4 protein levels then measured by Western blot. Briefly, cultured Caco-2 cells in a 6-well plate were washed twice with 1X PBS, 0.5-1ml ice-cold 1X PBS added per well and incubated on ice for 10 minutes. This resulted in detachment of cells from the surface of 6-well plate without affecting cell integrity. The cell suspension was then transferred into a sterile 1.5ml microcentrifuge tube, centrifuged at 1,500rpm for 5 minutes at room temperature and the pelleted cells were re-suspended in 200µl 1X PBS containing 0.1% (v/v) Triton. The cell suspension was sonicated twice for 10 seconds with a 30-50% pulse using a LAB SONIC U sonicator. This caused cell disruption. The cell debris was pelleted by centrifugation at 3,500rpm for 10 minutes at 4ºC. The supernatant fluid (cell lysate) was aliquoted into 30µl quantities, snap-frozen in liquid nitrogen and stored at -80ºC before use.

2.1.17 Separation of protein molecules by SDS-PAGE

Sodium dodecyl sulphate-polyacrylamide gel electrophoresis (SDS-PAGE) is an electrophoretic technique used to separate protein molecules on the basis of molecular weight. SDS binds to the polypeptide sequences, disrupts the non-covalent bonds to open their folding conformation and results in evenly distributed negative charges on the SDS-polypeptide, the amount of which are proportional to the polypeptide length. Polyacrylamide gels provide the matrix on which protein molecules migrate with

different electrophoretic mobility. Low concentration gels (e.g. 8%) can be used to separate large protein molecules whereas high concentration gels (e.g. 12.5%) are used to separate smaller protein molecules. In addition, a mix of protein molecules of known size (protein marker) is generally co-electrophoresized and used to estimate protein molecular weight.

Work described in this thesis used 12.5% SDS-polyacrylamide gels to separate protein molecules including the 19kDa GPx4 protein prior to western blot. The 12.5% SDS-polyacrylamide gel (resolving gel) solution was prepared with 3.125ml of 30% Acrylamide/Bis-acrylamide solution (ratio 29:1) (Sigma), 3.75ml of 1M Tris-Cl solution (pH=8.8) (Promega), 2.925ml of ddH_2O, 100µl of 10% SDS solution (obtained from 20% SDS stock solution, Sigma), 100µl of 10% Ammonium persulphate (APS) solution (Sigma, solution stored at -20ºC before use) and 10µl of N, N, N', N'-tetramethylethylenediamine (Sigma) in 10ml total volume. The stacking gel was prepared with 3.75ml of 1M Tris-Cl solution (pH=6.8) and Acrylamide/Bis-acrylamide solution, ddH_2O, 10% SDS solution and 10% APS solution in equal amounts as the resolving gel.

The SDS-PAGE running buffer (1X) was diluted from a 5X stock, which was prepared by dissolving 60.6g Tris-Cl, 144.1g Glycine and 5g SDS (all chemicals from Promega) in 800ml of water, adjusting pH to 8.8 and adding water to a 1000ml total volume. The 5X sample loading buffer was prepared by mixing and dissolving 2.25ml

of 1M Tris-Cl solution (pH=6.8), 5ml of Glycerol (Sigma), 0.5g SDS (Promega), 5mg Bromophenol Blue (Sigma) and 2.5ml of 1M DTT solution for each 10ml stock, aliquoted and stored at -20ºC before use.

For each sample, 20µg cell lysate protein was mixed gently with 5X sample loading buffer in a ratio of 1:4 (v/v) and incubated at 90ºC for 3-4 minutes to disrupt the non-covalent bonds of polypeptide (protein denaturation). The samples were loaded to the stacking gel and electrophoresis was carried out at 90-100 volts until the dye front reached the bottom of the gel.

2.1.18 Analysis of GPx4 protein expression by western blot

After separation by SDS-PAGE, the protein molecules on the gel were transferred onto a membrane and then probed using a specific antibody to quantitatively detect GPx4 protein. Transfer of protein molecules to a polyvinylidene difluoride (PVDF) membrane (Whatman) was carried out using semi-dry blotting in a transfer electroblotting machine. The polyacrylamide gel (approximately 7cm X 9cm) was placed upon a PVDF® membrane (7cm X 9cm) (Whatman) and two sets of three pieces of filter papers (Whatman) were placed on top of the gel and at bottom of the PVDF membrane. The entire stack was placed in the transfer machine and lightly wetted using a transfer buffer. The transfer buffer was prepared by mixing 1X SDS-PAGE running buffer and methanol (Fisher Scientific) in a ratio of 4:1 (v/v). A roller was used to roll over the stack gently to squeeze out any air bubbles between

the gel and the PVDF membrane. A small volume of transfer buffer was dripped on top of the stack to prevent the membrane becoming over-dry. Transfer was performed at 10 volts (constant voltage) for one hour.

After transfer of the proteins, the PVDF membrane was placed into 10ml of 5% (w/v) non-fat milk powder solution in TPBS and incubated at 4ºC overnight or at room temperature for 1 hour. TPBS was prepared by adding 0.05% (v/v) Tween-20 (Sigma) into 1X PBS and mixing thoroughly. Incubation in milk powder solution blocks (saturates) the protein-absorbing ability of PVDF and therefore prevents any non-specific binding of the antibodies to the membrane.

The PVDF membrane was then incubated for 1 hour with 10ml of rabbit polyclonal anti-GPx4 antibody (1^{st} antibody) (LF-PA0055, Ab Frontier, Korea) diluted 1/1000 (v/v) in 3% (w/v) milk-TPBS. The membrane was washed 3 times with 10ml of TPBS, each time for 10 minutes. The PVDF membrane was then incubated for 30 minutes with 10ml of horseradish peroxidase (HRP)-labeled anti-rabbit serum (2^{nd} antibody) diluted 1/3000 (v/v) in 3% (w/v) milk-TPBS. The membrane was washed 3 times with 10ml of TPBS, each time for 10 minutes and washed once with 10ml of 1XPBS for 10 minutes.

Detection of western blot was carried out using the Amersham Hyperfilm ECL™ reagent (GE Healthcare). For each membrane, 2ml of ECL solution mix was prepared

by adding Solution A and Solution B in a ratio of 40:1 (v/v) and mixed gently. The 2ml ECL mix was added to the PVDF membrane, sealed with 2 pieces of plastic film and incubated in darkness for 5 minutes. ECL emits fluorescence after being catalyzed by HRP and the fluorescent signal was captured on film.

2.1.19 Preparation of cell lysate using reporter lysis buffer (RLB) for luciferase assays

Caco-2 cells stably transfected with NFκB- or TATA-luciferase reporter constructs were tested for their ability to express luciferase at baseline and in response to known NFκB inducers. The samples of cell lysate from these cells were prepared using the reporter lysis buffer (RLB) and the luciferase assay reagent (LAR) used to measure luciferase activity (described in Section 2.1.21) following the protocols provided by the manufacturer (Promega).

Cells were washed 2-3 times using 1X PBS and 200µl of 1X RLB (provided as 5X RLB, diluted with water) added per well of a 6-well plate. Cells were lysed by freeze-thawing and vortexing. Cells were frozen in a -20ºC freezer for 15 minutes and then warmed at room temperature for 15 minutes. Cells were scraped off using a cell scraper and the cell suspension in 1X RLB was transferred into a sterile 1.5ml microcentrifuge tube. The cell suspension was then vortexed vigorously for 15 seconds and the cell debris was pelleted by centrifugation at 12,000 for 2 minutes at

4ºC. The supernatant fluid (cell lysate) was carefully collected in 2 aliquots (~70µl of each) and stored at -80ºC before use.

2.1.20 Quantification of protein concentration using bicinchoninic acid (BCA) protein assay

The BCA protein assay is a colorimetric assay that determines protein concentration based on the formation of Cu^{2+}-protein complex. Certain amino acids present in the proteins, such as cysteine and tyrosine, are able to convert Cu^{2+} to Cu^{1+} and therefore change the colour of protein solutions from blue to purple. As a result, the protein concentration, determining the efficiency of Cu^{2+} to Cu^{1+} conversion, can be measured at absorbance wavelength of 562 nm. The BCA protein assay is acceptable with the PBS-Triton buffer (see Section 2.1.16) and the reporter lysis buffer (see Section 2.1.19) and therefore was used to determine protein concentration for GPx4 western blot and for luciferase assay, respectively.

The BCA assay reagent (Sigma) was prepared by mixing the bicinchoninic acid solution and the 4% (w/v) $CuSO_4 \bullet 5H_2O$ solution (both provided in the kit) in a ratio of 50:1 (v/v). To build up the standard curve, standard solutions of bovine serum albumin (BSA) (provided in kit) were prepared at concentrations of 0, 0.2, 0.4, 0.6, 0.8 and 1µg/µl. The samples harvested from 6-well plate were estimated to be at concentrations of 1-3µg/µl and therefore were diluted in ratios of 1/4, 1/5, and 1/10 with water. The BSA dilutions and sample dilutions were loaded in a clear,

flat-bottomed 96-well plate. For each well, 25µl of protein dilution was mixed with 200µl of BCA assay reagent and incubated at 37ºC for 30 minutes. The 96-well plate was then read on a Multiskan Ascent plate reader at wavelength of 562 nm and the protein concentrations were evaluated on the reference of the standard curve.

2.1.21 Quantification of luciferase activities in NFκB- and TATA-luciferase transfected Caco-2 cells using a luminometer

To measure the luciferase activities in NFκB- and TATA-luciferase reporter transfected Caco-2 cells, assays used luciferase assay reagent (LAR, Promega) for sample preparation. Quantification was performed using a Truner TD-20e luminometer. LAR were prepared by dissolving 1 vial of luciferase assay substrate (lyophilized, provided with kit) with 105ml of luciferase assay buffer (provided with kit) and stored in darkness at -80ºC before use. The luciferase assay substrate is Beetle Luciferin, which can be oxidized by firefly luciferase in a few seconds releasing fluorescence as described below (instructions provided by the manufacturer):

$$\text{Luciferin} + \text{ATP} + O_2 \xrightarrow{\text{Firefly luciferase}} \text{Oxyluciferin} + \text{AMP} + \text{PPi} + CO_2 + \text{Light}$$

For each sample, 20µl of cell lysate and 100µl of LAR (stored at -80ºC, thawed in room temperature before use) were added to a luminometer tube and mixed thoroughly by repeatedly flicking the bottom of tube. A Truner TD-20e luminometer was set up with a 2-second measurement delay and a 10-second measurement read. Blank reading was repeated 3 times under the conditions of no luminometer tube being placed in the machine, or only LAR being present. Then the tube containing the sample mix was placed into the luminometer and reading of luciferase activity was performed with three repeats per sample. The average of the three reading numbers was taken and the luciferase activity was calculated per mg total cell lysate (luc/mg).

2.1.22 Semi-quantitative analysis of ROS levels in Caco-2 cells grown in Se-depleted medium and in cells treated with GPx1 siRNA using carboxy-H2DCFDA

5-(and-6)-carboxy-2´,7´-dichlorodihydrofluorescein diacetate (carboxy-H2DCFDA) is a cell membrane-permeable fluorescent dye for detection of reactive oxygen species (ROS). After being cleaved by ROS, the product emits a fluorescence signal that can be captured by a fluorescence microscope or read by a luminometer. A semi-quantitative analysis can be performed by comparing ROS levels in one group of cells (test) against another group of cells (control) and expressing data in a percentage relative to the level of control. This analytical method was used to estimate the effects of Se depletion and GPx1 knockdown on ROS levels and the ROS levels were determined by staining cells with Image-iT™ LIVE Green Reactive Oxygen Species

(ROS) Detection Kit (Invitrogen) following the protocol provided by manufacturer and reading carboxy-H2DCFDA fluorescence signal on a BMG LABtech Fluostar Omega luminometer.

Briefly, Caco-2 cells were seeded in a black, flat-bottomed 96-well plate at $6X10^4$ cells/well for Se depletion experiment and at $3X10^4$ cells/well for GPx1 knockdown and grown in 100µl of normal growth medium (Section 2.1.9) for 24 hours. Then cells were either changed with Se-depleted or Se-supplemented medium and grown for 3 days (Section 2.1.12), or treated with GPx1 siRNA or scrambled control siRNA (at a concentration of 30nM) (Section 2.1.11) and grown for 3 days. After 3 days, cells were washed gently once with 100µl/well of pre-warmed 1XHBSS/Ca/Mg solution (without phenol red, H8264, Sigma) and ROS measured.

The Image-iT™ LIVE Green Reactive Oxygen Species (ROS) Detection Kit (Invitrogen) contains Component A (carboxy-H2DCFDA as powder, 275µg/vial), Component B (Hoechst 33342, 400µl of a 1mM solution), Component C (tert-butyl hydroperoxide solution) and Component D (500µl DMSO). Preparation of a 10mM stock solution of carboxy-H2DCFDA was performed by adding 50µl of DMSO into one vial of carboxy-H2DCFDA and mixing until complete dissolving. Preparation of a 25µM working solution was performed by adding 5µl of 10mM stock solution into 2ml of pre-warmed 1XHBSS/Ca/Mg solution and mixing gently. In addition, Hoechst 33342 as a control dye that stains nucleic acid was also added. Each 2ml of 25µM

carboxy-H2DCFDA working solution was mixed with 2µl of 1mM Hoechst 33342 solution (at a final concentration of 1µM Hoechst 33342).

50µl of carboxy-H2DCFDA-Hoechst 33342 mix was added to each well of a 96-well plate and incubated at 37ºC for 30minutes. The 96-well plate was wrapped with foil to prevent disturbance by light. After incubation, cells were washed three times with 100µl/well of pre-warmed 1XHBSS/Ca/Mg solution and then 50µl of 1XHBSS/Ca/Mg solution was added per well. The carboxy-H2DCFDA fluorescent signal was then read at 495/529nm (excitation/emission) wavelength and the Hoechst 33342 fluorescent signal was read at 350/461nm wavelength in a BMG LABtech Fluostar Omega luminometer. For each well, reading was performed with 20 repeats for each signal and the signal value was calculated by taking the average of the 20 readings. To compare the difference in ROS levels between the Se-depletion and Se-supplementation cells, the average carboxy-H2DCFDA signal value of Se depleted cells was expressed in a percentage of the average value of Se-supplemented cells, which was standardized as "1". To compare the difference in ROS levels between the GPx1 siRNA and scrambled control siRNA treated cells, the average carboxy-H2DCFDA signal value of GPx1 siRNA treated cells was expressed in a percentage of the average value of control siRNA treated cells, which was standardized as "1". The Hoechst 33342 data for nucleic acid staining were used as a control of cell number and staining efficiency.

3. Development of NFκB-luciferase reporter model in Caco-2 cells

3.1 Introduction

In order to assess the influence by Se and antioxidant selenoproteins on the NFκB signalling in Caco-2 cells, a reliable and convenient method to monitor the activation status of NFκB transcriptional activity was established. To date, the widely-used methodologies to study NFκB activation include:

1) Western blotting or immunohistochemical methods to indicate the nuclear translocation of NFkB, i.e. increased NFkB subunits in nuclear and decreased NFκB subunits in cytoplasm (Prabhu et al., 2002, Crack et al., 2006, Tallant et al., 2004);

2) Electrophoretic mobility shift assay (EMSA) to show the DNA-binding affinity of NFκB to a target promoter, i.e. the transcriptional activity of NFκB factor (Brigelius-Flohe et al., 1997, Li et al., 2001);

3) Western blotting and/or PCR-based methods to assess the expressional status of one or more target genes under NFκB control (Roebuck, 1999a), including DNA-microarray and PCR-array (Atkinson et al., 2009, Takase et al., 2008);

4) Additional methods, most of which assess changes in activation of intermediate products involved in the activation of the NFκB signalling pathway, e.g. Western blot

to show changes in IκB protein expression (Li and Engelhardt, 2006), or enzymatic assays to assess changes of IκB kinase (IKK) activity (Tallant et al., 2004).

In addition to these methods, luciferase reporter approaches have also been used (Li et al., 2001, Carlsen et al., 2002, Vykhovanets et al., 2008). These take advantage of a luciferase gene driven by a promoter responsive to NFκB transcription activity. As a result, the luciferase activity, which can be easily measured and quantified, reflects the status of NFκB activation. One such reporter system has been constructed comprising of a firefly luciferase coding sequence fused to a promoter containing three NFκB binding sites (3X κB) (Maier et al., 2003, Kirillov et al., 1996) and applied to a number of *in vivo* studies assessing the NFκB response in different mouse tissues (Carlsen et al., 2002, Vykhovanets et al., 2008). For example, in transgenic mice carrying this reporter, activation of NFκB signalling has been monitored using *in vivo* imaging of various tissues following vein injection of NFκB inducers such as TNFα and LPS (Carlsen et al., 2002). In addition, in mouse prostate tissues increased NFκB activation was detected following the administration of IL1β and this method was suggested to be useful in drug screening of positive and negative NFκB regulators (Vykhovanets et al., 2008).

To investigate NFκB signalling in response to Se status in Caco-2 cells, the 3X κB luciferase reporter system was used by this study. This reporter system is detailed in Figure 9 and is based on a providing promoter that contains three binding sites responsive to various types of NFκB hetero- and homo- dimers, including two binding sites with affinity for the Class I NFκB (NFκB1 and NFκB2) motif: 5'-GGGRNNYYCC-3' and one κB-like site motif: 5'-HGGARNYYCC-3'. As a result, NFκB activation in response to various inducers can be detected through measuring luciferase activity. Also within the promoter and downstream of the 3X κB sites, is a TATA box which is used to maintain the baseline expression of luciferase in the unstimulated state.

A construct containing the 3XκB-luciferase sequence was obtained from Prof. Rune Blomhoff, University of Oslo (Carlsen et al., 2002). Before its use in this study, the construct required modifications which allowed it to be applied to *in vitro* experiments. These modifications included:

i. Firstly, a control construct was required that comprised only a TATA box and luciferase coding sequence (CDS) to that Caco-2 cells stably transfected with the construct could be used to assess the background luciferase expression not attributable to NFκB signalling. To make this construct, the TATA box and luciferase CDS were isolated by restriction digestion and inserted into an appropriate vector.

ii. Secondly, the required sequences were cloned into either pcDNA3.1 v5-his-TOPO or pBLUE-TOPO plasmids (respective maps are given in Figure 10) that can be expressed in mammalian cells.

(A) NFkB and TATA constructs

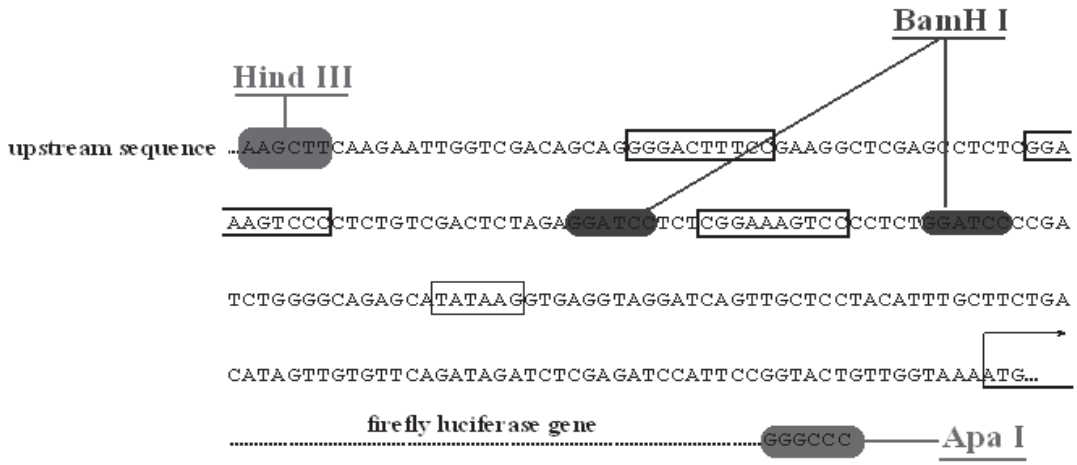

(B) Sequence information

Figure 9: Sequence information of the 3X κB-luciferase and TATA-luciferase sequences used in cloning strategy

(A): The construct of 3XκB-luciferase comprises of 3X κB binding sites, TATA box and luciferase CDS, and the control construct of TATA-luciferase comprises of TATA box and luciferase CDS. (B): The 3X κB-luciferase insert contains restriction sites of *Hind III* and *Apa I*, and the TATA-luciferase insert contains restriction sites of *BamH I* and *Apa I*. In addition, the 3 NFκB binding sites (**bold box**), the TATA core (light box) and the luciferase CDS initiation site (arrow) are shown.

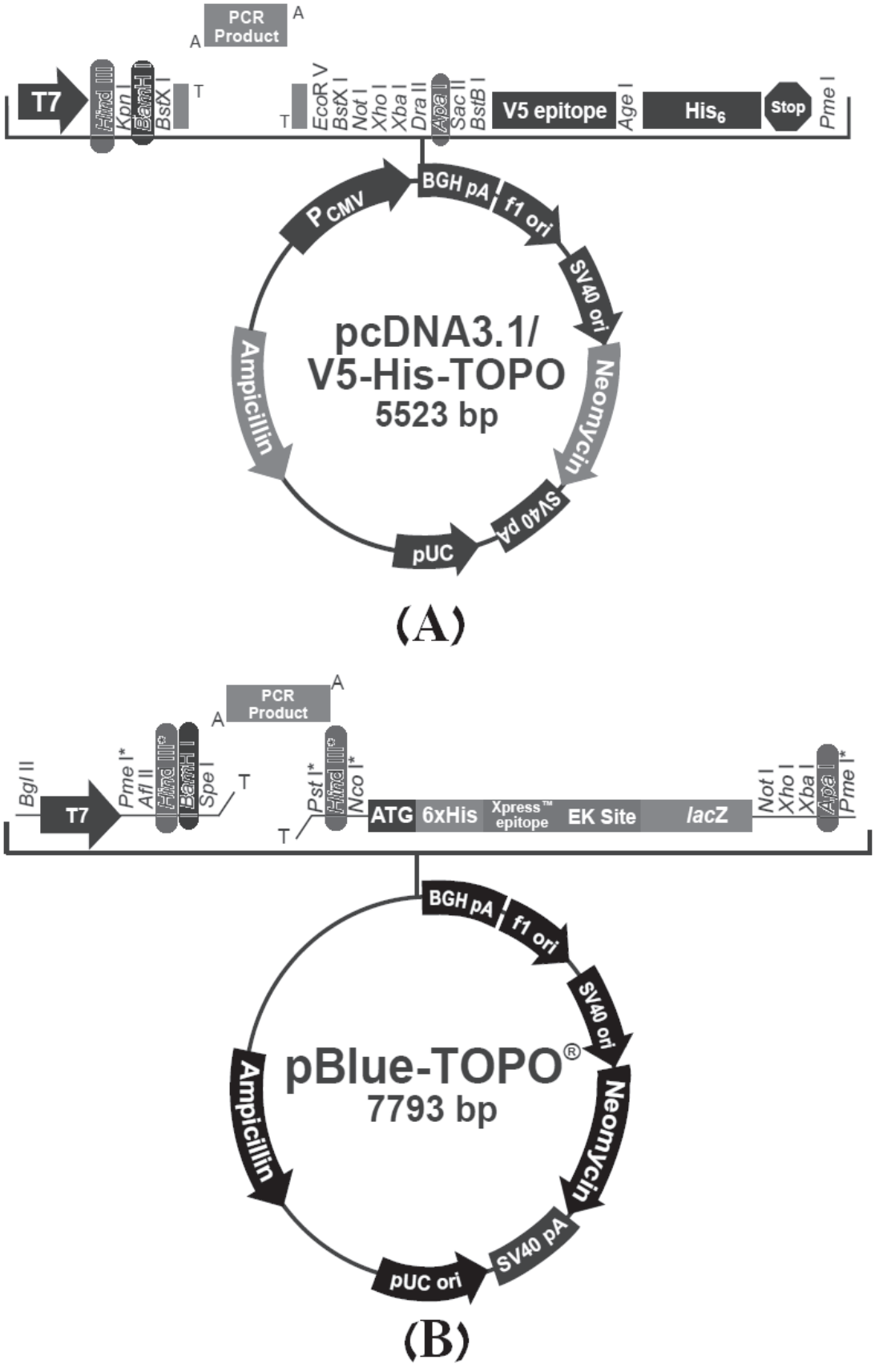

Figure 10: Plasmid maps of pcDNA3.1 v5-his-TOPO and pBLUE-TOPO

3.2 Cloning of the 3X κB-luciferase construct and TATA-luciferase construct in pcDNA3.1 v5-his-TOPO

The cloning strategy used by the present study was as follows:

I). pcDNA3.1 v5-his-TOPO or pBLUE-TOPO used as the plasmid vector were digested by either a.) *Hind III* and *Apa I* to clone the 3X κB-luciferase construct or b.) *BamH I* and *Apa I* to clone the TATA-luciferase construct (see Figure 7.2);

II). the 3X κB-luciferase and TATA-luciferase sequence used as inserts were obtained by *Hind III* and *Apa I* restriction digest and by *BamH I* and *Apa I* restriction digest, respectively (see Figure 9);

III). the respective vector and 3X κB-luciferase insert or TATA-luciferase insert were ligated and both the ligation products were confirmed by restriction digestion and sequencing.

Cloning of the 3X κB-luciferase construct and TATA-luciferase construct in pcDNA3.1 v5-his-TOPO was performed by Fan C, University of Newcastle.

The ligation product of 3X κB-luciferase in pcDNA3.1 v5-his-TOPO was checked by restriction digest using *Pst* I and/or *Sac* II. As shown in Figure 11 (A), since the expected construct contains one *Pst* I site and one *Sac* II site, double digestion would be expected to result in DNA fragments of 6519bp and 1396bp. As shown in Figure 11 (B), electrophoresis of the digestion product indicated that the 3XκB-luciferase sequence had been correctly inserted into the pcDNA3.1 v5-his-TOPO vector.

The ligation product of TATA-luciferase in pcDNA3.1 v5-his-TOPO was checked by restriction digest using *Sal* I, *Pst* I, *Cla* I, and *Pst* I and *Cla* I. As shown in Figure 11 (C), the expected TATA construct contains two *Sal* I sites, one *Pst* I site, and one *Cla* I site (located on the insert). Therefore, restriction digest would be expected to result in DNA fragments of 5608bp and 2222bp (*Sal* I), linearized plasmid (*Pst* I or *Cla* I), and DNA fragments of 5524bp and 2306bp (*Pst* I and *Cla* I), respectively. As shown in Figure 11 (D), electrophoresis of the digestion product from TATA construct indicated that the TATA-luciferase sequence had been inserted correctly. In comparison, restriction digest of the 3XκB construct by *Sal* I was found to result in DNA fragments of 4756bp, 2222bp, 885bp and 52bp, with two extra *Sal* I sites located within the 3X κB binding region (also shown in Figure 11 (A) and (D)).

The ligation products of 3X κB-luciferase in pcDNA3.1 v5-his-TOPO and TATA-luciferase in pcDNA3.1 v5-his-TOPO were confirmed by sequencing (data now shown), in which the presence of 3X κB binding sites on the 3X κB construct and the presence of TATA box together with the absence of 3X κB binding sites on the TATA construct were confirmed.

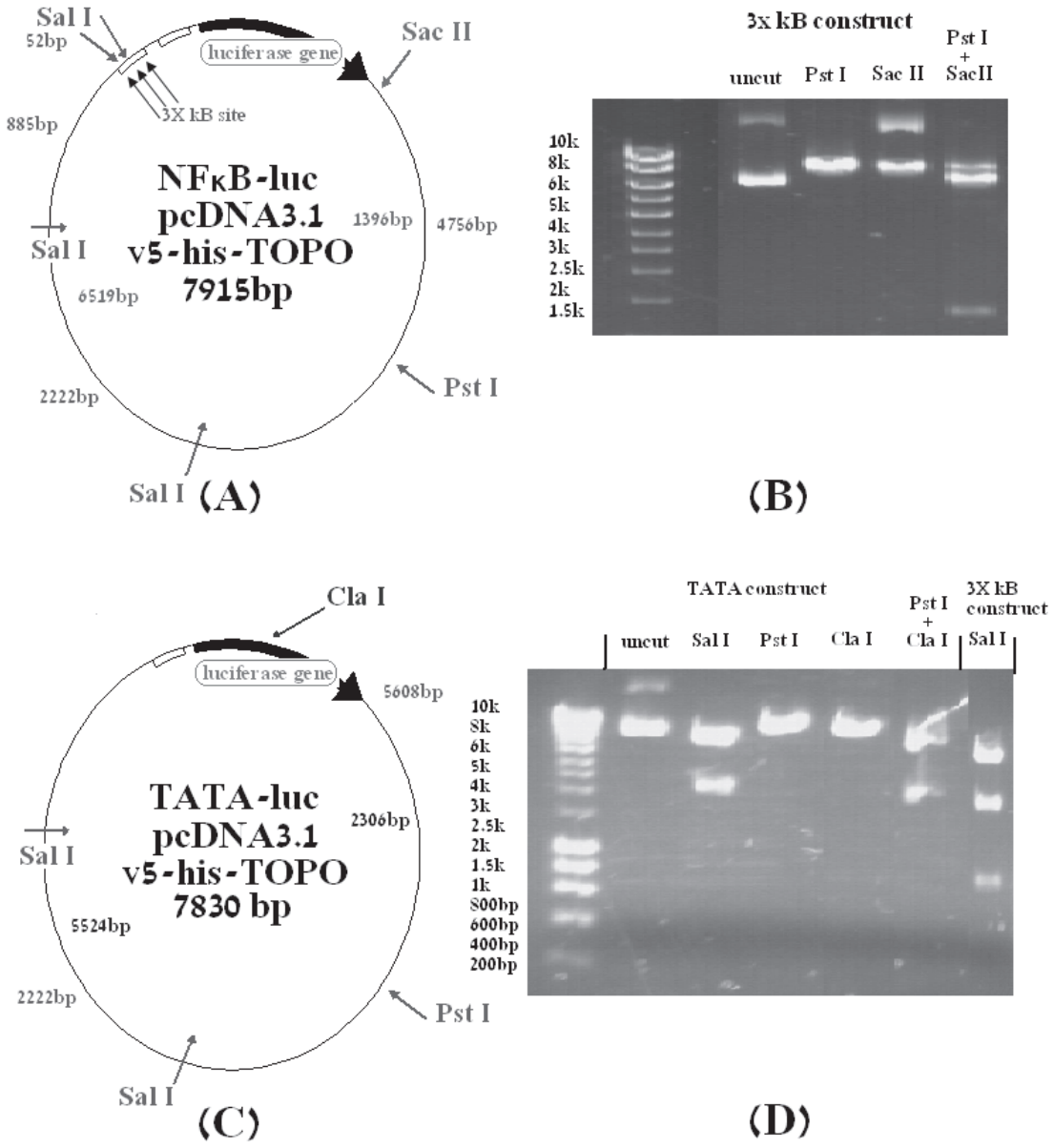

Figure 11: 3X κB-luciferase and TATA-luciferase sequences in pcDNA3.1 v5-his-TOPO and restriction digest of ligation product

Map of 3X κB-luciferase construct in pcDNA3.1 v5-his-TOPO (A) shows the position of 3X κB binding sites together with the TATA box and luciferase CDS and the position of restriction sites. Restriction digestion with *Pst* I and *Sac* II (B) suggested that the ligation product contained the 3X κB sequences. In addition, restriction digestion by *Sal* I on the 3X κB construct provided further evidence for the presence of 3X κB binding sites (D). Map of TATA-luciferase construct in pcDNA3.1 v5-his-TOPO (C) shows the position of TATA box and luciferase CDS and the absence of 3X κB binding sites and the position of restriction sites. Using restriction digest by *Sal* I, *Pst* I and *Cla* I, the ligation product was suggested to be the TATA construct (D).

3.3 Cloning of NFκB- (3X κB-) luciferase construct in pBLUE-TOPO

To clone the 3X κB-luciferase construct into pBLUE-TOPO (cloning strategy shown in Figure 12), the vector was prepared from a pBLUE-TOPO plasmid (kindly provided by Prof Dianne Ford, Newcastle University) and the 3X κB-luciferase insert was prepared from the previously established 3X κB-luciferase construct in pcDNA3.1 v5-his-TOPO. Both of vector and insert were obtained by restriction digestion using *Hind* III and *Apa* I.

Slightly different from the empty pBLUE-TOPO plasmid (map shown in Figure 10), the pBLUE-TOPO plasmid used in the experiment contained an insert of 1000bp within the PCR cloning site. This insert was flanked by *Hind* III recognition sites and could be completely removed in *Hind* III and *Apa* I restriction digestion. As shown in Figure 12 (A) (map of pBLUE-TOPO containing the 1000bp insert, 8793bp in length), restriction digestion by *Hind* III and *Apa* I generated DNA fragments of 1069bp, 3230bp and 4494bp (shown in Figure 12 (C)), of which the 4494bp fragment was the

pBLUE-TOPO vector to be used in ligation (Figure 12 (C)). The buffer, enzymatic activity and other details in experiment were as listed in **Table 4**.

In addition, the insert of 3XκB-luciferase was obtained by *Hind* III and *Apa* I restriction digest on the 3XκB-luciferase construct in pcDNA3.1 v5-his-TOPO. The restriction map of the 3XκB-luciferase in v5-his-TOPO (7915bp in length) shown in Figure 12 (B), restriction digest by *Hind* III and *Apa* I generated DNA fragments of 2500bp and 5415bp (results shown in Figure 12 (D)), of which the 2500bp fragment was the 3XκB-luciferase insert (Figure 12 (D)).

Cloning Procedure	Restriction Enzyme	Buffer	Activity	Product size
pBLUE-TOPO	*Hind* III	B	100%	1069bp 3230bp
Vector	*Apa* I		50-75%	4494bp
3XκB-luciferase	*Hind* III	B	100%	2500bp
Insert	*Apa* I		50-75%	5415bp
Confirmation of the NFκB-luciferase pBLUE-TOPO construct	*Sal* I	D	100%	52bp 4672bp 2200bp

Table 4: Procedure for restriction digestion in cloning of the NFκB-luciferase-pBLUE-TOPO construct

Restriction enzymes (Promega) used in cloning of NFκB-luciferase-pBLUE-TOPO construct was listed as above with respective buffer, enzymatic activity and production size instructed.

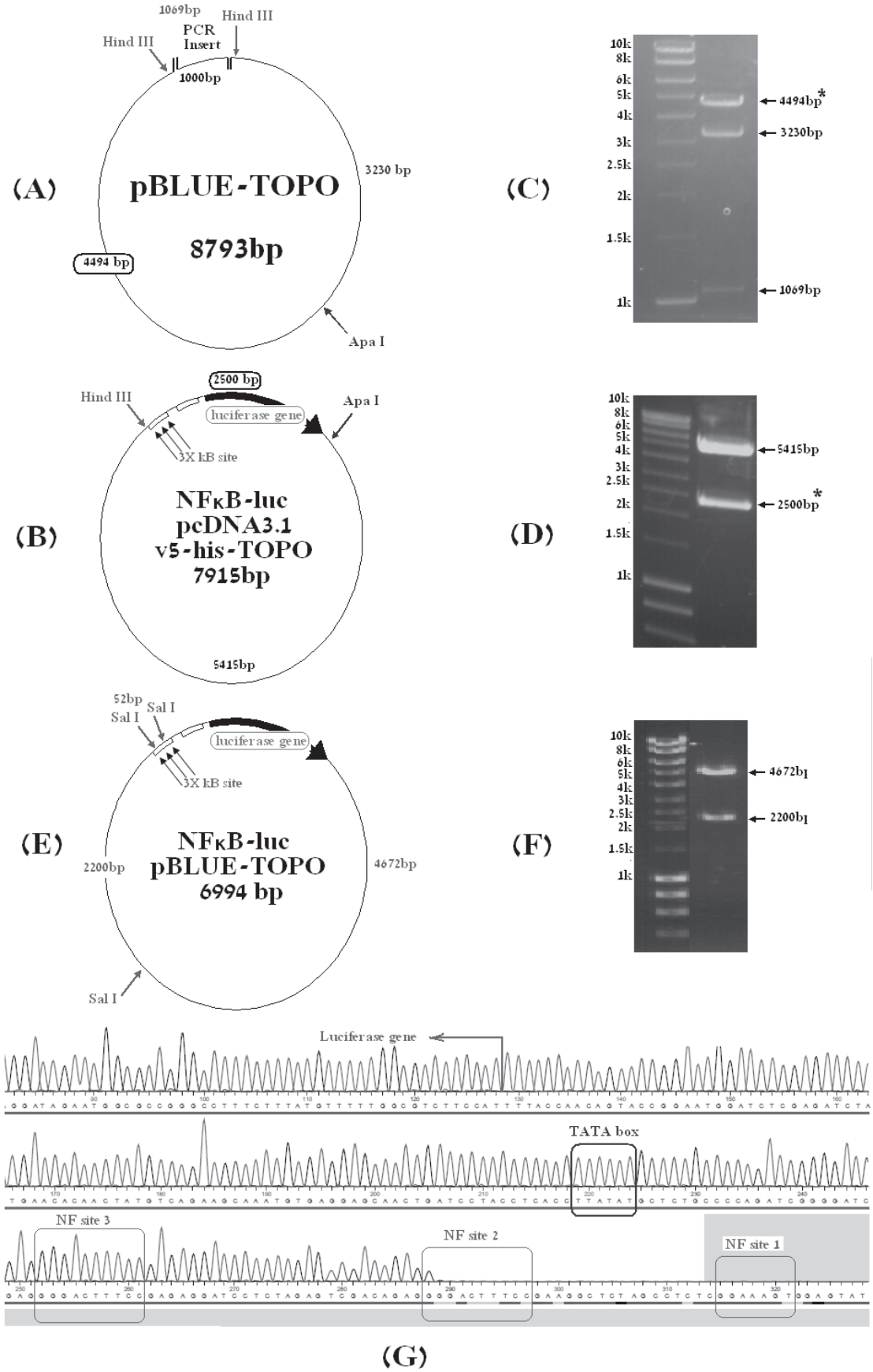

Figure 12: Cloning of the NFκB-luciferase pBLUE-TOPO construct

(A): pBLUE-TOPO vector with *Hind* III and *Apa* I restriction sites highlighted.
(B): pNFκB-luc-v5-his-TOPO construct containing 2.5kb *Hind* III-*Apa* I insert with 3XκB sites (red) and luciferase gene.
(C): pBLUE-TOPO vector restricted with *Hind* III and *Apa* I. DNA bands of ~4.5kbp, 3.2kbp and 1.0kbp correspond to *Hind* III-*Apa* I and *Hind* III fragments (see Fig A). * represents fragment isolated for cloning.
(D): pNFκB-luc-v5-his-TOPO construct restricted with Hind III and Apa I. DNA bands of ~5.4kbp and 2.5kbp correspond to Hind III-Apa I fragments (see Fig B).* represents fragment isolated for cloning.
(E): NFκB-luc-pBLUE-TOPO construct containing 2.5kbp NFκB-luciferase insert. *Sal* I restriction sites are highlighted.
(F): NFκB-luc-pBLUE-TOPO construct restricted with *Sal* I. DNA bands of ~4.7kbp and 2.2kbp correspond to *Sal* I fragments (see Fig E). The 52bp *Sal* I-*Sal* I fragment was lost from the electrophoresis gel.
(G): DNA sequence chromatograh to confirm cloning of the NFκB-luciferase fragment in pBLUE-TOPO. The NFκB sites are identified by the three red boxes; the TATA site is boxed in blue and the start of the luciferase gene is indicated in green.

Following restriction digest and electrophoresis, the DNA fragments of 4494bp (pBLUE-TOPO vector) and of 2500bp (3XκB-luciferase insert) were then extracted from the gel and purified to be used in ligation. Ligation of the NFκB-luciferase insert into the pBLUE-TOPO *Hind* III and *Apa* I- restructured vector was performed using T4 DNA ligase at 4°C overnight (details as shown in Chapter 2 Section 2.1.5). The ligation products were transformed into TOP10 cells and recombinant bacteria selected using Ampicillin (100mg/ml). Bacterial clonies were selected and each cultured in LB medium (Ampicillin 100mg/ml) overnight. Plasmids from each clone were purified (Miniprep Kit, Invitrogen) and screened by restriction digest to select those containing the 3XκB-luciferase-pBLUE-TOPO construct.

As shown in Figure 12 (E), the expected NFκB-luciferase-pBLUE-TOPO construct would generate three *Sal* I restriction sites, two positioned within the 3X κB binding sites and one positioned within the pBLUE-TOPO vector. As a result, digestion with *Sal* I was expected to generate three DNA fragments of 52bp, 2200bp and 4672bp respectively (Figure 12 (E) and Table 4), in contrast to the pBLUE-TOPO plasmid containing one *Sal* I site resulting in linearization. DNA electrophoresis of the *Sal* I digestion products showed several clones to be of the expected restriction pattern, i.e. ~4672bp and ~2200bp bands (Figure 12 (F)). The cloning of the NFκB-luciferase insert in the pBLUE-TOPO vector was confirmed by sequencing. This showed the presence of the 3XκB binding sites, the TATA box and the initial part of the

luciferase CDS (Figure 12 (G)) and confirmed that construct had been engineered successfully.

3.4 Cloning of TATA-luciferase construct (control) in pBLUE-TOPO

To clone the TATA-luciferase construct into pBLUE-TOPO (cloning strategy shown in Figure 13), which functioned as the control construct lacking the NFκB-binding sites, the pBLUE-TOPO plasmid was restructured using *BamH* I and *Apa* I. Restriction digestion by *BamH* I and *Apa* I were predicted to result in two DNA fragments of 4512bp and 4281bp, respectively (as shown in Figure 13 (A)). These would be difficult to separate by electrophoresis. Therefore, an additional restriction enzyme *EcoR* V was used in a triplet digestion. Complete restriction digestion by the three enzymes generated three DNA fragments of 1995bp, 2286bp and 4512bp (Figure 13 (C)), respectively, of which the 4512bp fragment was the required pBLUE-TOPO vector to be used in ligation. This fragment was gel extracted and purified (Figure 13 (C)). The buffer, enzymatic activity and other details in experiment were as listed in **Table 5**.

To obtain the TATA-luciferase insert, the previously established TATA-luciferase construct in pcDNA3.1 v5-his-TOPO was restructured with *BamH* I and *Apa* I. The restriction map of TATA-Luc-v5-his-TOPO plasmid (7830bp in length) is shown in Figure 13 (B) and digestion by *BamH* I and *Apa* I generated DNA fragments of

2397bp and 5433bp, of which the 2397bp fragment was the TATA-luciferase insert to be used in ligation (Figure 13 (D)) and gel extracted and purified.

Cloning Procedure	Restriction Enzyme	Buffer	Activity	Product size
pBLUE-TOPO Vector	*BamH* I	MC	75-100%	1995bp
	EcoR V		100%	2286bp
	Apa I		75-100%	4512bp
TATA-luciferase Insert	*BamH* I	MC	75-100%	2397bp
	Apa I		75-100%	5433bp
Confirmation of the TATA-luciferase pBLUE-TOPO construct	*Kpn* I	J	100%	6909bp (linearization)

Table 5: Procedure for restriction digestion in cloning of the TATA-luciferase-pBLUE-TOPO construct

Restriction enzymes (Promega) used in cloning of TATA-luciferase pBLUE-TOPO construct was listed as above with respective buffer, enzymatic activity and production size instructed.

The purified DNA fragments of 4512bp (pBLUE-TOPO vector) and of 2397bp (TATA-luciferase insert) were ligated together (procedure as described in Chapter 2 Section 2.1.5). The ligation products were transformed in TOP10 cells and bacteria selected on LB agar plates containing Ampicillin (100mg/ml). Bacterial colnies were selected, plasmids purified (Miniprep Kit, Invitrogen) and conformation of

TATA-luciferase construct in pBLUE-TOPO was screened by restriction digest using *Kpn* I (Figure 13 (E) and (F)) and determined by sequencing (Figure 13 (G)).

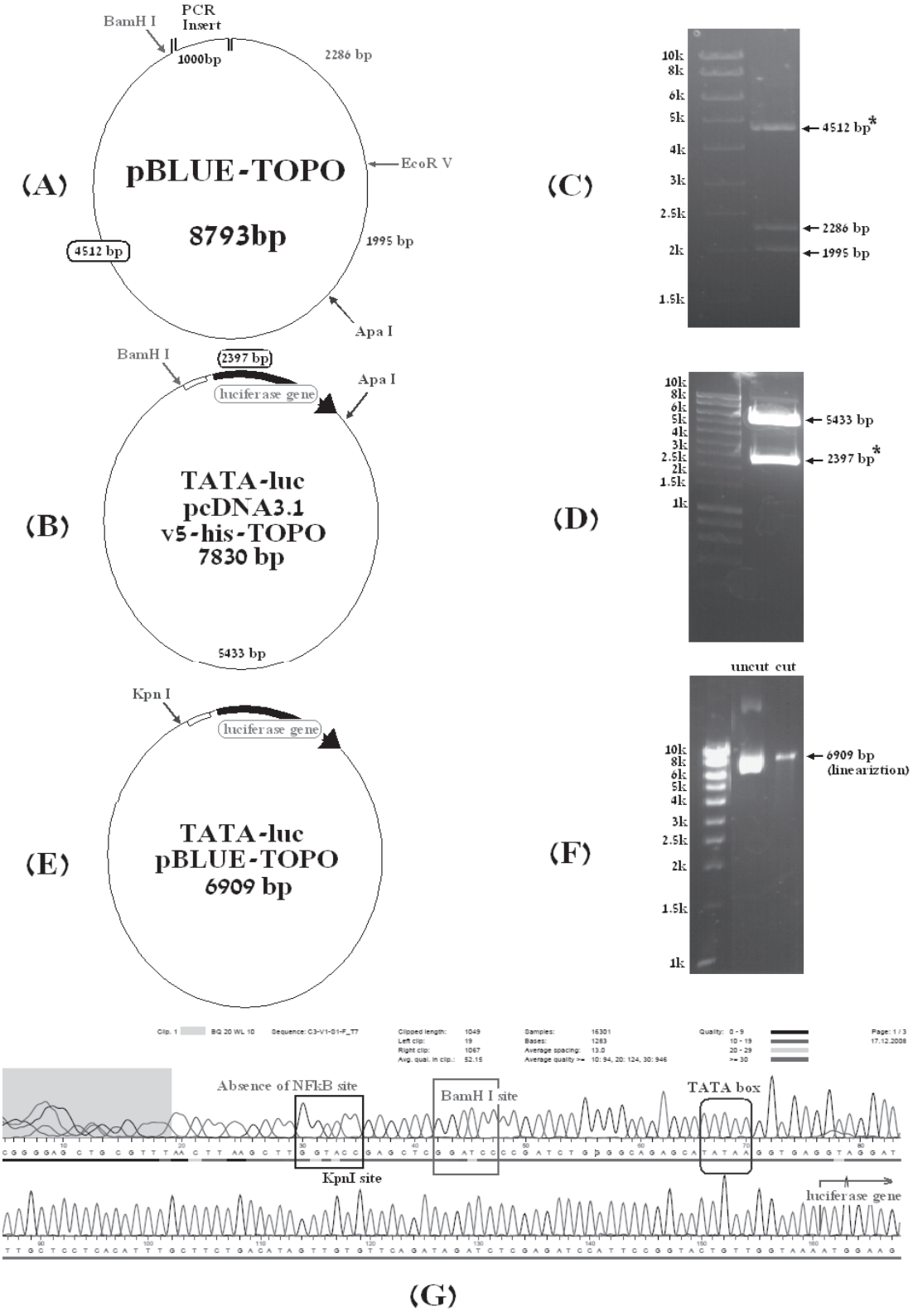

Figure 13: Cloning of the TATA-luciferase pBLUE-TOPO construct

(A): pBLUE-TOPO vector with *BamH*I, *EcoR*V and *Apa*I restriction sites highlighted.
(B): TATA-Luc-v5-his-TOPO construct containing 2.4kbp *BamH*I-*Apa*I insert with TATA site and luciferase gene.
(C): pBLUE-TOPO vector restricted with *BamH*I, *EcoR*V and *Apa*I. DNA bands of ~4.5kbp, 2.3kbp and 2.0kbp correspond to *BamH*I-*Apa*I, *BamH*I-*EcoR*V and *EcoR*V-*Apa*I (see Fig A). * represents fragment isolated for cloning.
(D): TATA-Luc-v5-his-TOPO construct restricted with BamHI and ApaI. DNA bands of ~5.4kbp and 2.4kbp correspond to *BamH*I-*Apa*I fragments (see Fig B). * represents fragment isolated for cloning.
(E): TATA-Luc-pBLUE-TOPO construct containing 2.4kb TATA-luciferase insert. A unique *Kpn*I restriction site derived from the pBLUE-TOPO MCS is highlighted.
(F): TATA-Luc-pBLUE-TOPO construct not restricted (uncut) or linearised (cut) using the unique *Kpn*I site derived from the pBLUE-TOPO MCS.
(G): DNA sequence chromatogram to confirm cloning of the TATA-luciferase fragment in pBLUE-TOPO. The *Kpn*I and *BamH*I restriction sites are highlighted; the TATA site is boxed in blue and the start of the luciferase gene is indicated in green.

As shown in Figure 13 (E), the TATA-luciferase construct in pBLUE-TOPO was expected to conserve one *Kpn* I restriction site positioned within the residual sequence of the pBLUE-TOPO vector. As a result, digestion with *Kpn* I would be expected to linearize the plasmid of 6909bp, in contrast to the NFκB-luciferase-pBLUE-TOPO which should remained uncut. This is because the Kpn I site originally locates between the *Hind* III and *BamH* I sites on the pBLUE-TOPO vector and in cloning of the NFκB-luciferase-pBLUE-TOPO construct it was abolished during the *Hind* III and *Apa* I digestion. DNA electrophoresis of the *Kpn* I digestion products confirmed several clones to be of the expected restriction pattern, i.e. linearized 6909bp plasmid (Figure 13 (F)) and differentiated the TATA-luciferase construct from the NFκB-luciferase construct in pBLUE-TOPO.

The cloning of the TATA-luciferase insert in the pBLUE-TOPO vector was confirmed by sequencing (Figure 13 (G)). This revealed the presence of *BamH* I site (as the fusion site of vector and insert), TATA box, and the beginning part of the luciferase CDS. In addition, as expected the NFκB-binding sites were absent on the control construct (Figure 13 (G)).

3.5 Stable transfection of the NFκB- and TATA- luciferase constructs in Caco-2 cells and preliminary study of the NFκB-luciferase Caco-2 cells

To obtain cell lines expressing the NFκB-luciferase reporter and its control, Caco-2 cells were stably transfected with each of the two constructs contained in either pcDNA3.1 v5-his-TOPO or pBLUE-TOPO vectors. Briefly, Caco-2 cells were seeded 24h before transfection in 6-well plate to reach ~90% confluency and washed 1X with PBS; For each transfection, 2-6μg of construct DNA and 5μl of transfection reagent Lipofectamine•• 2000 (Invitrogen) were diluted in 2.5ml Opti-mem (Gibco) and applied to the cells. Twenty-four hours later, cells were returned to normal growth medium for a further 24h, the transfected Caco-2 cells were detached from the 6-well plates by trypsin treatment, collected and transferred into 10mm Petri dishes for growth under the selection of Neomycin (750ug/ml).

The presence of Neomycin resistance gene encoded in the NFκB-luciferase pBLUE-TOPO construct and TATA-luciferase pBLUE-TOPO construct, as shown in Figure 10, allows cell survival when cells are grown in neomycin. Recombinant Caco-2 cells expressing the construct genes were able to survive, whereas non-recombinant Caco-2 cells would be killed by the neomycin. In order to select the Caco-2 cells, neomycin (G418), at a concentration of 750μg/ml, was added to the growth medium for 4 weeks until all untransfected cells had died. The Caco-2 cells transfected with either the NFκB-luciferase construct or the TATA-luciferase

construct were harvested as a mixed population, and these are described either as the NFκB-luciferase reporter model or the TATA-luciferase reporter model (control).

The NFκB- and TATA- luciferase constructs contained in pcDNA3.1 v5-his-TOPO were transfected in Caco-2 cells and the luciferase activities in these cells were assessed in the absence (to show baseline luciferase expression) and presence (to show the responsiveness to NFκB activation) of NFκB inducer TNFα (20ng/ml). Results are shown in Figure 14 (A) and (B). Details of the luciferase assay procedures are described in Chapter 2 Section 2.1.19-2.1.21. The luciferase activity was expressed as luciferase activity per mg total cell lysate (luc/mg).

As shown in Figure 14 (A), the mean baseline luciferase activity of the Caco-2 cells transfected with NFκB-luciferase v5-his-TOPO was 67.4 ± 6.2 luc/mg, whereas the mean baseline luciferase activity of the control TATA-luciferase v5-his-TOPO transfects was 242.1 ± 20.7 luc/mg. Compared with the models transfected with pBLUE-TOPO constructs (described later), the baseline luciferase activities of both NFκB and TATA models transfected with v5-his-TOPO constructs were considerably higher. In addition, the TATA-luciferase v5-his-TOPO Caco-2 cells showed a higher (~4 fold) level of baseline luciferase expression than the NFκB Caco-2 cells.

As shown in Figure 14 (B), the responsiveness of the v5-his-TOPO reporter cells to NFκB signalling was tested after TNFα (20ng/ml) stimulation. Owing to the large

difference in baseline luciferase activities, data for both NFκB model and TATA model are presented as fold-change relative to their baseline levels, respectively. In the NFκB-luc-v5-his-TOPO reporter cells, treatment of 20ng/ml TNFα for 4 hours resulted in approximately 8 fold increase of luciferase activity compared with the unstimulated level. However, in the TATA-luc-v5-his-TOPO reporter cells, the same treatment was also observed to result in approximately 4 fold increase of luciferase activity compared with its baseline level. Therefore, the responsiveness to NFκB signalling inducer TNFα was found in both NFκB- and TATA-luciferase reporter cells of the v5-his-TOPO transfect line, and the NFκB Caco-2 cells exhibited a larger responsive effect (8 fold) than the TATA Caco-2 cells (4 fold). The unexpected response by the TATA-luc-v5-his-TOPO cell line is analyzed in discussion.

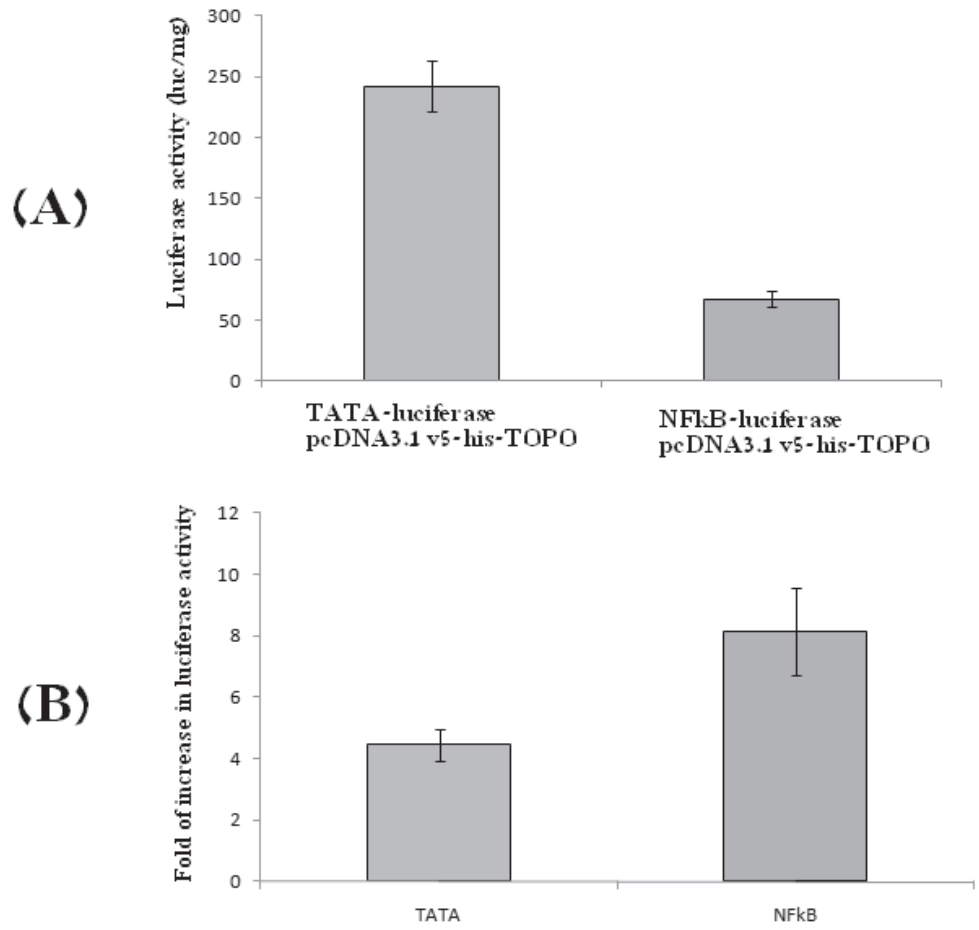

Figure 14: NFκB- and TATA- luciferase Caco-2 model based on pcDNA3.1 v5-his-TOPO constructs: Baseline luciferase activities and responsiveness to TNFα

Luciferase activity was measured in Caco-2 cells stably transfected with NFκB- or TATA- luciferase constructs in pcDNA3.1 v5-his-TOPO before or after stimulation with TNFα. The mean baseline luciferase activity of the TATA-luc reporter model was 242.1 ± 20.7 luc per mg total cell lysate whereas baseline luciferase activity of the NFκB-luc reporter model was 67.4 ± 6.2 luc/mg (shown in (A)). In the presence of NFκB inducer TNFα (20ng/ml), 4 hours treatment resulted in ~8 fold increase of luciferase activity in the NFκB-luc Caco-2 cells compared to the baseline level, and a ~4 fold increase of luciferase activity in the TATA-luc Caco-2 cells (shown in (B)).

The other pair of constructs, the NFκB- and TATA-luciferase constructs in pBLUE-TOPO, were also transfected in Caco-2 cells that harvested in a mix population. To show the baseline luciferase expression and the responsiveness to NFκB activation in these cells, the luciferase activities were measured in the absence and presence of known NFκB inducers TNFα and flagellin. Following stimulation of cells by 20ng/ml TNFα (Sigma) (Kelly et al., 2004), the luciferase activities were measured 0, 1, 2, 4, 6 and 8 hours. Stimulation by *Salmonella typhimurium* flagellin (Invivogen) was at a concentration of 100ng/ml (Kelly et al., 2004) and luciferase activities were measured 0, 1, 2, 4, 6, 8 and 12 hours after addition of flagellin.

As shown in Figure 15 (A), the mean baseline luciferase activity of the NFκB-luciferase pBLUE-TOPO Caco-2 cells was 22.7 ± 2.3 luc/mg, whereas the mean baseline luciferase activity of the TATA-luciferase pBLUE-TOPO Caco-2 model was 10.7 ± 0.5 luc/mg. The NFκB-luciferase Caco-2 model showed a higher (~2 fold) level of baseline luciferase expression compared to the control TATA Caco-2 cells (Figure 15 (B)). However, the baseline luciferase activities of both models were low.

The responsiveness of the reporter cells to NFκB activation by TNFα and flagellin are shown in Figure 15 (C) and (D). NFκB-luciferase pBLUE-TOPO Caco-2 cells treated with 20ng/ml TNFα exhibited increased luciferase activity starting 1 hour after TNFα addition and peaking at 4h about approximately 12 fold above baseline levels (Figure

15 (C)). In contrast, the control TATA-luciferase pBLUE-TOPO Caco-2 cells exhibited no increase in luciferase activity after addition of TNFα and remained baseline levels. Similarly, as shown in Figure 15 (D), treatment of the NFκB-luciferase pBLUE-TOPO Caco-2 cells with 100ng/ml flagellin resulted in increased luciferase activity but no change in activity was observed in the TATA-luciferase pBLUE-TOPO control cells. The luciferase activities of the NFκB cells started to increase at 2h after the addition of flagellin, peaked between 4-8 hours ~6.4 fold of the baseline level and then started to decrease.

In summary, these results confirmed the ability of the NFκB-luciferase pBLUE-TOPO Caco-2 cells to report the status of NFκB activation in response to potential inducers. In addition, the responsiveness was specific to the NFκB signalling. The establishment of the luciferase reporter model by the present study therefore provided a convenient tool to assess the activation of NFκB signalling in Caco-2 cells and allowed investigation of the regulatory effects of Selenium and selenoproteins on the NFκB signalling pathway.

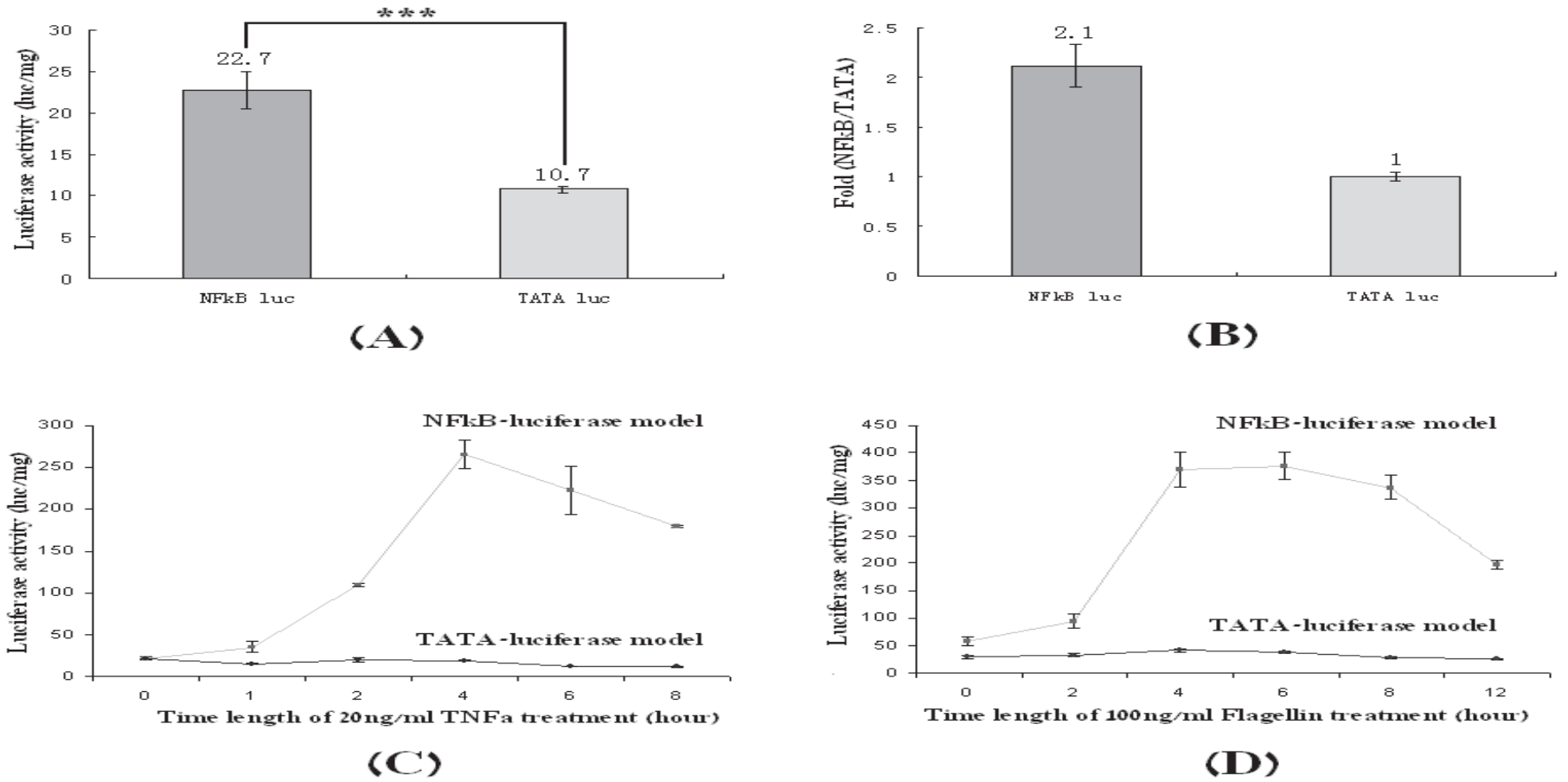

Figure 15: NFκB- and TATA- luciferase pBLUE-TOPO Caco-2 cells: Baseline luciferase activities and responsiveness to TNFα and flagellin

Luciferase activity was measured in Caco-2 cells transfected with either NFκB-luciferase or TATA-luciferase construct in pBLUE-TOPO. (A): the baseline luciferase activity of NFκB Caco-2 cells was 22.73luc/mg on average and the baseline luciferase activity of TATA Caco-2 cells was 10.74luc/mg on average. (B): the luciferase expression was also found to be ~2 fold higher in NFκB Caco-2 cells compared with TATA Caco-2 cells.

After stimulation with TNFα (20ng/ml) or *Salmonella typhimurium* flagellin (100ng/ml), there was a dramatic increase of luciferase activity in the NFκB Caco-2 cells but not in the control TATA Caco-2 cells (C and D). The increase started 1h and peaked by up to ~12 fold 4h after TNFα addition (C). Similarly, the increase started 2h after flagellin addition and reached a plateau of a 6.4 fold increase stage after between 4 and 8 hours (D). These results indicate that the NFκB-luciferase Caco-2 model is able to sensitively and specifically report the activation of NFκB signalling. Groups were compared using a 2-tailed Student t-test (***: $p<0.001$).

3.6 Discussion

The transcription factor NFκB modulates the expression of a large number of proteins many of which are inflammatory cytokines or peptides involved in the inflammatory process (Vallabhapurapu and Karin, 2009). Studies in these pathways have provided insights into how inflammatory events develop and are controlled in human tissues (Neurath et al., 1998, Karin and Greten, 2005). The aim of the research described in this thesis is to investigate the regulatory effects of micronutrient Selenium and Se-dependent antioxidants on the NFκB inflammtory signalling pathway in human colonic epithelial Caco-2 cells. The present Chapter describes the work that established a reliable and convenient method to assess the activation status of NFκB signalling.

Compared to the other methods to study the NFκB signalling pathway (as listed in Section 3.1), the NFκB-luciferase reporter system takes advantage of a luciferase gene driven by a promoter sequence containing NFκB binding sites and therefore reports NFκB signalling into luciferase expression when NFκB sites are activated. In this study, Caco-2 epithelial cells were stably transfected with constructs modified from a previously proven NFκB reporter construct (Carlsen et al., 2002, Vykhovanets et al., 2008), in which a promoter containing 3X κB binding sites was fused to the luciferase coding sequence (Kirillov et al., 1996, Maier et al., 2003). However, for use in Caco-2 cells and *in vitro* experiments by this study, re-cloning of the NFκB-luciferase sequence into a new vector was required. The main reason of this was to generate a

control construct to specify the background and changes of luciferase expression which are not attributable to NFκB signalling.

Selective cloning of the NFκB-luciferase or the TATA-luciferase (control) construct employed pcDNA3.1 v5-his-TOPO or pBLUE-TOPO as vector and Caco-2 cells stably transfected with each construct were harvested as a mixed population. In the pBLUE-TOPO transfection cell lines, the NFκB-luciferase-pBLUE-TOPO and the TATA-luciferase-pBLUE-TOPO Caco-2 cells exhibited luciferase expression in the absence and presence of NFκB inducers. As shown in Figure 15 (A), in unstimulated cells the NFκB-luc pBLUE-TOPO Caco-2 model displayed mean luciferase activity of 22.7luc/mg whereas the TATA-luc pBLUE-TOPO Caco-2 model displayed mean luciferase activity of 10.7luc/mg. Possible reasons for the difference in baseline luciferase expressions between the two models include:

1. the background NFκB tone in Caco-2 cells drives luciferase expression in the NFκB-luciferase reporter but not in the TATA-luciferase reporter which lacks any NFκB binding sites. Since that NFκB is an essential modulator for cell inflammatory response (Wong and Tergaonkar, 2009), complete silence of NFκB signalling might be hazardous and a background tone of NFκB signalling is almost inevitable, which has been previously observed in other cell types (Coiras et al., 2007, Carlotti et al., 2000). Also, NFκB signalling is responsive to various endogenous physiological mediators (Jang et al., 2004, Ramakers et al., 2007) or apoptotic mediators (Schneider

et al., 1997) which naturally maintain cell function and background NFκB signalling might be activated by these endogenous inducers. In addition, for long time NFκB signalling has been known to be activated by oxidative stress (Schreck et al., 1991, Gloire et al., 2006), which occurs at a certain level during the cell respiration.

2. the difference in copy numbers of NFκB and TATA constructs transfected in Caco-2 cells;

3. the difference in the recombinant sites where the NFκB and TATA constructs were integrated into the Caco-2 genome.

If the possibilities 2 and 3 occur during transfection they might result in variability of the baseline luciferase expression in different cells. In the present study, the transfected Caco-2 cells were harvested as a mix population. Alternatively, the transfected cells could be harvested from individual clones and as a result, those cells expressing luciferase on a comparable level could be screened out and cultivated further. Using this strategy, the uneven expression of baseline luciferase activity could be avoided. However, in this study the baseline luciferase expressions in both NFκB and TATA Caco-2 models are low and the difference between the two should not be problematic.

The ability of the NFκB-luciferase pBLUE-TOPO Caco-2 model to respond to NFκB activators was also tested using known NFκB inducers TNFα and flagellin. TNFα is an inflammatory cytokine responsible for activation of NFκB through the endogenous signalling pathway (Li and Lin, 2008), whereas flagellin is a bacterial component activating NFκB through an exogenous signalling pathway (Tallant et al., 2004). Luciferase activities of the NFκB Caco-2 cells were increased by ~12 fold compared with the baseline level when cells were stimulated with 20ng/ml TNFα for 4 hours, and increased by ~6.4 fold compared with the baseline level when cells were stimulated with 100ng/ml flagellin for 4-8 hours (Figure 15 (C) and (D)). Despite of the variations in the peaking time for NFκB activation (4h for TNFα and 4-8h for flagellin) and in the extent of increase of luciferase activities (12 fold by TNFα and 6.4 fold by flagellin), which are mostly likely resulted from the different NFκB-inducing signalling pathways, the responsiveness of the NFκB reporter model was found sensitive to inducers. In contrast, increased luciferase activity was not observed in the control TATA-luciferase Caco-2 model which contained no NFκB binding sites, suggesting that the reporter system was specific. Therefore, the NFκB reporter Caco-2 model established in the present study work well in response to stimulation and the regulatory effects of Se supply and antioxidant selenoproteins on the NFκB signalling pathway were investigated and results described and discussed in the following Chapters.

In addition to the NFκB reporter model constructed using the pBLUE-TOPO vector, a similar reporter system was established using constructs contained in the pcDNA3.1 v5-his-TOPO vector. However, both the NFκB- and TATA- luciferase reporter cells transfected with the v5-his-TOPO constructs exhibited considerably higher level of baseline luciferase activity (242.1 luc/mg for TATA cells and 67.4 luc/mg for NFκB cells), and an unexpected responsiveness to NFκB inducer TNFα was observed (4 fold increase of luciferase activity compared to the baseline level) in the control TATA-luciferase reporter cells, which was not engineered with the 3X κB binding sites.

A possible explanation of these effects is the CMV promoter contained in the pcDNA3.1 v5-his-TOPO plasmid vector but not the pBLUE-TOPO vector. CMV promoter is a strong promoter originated from the human cytomegalovirus and is used to promote strong expression of the gene cloned in the construct (Schlabach et al., 2010), i.e. the NFκB- or TATA- luciferase gene in the present study. CMV promoter has been reported to contain NFκB binding sites and therefore responsive to NFκB signalling (Sambucetti et al., 1989). As a result, the transfected Caco-2 cells with the v5-his-TOPO constructs are able to express luciferase at a high level when driven by CMV promoter. In addition, following the NFκB induction by TNFα, the TATA-luciferase-v5-his-TOPO Caco-2 transfects were also stimulated to express luciferase under the control of CMV promoter (4 fold increase), whereas the NFκB-luciferase-v5-his-TOPO transfects expressed luciferase under the control of

both CMV promoter and 3X κB binding region (8 fold increase). Owing to the disturbance by CMV promoter, the NFκB reporter system based on pcDNA3.1 v5-his-TOPO constructs was abandoned and not used in the experiments described in the following chapters.

Lastly, it is worth emphasizing that in the studies described in this thesis, TNFα at a concentration of 20ng/ml and flagellin at a concentration of 100ng/ml, which were used to induce NFκB signalling, are on an experimental level aiming to achieve maximal inflammatory response. A concentration of 20ng/ml TNFα is much higher than that found under physiologial and pathogenic conditions (Turner et al., 2010). Plasma TNFα concentration has been documented to be 75 +/- 15 pg/ml in the normal population (physiological condition) and 100-5000 pg/ml in sepsis patients (pathogenic condition) (Damas et al., 1989). Flagellin at a concentration ranging 10-100ng/ml has been suggested sufficient to stimulate TLR5 (Hayashi et al., 2001) and its pathogenic level has not been documented. Using 20ng/ml TNFα or 100ng/ml flagellin, two models of NFκB signalling pathways in response to immune cytokine or bacterial components were established in Caco-2 cells and further investigations of the regulatory mechanisms of these pathways are presented in the following chapters.

4. Study of the relationship between selenium and NFκB inflammatory signalling pathways

4.1 Introduction

Until recently, knowledge of Se was limited mainly to antioxidant protection in the cellular environment through its relatively well-characterized GPx and TrxR selenoprotein families (Brigelius-Flohe, 1999). Yet increasing evidence has linked Se to additional protective functions, such as the reduced incidence of inflammation and carcinogenesis (Brigelius-Flohe, 2008). This evidence includes:

1) epidemiological studies that have linked low Se intake with a susceptibility to inflammatory bowel disease (IBD) and its associated complications (Karp and Koch, 2006);

2) clinical trials that have shown Se supplementation to be linked to a reduction in IBD symptoms and the decreased usage of therapeutic drugs (Karp and Koch, 2006);

3) biochemical studies that have suggested that Se and/or selenoprotein GPxs are involved in arachidonic acid metabolism (the LOX and COX pathways) and the control of leukotriene (LT) and prostaglandin (PG) synthesis (Sordillo et al., 2008, Seiler et al., 2008, Chen et al., 2003);

4) data indicating that Se and/or selenoprotein GPxs participate in the NFκB signalling pathway regulating its activation and the expression of NFκB target genes (Brigelius-Flohe, Banning et al. 2004; Kim, Johnson et al. 2004; Vunta, Davis et al. 2007).

The potential for Se to regulate the NFκB signalling pathway could be linked to Se modulating ROS production in the cell. ROS are known to activate NFκB directly, or to indirectly serve as a secondary messenger in NFκB activation through cytokines such as IL1β, and bacterial components such as lipopolysaccharide (LPS) (Brigelius-Flohe, Banning et al. 2004; Vunta, Davis et al. 2007). Thus ROS may function as links that extend the function of Se from one of antioxidant protection to NFκB regulation.

For example, Se has been identified as an inhibitory factor in NFκB activation by LPS (Kim et al., 2004) or IL1β (Brigelius-Flohe et al., 2004). This inhibitory effect was proposed to function through modification of ROS production, stimulated by cytokines, by the activity of GPx antioxidant selenoproteins (Brigelius-Flohe et al., 2004, Li et al., 2001). In macrophages the inhibition of LPS-induced NFκB activation via Se was suggested to be through regulation of the COX-1 arachidonic acid metabolism pathway and the resultant production of prostaglandin 5d-PGJ2 which, in turn, inhibited the activation of NFκB signalling (Vunta et al., 2007).

Intriguingly, evidence for protective effects of Se against the development of inflammation has been found in specific tissues, including gastrointestinal (GI) tract, lung and prostate (Duffield-Lillico, Reid et al. 2002; Whanger 2004; Karp and Koch 2006), all of which have constant exposure to oxidative stress and microbial challenge. However, the present knowledge of the anti-inflammatory effects of Se in these tissues remains limited. Essentially little is known about how Se and the selenoproteins impact on NFκB signalling pathway in human GI cells. For this reason, in the present study the human colonic epithelial cell line, Caco-2, was used to investigate whether the activation of NFκB by the inflammatory cytokine TNFα or the bacterial component flagellin was modulated by Se.

Being an endogenous cytokine participating in the innate immunity, TNFα is known to induce NFκB signalling through its receptor TNF receptor 1 (TNFR1) and associated ligands TRAF2 and RIP (Li and Lin, 2008). ROS production linked to TNFα is thought to be mitochondrial (Hsu et al., 1996, Morgan et al., 2008) or from activity of NAPDH oxidases (Li et al., 2009, Yazdanpanah et al., 2009) and associated with the activation of NFκB signalling. In comparison, flagellin, a component of bacteria, including pathogens, is known to induce NFκB activation through Toll-like receptor 5 (TLR5) signalling and associated ligands IRAK and TRAF6 (Tallant et al., 2004). ROS production by flagellin is probably through the apoptotic effects of MAPK pathway (p38 and JNK), since both NFκB and MAPK signalling has been suggested to be activated following flagellin stimulation (Harrison

et al., 2008, Zeng et al., 2006). In addition, a further TLR member TLR4 when bound by bacterial Lipopolysaccharide (LPS) has been suggested to be linked to NAPDH oxidase activity (Nox4) and ROS production resulting in NFκB activation (Park et al., 2006). Similar events could be presumed to occur in the flagellin-TLR5 pathway. Taken together, these two NFκB signalling pathways represent alternative NFκB activation models and were investigated in the present study.

To monitor NFκB activation, a previously established 3X NFκB-luciferase reporter construct (Carlsen et al., 2002, Vykhovanets et al., 2008) was modified for experiments in Caco-2 cells and the establishment of NFκB-luciferase reporter Caco-2 model was as described in Chapter 3. In addition, interleukin 8 (IL8), as a known NFκB target gene was assessed by semi-quantitative PCR to quantify its expression at the mRNA level, following stimulation of the Caco-2 cell models with either TNFα or flagellin.

4.2 Results

4.2.1 Se depletion and decrease of GPx1 expression

To study the effect of Se supply on NFκB activation, Se depletion experiments were performed using a previously established protocol (Pagmantidis et al., 2005) in which Caco-2 cells were grown for 3 days in Se-depleted or Se-supplemented culture medium (see Chapter 2 Section 2.1.12). Se depletion is known to lead to a lowering of mRNA expression, synthesis and activity of a number of selenoproteins (Bermano et al., 1995, Pagmantidis et al., 2005, Sunde et al., 2009) and GPx1 and SelW expression are particularly sensitive to Se supply (Pagmantidis et al., 2005, Kipp et al., 2009). In order to verify that Se depletion had occurred in the experiments, Caco-2 cells were grown for 3 days in Se-depleted or Se-supplemented culture medium, RNA extracted and then semi-quantitative PCR was used to assess the expression of GPx1.

As shown in Figure 16, the expression of GPx1 was significantly lower in Se-depleted cells compared to those grown in Se-supplemented medium ($p<0.001$). Quantification of the data (Figure 16) showed that the mean relative expression of GPx1 was lowered by 60% compared to the Se-supplemented controls. The reduction of GPx1 expression, which is in agreement with the previous findings (Pagmantidis et al., 2005), indicated that the cells were indeed in a Se-depleted state using this established method.

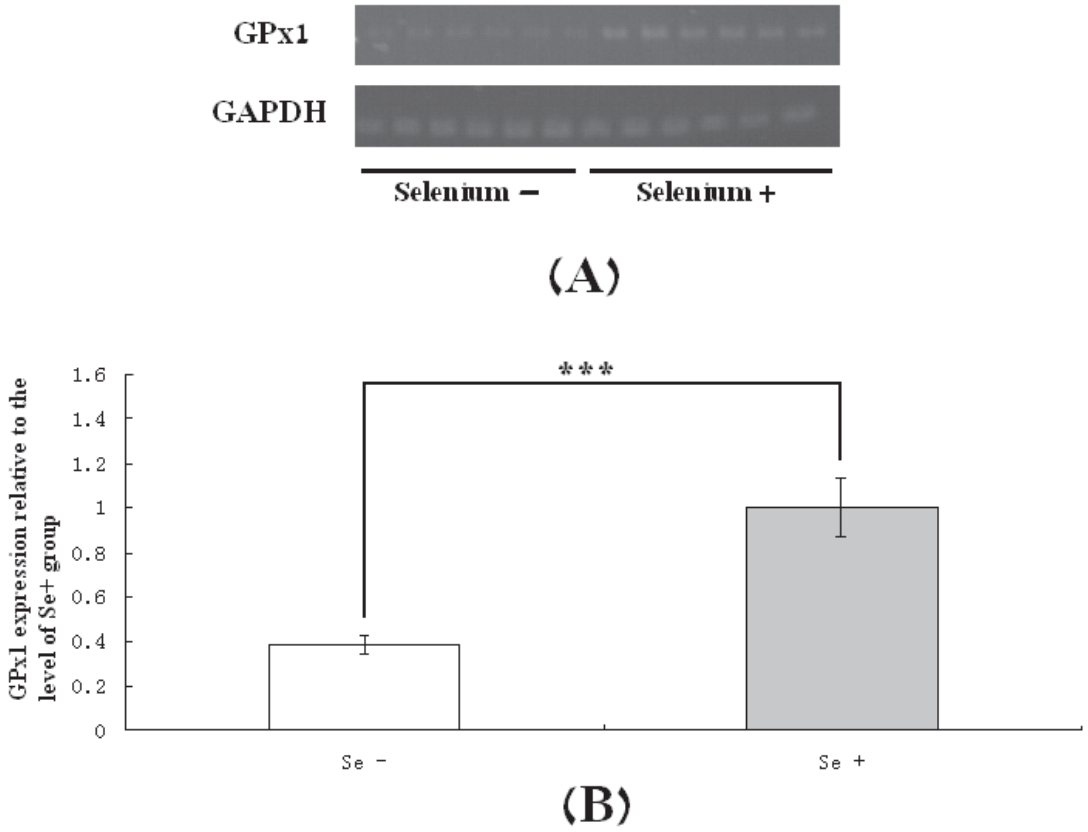

Figure 16: Se depletion and GPx1 mRNA expression in Caco-2 cells

Caco-2 cells were grown for 3 days in Se-depleted or Se-supplemented culture medium, RNA extracted and GPx1 expression assessed by semi-quantitative RT-PCR (A). GPx1 expression was quantified by densitometry and normalized to the housekeeping gene GAPDH (B). GPx1 expression was lowered by ~60% in cells grown in Se-depleted medium compared with supplemented cells (B). Groups were compared using a 2-tailed Mann-Whitney U-test (***$p<0.001$)

4.2.2 The impact of Se depletion on TNFα-induced NFκB-activation in the Caco-2 luciferase reporter model

The impact of Se depletion to NFκB signalling pathway was studied using the Caco-2 cell models transfected with the luciferase reporter constructs as described previously (Chapter 3). Firstly the effects of Se supply on NFκB signalling were assessed by growing the transfected cells +/- Se and quantififying luciferase activity. Luciferase activity was calculated per mg total lysate protein and expressed as relative luciferase activity (RLA, luciferase activity relative to the standard protein concentration).

As shown in Figure 15A, depleting the amount of Se in the cell growth medium did not affect the baseline luciferase activities in either the cells transfected with NFκB- or TATA-luciferase reporter. Therefore, deprivation of Se in the culture medium did not result in major changes to the background luciferase reporter activity.

The effect TNFα challenge on the NFκB pathway was studied in the Se-depleted and Se-supplemented Caco-2 cells by treating the cells with 20ng/ml TNFα for 2 or 4 hours respectively. To compare the Se+ and Se- treatments, the data was expressed as ratios relative to the level of luciferase activity in Se+ treatment group, which was standardized as 100% (see Figure 17B).

When the cells were challenged with TNFα, an increase in NFκB-driven luciferase activity was observed and this was greater in the Se-depleted cells, with an

approximate 30% increase in TNFα-NFκB activation resulting from Se depletion. Such an increase was not observed in Caco-2 cells transfected with the TATA-luciferase construct, suggesting that the effect was NFκB specific. In addition, the increase was observed at both 2 hours and 4 hours after addition of TNFα. The data suggest that depletion of Se in the culture medium amplified NFκB activation in response to TNF stimulation.

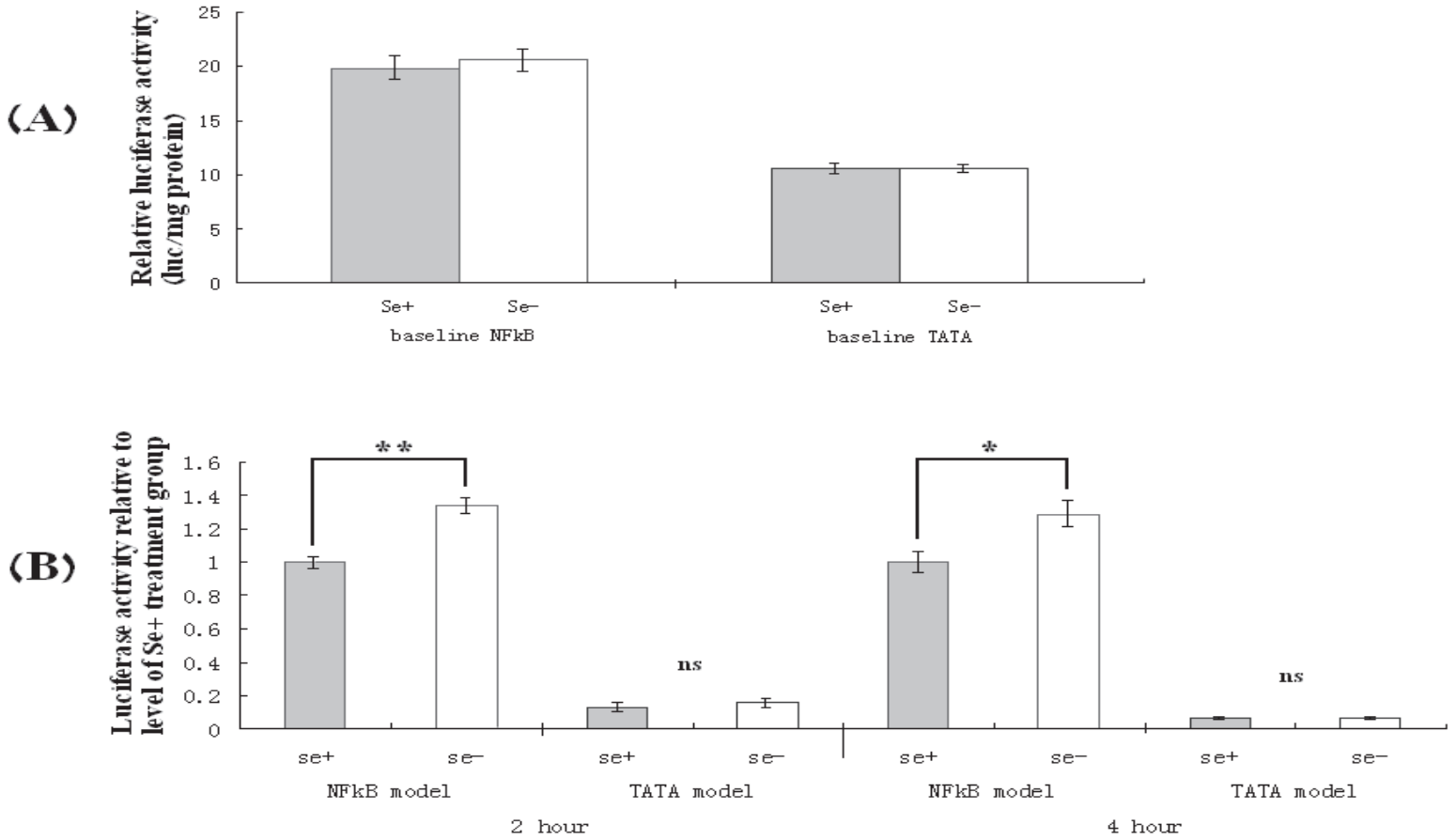

Figure 17: Effect of Se depletion on baseline luciferase activity & TNFα-induced luciferase activity of NFκB and TATA reporter constructs in Caco-2 cells

Caco-2 cells transfected with either NFκB- or TATA- luciferase constructs were grown for 3 days in Se-depleted (Se-) or Se-supplemented (Se+) culture medium, followed by treatment with 20ng/ml TNFα.
Protein lysate was harvested using 1X Reporter lysis buffer, and luciferase activity was determined and expressed per mg total lysate protein and as relative luciferase activity (RLA). Results relating to unstimulated Caco-2 cells, without TNFα addition, are shown in (A). Results relating to TNFα stimulated Caco-2 cells are shown in (B). Groups were compared using a 2-tailed Mann-Whitney U-test (** $p<0.01$; * $p<0.05$).

4.2.3 The impact of Se depletion on IL-8 mRNA expression

To further extend the findings obtained using the NFκB-luciferase reporter model and investigate the impact of Se depletion on NFκB-signalling pathways, the expression of a known NFκB target gene, encoding the cytokine IL8, was assessed by semi-quantitative RT-PCR. To show the response of IL8 to TNFα-NFκB activation, Caco-2 cells +Se were treated with 20ng/ml TNFα for 1, 2, 4 and 6 hours respectively, and IL8 mRNA expression determined. As shown in Figure 18, IL8 levels in unstimulated Caco-2 cells were barely detectable but following stimulation of the cells with TNFα, IL8 expression was elevated with the highest level observed after 1 hour.

To explore the effects of Se supply on IL8 expression, Caco-2 cells were grown for 3 days in Se-depleted or Se-supplemented culture medium followed by addition of 20ng/ml TNFα for 1 hour. RNA was extracted and semi-quantitative PCR was used to assess the expression of IL8, GPx1 (to validate Se depletion) and GAPDH. The expression levels of IL8 and GPx1 were normalized to the house keeping gene GAPDH. After TNFα treatment, Figure 19 (A), the PCR bands for IL8 expression in the Se-depleted Caco-2 cells were considerably more intense compared with those in Se-supplemented cells. These data expressed as a ratio relative to the level of the Se+ control (shown in Figure 19 (B)), indicated Il-8 expression to be significantly increased ($p<0.001$), about 50% compared to control. GPx1 expression was found to be significantly decreased ($p<0.001$), approximately 60% compared to control, which

was in agreement with previous findings. Therefore Se depletion was associated with an increased IL8 response in the TNFα-NFκB activation pathway

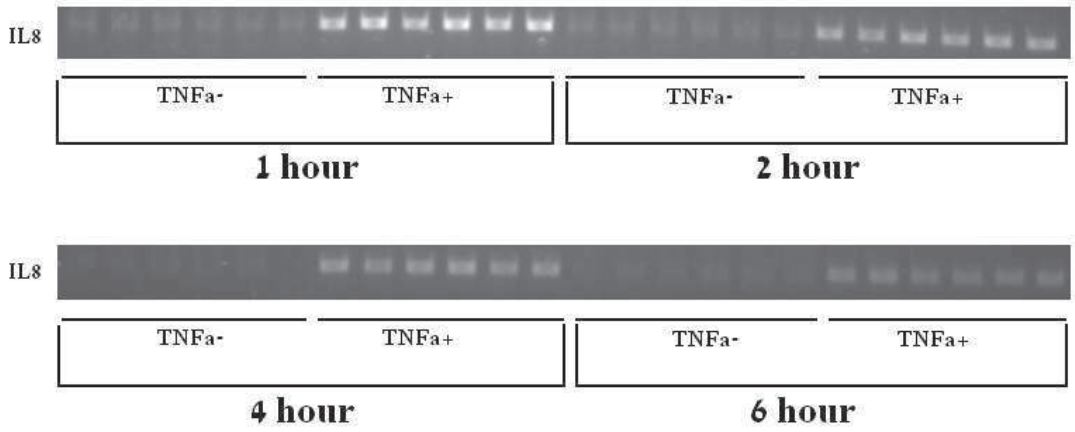

Figure 18: Induction of IL8 mRNA expression in Caco-2 cells following 1, 2, 4 and 6 hours of TNFα treatment

Caco-2 cells were cultured with or without 20ng/ml TNFα for 1, 2, 4 and 6 hours, RNA extracted and IL8 expression assessed by semi-quantitative RT-PCR. At all time points, IL8 expression in the absence of TNFα was barely detectable but when cells were stimulated with TNFα, IL8 expression was detected.

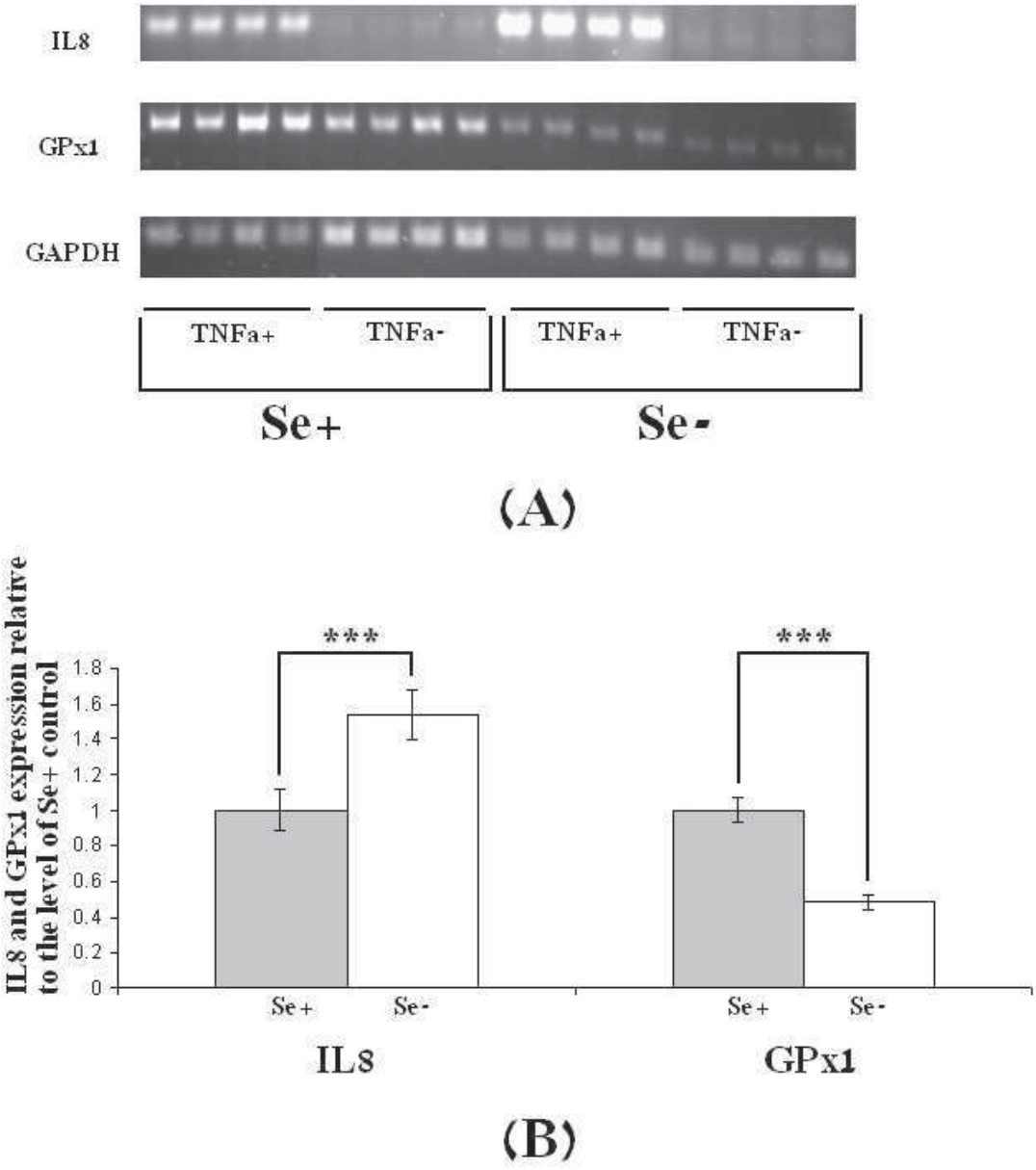

Figure 19: Effect of Se depletion on TNFα-induction of IL-8 expression in Caco-2 cells

Caco-2 cells were grown for 3 days in Se-depleted (Se-) or Se-supplemented (Se+) culture medium and incubated with 20ng/ml TNFα for one hour. IL8 expression was determined by semi-quantitative RT-PCR and normalized to the house keeping gene GAPDH. PCR bands of IL8, GPx1 and GAPDH are shown in (A). Bands were quantified by densitometry and data plotted as ratios relative to the level of Se+ control (B). (***$p<0.001$) indicates significance using 2-tailed Mann-Whitney U-test

4.2.4 The impact of Se depletion on flagellin-induced NFκB-activation in a luciferase reporter model

The impact of Se depletion on the NFκB signalling pathway, which has been shown previously to up-regulate NFκB activation and target gene IL8 expression in response to activator TNFα, was further investigated but using an alternative NFκB activator, bacterial flagellin. Unlike TNFα, which is synthesized by host cells, flagellin is an exogenous ligand, and synthesised by bacteria. This experiment was to test if, in response to flagellin, Se supply affects NFκB signalling through a different or similar mechanism to that of TNFα. In this study, the luciferase reporter model was used to monitor NFκB activation following Se depletion.

As shown in Figure 15 (Chapter 3), NFκB activation as indicated by luciferase activity in the transfected Caco-2 cells showed that NFκB activation by flagellin occurred 2-8 hours after addition of the ligand, with activation peaking at 4-8 hours. Therefore, to investigate possible effects of Se on flagellin-induced NFκB activation, the measurement of luciferase activity was performed at 2 and 6 hours after treatment. Cells were grown for 3 days in Se- or Se+ culture medium and afterwards treated with 100ng/ml flagellin for either 2 or 6 hours. The cell lysates were extracted and data expressed as RLA per mg total cell lysate and further expressed as a ratio relative to the level of Se+ control.

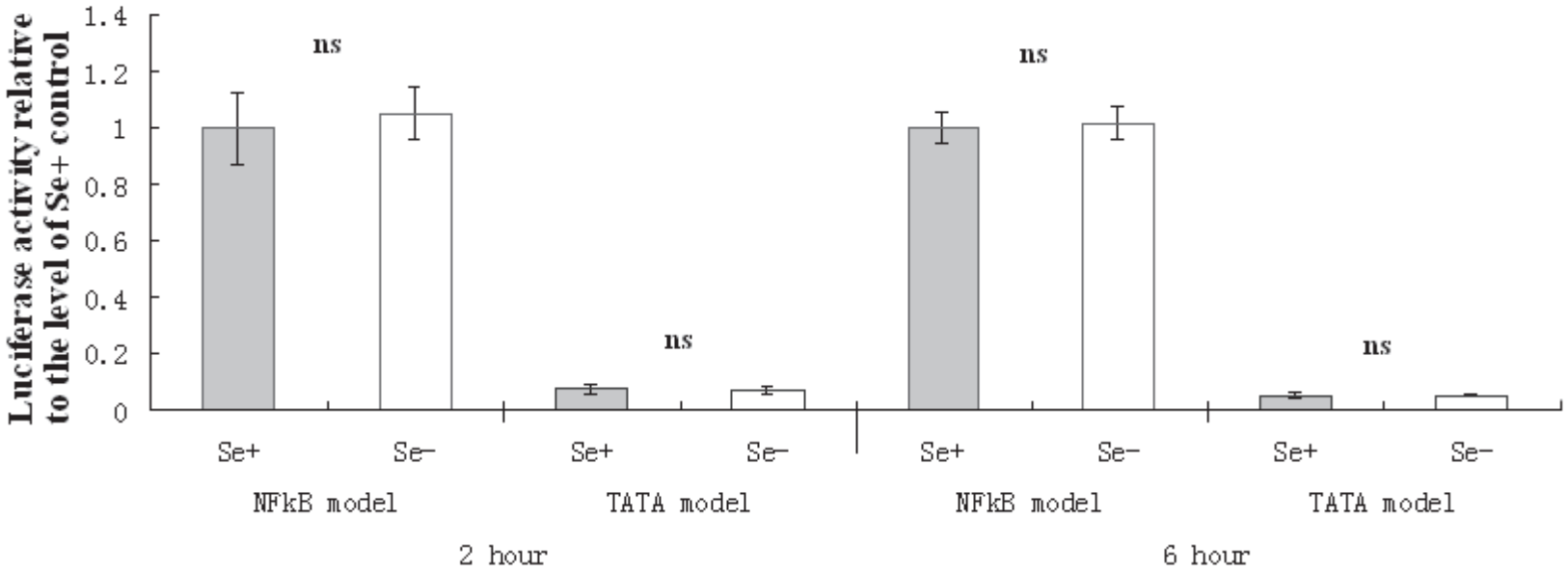

Figure 20: Effect of Se depletion on flagellin-induced luciferase activity of NFκB and TATA reporter constructs in Caco-2 cells

Caco-2 cells transfected with NFκB- and TATA- luciferase constructs were cultured in Se-depleted or Se-supplemented medium for 3 days, followed by incubation with 100ng/ml flagellin for either 2 or 6 hours. Data were expressed as RLA (relative luciferase activity per mg total cell lysate) and further assessed as a ratio relative to the level of Se+ control to show the effect of differential Se supply. Groups were compared using a 2-tailed Mann-Whitney U-test (ns: non-significant, $p>0.05$)

As shown in Figure 20, the induction of luciferase activity by 100ng/ml flagellin was specific to NFκB, as the cells transfected with the TATA- luciferase construct showed only low-level activity. However, following the flagellin challenge there was no significant difference in luciferase activity between cells cultured in Se-depleted or Se-supplemented medium, indicating that Se supply did not affect NFκB activation by flagellin. In addition, the data were similar in both 2 and 6 hour treatment groups, suggesting that Se depletion had no effect at any stage of NFκB activation in response to flagellin. These data therefore suggested that while Se supply effected the TNF-NFκB induction it did not influence flagellin-NFκB induction, suggesting the involvement of different pathways with different Se sensitivity.

4.3 Discussion

Aiming to contribute to knowledge of the mechanisms by which selenium influence health, studies in this chapter investigated the regulatory effects of Se supply on the NFκB inflammatory signalling pathways in colonic epithelial Caco-2 cells. For these studies cells were cultured plus and minus Se to study differential Se supply, and the endogenous cytokine TNFα and the exogenous bacterial flagellin were used as inducers of NFκB activation. To assess the activation status of NFκB signalling, a previously established 3X luciferase reporter construct (Carlsen et al., 2002), which was modified to be used in *in vitro* rather than *in vivo* experiments (described in Chapter 3, also see Figure 15) was employed. The response in endogenous expression of a known NFκB target gene, IL8, and a mediator of the inflammatory response was also investigated.

Se depletion was found to increase NFκB activation by TNFα. In studies using the NFκB luciferase reporter, a 1.3 fold increase in luciferase activity was found in cells grown in Se-depleted culture medium, compared with the luciferase activity detected in cells grown in Se-supplemented culture medium (see Figure 17 (B)). This increase was restricted to NFκB activation by TNFα as the baseline luciferase activity was maintained in Se- or Se+ groups (Figure 17 (A)). Consistently, in studies using semi-quantitative PCR to assess IL8 expression, Caco-2 cells cultured in Se-depleted medium exhibited a 1.5 fold increase in IL8 induction in response to TNFα, when compared to the IL8 level in the control Se-supplemented cells (see Figure 19). These

results suggested that Se supply regulates the TNFα-NFκB signalling pathway, and insufficient Se results in increased NFκB activation. Further, the increased NFκB status in Se depletion was found at both 2 and 4 hours after TNFα stimulation (Figure 17 (B)), suggesting that Se depletion affected NFκB activation by resulting in both faster and greater response to TNFα.

In comparison, in the studies of NFκB activation by flagellin using the NFκB luciferase reporter, no difference in induced luciferase activity was found in cells cultured in Se-depleted or Se-supplemented medium (see Figure 20), suggesting that Se supply was unable to affect the NFκB signalling pathway activated by flagellin. The investigation of flagellin-NFκB activation was also performed at the earlier and peaking stages (2 and 6 hours, respectively, see Figure 15) and neither time points were found with significantly change. Therefore, Se supply was found to differentially affect NFκB activation induced by different stimuli.

These results provide evidence of a regulatory effect of Se on NFkB activation in human gastrointestinal epithelial cells. In the human gut, constant exposure to bacteria and oxidative stress occurs (Hisamatsu et al., 2008, Duerkop et al., 2009), and Se has been suggested to help protect against the development of inflammation (Karp and Koch, 2006, Whanger, 2004). However, there is only limited knowledge of the underlying mechanism. The results in this chapter suggest that Se supply regulates NFkB signalling and target gene induction in gut epithelial cells in response to TNFα,

i.e. Se helps dampen the inflammatory response. Therefore, in addition to the established findings that Se affects the generation of inflammatory metabolites including the leukotrienes and prostanoids from arachidonic acid (Dey et al., 2009, Huang et al., 1999), these findings associating Se with regulation of NFkB signalling provide further insights into how Se is involved in mediating the cellular signalling responsiveness to endogenous or exogenous inflammatory stimuli.

The NFkB signalling pathway controls over 200 downstream target genes, many of which may directly participate in the development of inflammation, such as inflammatory cytokines, immuno-receptors and antigen presentation proteins (Pahl, 1999) (also see the NFkB target genes being collected on website: nfkb.org, updated up to 2008). As a result, the increased NFkB signalling response found in Se depletion may be expected to result in multiple inflammatory consequences through excessive expression of target genes. For instance, IL8 as a model NFkB target in this study is a chemoattractant to recruit neutrophils and to activate downstream immune cascades (Kucharzik and Williams, 2002, Roebuck, 1999a). IL8 has been suggested to be expressed in colonic epithelial cells and is associated with the development of inflammatory bowel disease (IBD) (Kucharzik and Williams, 2002, Ohkusa et al., 2009, Subramanian et al., 2008). Therefore, when Se is insufficient, the activities of TNFα, synthesized by epithelial cells and macrophages, could generate excessive IL8 production through the NFkB signalling pathway, which may further recruit lymphocytes and macrophages to the colonic epithelium and lead to excessive

inflammation. In this study, only the expression of IL8 was examined, but it would be interesting to examine the expression of other NFkB activated genes, for example, interleukin 6 (inflammatory cytokine), interleukin 12 (inflammatory cytokine), vascular cell adhesion molecule-1 (VCAM-1) and COX-2 (prostaglandin synthase), to assess the wider effects of Se depletion on inflammatory pathways.

The increase in NFkB activation, as detected using the reporter construct, and the increase in IL8 expression, as detected by semi-quantitative RT-PCR were consistent, but the extent of the changes was different. This variability may have arisen from the different techniques used in the analyses but it could also have been due to cis- or trans- elements in the promoter of the IL8 gene modifying the response to NFkB (Hoffmann et al., 2002b, Roebuck, 1999b). Therefore, although a 30% increase in NFkB activation in response to Se depletion appeared moderate, the resulting positive and/or negative effects on NFkB target genes cannot be predicted.

Compared with the TNFα-NFκB pathway, Se was shown to have no effect on the flagellin-associated NFκB activation pathway. Given the fact that these two NFκB activation signalling pathways utilized different receptors and signalling pathways (TNFα• TNFR1• NFκB and flagellin• TLR5• NFκB)••(Li and Lin, 2008, Simon and Samuel, 2007), it was perhaps not unexpected to find that Se depletion affected them differently. In addition, different catalytic processes are also involved in their respective activation mechanisms (details in Chapter 1, Section 1.2b and 1.2c, also see

previously in section 4.1). Therefore, based on the difference in these aspects, it is reasonable to conclude that Se depletion regulates the inflammatory signalling in some types of NFκB activation pathways but not in all. Further investigations to test the ability of Se to modulate the NFκB pathway activated by other inducers, e.g. H_2O_2 (as oxidative stress), IL1β (as another inflammatory cytokine) and LPS (as another bacterial component), would be potentially informative and helpful.

In summary, studies in this chapter investigated the regulatory effects of Se on NFκB signalling pathways and showed that Se depletion leads to greater NFκB activation by TNFα but not flagellin. However, these studies provide clues as to how Se exerts this effects; for example, if its effects are due to reduced activities of one or more of the selenoproteins. Therefore the next step in these studies was to investigate through which selenoprotein(s) Se regulates NFκB activation. It has been suggested that some of the major effects of Se are through its antioxidant proteins that protect the cells against oxidative stress and Redox signalling. Thus the effects of knockdown of GPx1 and GPx4 were studied in association with the NFκB signalling pathway and these studies will be described in the following chapters.

5. Effects of GPx1, SelW, SelH on NFκB inflammatory signalling

5.1 Introduction

In the previous Chapter the effects of Se depletion on the NFκB signalling pathway were studied in Caco-2 cells and found to result in increased NFκB activation in response to TNFα (Figures 17 and 19). Following on from this observation, the particular mechanisms underlying this connection were explored by investigating the role of individual selenoproteins in the modulation of NFκB inflammatory signalling by Selenium.

Of the selenoproteins identified so far, GPx1 has a relatively well-characterised antioxidant function (Brigelius-Flohe, 2006), and a high sensitivity to Se supply (Pagmantidis et al., 2005, Sunde et al., 2009). GPx1 is expressed in all tissues including the gastrointestinal epithelium (Moghadaszadeh and Beggs, 2006, Brigelius-Flohe, 1999), is present in the cytoplasm, and catalyzes the removal of the soluble hydroperoxides, such as H_2O_2 (Forstrom et al., 1979), but when coupled with phospholipase, also removes some membrane-associated oxidative fatty acids (Grossmann and Wendel, 1983). Because of these features of GPx1, and also because of the fact that the production of oxidative species has been frequently found associated with the activation of NFκB signalling in response to various types of inducers, including IL1β (Li and Engelhardt, 2006), TNFα (Jamaluddin et al., 2007) and Lipopolysaccharide (LPS) (Bhattacharyya et al., 2008), GPx1 has been suggested to be one of the selenoproteins potentially capable of regulating NFκB signalling pathway through its antioxidant ability (Li et al., 2001, Kretz-Remy et al., 1996, Crack et al., 2006).

In the breast cancer cell line MCF7, NFκB activation by endogenous cytokine IL-1β was found to be partially inhibited by overexpressed GPx1, as assessed by EMSA (to show NFκB DNA-binding) and measurement of luciferase activity of an NFκB reporter gene (Li and Engelhardt, 2006). In addition, this inhibitory effect was shown in parallel with decreased H_2O_2 production after IL-1β stimulation, so linking the regulatory effects of GPx1 on the IL-1β-NFκB response to its antioxidant ability. Moreover, the inhibition of NFκB activation by GPx1 overexpression was also found in the other pathways activated by UV irradiation, TNFα (0.5ng/ml) and H_2O_2 (1mM), with the recorded reductions being 25~30%, 25~30% and >50%, respectively (Li et al., 2001). Overall these results suggest that GPx1, as an antioxidant selenoprotein, is able to regulate the NFκB signalling pathway in the breast cancer cells. However, the transduction signal and the regulatory mechanisms controlling NFκB signalling pathways have been suggested to be hugely variable according to the cell-type and inducer (Gloire et al., 2006, Vallabhapurapu and Karin, 2009).

The effects of GPx1 on NFκB signalling in human gut cells remain to be determined. Therefore, the first aim of the work described in this chapter was to assess the function of GPx1 in relation to NFκB activation by TNFα in Caco-2 cells, so as to contribute to our understanding of the regulatory role of GPx1 in the functioning of the colonic epithelium. In addition, a second aim was to investigate the roles of two other selenoproteins, SelW and SelH, in the activation of NFκB signalling. SelW and SelH are two selenoproteins also known to be highly sensitive to Se supply (Pagmantidis et al., 2005, Kipp et al., 2009), and therefore they might also be responsible for the NFκB-regulatory effects observed in Se depletion. Moreover, SelW and SelH have also been suggested to have possible antioxidant functions

(Dikiy et al., 2007, Jeong et al., 2002b), but are not as well-defined as the GPx family, and therefore exploration of their individual impacts on NFκB signalling could contribute to our understanding of their function.

In order to assess the roles of these selenoproteins, the expression of GPx1, SelW and SelH was knocked down using siRNA in Caco-2 cells and then their respective effects on the TNFα-NFκB response were studied. Using this strategy, the experiments described in this chapter aimed to address the question of which selenoprotein(s) are involved in regulating NFκB inflammatory signalling pathways in Caco-2 cells.

Importantly, the biological effects observed following the knockdown of selenoproteins should provide different information compared with previous studies using the overexpression technique (Li and Engelhardt, 2006, Fan et al., 2003). The latter takes advantage of the selective delivery of DNA constructs containing a specific gene into cells to obtain a cell line with higher expression of the targeted gene and highlight its biological impacts. In contrast, siRNA knockdown inhibits gene expression by delivering small exogenous antisense oligoneucleotides into cells, which bind to the target mRNA sequence and cause a mRNA degradation process called RNA interference (Reynolds et al., 2004). Therefore the knockdown experiments serve as a model of loss-of-function study and can provide useful information in parallel with the previous studies by Se depletion.

In summary, the work described in this chapter aimed to investigate if any of the three particular selenoproteins, GPx1, SelW and SelH, were involved in the regulation of the TNFα-NFκB signalling pathway by Se depletion. The experiments used siRNA

knockdown to assess the individual functions of GPx1, SelW and SelH in relation to the TNFα-NFκB response. NFκB activation was assessed by NFκB luciferase reporter activity and/or the expression of NFκB target gene IL8, as assessed by semi-quantitative RT-PCR. In addition, investigations to assess the effects of Se depletion and GPx1 knockdown on ROS levels, and their influence on the system of redox control, were also conducted.

5.2 Results

5.2.1 Design of GPx1-specific siRNA and knock-down of GPx1 expression

In order to assess the function of GPx1, a siRNA specific to the *GPX1* gene was designed and used to knock down GPx1 expression in Caco-2 cells. The design of GPx1 siRNA was performed according to published methods (Reynolds et al., 2004, Ui-Tei et al., 2004). The GPx1-specific siRNA, 21nt in length, shared sequence homology of less than 15nt with the other human mRNA transcripts and therefore is expected to be specific to *GPX1* gene.

The GPx1-specific siRNA is complementary to sequences within exon 1, which are common to GPx1 transcript variants. *GPX1* gene has been suggested to encode at least two well-documented isoforms (Thierry-Mieg and Thierry-Mieg, 2006), variant 1 (NM_000581.2) (containing exon 1 and 2) and variant 2 (NM_201397.1) (containing mainly exon 1). However, the two GPx1 transcript variants appear not to function with major difference, since both of them encode the catalytic SeCys using the UGA codon within exon 1 (Mullenbach et al., 1988). Therefore GPx1 siRNA was designed to target exon 1. The sequence information of GPx1 siRNA and of GPx1 mRNA is shown as below:

Sequence Information of GPx1 siRNA

Target mRNA: aaggtactacttatcgagaat
SiRNA: gguacuacuuaucgagaau -uu (sense strand)
uu-ccaugaugaauagcucuua (antisense strand)

Sequence Information of GPx1 gene (exon 1 and exon 2)

[atgtgtgctgctcggctagcggcggcggcggcggcccagtcggtgtatgcctt
ctcggcgcgcccgctggccggcggggagcctgtgagcctgggctccctgcggggcaa
ggtactacttatcgagaatgtggcgtccctctgaggcaccacggtccgggactacac
ccagatgaacgagctgcagcggcgcctcggaccccggggcctggtggtgctcggctt
cccgtgcaaccagtttgggcatcag][gagaacgccaagaacgaagagattctgaat
tccctcaagtacgtccggcctggtggtgggttcgagcccaacttcatgctcttcgag
aagtgcgaggtgaacggtgcgggggcgcaccctctcttcgccttcctgcgggaggcc
ctgccagctcccagcgacgacgccaccgcgcttatgaccgaccccaagctcatcacc
tggtctccggtgtgtcgcaacgatgttgcctggaactttgagaagttcctggtgggc
cctgacggtgtgcccctacgcaggtacagccgccgcttccagaccattgacatcgag
cctgacatcgaagccctgctgtctcaagggcccagctgtgcctag]

- GPx1 exon 1 and exon 2 are separated and GPx1 siRNA mRNA target is underlined.

To test the ability of siRNA to knock down GPx1 expression, 5 X 10^5 Caco-2 cells were seeded into each well of a 6-well plate 24h before transfection. At 40-50% confluency, cells were treated with 5µl transfection reagent Lipofectamine 2000™ (Invitrogen) together with either 40, 80 and 120 pmol of GPx1 siRNA or an equal amount of a "scrambled" control siRNA. After 2 days, total RNA was harvested and semi-quantitative RT-PCR used to assess the expression of GPx1 and GAPDH transcripts (Figure 21 (A)). The scrambled control siRNA did not match any human mRNA transcripts and cells treated with this siRNA served as the control for normal GPx1 expression. GAPDH is a housekeeping gene and its transcript level was used as internal control. GPx1 expression in the GPx1-specific siRNA or the scrambled control siRNA treatment groups was calculated as a ratio of GPx1/GAPDH transcript levels (Figure 21 (B)). To show the knock-down, the adjusted GPx1 expression (GPx1/GAPDH ratio), of the GPx1 siRNA treatment group were further compared relative to the level of the scrambled control siRNA group, in which the level of the scrambled control group was standardized as '1' (Figure 21 (C)).

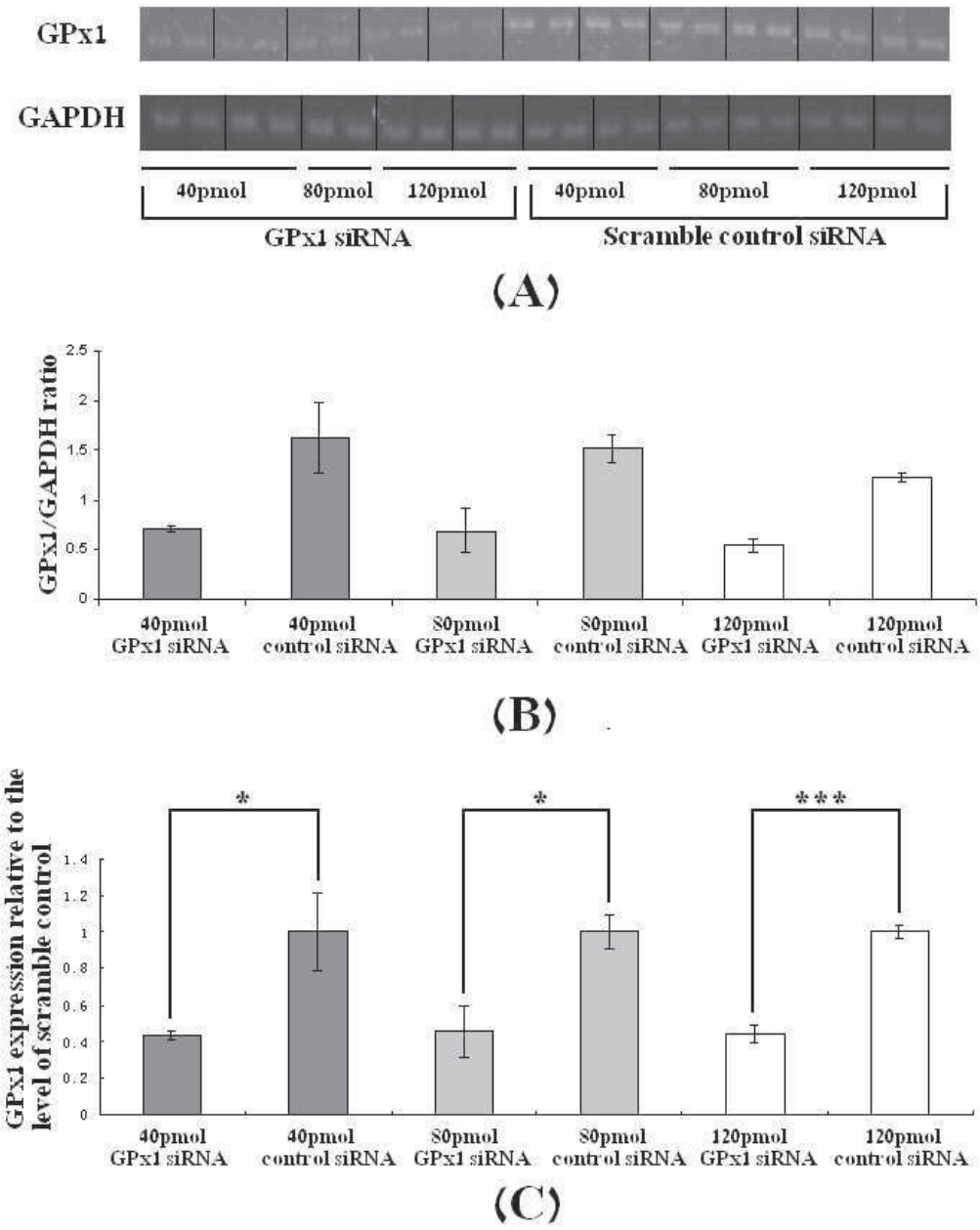

Figure 21: siRNA knock-down of GPx1 expression

(A): GPx1 expression as assessed by RT-PCR, was decreased following treatment with GPx1 specific siRNA, but no obvious change was found in the expression of GAPDH. (B): for quantification, the mRNA level GPx1 expression was adjusted to the GAPDH expression, and calculated as a ratio of GPx1/GAPDH. (C): the data were expressed in a ratio relative to the level of control siRNA group (standardized as '1'). Groups were compared using a Student 2-tail t test (*** p• 0.001; * 0.01<p• 0.05). n=4

As shown in Figure 21 (A), the GPx1 expression exhibited a clear decrease in the GPx1 siRNA treatment group, but not in the "scrambled" control siRNA treatment group, whereas the GAPDH levels were unchanged. This was confirmed by quantification of the bands and expression of the data as a ratio of GPx1 and GAPDH transcript levels (Figure 21 (B)). In this preliminary study, GPx1 knockdown assessed by comparing the GPx1 siRNA and the control siRNA treatment groups (Figure 21 (C)) was shown to be 55% at mRNA level and this effect was similar with 40, 80 and 120pmol siRNA treatments. This 55% knock down by siRNA was similar to the lowering of GPx1 level (60%) in the Se depletion experiments (Chapter 4, Section 4.2.1).

5.2.2 The impact of GPx1 siRNA knockdown on TNFα-induced NFκB-activation in NFκB luciferase reporter model

In order to study the effect of GPx1 siRNA knockdown on the NFκB signalling pathway activated by TNFα, Caco-2 cells transfected with NFκB or TATA (control) luciferase constructs were treated with 80pmol GPx1siRNA or scrambled control siRNA for 3 days to knock down GPx1 expression on protein level, incubated with 20ng/ml TNFα for 2-4 hours to activate NFκB and the total cell lysate harvested using 1X Reporter lysis buffer. To assess the extent of activation of NFκB signalling, quantification of luciferase activity was calculated per mg total cell lysate (data shown as relative luciferase activity (RLA)).

Incubation with TNFα for 2-4 hours resulted in NFκB activation in Caco-2 cells (Figure 15 (C)). To assess if GPx1 knock-down resulted in a faster or greater NFκB response, luciferase activity was assessed at baseline and 2 and 4 hours after addition of TNFα. As shown in Figure 22 (A), the baseline luciferase activities in NFκB and TATA Caco-2 cell models exhibited no difference in groups treated with lipofectamine, GPx1siRNA + lipofectamine, or scrambled control siRNA + lipofectamine. Therefore a decrease in GPx1 expression by siRNA treatment appeared to cause no change in the background luciferase reporter activity. To compare the difference between GPx1siRNA and scrambled control siRNA treatment groups after stimulation with TNFα, the RLA values were further calculated relative to the level of scrambled control siRNA group, which was standardized as '1'. The effects of GPx1 knockdown on luciferase activity 2 and 4 hours after TNFα activation are shown in Figure 22 (B) and (C), respectively.

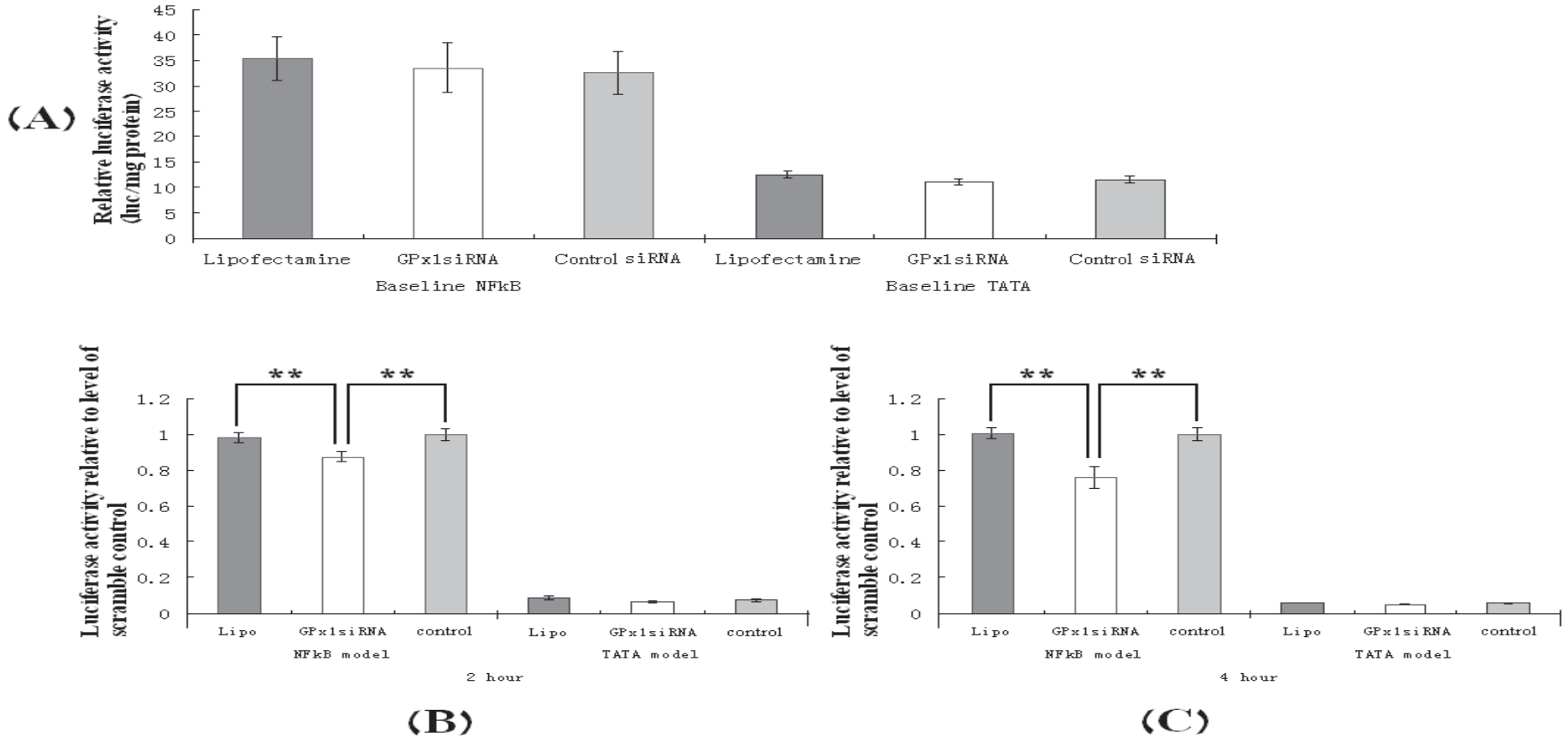

Figure 22: Imact of GPx1 siRNA knock-down on TNFα-induced luciferase activity of NFκB- and TATA-luciferase expressing Caco-2 cells

(A): Baseline luciferase activities (expressed as relative luciferase activity per mg protein, RLA) measured in both the NFκB- and TATA-luciferase Caco-2 cells following treatment with lipofectamine, lipofectamine and GPx1 siRNA, and lipofectamine and scrambled control siRNA for 3 days. (B) and (C): the luciferase activities measured in the NFκB- and TATA-luciferase Caco-2 cells following the same treatments (as above), and stimulation with 20ng/ml TNFα for 2 (shown in (B)) and 4 hours (shown in (C)). To show the effects of GPx1 knockdown, the luciferase activities (RLA values) in all groups were further calculated relative to the level of the scrambled control siRNA group (standardized as '1'). Groups were compared using a 2-tailed Mann-Whitney U-test (**$p<0.01$). n=9 in (B), 6 in (C).

Following stimulation with TNFα, NFκB activation, as reported by luciferase activity, was decreased in cells treated with 80pmol GPx1siRNA, as compared with the control cells treated with either lipofectamine, or lipofectamine and a scrambled control siRNA (Figure 22 (B) and (C)). The decrease was by ~13% at 2 hours and by ~25% at 4 hours after TNF treatment, respectively, and these effects were statistically significant (Figure 22 (B) and (C)). Therefore, GPx1 siRNA treatment appeared not to affect the baseline activity of the luciferase reporter, but resulted in decreased luciferase reporter activity in response to TNFα stimulation. No effect was observed in cells stably transfected with the TATA- (control) luciferase construct, suggesting that this observed effect was specific to the NFκB signalling pathway (Figure 22 (B) and (C)). In summary, in the present study using an NFκB luciferase reporter, GPx1 siRNA knockdown was found to down-regulate the TNFα-NFκB response by 13-25%, compared to the control treatment with scrambled control siRNA.

5.2.3 The impact of GPx1 siRNA knock-down on the expression of NFκB target gene IL8

The impact of GPx1 siRNA knockdown was further assessed by measuring the expression of the NFκB target gene, IL8, following TNFα stimulation. As shown in Chapter 4 (Figure 18), IL-8 was found to be expressed at low levels in Caco-2 cells but was up-regulated quickly after 1h TNFα stimulation (20ng/ml) of the cells. Therefore, in this study, Caco-2 cells were treated with 80pmol GPx1 siRNA or scrambled control siRNA for 3 days, incubated with 20ng/ml TNFα for 1 hour to induce IL8 expression, the total RNA harvested and semi-quantitative RT-PCR used to assess the expression of IL8, GPx1 and GAPDH. Semi-quantitative RT-PCR analysis of GPx1 expression was to validate that the siRNA treatment had decreased GPx1 mRNA expression. RT-PCR amplification of GAPDH as a house keeping gene was used as the internal control. The expressions of IL8 and GPx1 were calculated as a ratio of IL8/GAPDH or GPx1/GAPDH transcript levels, respectively. To compare the different effects of GPx1 siRNA and scrambled control siRNA treatments on the IL8 response, the IL8 expressions (IL8/GAPDH ratio) were calculated relative to the IL8 expression of the scrambled control siRNA group, which was standardized as '1'.

As shown in Figure 23 (A), GPx1 expression was clearly reduced in the GPx1 siRNA treatment groups, compared with the lipofectamine control or the scrambled control siRNA treatment groups, suggesting that GPx1 knockdown had occurred. In addition, as shown in Figure 23 (A), the IL8 PCR bands appeared slightly less intense in the GPx1 siRNA treatment group compared with those in the control treatment groups. The GAPDH PCR bands were unchanged in the groups of Lipofectamine treatment, GPx1 siRNA treatment and scrambled control siRNA treatment, confirming that the

expression of GAPDH, as an internal control gene, was not affected by the GPx1 siRNA.

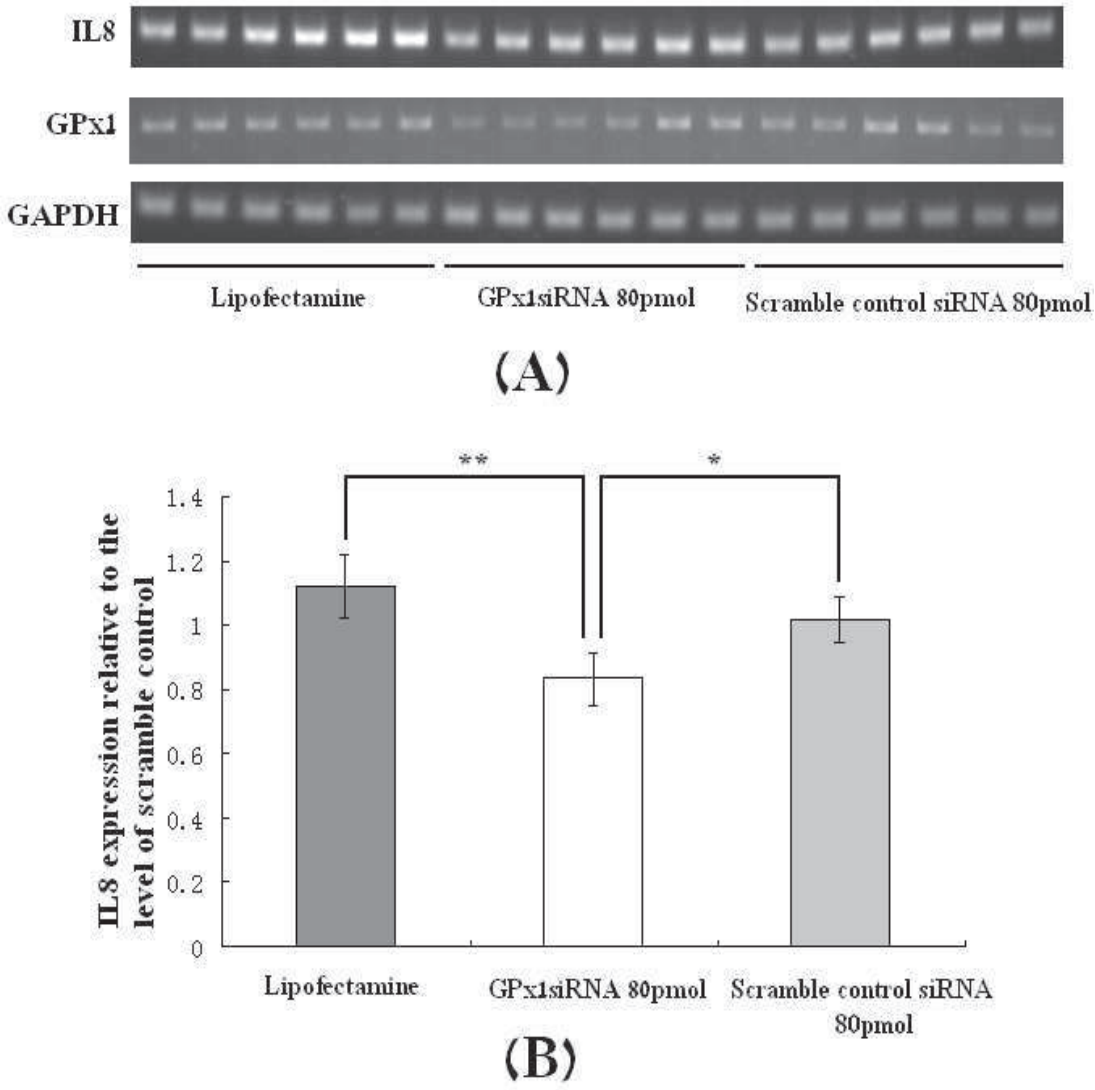

Figure 23: Impact of GPx1 siRNA knock-down on TNFα-induced IL-8 expression

(A): Semi-quantitative RT-PCR analysis of IL8, GPx1 and GAPDH transcript levels in Caco-2 cells treated with lipofectamine, lipofectamine and GPx1 siRNA, and lipofectamine and scrambled control siRNA and stimulated with 20ng/ml TNFα for 1 hour.
(B): quantitative analysis comparing the IL8 levels in the GPx1 siRNA and scrambled control siRNA treatment groups. IL8 expressions in the three treatment groups (as above) were calculated as a ratio of IL8/GPADH transcript levels, and then further expressed in ratios relative to the level of the scrambled siRNA treatment group, which was standardized as "1". Groups were compared using a 2-tailed Mann-Whitney U-test (** p• θ.01; * p• θ.05). n=8

As shown in Figure 23 (B), quantification of the data showed that IL8 expression in the GPx1 siRNA treatment group was approximately 80% relative to the IL8 level of the scrambled control siRNA treated cells, and this decrease in expression was statistically significant ($p<0.05$). Therefore, a 17% decrease of IL8 expression in response to TNFα was observed following GPx1 knockdown, and this is in concordance with the decreased NFκB-luciferase activity described in last section.

In summary, the results of both luciferase and IL8 measurements indicated that GPx1 knockdown negatively affected the NFκB response to TNFα in Caco-2 cells. This result was different to what would have been predicted from results of Se depletion experiments. To attempt to understand the potential mechanism(s) responsible for this difference, several additional experiments were performed:

1) A siRNA approach was used to test whether the knockdown of either of two other selenoproteins sensitive to Se nutritional status modulated NFκB signalling as assessed by the luciferase reporter;

2) Since ROS have been suggested to be both an essential mediator of NFκB activation and the target of Se depletion and GPx1 knockdown, ROS production in the Se depletion and GPx1 knockdown experiments were compared;

3) The expression profiles of major selenoproteins were compared between the two treatments, so as to assess if the differences in effects due to knockdown or Se depletion were related to the expression of other selenoproteins.

5.2.4 The impact of siRNA knockdown of SelW and SelH on TNFα-induced NFκB-activation

Two other selenoproteins sensitive to Se supply are SelW and SelH (Sunde et al., 2009). These particular selenoproteins may be involved in antioxidant protection and yet not fully characterized (Dikiy et al., 2007). Therefore, SelW and SelH could have a role in the up-regulated NFκB inflammatory signalling observed in Se depletion. To test this, the expressions of SelW and SelH were independently knocked down in Caco-2 cells using siRNA, and their resulting effects on the TNFα-NFκB response were studied using the luciferase reporter model.

Briefly, Caco-2 cells ($5X10^5$/well) transfected with NFκB- or TATA- (control) luciferase constructs were treated with lipofectamine and 80pmol SelW or SelH siRNA to knock down either SelW or SelH expression, or a "scrambled" control siRNA. Treatment with siRNA was for 3 days to reach an expected maximal knockdown of protein, the cells were incubated with 20ng/ml TNFα for 4 hours and total cell lysates were prepared from harvested cells using 1X Reporter lysis buffer. To assess the effects of SelW or SelH knockdown on NFκB activation, luciferase activity was calculated per mg total cell lysate and expressed as RLA value. To compare the difference in luciferase activity between the SelW/SelH siRNA and control siRNA treatment groups, the RLA values in all groups were further expressed in ratios relative to the level of the scrambled control siRNA treatment group, which was standardized as "1". In addition, total RNA from the cells treated with SelW or SelH siRNA, or control siRNA, was extracted 2 days after treatment and knockdown of mRNA expression assessed by RT-PCR. The SelW and SelH knockdown and their effects at 4 hours of TNFα-induced NFκB activation are shown in Figure 24.

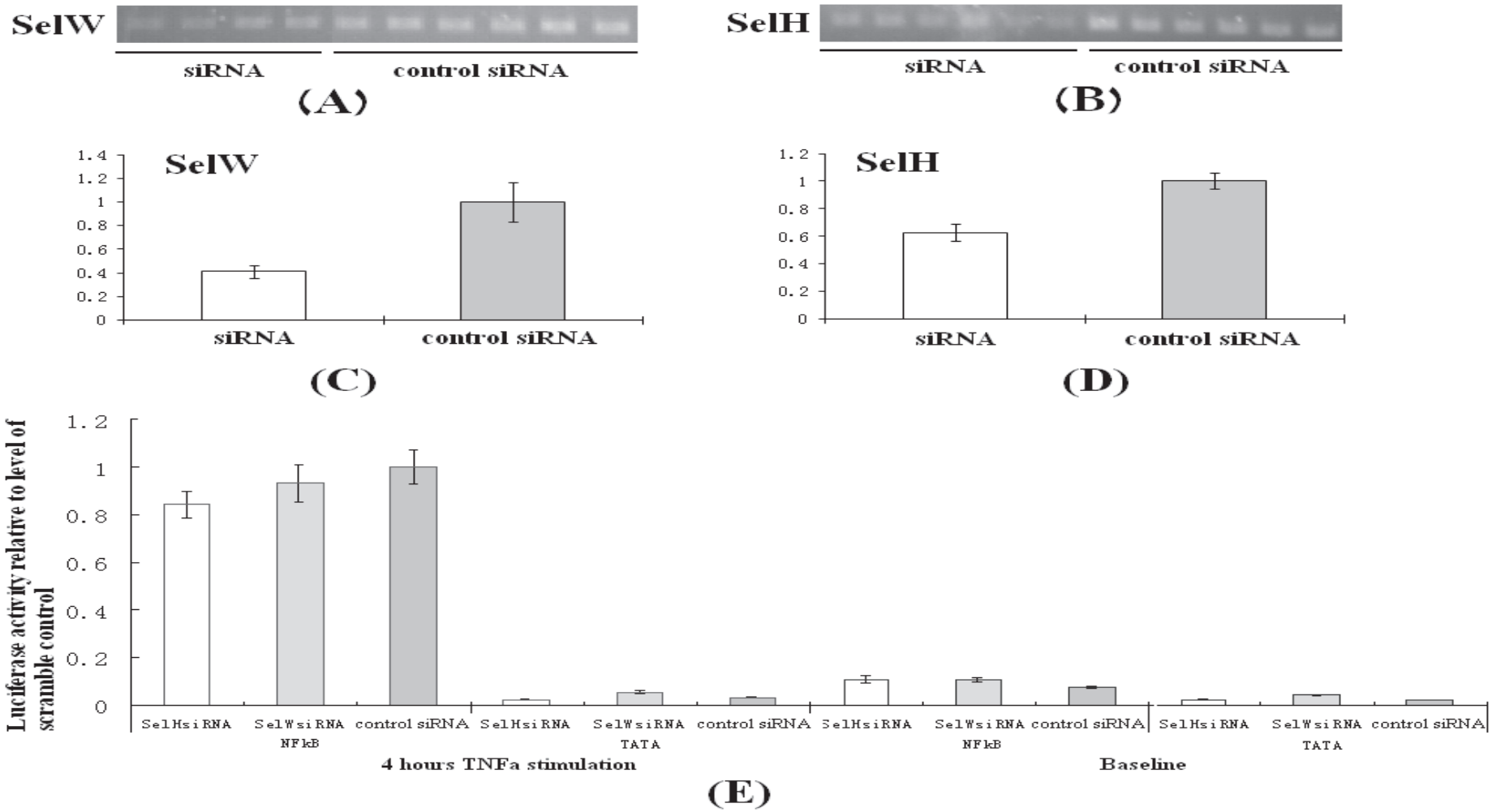

Figure 24: Impact of siRNA knock-down of SelH and SelW: TNFα-induced luciferase activity of Caco-2 reporter model

(A) and (B): Semi-quantitative RT-PCR analysis of SelW and SelH expression in Caco-2 cells treated with 80pmol SelW siRNA, SelH siRNA, or a scrambled control siRNA; (C) and (D): densitometry quantification of the PCR bands present in (A) and (B), to show the extents of SelW and SelH knockdown on mRNA level. (n=3)
(E): luciferase activities in cells treated with SelW siRNA, SelH siRNA, and control siRNA, and after stimulation with 20ng/ml TNFα for 4 hours (left panel), or at baseline (right panel). To show the effects of SelW or SelH knockdown, the luciferase activities (RLA values) in all groups were calculated relative to the level of the group treated with the control siRNA and stimulated with TNFα (standardized as '1'). Groups were compared using a 2-tailed Mann-Whitney U-test. (n=6)

As shown in Figure 24 (A) and (B), Caco-2 cells treated with either SelW or SelH siRNA, respectively, compared with the scrambled control siRNA treatment group, displayed decreased SelW and SelH expression. As shown in Figure 24 (C) and (D), data quantification revealed that the knockdowns of SelW and SelH were 60% and 40%, respectively.

As shown in Figure 24 (E), using luciferase activity to assess NFκB activation following 20ng/ml TNFα stimulation, no significant differences in RLA values were found between either the SelW siRNA or SelH siRNA treatment groups, and the scrambled control siRNA treatment group. Therefore, knockdown of SelW and SelH appeared to confer no change in the TNFα-NFκB response compared with the scrambled control, as assessed by the NFκB-luciferase reporter system. These results suggested that although the decreased expression of SelW and SelH would have occurred in Se depletion, the decreases of these proteins would not be expected to influence the NFκB activation in response to TNFα in Caco-2 cells.

5.2.5 Comparison of ROS production in Se depletion and GPx1 siRNA knock-down

Results described previously indicated that NFκB activation by TNFα was increased following Se depletion (Figures 12 and 14), and yet decreased by GPx1 siRNA knock-down (Figures 16 and 17). Thus, while Se depletion and GPx1 siRNA knock-down both reduced the expression of GPx1 by approximately 60%, their effects on the regulation of the NFκB signalling pathway were contrary. In order to try to explain this apparent contradiction, the differences in background cellular environment between the Se depletion and GPx1 knockdown experiments were investigated. The aim was to try to understand which mechanisms were essential for regulation of NFκB signalling and responsible for the different effects observed in response to the two treatments.

As mentioned previously, ROS have been suggested to be one of the key mediators during the activation process of the NFκB signalling pathways (Vallabhapurapu and Karin, 2009). Specific to TNFα-NFκB signalling transduction, the production of oxidative species following TNFα stimulation has also been suggested to be crucial for the activation of the TNF receptor complex (TNFα-TNFR1-TRADD-RIP-TRAF2), phosphorylation of NFκB inhibiting protein IκB and release of NFκB into nucleus (Jamaluddin et al., 2007, Gloire et al., 2006, Li and Lin, 2008). ROS production, as a result of TNFα stimulation, has been suggested to arise from TNF-induced caspase-8 apoptosis in mitochondria (Gloire et al., 2006) and/or from the NADPH oxidases responding to the activated TNFR1 receptor (Kim et al., 2007, Yazdanpanah et al., 2009, Li et al., 2009). To investigate this factor, ROS levels in Caco-2 cells grown in

Se-depleted and Se-supplemented medium, and ROS levels in cells treated with GPx1 siRNA and scrambled control siRNA, were measured and compared.

To test the potential changes in ROS levels induced by Se depletion, Caco-2 cells seeded in a 96-well plate were grown for 3 days in Se-depleted (Se-) or Se-supplemented (Se+) culture medium (90% confluent at day 3). To investigate the changes in ROS production caused by GPx1 siRNA knockdown, Caco-2 cells seeded in a 96-well plate were treated with lipofectamine and GPx1 siRNA or scrambled control siRNA for 3 days (in 90% confluency at day 3). Cells were washed 3 times with 1XHBSS and incubated with 25μM 5-(and-6)-carboxy-2´7´-dichlorodihydrofluorescein diacetate (Carboxy-H_2DCFDA) for 15 minutes (as described in Chapter 2, Section 2.1.22). Carboxy-H_2DCFDA is a fluorescent dye permeable to the cell membrane and is able to label the oxidative species in a subcellular environment (Shimizu et al., 2004). The labelled Caco-2 cells were washed 3 times with 1XHBSS and the ROS levels measured at 495/529nm wave length. Comparisons in ROS levels following Se depletion or GPx1 knockdown are shown in Figure 25.

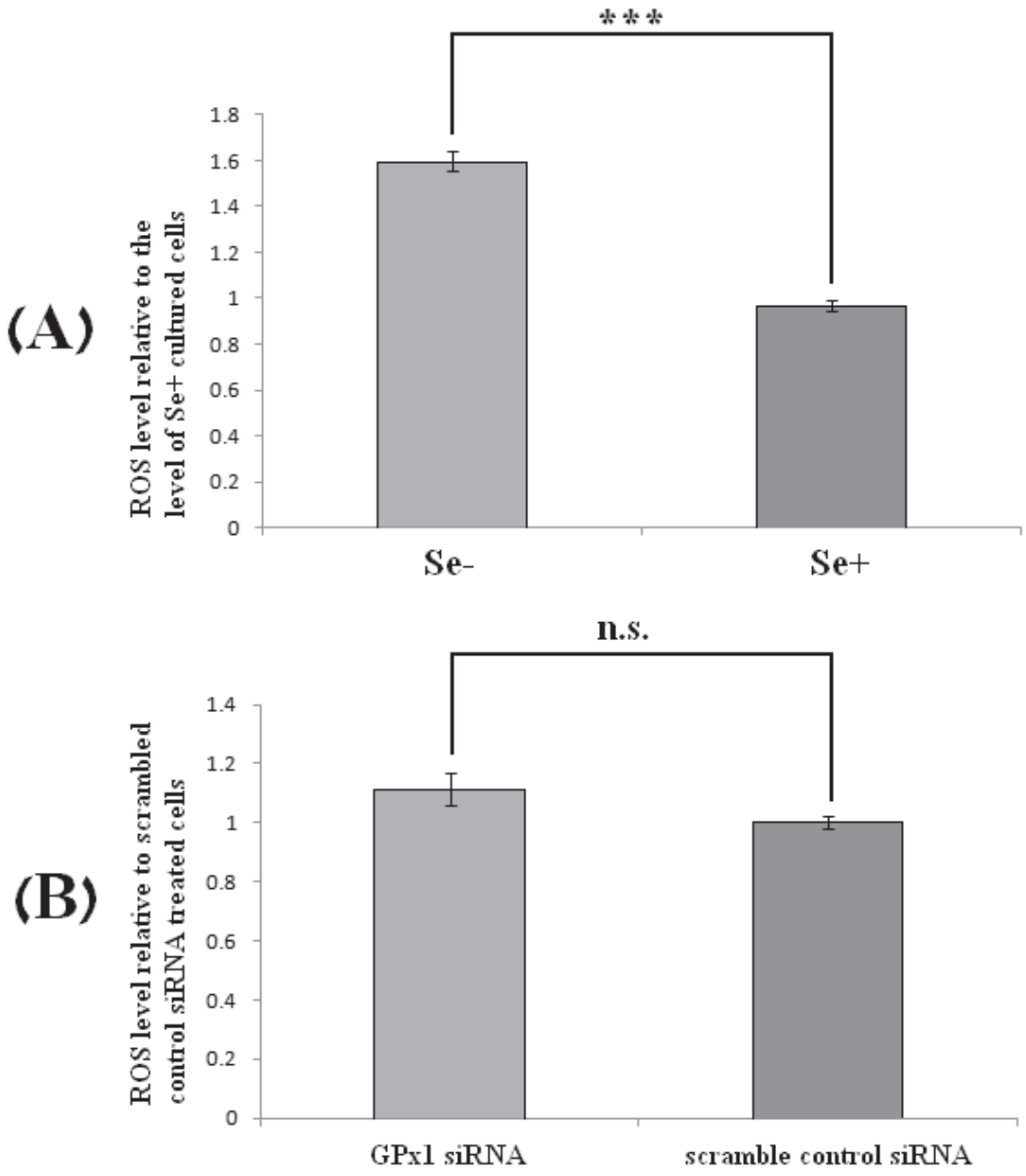

Figure 25: Impact of Se depletion and GPx1 knock-down on ROS levels

(A): Comparison of ROS levels in Caco-2 cells grown in the Se-depleted (Se-) and Se-supplemented (Se+) culture medium. ROS levels were determined by measuring the fluorescent activity of the oxidized Carboxy-H_2DCFDA and expressed relative to the level of the Se+ group (standardized as "1").
(B): Comparison of ROS levels in Caco-2 cells treated with GPx1 siRNA and scrambled control siRNA. The ROS level of the GPx1 siRNA treatment group was expressed relative to the level of the control siRNA group (standardized as "1"). Groups were compared using a 2-tailed Mann-Whitney U-test (*** p• 0.001; n.s: not significant). n=12 for (A) or 24 for (B)

To compare the effects of Se depletion with Se supplementation, the average fluorescent activity of the oxidized Carboxy-H_2DCFDA measured in the Se- medium-grown cells were expressed in a ratio relative to the average activity measured in the Se+ medium-grown cells, which was standardized as '1' (Figure 25 (A)). Results showed that Caco-2 cells cultured in Se- medium exhibited higher (~1.6 fold, $p<0.001$) ROS levels than the cells cultured in Se+ medium, suggesting that Se depletion resulted in an increase of ROS levels in Caco-2 cells.

In addition, the results shown in Figure 25 (B) compared the ROS levels in the GPx1 siRNA and control siRNA-treated Caco-2 cells (standardized as '1') and found that these cells exhibited comparable ROS levels between the two treatment groups, the difference between which was not statistically significant ($p=0.07$). Therefore, GPx1 knockdown appeared not to cause any obvious effects on ROS levels in Caco-2 cells.

In summary, the results of studies suggested that Se depletion elevated ROS levels in Caco-2 cells whereas GPx1 knockdown had no effect. This therefore provides a potential explanation of why the TNFα-induced NFκB activation was differentially affected by Se depletion and by GPx1 knockdown. To further search for any differences in background cellular environment between Se depletion and GPx1 knockdown, the effects of these treatments on the selenoprotein gene expression were studied.

5.2.6 Comparison of the expression of antioxidant selenoproteins in Se depletion and GPx1 siRNA knock-down

As described previously, Se depletion and GPx1 siRNA knockdown in Caco-2 cells were shown to have different regulatory effects both on the TNFα-NFκB signalling pathway, and on the production of cellular oxidative stress. Yet in both experiments the regulatory effects on NFκB signalling and ROS was in concordance (increased NFκB activation and increased ROS production in Se depletion; decreased NFκB activation and unchanged ROS production in GPx1 knockdown). These results suggested that the differential regulation of NFκB activation induced by TNFα, relied on the differential control of ROS production in Caco-2 cells either by Se depletion or by GPx1 knockdown. Therefore, a retrospective study to investigate the upstream antioxidant system was carried out to interpret the present data, and the expression of antioxidant selenoproteins was compared between Se depletion and GPx1 knockdown experiments.

Selenoproteins incorporate Se and depleted Se supply is known to decrease the synthesis and activity of a number of selenoproteins including GPx1, GPx4, SelW, SelH and TrxR1, and increase the expression of GPx2 (Pagmantidis et al., 2005, Bellinger et al., 2009). In some cases this is paralleled by a decrease in mRNA expression (Pagmantidis et al., 2005, Kipp et al., 2009). Among the selenoproteins affected by Se depletion, GPx1, GPx4, TrxR1, TrxR2 and GPx2 are well-characterized antioxidants with different substrate specificity. For example,

GPx1 and GPx2 matabolise water soluble oxidative species such as H_2O_2, whereas GPx4 is also able to catalyze the lipid hydroperoxides present on the cell membrane (Brigelius-Flohe, 1999). SelW and SelH, on the other hand, have also been suggested to have possible antioxidant functions (Whanger, 2009, Dikiy et al., 2007). Therefore, depleted Se supply would be expected to cause dramatic changes in the balance of the antioxidant system, by affecting multiple antioxidant selenoproteins and as a result, releasing variable types of oxidative substrates. In comparison, GPx1 knockdown would be expected to affect only the expression of GPx1, and release the water soluble oxidative species. However, the expression of the other antioxidant selenoproteins, despite presumably not being directly affected by the siRNA treatment, had not been assessed following GPx1 knockdown.

To assess the expression of the selenoproteins, Caco-2 cells were cultured for 3 days in Se-depleted (Se-) or Se-supplemented (Se+) medium, or treated with lipofectamine and GPx1 siRNA or scrambled control siRNA for 3 days to induce GPx1 knockdown. In all groups, total RNA was harvested and semi-quantitative RT-PCR was used to assess the mRNA expression of GPx1, GPx4, GPx2, SelW, SelH and the house keeping gene GAPDH as an internal control. In order to show the effects of Se depletion or GPx1 knockdown, the expression of each selenoprotein gene was further compared between Se- and Se+ culture conditions (expressed in a ratio relative to the level of Se+ group), or between GPx1 siRNA and scrambled control siRNA treatments (expressed in a ratio relative to the level of scrambled control siRNA

group). The expression profiles of GPx1, GPx4, SelW, SelH and GPx2 in Se depletion and GPx1 knockdown are presented in Figure 26.

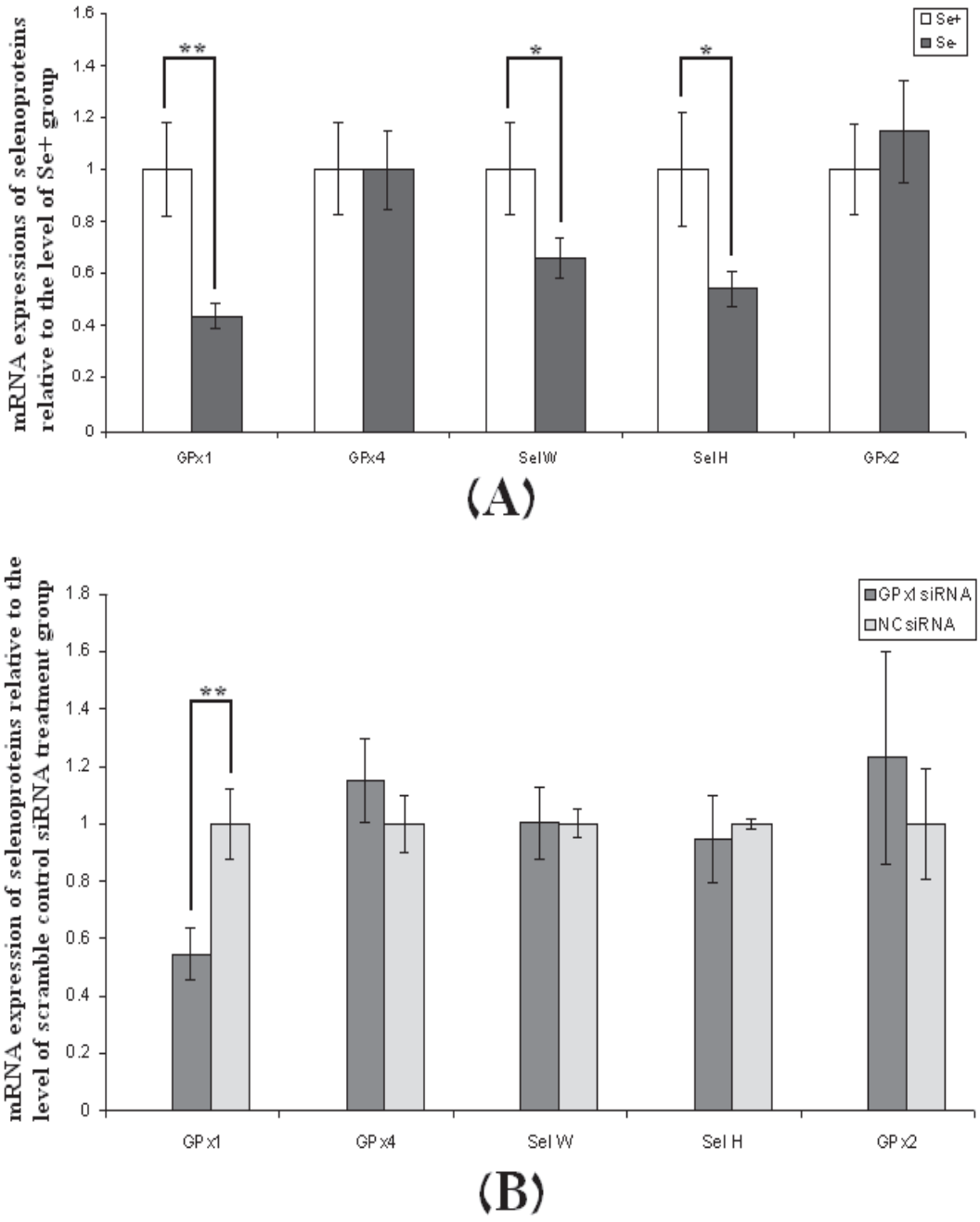

Figure 26: Expression profile of antioxidant selenoprotein mRNA in Se depletion and GPx1 knockdown

(A): The expression of the selenoprotein mRNAs encoding GPx1, GPx4, SelW, SelH and GPx2 in Caco-2 cells grown in Se- and Se+ medium. Expression was adjusted to the GAPDH transcript level and in all comparisons the Se- group data expressed in a ratio relative to the Se+ group data (standardized as '1'). (B): The expression of the above selenoproteins in the cells treated with GPx1 siRNA and control siRNA. Data in the GPx1 siRNA treatment group expressed relative to the data in the control siRNA treatment group. Groups were compared using a Student 2 tail t-test. (**$p<0.01$; * $p<0.05$). n=3

mRNA expression of the antioxidant selenoproteins was found to be differently affected by Se depletion and by GPx1 knockdown. In Se depletion (Figure 26 (A)), the Se- group exhibited significant decrease of expression of GPx1 (~60%), SelW (~40%) and SelH (~50%) mRNAs, compared with the Se+ control group. The expression of GPx4 and GPx2 mRNAs were not significantly changed between Se- and Se+ groups. In comparison, in GPx1 knock-down (Figure 26 (B)), which was shown to reduce the GPx1 mRNA level by ~50%, the expression of SelW and SelH mRNAs were not affected compared with the control siRNA treatment group. The expressions of GPx4 and GPx2 were also unchanged. Therefore, Se depletion was found to result in the decreased expression of several antioxidant selenoprotein genes, whereas GPx1 knockdown was found only to decrease the expression of GPx1. These results indicated that the overall antioxidant system was regulated differently by Se depletion and GPx1 knockdown, and therefore suggested a possible explanation of how the different regulation of ROS level and NFκB activation occurred following the two experimental treatments.

5.3 Discussion

In the previous chapter the effect of Se supply on the NFκB inflammatory signalling pathway was studied. An increased activation of an NFκB-driven reporter together with increased expressional response of NFκB target gene IL8 to TNFα were found in Caco-2 cells, when Se was depleted in the culture medium. To understand how Se depletion exerts this effect and elevates NFκB signalling, the individual functions of the selenoproteins GPx1, SelW and SelH in relation to NFκB regulation were examined, the different impacts on cellular ROS level between Se depletion and GPx1 knockdown were compared, and the influence on the antioxidant system between Se depletion and GPx1 knockdown was examined by assessing the expression of the antioxidant selenoproteins under the two conditions.

GPx1, SelW and SelH, whose expression is dramatically decreased in Se depletion (Pagmantidis et al., 2005, Kipp et al., 2009), were studied using the siRNA knockdown technique, and the impact of knockdown on the activation of NFκB signalling pathway was assessed. As shown in Figure 21 and Figure 24 (A-D), treatment of Caco-2 cells with 80pmol (~30nM) siRNA resulted in ~55%, ~50% and ~40% knockdown of gene expression of GPx1, SelW and SelH, respectively, as judged by mRNA levels. These knockdown levels were comparable to the levels of reduction in gene expression observed following Se depletion, which were ~60%, ~40% and ~50% for GPx1, SelW and SelH, respectively (shown in Figure 26, also discussed later). Since a siRNA knockdown experiment is generally specific to the

gene of target (Reynolds et al., 2004), experiments using siRNA knockdown were carried out to help to dissect the complicated picture of Se depletion, and provide useful information about whether, and if so, how, the decrease of expression of each selenoprotein may affect the TNFα-induced NFκB signalling in Caco-2 cells.

Using an NFκB-luciferase reporter to monitor the transcriptional activation of NFκB signalling, and using semi-quantitative PCR to assess the expression of the NFκB target gene IL8, GPx1 siRNA knockdown by 55% was found to result in significantly decreased luciferase activity (by 25% at 4 hours after addition of TNFα), and decreased IL8 expression (by 17% at 1 hour after addition of TNFα), compared with the groups treated with a scrambled control siRNA (shown in Figure 22(B) and Figure 23(B)). In addition, this regulatory effect was found specific to the NFκB signalling in response to TNFα, since the baseline luciferase activities were similar between the GPx1 siRNA and scrambled control siRNA treatment groups. Therefore, GPx1 knockdown was found to inhibit the TNF-NFκB signalling pathway and its effect was contrary to the effects of Se depletion, where a 30% increase of NFκB-luciferase activity and a 50% increase of IL8 expression were observed.

Using the NFκB-luciferase reporter, siRNA knockdown of SelW (50%) and siRNA knockdown of SelH (40%) did not change the NFκB signalling response to TNFα (shown in Figure 24 (C)). These data indicated that these two selenoproteins were not responsible for the effects on NFκB signalling caused by Se depletion.

Knockdown of each of three individual selenoproteins known to respond to Se depletion did not reproduce the elevated NFκB signalling found in Se depletion. Therefore the regulatory effects of Se depletion cannot be explained by the reduced expression of either GPx1, SelW or SelH, suggesting that either an alternative selenorprotein is affected by depleted Se supply and is responsible for the increased NFκB signalling, or that the combined reduced expression of multiple selenoproteins, together, caused the increased TNFα-NFκB response. The other selenoproteins known to be affected by Se supply include TrxR1 (Crosley et al., 2007) and GPx4, the expressions of which have been reported to be reduced mildly, by~30%, in cells grown in the Se-depleted medium (Pagmantidis et al., 2005). TrxR1 and GPx4 are also essential antioxidant enzymes and therefore potential modulators for NFκB signalling. Thioredoxin and thioredoxin reductases (TrxRs), particularly TrxR1 (cytosolic TrxR) and TrxR2 (mitochondrial TrxR), have been previously described as negative and positive regulators of NFκB activation, respectively, in Hela cells and vascular endothelial cells (see Chapter 1 Section 1.1d) (Schenk et al., 1994, Glineur et al., 2000, Sakurai et al., 2004). GPx4 overexpression has been previously associated with decreased NFκB nuclear translocation in response to UV-irradiation in fibroblasts (Wenk et al., 2004). Therefore these additional two or three selenoproteins are possible candidates responsible for the elevated TNFα-NFκB activation seen in Se depletion and need to be further examined. It is also possible that the increased NFκB signalling found in Se depletion was caused by the overall repression of multiple selenoproteins, which was supported by later experiments when the regulatory effect

on ROS was studied, in Caco-2 cells either Se depleted or subject to GPx1 siRNA knockdown.

The close correlation of ROS levels with activation of the NFκB signalling pathway has been suggested in the previous publications, in which ROS have been documented either to directly activate NFκB signalling (Gloire et al., 2006, Fan et al., 2003, Taylor et al., 2004), or in some other circumstances, function as a secondary messenger to mediate the activation of NFκB when the signalling cascade was initiated by either cytokines such as TNFα or IL1β (Jamaluddin et al., 2007, Bol et al., 2003, Li et al., 2009), or bacterial components such as LPS (Bhattacharyya et al., 2008, Sanlioglu et al., 2001). Of particular relevance to the present study, ROS have also been suggested to be critical for the NFκB activation induced by TNFα, and the major findings in this regard are summarized briefly as follows:

1. In breast cancer cells, an increase of endosomal H_2O_2 production has been observed after TNFα stimulation (Li and Lin, 2008). When this H_2O_2 production was inhibited by either GPx1 overexpression (Li et al., 2001) or NADPH oxidase 2 (Nox2) siRNA (Li et al., 2009), TNFα-induced NFκB signalling was decreased. In addition, this H_2O_2 production has also been associated the recruitment of TRAF2 to the TNFR1 receptor (Li et al., 2009). Therefore, ROS production by TNFα has been suggested to be essential for the TNFα-NFκB response in certain cell types.

2. The ROS production by TNFα may be from at least two sources, the mitochondria and/or the NADPH oxidases. TNFα is capable of inducing the caspase-8 apoptosis pathway and the latter could result in the release of ROS from mitochondria (Morgan et al., 2008, Hsu et al., 1996, Tang et al., 2009). In addition, endosomal H_2O_2 production by TNFα has been suggested to be from the Nox2 complex (Li et al., 2009, Yazdanpanah et al., 2009).

3. As described in Chapter 1 Section 1.2b-1.2d, ROS production can mediate the NFκB signalling through several possible mechanisms. ROS are capable of enhancing the activities of the MAP3Ks, including NFκB inducing kinase (NIK) (Li and Engelhardt, 2006, Kim et al., 2008) and MAP3K1 (Lee and Koh, 2003, Lee et al., 2008), which participate in the phosphorylation cascade (MAP3Ks→IKK→IκB →NFkB) for NFκB activation. ROS are also capable of inhibiting the MAPK phosphatases that counteract with the MAP3Ks, and therefore help to maintain the active state of NFκB signalling (Kamata et al., 2005, Farooq and Zhou, 2004). Although in the present study the particular MAP3K kinase and regulatory mechanisms, by which ROS might mediate the TNFα-NFκB response in Caco-2 cells, remained not characterized, it is clear that ROS play an essential role in the activation of TNFα-induced NFκB signalling (Jamaluddin et al., 2007, Li and Lin, 2008).

4. The production of ROS has also been suggested to mediate the cross-talk between apoptosis signalling and the NFκB inflammatory signalling, both of which can be

activated by TNFα (Chen and Goeddel, 2002). ROS production, in large amounts, has been suggested to lead to apoptosis and/or necrosis, and in moderate to small amounts, has been suggested to activate the JNK and NFκB signalling pathways (Gloire et al., 2006). Particularly, NFκB signalling, after being activated, can repress apoptosis by expressing anti-apoptotic cytokines (Nakano et al., 2006, Kamata et al., 2005). Therefore, in the present study, the ROS production by TNFα in Caco-2 cells was expected to be in a relative small amount and subject to the regulation by Se and antioxidant selenoproteins.

Because of the critical impact that ROS could have in modulating the activation of NFκB signalling pathway, it was essential for the present study to compare the regulatory effects of Se depletion and GPx1 knockdown on the ROS levels in Caco-2 cells. As assessed by ROS-indicating dye Carboxy-H_2DCFDA((Shimizu et al., 2004), Figure 25 (A)), a statistically significant increase of ROS level, by ~1.6 fold, was found in Caco-2 cells grown in Se- medium, compared with the ROS level in control cells grown in Se+ medium. In contrast, in the GPx1 knockdown experiment (Figure 25 (B)), no difference in ROS level was found in cells treated with GPx1 siRNA or scrambled control siRNA. Therefore, these results suggested that the ROS level was differently affected by Se depletion and by GPx1 knockdown.

Taking together the NFκB reporter data, the IL8 expression measurements, and the ROS data, it is clear that effects of Se depletion and GPx1 knockdown are distinct.

Whereas Se depletion resulted in both the up-regulated NFκB signalling in response to TNFα (Figure 17 and 19) and the increased ROS level in Caco-2 cells (Figure 25 (A)), siRNA knockdown of GPx1 (Figure 21) resulted in down-regulated NFκB signalling (Figure 22 and 23) and no change of the ROS level (Figure 25(B)). Therefore, the regulatory effects of Se depletion and GPx1 knockdown on the TNF-NFκB activation are largely concordant to their regulatory effects on ROS. Since ROS has been suggested widely to be an essential mediator in the activation of NFκB signalling, it would be logical to speculate that the NFκB-regulatory effects of Se depletion and GPx1 knockdown were *via* their respective impacts on ROS, with the increased activation of NFκB signalling by Se depletion being associated with increased ROS levels, and the decreased activation of NFκB signalling by GPx1 knockdown occurring in the absence of any changes in ROS levels.

Se depletion is known to cause expressional changes in a number of selenoproteins (Bellinger et al., 2009), whereas GPx1 knockdown by siRNA was expected to specifically decrease the expression of GPx1. Using semi-quantitative RT-PCR to assess the mRNA expression of antioxidant selenoproteins including GPx1, GPx4, SelW, SelH and GPx2, Se depletion was shown to dramatically decrease the expressions of GPx1 (by 60%), SelW (by 40%) and SelH (by 50%), but to have no obvious effect on the expressions of GPx4 and GPx2 (Figure 26 (A)). Sensitivity of GPx1, SelW and SelH to Se depletion is similar to previous studies in Caco-2 cells (Pagmantidis et al., 2005) and in mouse colon (Kipp et al., 2009). Whereas early work

showed changes in GPx4 (decrease by ~24%) and GPx2 (increase by ~63%) mRNA expression (assessed by RNA hybridisation) following Se depletion in Caco-2 cells (Pagmantidis et al., 2005), the present work showed no changes. This was likely to be an effect of different techniques used for assessing mRNA expression. However, it is clear that Se depletion alters the balance of multiple antioxidant selenoproteins.

Using the same method, GPx1 siRNA knockdown was shown to decrease the expression of GPx1 but did not affect the gene expression of the other antioxidant selenoproteins investigated (Figure 26 (B)). Therefore, the sustained expression of these selenoproteins, including GPx2 and GPx4, which are both known antioxidants more efficient than GPx1 (Brigelius-Flohe, 2006, Brigelius-Flohe, 1999), was found to be a major difference between the Se depletion and GPx1 knockdown experiments. This difference could be responsible for the different impact on the control of redox-signalling and NFκB signalling.

In GPx1 knockdown, although no direct evidence has been found by the present study to support this, compensation by the other Se dependent and/or independent antioxidants could occur, resulting in consistent ROS levels and decreased NFκB activation following TNFα stimulation. Indeed, as shown in Figure 26 (B), there was a trend towards the average GPx2 expression being higher in the GPx1 siRNA treatment group compared with the control group but the difference was not significantly different, probably due to the large standard errors caused by the limited

number of the experiment repeats. Therefore, it would be useful to carry out repeat measurements of GPx2 mRNA expression in the GPx1 siRNA treated cells.

In the present study, the investigations using semi-quantitative RT-PCR fundamentally revealed how antioxidant selenoproteins respond to changes in Se supply (Se depletion) or selenoprotein expression (GPx1 knockdown), resulting in different biological consequences (NFκB inflammatory signalling). However, additional or even more precise information could have been obtained, if time had been allowed, using real-time PCR to strengthen the current investigation assessing the mRNA level, using Western bloting to assess the protein levels or enzymatic assays to assess protein activity (for example, measurement of GPx1, GPx4 and TrxR1 activities in reduction of their specific ROS targets would have complemented this work) (Crane et al., 2009, Campbell et al., 2007). In addition, TrxR1 and TrxR2 are other essential antioxidant selenoproteins (briefly reviewed in Section 1.1d) but have not been included in the present data (Figure 26) and their expression profiles in the Se depletion and GPx1 knockdown experiments remain to be determined in future. The proposed compensation in antioxidant expression could possibly occur at the protein expression or protein activity level.

Moreover, a further possible strategy would be to knock down more than one antioxidant selenoprotein together using combined siRNA treatments. For example, double transfection of Caco-2 cells with both GPx1 and GPx2 siRNAs would

decrease the expression of both GPx1 and GPx2, mimicking the double knock-out (GPx1 -/- and GPx2 -/-) mouse model which exhibited susceptibility to bacterial infection in colon (Esworthy et al., 2003). Investigations of the effects of double knock-down (GPx1 and GPx2, or GPx1 and GPx4) on NFκB response in Caco-2 cells would provide additional insights in how the antioxidant selenoproteins compensate for each other's function and contribute to the control of inflammatory signalling pathways.

In summary, the experiments described in this chapter investigated the influence of siRNA knockdown of GPx1, SelW and SelH on the TNFα-induced activation of NFκB signalling pathway. The results showed that none of these knockdown experiments was able to reproduce the increased NFκB response observed following Se depletion, but resulted in either decreased NFκB response (by GPx1 knockdown, opposite to the influence by Se depletion) or unchanged NFκB response (by SelW or SelH knockdown). Although in these studies the knockdown levels of these selenoproteins were comparable to their respective reductive levels by Se depletion, their distinct regulatory effects suggested that, individually, the decreased expression of GPx1, SelW or SelH was not able to cause the increased response of NFκB signalling. These results suggested that most likely, Se depletion elevates the TNFα-NFκB activation through repressing the expression of multiple antioxidant selenoproteins, rather than through the decreased expression of any single one. Alternatively, it remains possible that the effect of Se depletion resulted from the

decreased expression of a selenoprotein other than GPx1, SelW and SelH. In the next Chapter the effects of GPx4 knockdown were studied in relation to the NFκB signalling induced by TNFα and flagellin.

The present finding that GPx1 knockdown resulted in decreased TNF-NFκB response and IL8 gene expression is, interestingly, contrary to the suggestions from earlier publications, which described stably-transfected cells overexpressing GPx1 and found that in these cells the H_2O_2 production was lowered and the activation of NFκB signalling was repressed (Li et al., 2001, Kretz-Remy et al., 1996, Fan et al., 2003, Ishibashi et al., 1999, Li and Engelhardt, 2006). This conflict in the data might be explained by the different techniques in use. GPx1 knockdown models loss of function, whereas GPx1 overexpression models gain of function. Although gain of GPx1 function could enhance its beneficial effects on antioxidant protection and inhibition of the inflammatory signalling, partial loss of GPx1 function may not result in the converse effects, perhaps due to the compensatory activities of the other antioxidant proteins.

In previous studies using the GPx1 knock-out (GPx1 -/-) mouse model, no obvious developmental abnormalities were observed and the mice remained healthy in hyperoxia, a condition causing excess hydroperoxide challenge (Ho et al., 1997). However, when GPx1 -/- knockout was coupled with GPx2 -/- knockout, the double knockout mouse model exhibited increased sensitivity to microflora challenges,

developed excessive colonic inflammation (Esworthy et al., 2003) and showed increased accumulation of cell DNA errors (transition, transversion or small deletion for DNA damage), which is an important event in cancinogenesis (Lee et al., 2006). In addition, GPx1 -/- mice in other studies were also shown to have no difference in TNF-induced primary apoptosis signalling, but had increased susceptibility to secondary necrosis/T-cell induced liver cell injury (Bajt et al., 2002), exhibited increased NFκB signalling (assessed by EMSA for chromatin binding affinity of p65 NFκB subunit) after ischemia-reperfusion injury in neuron (Crack et al., 2006), and exhibited increased apoptosis and NFκB response to H_2O_2 challenge in their fibroblasts (de Haan et al., 2004). Taken together, these observations suggest that a loss of GPx1 function is relatively benign, unless a second strike stressing the redox-system occurs, such as that which occurs in Se depletion, ischemia-reperfusion injury and H_2O_2 challenge.

Secondly, in GPx1 overexpression studies, culture medium supplemented with Se was used to enhance the additional expression of GPx1 (Li et al., 2001). It cannot be excluded that the expressions and/or activities of other selenoproteins might also have been affected by the Se supplementation, but these were not carefully determined. Therefore, the studies of GPx1 overexpression with Se supplementation might potentially have brought additional beneficial effects on other antioxidant selenoproteins and this should also be taken into consideration.

Thirdly, the cell models used in the present and previous studies were different and involved a colonic epithelial Caco-2 cell line in the present work, but breast cancer MCF-7 or T47D cell lines (Li et al., 2001, Li and Engelhardt, 2006, Kretz-Remy et al., 1996), and mouse renal cells (Ishibashi et al., 1999) in ealier experiments. The different cell types might be distinct in their properties relating to redox-control and NFκB signalling transduction. For example, MCF7 cells have been suggested to express endogenous GPx1 at a very low level (Li et al., 2001, Kretz-Remy et al., 1996) and not to express GPx2, which is expressed mainly in the gastrointestinal epithelium. In comparison, Caco-2 cells express both GPx1 and GPx2 at high levels (Brigelius-Flohe, 1999). Therefore, the MCF7 and Caco-2 cells might also respond differently to changes in GPx1 expression.

6. Effects of GPx4 on NFκB inflammatory signalling

6.1 Introduction

Changes in Se supply to either the host cell environment or a cell culture system are known to affect the transcript expression, protein synthesis and enzymatic activity of sensitive selenoproteins such as GPx1 and SelW, but have also been suggested to influence some other selenoproteins such as GPx4 and TrxR1, which rank in the middle of the selenoprotein incorporation hierarchy (Pagmantidis et al., 2005, Kipp et al., 2009). For example, GPx4 expression, as assessed by mRNA levels using a macroarray, was found to be reduced by 24% and TrxR2 expression by 27% in Caco-2 cells cultured in Se-depleted medium (Pagmantidis et al., 2005). A recent study using a microarray and quantitative PCR approach, to screen genes expressed in the colon of mice fed with Se deficient or adequate diets, have reported a decrease of ~35% in TrxR1 expression in mice fed a marginally low Se diet, but no obvious changes in GPx4 and TrxR2 expression (Kipp et al., 2009). In Chapter 5 Section 5.2.6, Se depletion was found not to change GPx4 mRNA expression in Caco-2 cells as assessed by semi-quantitative RT-PCR (Figure 26). Taking these results together, it is reasonable to suggest that during insufficient Se supply, although the most dramatic changes of gene expression, protein synthesis and activity occur in the sensitive selenoproteins, such as GPx1, the other selenoproteins, such as GPx4 and TrxR1, may also be mildly affected by Se depletion and their influence on NFκB signalling should be taken into consideration.

Furthermore, selenoproteins such as GPx4 have been suggested to be of particular biological importance, especially in the repression of cellular oxidative stress and regulation of the redox-signalling pathways (Imai and Nakagawa, 2003, Brigelius-Flohe, 2006). Like GPx1, GPx4 is also widely distributed in tissues including the gastrointestinal epithelium (Chu et al., 1993). However, whereas GPx1 catalyzes mainly the water-soluble oxidants, e.g. H_2O_2, GPx4 catalyzes a much wider selection of oxidative targets such as phospholipid hydroperoxides (Chu et al., 1993) and lipid hydroperoxides (Thomas et al., 1990), most of which are associated with lipid peroxidization in cell and mitochondrial membranes. Moreover, GPx4 is able to employ substrates for ROS reduction other than glutathione (GSH) (Aumann et al., 1997). GPx4 comprises three isoforms including mitochondrial GPx4, cytosolic GPx4 and nuclear GPx4 (Arai et al., 1996, Pfeifer et al., 2001), of which mitochondrial GPx4 has been suggested to be particularly important in preventing pro-apoptotic oxidative stress in mitochondria (Liang et al., 2007, Imai et al., 2003b). Taking these aspects together, GPx4 has been suggested to be an essential antioxidant in the cell environment.

GPx4's regulatory effects on redox-signalling are based on its ability to repress a wide range of reactive oxidative species that the other GPxs do not reduce. For example, GPx4 may regulate eicosanoid biosynthesis through inhibition of the oxidative signalling involved in the positive feedback of the lipoxygenase (LOX) and cyclooxygenase (COX) pathways (details included in Chapter 1 Section 1.3a). In

comparison, any regulatory effects of GPx4 on the NFκB signalling pathway, which has also been widely suggested to use redox-signalling to mediate its activation (see Chapter 1 Section 1.2b-1.2d), has not yet been systematically investigated. A major difficulty is the variable transductional signalling used in NFκB activation according to different cell-types and inducer-types. However, a limited number of previous studies have suggested a close association between GPx4's repression of redox-signalling and the inhibition of NFκB activation in certain cell types. For example, in human vascular endothelial cells (ECV304 cells), overexpression of GPx4 was found to result in decreased NFκB activation by IL-1, which was also observed following Se supplementation and in fact caused complete cancellation of NFκB activation (Brigelius-Flohe et al., 1997). In epidermal fibroblast cells, NFκB activation by UV irradiation and phospholipid hydroperoxides, known inducers as oxidative stress, was found to be repressed by GPx4 overexpression (Wenk et al., 2004). In addition, in rabbit muscle cells, inhibition of active NFκB signalling in response to lipid hydroperoxides, an oxidative substrate preferentially catalyzed by GPx4, was also achieved by GPx4 overexpression (Brigelius-Flohe et al., 2000). Together, these findings provide evidence that in certain cells, the antioxidant ability of GPx4 is associated with its regulatory effects on NFκB signalling pathways. However, GPx4's effect on NFκB signalling in many other cells or tissues, including the gastrointestinal epithelial cells, remains to be determined.

In Chapter 4 and 5, Se depletion was shown to increase NFκB signalling in response to TNFα, but not flagellin, in Caco-2 cells. In addition, it was found that the TNFα-NFκB response was decreased by GPx1 knockdown but unaffected by SelW or SelH knockdown. The distinct effects on NFκB signalling by Se depletion and by knockdown of GPx1, SelW or SelH raised the possibility of an alternative mechanism being involved in the increased TNFα-NFκB response observed in Se depletion. Since reduced synthesis and expression of GPx4 has also been suggested to occur in Se depletion, and GPx4 as an essential antioxidant has been suggested to be associated with regulation of NFκB signalling by earlier findings, experiments using the NFκB-luciferase reporter model were carried out to investigate GPx4's regulatory effect on NFκB signalling pathway in Caco-2 cells. The approach taken was to lower GPx4 expression using siRNA and then stimulate cells with either TNFα or flagellin.

6.2 Results

6.2.1 Design of GPx4 siRNA and siRNA knock-down of GPx4

In order to study the function of GPx4 in Caco-2 cells, siRNAs specific to the *GPX4* gene were designed and used to knockdown GPx4 expression. The *GPX4* gene has been reported to encode three different transcript variants, namely cytosolic GPx4 (cGPx4), mitochondrial GPx4 (mGPx4) and nuclear GPx4 (nGPx4) (Arai et al., 1996, Pfeifer et al., 2001). Experiments were performed initially to determine which GPx4 transcript variants are expressed in Caco-2 cells. These experiments used RT-PCR and, as shown in Figure 27, amplification of both cGPx4 and mGPx4 isoforms was achieved, but there was no evidence for expression of nGPx4, which has been suggested to be expressed specifically in sperm cells (Pfeifer et al., 2001). These data indicate that the mitochondrial and cytosolic GPx4 are expressed in Caco-2 cells.

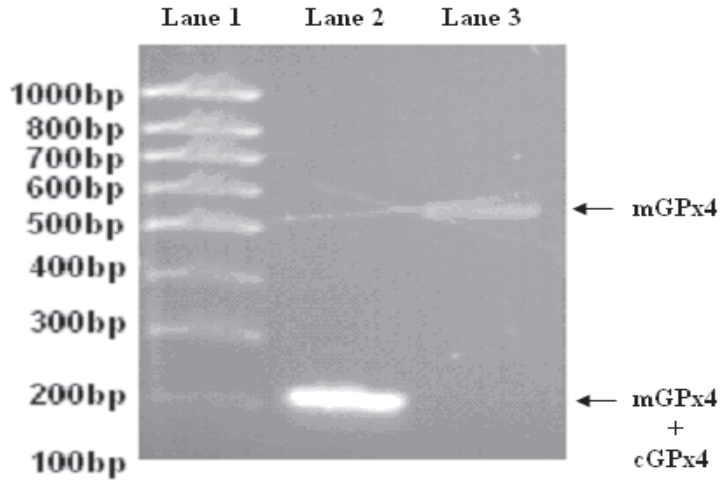

Figure 27: Detection of GPx4 transcript variants in Caco-2 cells

The expression of GPx4 transcript variants in Caco-2 cells was detected using RT-PCR. Lane 1: molecule weight markers; Lane 2: amplification of both cGPx4 and mGPx4; Lane 3: amplification of mGPx4 only.

Design of the GPx4 siRNA was carried out following the published methods (Reynolds et al., 2004, Ui-Tei et al., 2004). Low sequence homology (• 15nt out of 21nt length of siRNA) with the other human mRNA transcripts was achieved so as to limit the non-specific binding of siRNA to the off-target mRNAs. As a result, two siRNA sequences, GPx4siRNA01 and GPx4siRNA02, were designed. The sequence information of the two GPx4 siRNA together with the sequence information of the GPx4 mRNA transcripts is shown in Figure 28:

Sequence Information of GPx4 mRNA transcripts

Exon 1a:

[atgagcctcggccgcctttgccgcctactgaagccggcgctgctctgtggggctct
ggccgcgcctggcctggccgggaccatg]

Exon 2-7:

[tgcgcgtcccgggacgactggcgctgtgcgcgctccatgcacgagttttccgccaa
ggacatcgacgggcacatggttaacctggacaagtaccg][gggcttcgtgtgcatc
gtcaccaacgtggcctcccagtgaggcaagaccgaagtaaactacactcagctcgtc
gacctgcacgcccgatacgctgagtgtggtttgcggatcctggccttcccgtgtaac
cagttcgggaagcag][gagccagggagtaacgaagagatcaaagagttcgccgcgg
gctacaacgtcaaattcgatatgttcagcaagatctgcgtgaacggggacgacgccc
acccgctgtggaagtggatgaagatccaacccaagggcaagggcatcctgggaaa][
tgccatcaagtggaacttcaccaag][ttcctcatcgacaagaacggctgcgtggtg
aagcgctacggacccatggaggagcccctg][gtgatagagaaggacctgccccact
atttctag]

Sequence Information of GPx4siRNA01

Target mRNA: aagaccgaagtaaactacact
SiRNA: gaccgaaguaaacuacacu –uu (sense strand)
uu–cuggcuucauuugauguga (antisense strand)

Sequence Information of GPx4siRNA02

Target mRNA: aattcgatatgttcagcaaga
SiRNA: uucgauauguucagcaaga –uu (sense strand)
uu–aagcuauacaagucguucu (antisense strand)

Figure 28: Scheme showing GPx4 isoforms and design of GPx4 siRNA

GPx4 gene encodes 7 exons (exon 1a and exon 2 to 7). mGPx4 is transcribed from exon 1a to exon 7 and cGPx4 is transcribed from exon 2 to 7. GPx4 gene also encodes an alternative exon 1 as exon 1b, which is used to transcribe nGPx4 but this is not shown above. Exon 1a was suggested to translate a mitochondrial translocation leader sequence whereas exon 2 to 7 was suggested to translate the main part of GPx4 with catalytic function (Arai et al., 1996). Exons are separated by brackets and the mRNA targets of GPx4siRNA01 (design 1) and GPx4siRNA02 (design 2) are respectively underlined.

The target sequences of GPx1siRNA01 and GPx4siRNA02 were present in both cGPx4 and mGPx4 transcripts and therefore these siRNA were unable to differentiate between the cGPx4 and mGPx4 transcripts expressed in Caco-2 cells. This was mainly due to the difficulty of selecting a siRNA target within exon1a, a short sequence of 84nt, which is the only differential sequence uniquely found in mGPx4. As a result, GPx1siRNA01 and GPx4siRNA02 were designed to sequences in exon 3 and exon 4, respectively, and the two GPx4 siRNAs would be expected to knockdown cGPx4 and mGPx4 transcript variants.

In order to test the ability of siRNA to knockdown GPx4 expression, Caco-2 cells of ~50% confluency were seeded in a 6-well plate one day before addition of 5μl transfection reagent Lipofectamine 2000™ and 80pmol of either GPx4siRNA01 or GPx4siRNA02. To assess the knockdown at the mRNA level, treatment by each GPx4 siRNA was maintained for 2 days, total RNA harvested and semi-quantitative RT-PCR carried out to measure the expression of GPx4 and GAPDH. GAPDH is a house keeping gene and was used as the internal control. To assess the knockdown at the protein level, treatment by each GPx4 siRNA was maintained for 3 days, total cell lysate was harvested and GPx4 expression was determined by western blot using polyclonal anti-GPx4 as described in Section 2.1.17 (Chapter 2 Materials and Methods). The results of siRNA treatment on GPx4 expression at the mRNA and protein levels are shown in Figure 29 and Figure 30, respectively.

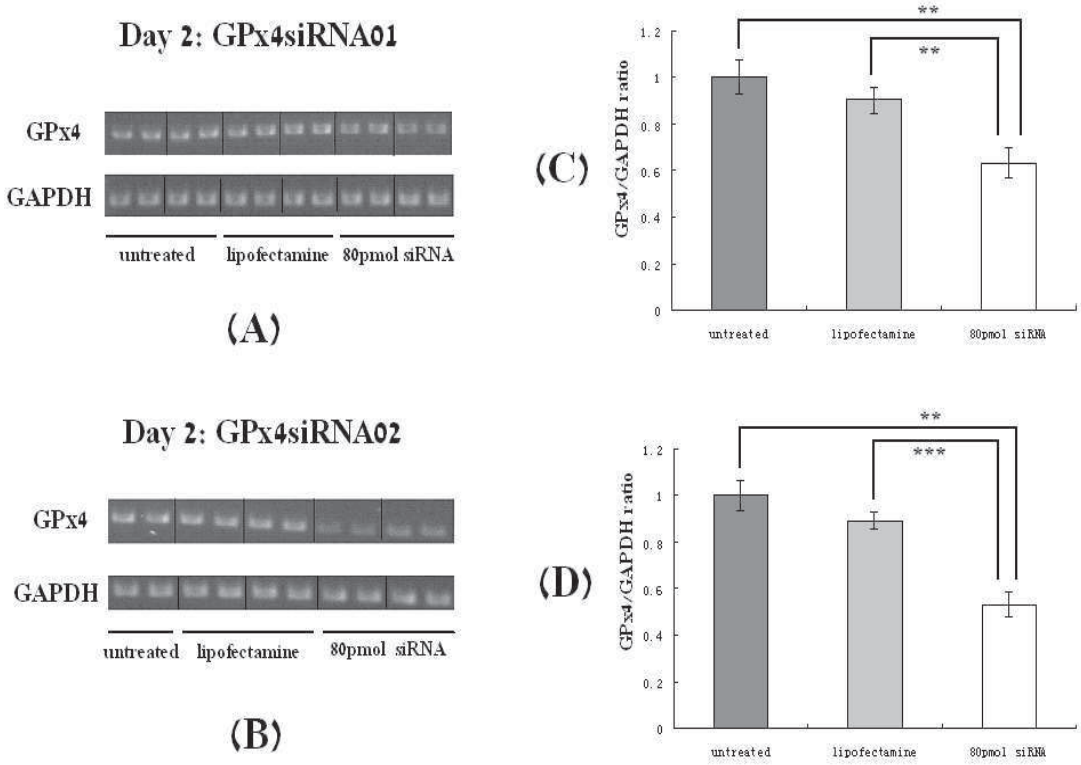

Figure 29: siRNA knockdown of GPx4 expression at the mRNA level

Caco-2 cells were treated with either GPx4siRNA01 or GPx4siRNA02 (80pmol) for 2 days. (A) and (B): the results assessed using semi-quantitative RT-PCR to show the expression of GPx4 and GAPDH (internal control) at the mRNA level in the groups of GPx4siRNA01 and GPx4siRNA02, respectively. (C) and (D): quantification of the data indicating the knockdown of GPx4 expression by 80pmol GPx4siRNA01 and GPx4siRNA02, respectively. GPx4 expression was calculated as a ratio of GPx4/GAPDH transcript levels and further compared between the siRNA treatment group and the control groups (untreated or treated with lipofectamine). Groups were compared using a 2-tailed Mann-Whitney U-test (***: $p<0.001$; **: $p<0.01$). n=6

.

As shown in Figure 29 (A) and (B), treatments with 80pmol of GPx4siRNA01 and GPx4siRNA02 for 2 days, respectively, resulted in a slight decrease and a clear decrease in GPx4 mRNA expression, compared to the control groups without any treatment or treated only with lipofectamine. In addition, GAPDH expression was not affected by GPx4 siRNA treatments. Quantification by densitometry of the RT-PCR bands allowed calculation of the GPx4 expression as a ratio of GPx4/GAPDH transcript levels, and the GPx4 expressions were further compared between the siRNA treatment group and the control groups. Knockdown of ~40% was achieved with 80pmol GPx4siRNA01, whereas knockdown of ~50% was achieved with GPx4siRNA02, compared with the control group of untreated Caco-2 cells (standardized as '1') (Figure 29 (C) and (D)). Therefore, both GPx4 siRNA appeared to be capable of GPx4 knockdown in Caco-2 cells. However, GPx4siRNA02 appeared to have the greater knockdown effect and therefore its effects were investigated further.

In order to test GPx4 knockdown at the protein level, treatments with 40, 80 and 120pmol GPx4siRNA02 were maintained for 3 days. As shown in Figure 30 (A), groups treated with this GPx4 siRNA exhibited reduced GPx4 protein expression to various extents when compared to the control groups, i.e. untreated cells or cells treated only with lipofectamine. Considerable knockdown of GPx4 protein were observed in groups treated with 80 and 120pmol siRNA, with GPx4 protein being barely detectable in the 120pmol treatment group. After quantification (shown in

Figure 30 (B)) using the untreated group standardized as '1', GPx4 knockdown by 40, 80 and 120pmol siRNA was found to be by ~20%, ~60% and >85% at the protein level, respectively. Therefore, treatment with 80pmol siRNA was found to achieve a similar knockdown in GPx4 expression (50~60%) at both mRNA and protein levels, and treatment with 120pmol siRNA was found to result in a much larger effect on GPx4 protein expression with knockdown of over 85%.

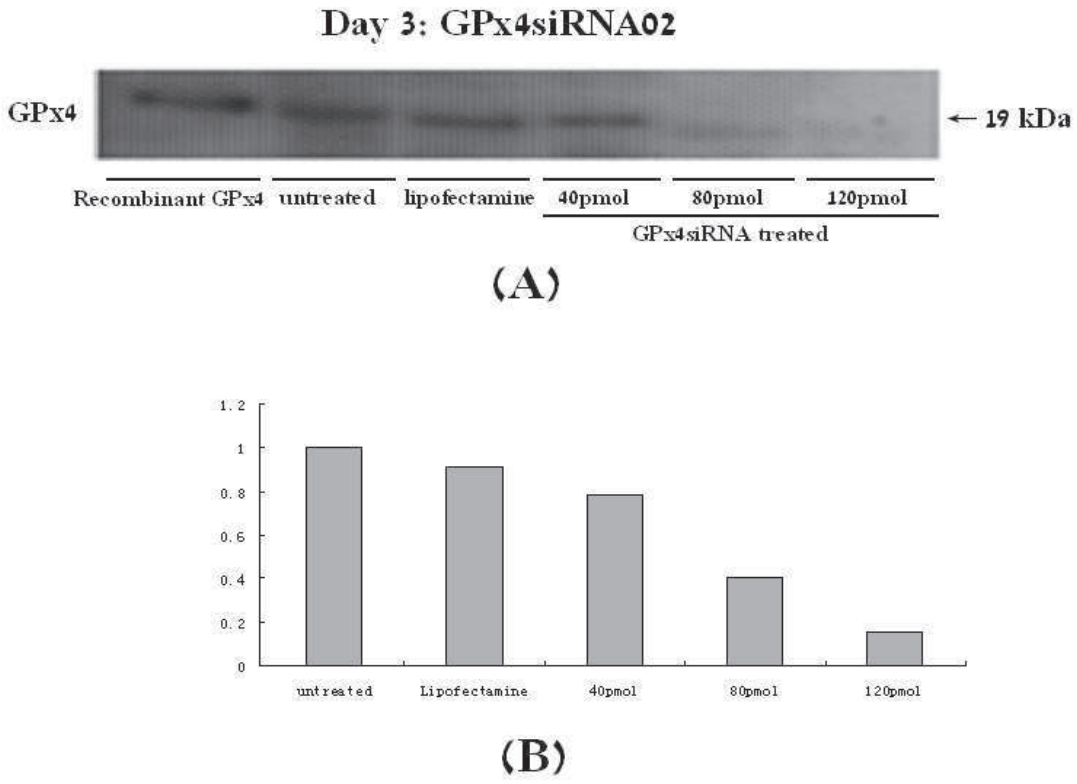

Figure 30: siRNA knockdown of GPx4 expression at the protein level

Caco-2 cells treated with 40, 80, 120pmol of GPx4siRNA02 were assessed by western blotting using an anti-GPx4 antibody. Results showed various extents of reduced GPx4 expression at the protein level, compared with the control group (standardized as '1') of untreated cells; 40, 80 and 120pmol GPx4 siRNA were found to result in approximately 20%, 60% and more than 85% knockdown of GPx4 protein, respectively. n=3

In summary, to establish a method to study GPx4's function in Caco-2 cells, the design and experimental use of two siRNA specific to the GPx4 transcript showed that it is possible to knockdown GPx4 expression in Caco-2 cells. Using 80pmol siRNA treatment, ~40% knockdown of GPx4 mRNA expression was achieved using GPx4siRNA01 and a larger knockdown effect (50%) was achieved with GPx4siRNA02. Further investigation using GPx4siRNA02 showed that knockdown of GPx4 expression at the protein level was ~60% using 80pmol siRNA and >85% using 120pmol siRNA. Therefore, in further experiments assessing GPx4's regulatory effect on NFκB signalling, knockdown of GPx4 expression was carried out using 120pmol GPx4siRNA02.

6.2.2 The impact of GPx4 knockdown on TNFα-induced NFκB-activation in the NFκB luciferase reporter model

The impact of GPx4 on the NFκB signalling pathway in response to TNFα induction was studied using siRNA knockdown in Caco-2 cells expressing the NFκB luciferase reporter. Caco-2 cells transfected with NFκB or TATA (control) luciferase constructs were treated with 120pmol GPx4siRNA or a "scrambled" control siRNA for 3 days to reach maximal knockdown at the protein level, then incubated with 20ng/ml TNFα for 2 or 4 hours to activate NFκB signalling. TNFα treatment has been shown previously to result in activation of the NFκB signalling-driven reporter after 2-4 hours stimulation (Figure 15). Total cell lysate was harvested using 1X Reporter lysis buffer and luciferase activity was measured, at baseline, and at 2 and 4 hours after addition of TNFα. Activity was calculated per mg total cell lysate protein (relative luciferase activity, RLA) and then expressed as a ratio relative to the level of the "scrambled" control siRNA treatment group, which was standardized as "1".

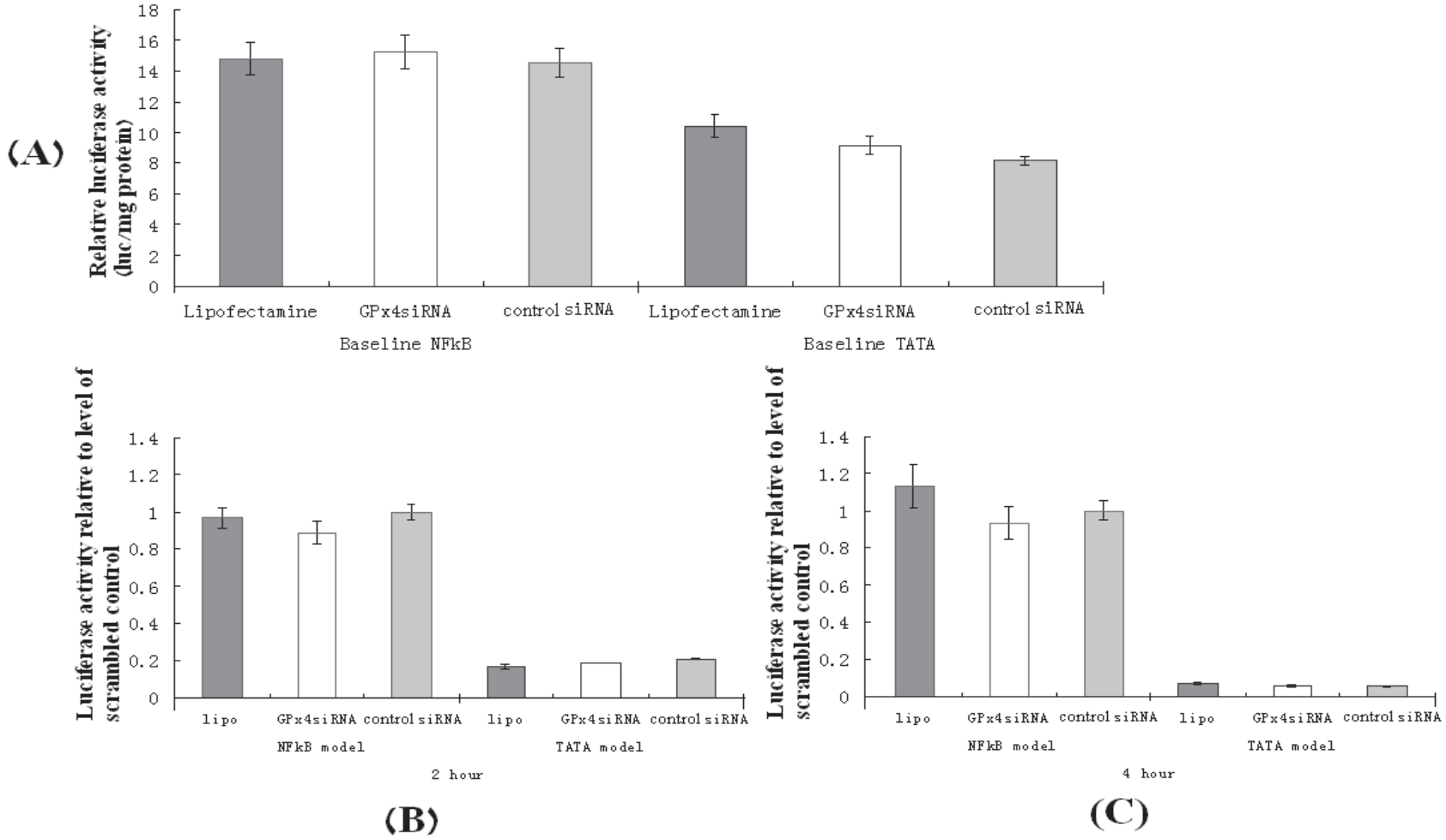

Figure 31: Imact of GPx4 siRNA knockdown: TNFα-induced luciferase activity of NFκB and TATA reporter Caco-2 cells

(A): Baseline RLA values measured in both NFκB- and TATA- luciferase transfected Caco-2 cells and for each cell type, in the three treatment groups: only with lipofectamine, with GPx4 siRNA, and with scrambled control siRNA. (B) and (C): after 2 hours and 4 hours TNFα treatment, luciferase activity increased dramatically in the cells transfected with NFκB-luciferase construct, compared with the TATA construct-transfected cells. Moreover, the levels of luciferase activity were compared within the treatment groups and expressed as a ratio relative to the control group (scrambled control siRNA treatment). Groups were compared using a 2-tailed Mann-Whitney U-test (non-significant: $p>0.05$). n=6

In Caco-2 cells transfected with either NFκB- or TATA- luciferase constructs, baseline RLA values exhibited a difference between the cell types but exhibited no difference among the three treatments (lipofectamine, lipofectamine and GPx4 siRNA, or lipofectamine and "scrambled" control siRNA) (Figure 31 (A)). Therefore, the background luciferase reporter activity appeared not to be affected by the GPx4 knockdown. Furthermore, although large differences in RLA values between the NFκB- and TATA- luciferase cell models were found both 2 hour and 4 hour after TNF addition, indicating that an induction of NFκB signalling had indeed occurred in this experiment, there was no significant difference between the three treatment groups (Figure 31 (B) and (C)). Therefore, these results suggested that in Caco-2 cells GPx4 knockdown to ~85% by 120pmol siRNA treatment resulted in no obvious changes of NFκB-driven luciferase reporter after stimulation with TNFα.

6.2.3 The impact of GPx4 knockdown on Flagellin-induced NFκB-activation in the NFκB luciferase reporter model

Studies of the correlation between GPx4 knockdown and flagellin-induced NFκB-luciferase activity were carried out as follows: Caco-2 cells transfected with NFκB or TATA (control) luciferase constructs were treated with 120pmol GPx4siRNA or "scrambled" control siRNA for 3 days, then incubated with 100ng/ml *Salmonella typhimurium* flagellin to activate NFκB signalling. As shown previously, treatment of Caco-2 cells with 100ng/ml flagellin resulted in increased luciferase activity 2-8 hours after addition of flagellin in the luciferase reporter model (Figure 15 (D)). Therefore, in order to assess if GPx4 knockdown caused any effects on the flagellin-induced NFκB signalling response, total cell lysate harvested and luciferase activities were measured at baseline, and at 2 and 6 hours after treatment. Activity was calculated per mg total cell lysate (relative luciferase activity, RLA) and expressed in a ratio relative to the level of the control siRNA treatment group.

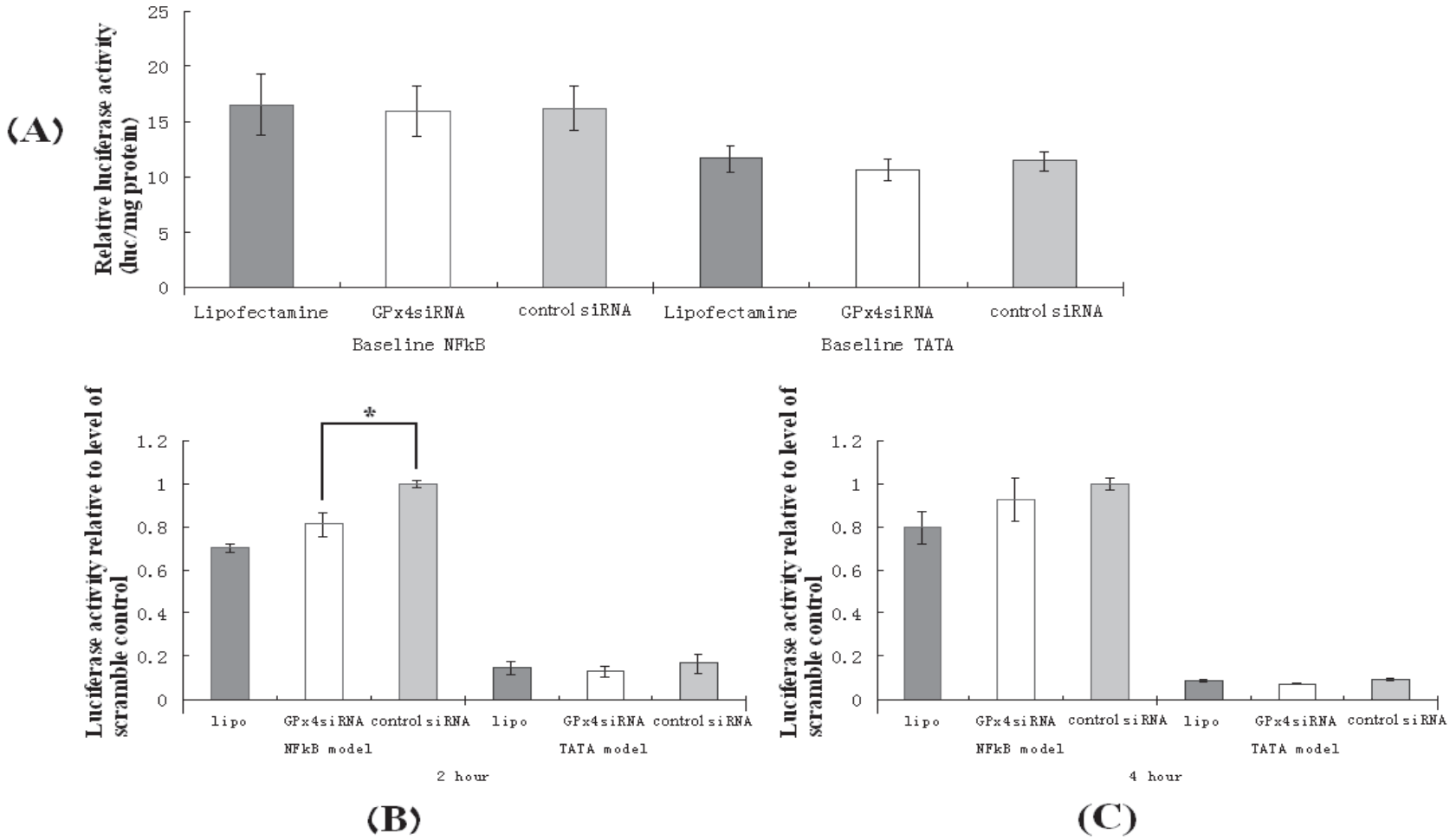

Figure 32: Imact of GPx4 siRNA knockdown: flagellin-induced luciferase activity of NFκB and TATA reporter Caco-2 cells

(A): the luciferase activities at baseline in the NFκB- and TATA- luciferase construct transfected Caco-2 cells and for each cell type, in three different treatment groups (lipofectamine only, lipofectamine and 120pmol GPx4 siRNA, and lipofectamine and 120pmol control siRNA). (B): the luciferase activity levels expressed in a ratio relative to the level of control siRNA group after 2 hours flagellin treatment. (C): the luciferase activity levels expressed in a ratio relative to the level of control siRNA group after 6 hours flagellin treatment. Groups were compared using a 2-tailed Mann-Whitney U-test (*: $p<0.05$). n= 6

Similar to the TNFα-NFκB experiment, the baseline luciferase activities exhibited comparable values between the GPx4 siRNA and the scrambled control siRNA treatment groups, again indicating that the background luciferase reporter activity was not affected by GPx4 knockdown (Figure 32 (A)). When Caco-2 cells were stimulated with *Salmonella typhimurium* flagellin (100ng/ml) for 2-6 hours, there was a clear increase in luciferase activity in the NFκB-luciferase but not the TATA-luciferase transfected cells, suggesting that NFκB signalling was activated (Figure 32 (B) and (C)). Comparison between the GPx4 siRNA and the scrambled control siRNA treatment groups showed that 2 hours after flagellin stimulation, GPx4 knockdown led to a small (20%) but statistically significant ($p<0.05$) decrease in luciferase activity (shown in Figure 32 (B)). However, 6 hours after flagellin stimulation, knockdown of GPx4 had no significant effect (shown in Figure 32 (C)).

To further investigate the impact of GPx4 knockdown on the NFκB signalling, expression of the NFκB target gene IL8 was measured after flagellin stimulation.

6.2.4 The impact of GPx4 knockdown on expression of the NFκB target gene IL8 following flagellin induction

Semi-quantitative RT-PCR was used to assess the response of NFκB target gene IL8 to flagellin induction. Caco-2 cells were stimulated with *Salmonella typhimurium* flagellin (100ng/ml) for 0, 2, 4, 6 and 16 hours. IL8 expression in unstimulated Caco-2 cells was found to be very low, whereas following the stimulation by flagellin, the expression of IL8 increased dramatically with the highest level observed after 2 hours (Figure 33).

In order to assess the regulatory effect by GPx4 knockdown on the response of IL8 expression to flagellin, Caco-2 cells were treated with 120pmol GPx4 siRNA or the "scrambled" control siRNA for 3 days, incubated with 100ng/ml flagellin for 2 hours to stimulate IL8 expression, and total RNA harvested. Semi-quantitative RT-PCR was used to assess the mRNA expression of IL8, GPx4 and GAPDH. The expression levels of IL8 and GPx4 (to show the effect of knockdown) were normalized to the level of house keeping gene GAPDH.

A clear decrease in GPx4 expression was observed in the GPx4 siRNA treatment group compared with the control siRNA group, confirming that siRNA knockdown had occurred (Figure 34 (A)). In addition, a decrease in IL8 expression was also found in the GPx4 siRNA treatment group compared with the IL8 level in the scrambled control siRNA treatment group. Quantification of the data indicated a decrease in IL8 expression by GPx4 knockdown, which was ~40% and of statistical significance ($p<0.01$) (Figure 34 (B)). Therefore, in addition to the finding that GPx4 knockdown resulted in decreased luciferase activity assessed by the NFκB-luciferase reporter,

siRNA knockdown of GPx4 expression also resulted in decreased IL8 expression in response to flagellin. Together, these results suggested that GPx4 knockdown was associated with down-regulation of NFκB signalling in response to flagellin challenge in Caco-2 cells.

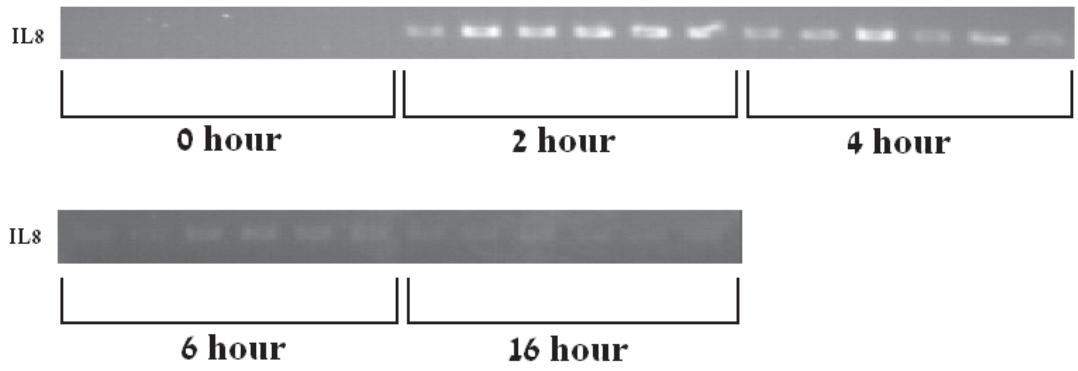

Figure 33: Induction of IL8 mRNA expression by flagellin for 0, 2, 4, 6 and 16 hours treatment

Caco-2 cells treated with 100ng/ml flagellin for 0, 2, 4, 6 and 16 hours and IL8 expression assessed by RT-PCR. In treated cells (0 hour), IL8 expression was very low, whereas in cells treated with flagellin for 2 hours, IL8 expression was stimulated and at the highest level, compared with the other groups (4, 6 and 16 hours flagellin stimulation).

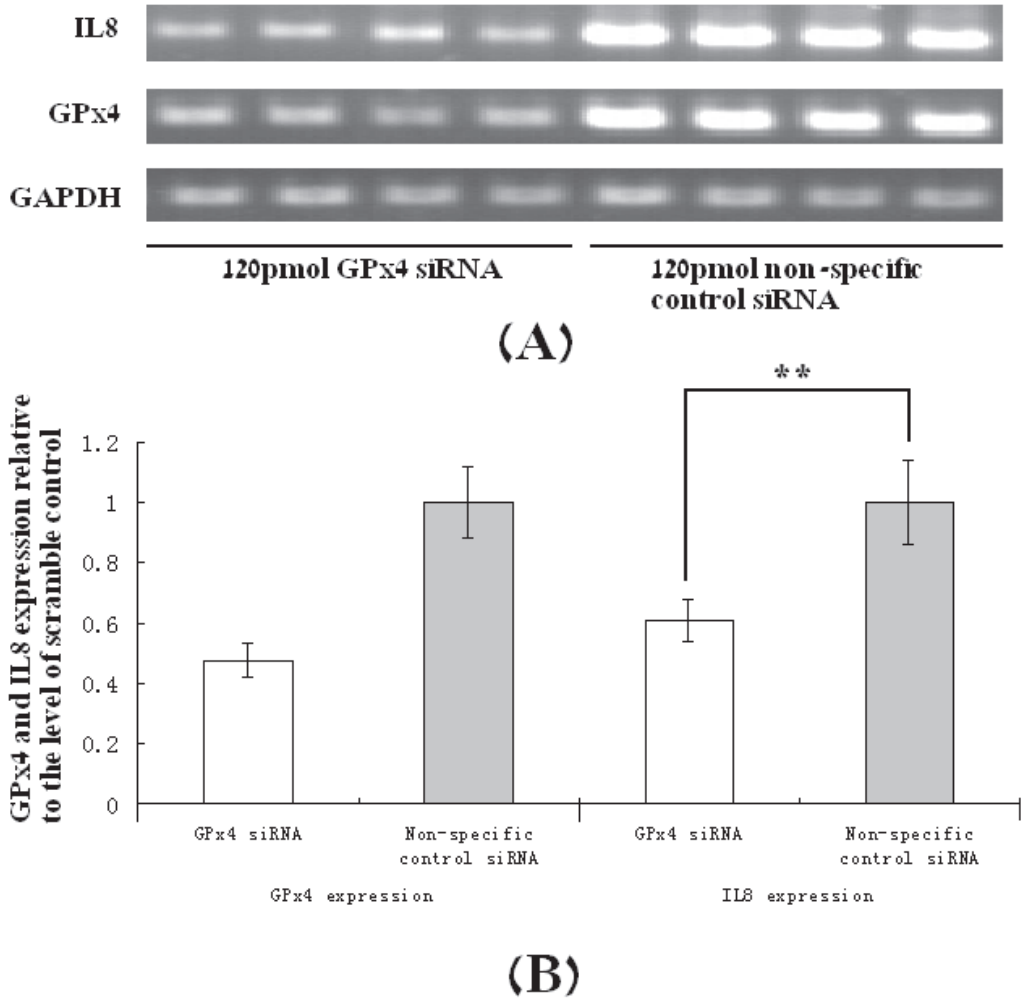

Figure 34: Imact of GPx4 siRNA knockdown: flagellin-induced IL8 expression in Caco-2 cells

(A): Expression of IL8, GPx4 and GAPDH mRNAs in Caco-2 cells treated with 120pmol GPx4 siRNA or scrambled control siRNA and incubated with 100ng/ml flagellin for 2 hours (assessed by semi-quantitative RT-PCR). (B): Quantification of the data comparing GPx4 and IL8 expression in the cells stimulated with flagellin and treated with GPx4 siRNA and scrambled control siRNA. Data were expressed in a ratio relative to the level of control siRNA treatment group. Groups were compared using a 2-tailed Mann-Whitney U-test (**: $p<0.01$). n=9

6.3 Discussion

In the present study siRNA knockdown was used to investigate the role of GPx4 in the NFκB signalling pathway in Caco-2 cells following activation by TNFα and flagellin. The aim was to test whether GPx4, as an essential antioxidant selenoprotein, exerts any regulatory effects on NFκB activation, which has been suggested frequently to be associated with the redox-signalling. Using both the luciferase reporter model and measurement of endogenous IL8 mRNA level, the TNFα-induced NFκB signalling was not affected by GPx4 knockdown (Figure 32), whereas flagellin-induced NFκB signalling was found to be decreased by GPx4 knockdown; luciferase activity was decreased by ~20% (Figure 33) and mRNA expression of the NFκB target gene IL8 was decreased by ~40% (Figure 34). Critically, these experiments indicate that GPx4 knockdown has different effects on NFκB signalling depending on the inducers. This suggests that knockdown of GPx4 affects part of the signalling pathways that are distinct between TNFα and flagellin-activated receptors.

The inability of GPx4 knockdown to alter the luciferase expression by activated NFκB signalling in response to TNFα provided additional information to the previous findings that knockdown of GPx1, SelW and SelH resulted in either decreased (Figure 22) or unchanged (Figure 24) NFκB-luciferase reporter activities by the same inducer. These selenoproteins tested were found (Figure 26) or have been suggested to be decreased in expression by Se depletion (also see Section 6.1 introduction). GPx4 expression has been observed to be mildly decreased, by ~24%, in Caco-2 cells grown in Se-depleted medium (Pagmantidis et al., 2005), whereas GPx4 expression was decreased by >85% in the present study using 120pmol GPx4 siRNA, which was a much larger decrease than the effect caused by Se depletion. However, no significant

difference in luciferase activity driven by TNFα-NFκB signalling was identified in the GPx4 knockdown treatment group compared to the control groups treated with lipofectamine or treated with "scrambled" control siRNA. Therefore, in addition to the previous findings that knockdowns of either GPx1, SelW or SelH expression were unable to reproduce the up-regulated TNFα-NFκB signalling observed in Se depletion, findings by this study further suggested that knockdown of GPx4 expression, by >85%, was also unable to cause obvious effects on the TNFα-NFκB response.

Therefore, comparing the results of increased NFκB activation by Se depletion and the results from knockdown experiments (GPx1, SelW and SelH knockdown described in last chapter and GPx4 knockdown described in the present chapter), it is reasonable to suggest that the regulation of the NFκB signalling pathway following TNFα induction by Se depletion, occurs through alternations in the redox-balance by systematic changes in the expression of multiple selenoproteins.

The down-regulated NFκB signalling in response to flagellin by GPx4 knockdown was identified using the luciferase reporter system and confirmed by semi-quantitative RT-PCR measurements of IL8 mRNA expression. This contrasts with the earlier finding (Chapter 4) that this particular NFκB response was not affected by Se depletion. The mechanisms in regard to the decreased flagellin-NFκB signalling remained to be explored. However, this pathway activates NFκB signalling through the TLR receptors and therefore is different from the TNFα pathway.

Owing to its effects on ROS clearance, GPx4 has been suggested to exert a repressive role in the activation of the NFκB signalling (Banning and Brigelius-Flohe, 2005,

Wenk et al., 2004), but so far only limited evidence has been directly provided in this regard. Much of this evidence is based on observation of activation status of NFκB signalling using overexpression experiments, rather than the knockdown approach used in the present work. Particularly, the targets of redox-signalling responsible for activation of NFκB signalling need to be defined to explain the underlying mechanism(s). Intriguingly, in the previous Chapter, knockdown of GPx1 expression was also correlated with decreased NFκB-luciferase reporter activities and IL8 expression in response to TNFα in Caco-2 cells. These findings suggest that different selenoproteins have different effects on NFκB signalling. In addition, it is possible that the regulatory role of the antioxidant selenoproteins in NFκB signalling might be distinct when their levels are either overexpressed or knocked-down. Finally, this raises the question of how the antioxidant selenoproteins, together with the other antioxidants, are integrated into the control of NFκB signalling, and how this explains the response to Se depletion.

7. Final discussion

The micronutrient Se, together with selenoproteins, has been widely studied in respect to its health implications in areas including antioxidant protection, immune function and inflammation, cancer risk, thyroid hormone metabolism (DIO family), calcium homeostasis (SelN) (Arbogast and Ferreiro, 2010), protein folding and ER-stress response (SelS, Sep15 and others) (Labunskyy et al., 2009, Shchedrina et al., 2010). In relation to this thesis, specifically, Se can provide significant protection of the gastrointestinal tract against inflammation and carcinogenesis (Karp and Koch, 2006, Duffield-Lillico et al., 2002). For example, Se intake has been associated inversely with the risk of colon cancer (Russo et al., 1997) and Se supplementation has been used as a non-therapeutic method to control the symptom of Inflammatory bowel disease (Halliwell et al., 2000).

The anti-inflammatory effects of Se in the colon have been related to the function of the antioxidant selenoproteins. GPx1 -/- and GPx2 -/- double knock-out mice are sensitive to microbial challenges and vulnerable to development of colitis and colonic cancer (Esworthy et al., 2003). In addition, the antioxidant selenoproteins, GPx1, GPx2 and GPx4, can repress the biosynthesis of eicosanoids in various cells (summarized in Table 2). Se and selenoproteins GPx1 and GPx4 also have regulatory effects on the NFκB inflammatory signalling pathways in the breast cancer cells and macrophages (reviewed in Section 1.3). However, it is unknown whether, and how, Se together with antioxidant selenoproteins has any regulatory effects on the NFκB signalling pathway functioning in the human gastrointestinal tract, which system constantly requires the healthy maintenance of immune homeostasis.

The NFκB signalling pathways are critical control factors for the inflammatory response. The potential linkage between Se/selenoproteins and the NFκB signalling pathways is that NFκB signalling pathways are frequently mediated by ROS (reviewed in Section 1.2b and 1.2c), and Se and antioxidant selenoproteins repress ROS. This potential link provides the rationale that supports the present studies. However, the NFκB signalling pathways are complicated and many NFκB inducers may also activate alternative pathways. For example, TNFα and flagellin both activate the MAPK and apoptosis pathways, in addition to the NFκB pathway (Li and Lin, 2008, Yu et al., 2003).

The present study addressed the hypothesis that Se and selenoproteins modulate the NFκB signalling pathways in human colonic epithelial cells in response to inflammatory challenges. To test the hypothesis, an NFκB-luciferase reporter system was developed in Caco-2 cells and the effects of Se depletion and selenoprotein knockdown (GPx1, SelW, SelH and GPx4) were studied using both the reporter system and measurement of endogenous expression of the NFκB target gene IL8, following stimulation of cells with the known NFκB inducers TNFα and flagellin. Using this strategy, the activation of the NFκB transcription activity was specifically reported as luciferase expression and its impact on the expression of selected target genes examined and used as confirmation.

The other important selenoproteins not examined in the present study include TrxR1, TrxR2, GPx2, SelS and SelP, owing to the limition in time. TrxR1 and TrxR2 are essential antioxidants which reduce thioredoxin (Lu et al., 2009) and subsequently generate ROS and therefore interact with the GSH-GPx redox system. Thioredoxin

and Thioredoxin reductases (TrxRs) predominantly modulate DNA-binding affinity of NFκB subunits, an event after IκB-NFκB disassociation. Thioredoxin has previously been shown to crosslink the thiol compounds (-SH) between the cysteine residues of p50 (for example, Cys_{62} of p50) (Hayashi et al., 1993) or c-Rel (Glineur et al., 2000) and promote oxidation and inhibition of the NFκB DNA-binding ability (Hayashi et al., 1993). Therefore, TrxRs may unlock this inhibition by reducing thioredoxin and fully activate the NFκB transcription factors (Sakurai et al., 2004). Particularly, TrxR1, the cytosolic form of TrxR, is expressed ubiquitously in all tissues and its expression has been shown to be sensitive to changes in Se supply (~4 fold increase in Se supplementation (40nM) and ~60% reduction in Se depletion for 7 days in endothelial EAhy926 cells (Crane et al., 2009), or ~35% reduction in mouse colon fed Se-deficient diet (Kipp et al., 2009)). Therefore, it will be important to study the influence of TrxR1 knock-down on TNFα-NFκB signalling in the future.

GPx2 is an antioxidant selenprotein specificially expressed in the human gastrointestinal tract. The expression of GPx2 is highly stable (highest in Se incorporation hierarchy) and hardly lowered by Se depletion (Brigelius-Flohe and Kipp, 2009). Similarly, TrxR2 has also been suggested to be relatively stable and its expression is difficult to influence unless under prolonged Se depletion (7 days) (Crane et al., 2009). Therefore GPx2 and TrxR2 were not considered a priority for investigation in the present study of NFκB signalling during Se depletion. In addition, the functions of SelP and SelS (see Section 1.1d) are only poorly characterized (Curran et al., 2005, Moghadaszadeh and Beggs, 2006) and their roles in NFκB activation were not established.

To develop the NFκB-luciferase reporter model in Caco-2 cells, the NFκB-luciferase (test) and the TATA-luciferase (control) constructs were made by modification of the previously established 3XκB-luciferase reporter (Carlsen et al., 2002). The modification was necessary because the TATA control construct, which has no NFκB binding sites, was not provided with the original reporter system. These constructs were integrated with either the pBLUE-TOPO or the pcDNA3.1 v5-his-TOPO plasmid vector and stably transfected in Caco-2 cells. However, the preliminary studies of the v5-his-TOPO constructs found that the TATA control cells expressed baseline luciferase activity at a relatively high level (~242 luciferase units per mg protein lysate) and exhibited an unexpected responsiveness to TNFα, by showing a 4-fold increase of luciferase activity (Figure 14). A possible explanation was the presence of the CMV promoter in the pcDNA3.1 v5-his-TOPO plasmid. The CMV promoter has been suggested to be responsive to NFκB transcription factors (Sambucetti et al., 1989), and it contains four binding sites of Class I NFκB, 3X GGGACTTTCC and 1X GGGGATTTCC, corresponding to motif GGGRNNYYCC (R: purine, Y: pyrimidine, N: any base). Therefore, potential NFκB binding sites of the CMV promoter were predicted to be causing the responsiveness of the TATA control cells.

In comparison, the other pair of reporter cell lines, transfected with the NFκB- and TATA-luciferase constructs in pBLUE-TOPO vector, that has no CMV promoter, exhibited low baseline luciferase activities and good responsiveness to TNFα and flagellin. The baseline luciferase activity was ~23luc units/mg in the NFκB cells and ~11luc units/mg in the TATA cells (Figure 15). Following treatment with TNFα for 4 hours or flagellin for 6 hours, respectively, the NFκB cells exhibited increases of

luciferase activity of 12 fold and 6.4 fold, respectively, whereas under both conditions the TATA cells exhibited no increase (Figure 15). Therefore, the NFκB- and TATA-luciferase pBLUE-TOPO transfected Caco-2 cells are able to report, specifically, the activity of NFκB transcription factors and were used to test the regulatory effects of Se and selenoproteins on the NFκB signalling pathways.

The impact of Se depletion on NFκB signalling was studied using a previous established method that depletes Se in the cell growth medium, i.e. growing cells without FCS but in presence of insulin and transferrin, and in the control group, supplementing cells with sodium selenite (Pagmantidis et al., 2005). This method decreased the expression of mRNAs encoding selenoproteins such as GPx1, SelW and SelH (Figure 26 (A)). Following Se depletion/Se supplementation, the NFκB- and TATA-luciferase Caco-2 cells were stimulated with TNFα (20ng/ml) and flagellin (100ng/ml) and luciferase activity was measured in these cells before and after stimulation. Without stimulation, the baseline luciferase activities of the NFκB or TATA cells were comparable under the conditions of Se-depletion and Se-supplementation (Figure 17 (A)). Therefore, Se depletion itself did not affect the basic luciferase expression and the non-specific background NFκB signalling in Caco-2 cells.

When the NFκB-luciferase cells were stimulated with TNFα, there was a difference in luciferase activity between cells grown in Se depleted and Se supplemented medium. The Se- NFκB-luciferase cells exhibited higher, an average of 30% more, luciferase activities than the Se+ NFκB-luciferase cells 2 or 4 hours after TNFα stimulation (Figure 17 (B)). This difference was statistically significant ($p<0.05$ in the 4h TNFα

treatment group and $p<0.01$ in the 2h TNFα treatment group). It was only observed in the NFκB-luciferase cells and not in the TATA control cells, which maintained low luciferase activities throughout (Figure 17 (B)). Similarly, in the untransfected Caco-2 cells after 1h TNFα stimulation, IL8 expression changed accordingly to whether the cells were cultured either minus Se or plus Se, with the Se-depleted group expressing on average 50% more IL8 mRNA than the Se+ group ($p<0.001$) (Figure 19 (B)). Thus, these observations support the hypothesis that Se supply has regulatory effects on the NFκB signalling pathway in response to TNFα in Caco-2 cells, such that when Se supply is depleted elevated NFκB activation occurs.

When the reporter cells were, in parallel, stimulated with *Salmonella typhimurium* flagellin (100ng/ml), no difference was found between the luciferase activities measured in the Se- and Se+ growing cells (Figure 20). After 2h or 6h induction by flagellin, the NFκB reporter cells exhibited increased luciferase activity indicating activated NFκB signalling, but this response was similar in the cells either Se depleted or supplemented. Therefore, these findings suggest that, unlike the TNFα-activated NFκB signalling response, flagellin-activated NFκB signalling is not influenced by Se supply. However, further experiments to monitor NFκB activation by measurements of expression of a NFκB target gene, such as IL8 mRNA, or the NFκB DNA-binding affinity, would strengthen this conclusion.

It is not surprising that Se depletion had different regulatory effects on the TNFα-NFκB and the flagellin-NFκB signalling pathways, because these two pathways are processed independently through different signalling transduction cascades. TNFα activates NFκB transcription factors using the adaptor proteins

TRADD, RIP and TRAF2, and it has been suggested that this activation is essentially associated with redox-signalling attributed to the flavokinase-Nox2 complex (Yazdanpanah et al., 2009) (Chapter 1 Section 1.2b). In comparison, flagellin activates NFκB signalling using the adaptor proteins MyD88, IRAK4-IRAK1 and TRAF6, and pathway activation has been linked to redox-signalling produced from the IRAK4-Nox1 complex (Chapter 1 Section 1.2c). Furthermore, the phosphorylation of IKK subunits functions through TAK1, NIK, MAP3K1 or MAP3K3 in cells including lymphocytes, fibroblasts, breast cancer cells and fibroblast-like synovial cells for the TNFα-NFκB activation (reviewed in Section 1.2b), and through TAK1 for the flagellin-NFκB activation in human colonic epithelial T84 and Caco-2 cells (Kawahara et al., 2004). These distinct features in NFκB-activation by TNFα and flagellin could potentially be responsible for the different effects seen in the Se depletion studies. Based on these observations, it is reasonable to suggest that Se supply might influence certain, but not all, types of NFκB response in Caco-2 cells (see the latter parts of this discussion).

The mechanism by which Se depletion resulted in an elevated NFκB response to TNFα was further analyzed by using siRNA to knockdown expression of individual selenoproteins, including GPx1, SelW and SelH, and then assessing the impact on the NFκB response to TNFα (Chapter 5). The reason for selectively studying these selenoproteins was because they all have well-characterized (GPx1) or suggested (SelW and SelH) antioxidant activity and, in addition, their expression is most affected by Se depletion (Sunde et al., 2009, Kipp et al., 2009). In Se depletion, the expressions of GPx1, SelW and SelH mRNA were lowered by 60%, 40% and 50%, respectively (Figure 26). Using siRNA, their mRNA expression was knocked down to

comparable levels, by 55%, 50%, 40%, respectively, which allows reasonable comparison of these data in the siRNA and Se depletion experiments. GPx1 knockdown decreased the TNFα-NFκB response by ~13-25% ($p<0.01$), an effect contrary to that of Se depletion, when assessed by luciferase reporter activity (Figure 22 (B)). This decrease was specific to TNFα stimulation, since the baseline luciferase activities were similar in the GPx1 siRNA and control siRNA groups. Moreover, following 1 hour of TNFα stimulation, the IL8 mRNA level also showed a significant decrease (17%, $p<0.05$) in the cells with GPx1 knockdown when compared to the cells without knockdown (Figure 23 (B)). Overall, these observations suggest that the knockdown of the antioxidant selenoprotein GPx1 alters the TNFα-NFκB response in Caco-2 cells, and yet this effect is contrary to the effect of Se depletion and is an inhibition of the activation of NFκB signalling.

In addition, the effects of SelW and SelH knockdown appeared not to change the TNFα-NFκB response in Caco-2 cells, as assessed by NFκB-luciferase activity (Figure 24). Thus the TNFα-induced NFκB transcription activity seems not to be influenced either by SelW or SelH. Similarly, when GPx4 was knocked down by >85%, the Caco-2 reporter cells also exhibited no difference in luciferase activity after TNFα stimulation (Figure 31). The distinct effects of Se depletion and selenoprotein knockdown (GPx1, SelW, SelH and GPx4) raise the challenging question of how Se supply exerts its regulatory effects on the TNFα-NFκB response when its effects cannot be simply explained by the altered expression of one of the individual antioxidant selenoproteins. It is possible that Se depletion results in elevated NFκB signalling by decreasing the expression of multiple selenoproteins, including GPx1, SelW, SelH (Figure 26), TrxR2 and GPx4 (Pagmantidis et al., 2005).

In comparison, siRNA knockdown only resulted in decreased expression of a single antioxidant selenoprotein which might not be enough to modulate the redox system sufficiently to affect the TNFα-NFκB response. This explanation was supported by the experiments measuring the ROS levels in the Se- cells and in the GPx1 siRNA-treated cells. Compared with the Se+ cells, Se- cells exhibited 60% higher levels ($p<0.001$) of ROS (Figure 25 (A)), whereas compared with the scramble control siRNA-treated cells, the GPx1 siRNA-treated cells exhibited no obvious difference in ROS level (Figure 25 (B)). Since NFκB activation has been suggested to be partly mediated through ROS (Gloire et al., 2006, Haddad, 2002), it is possible that Se depletion and GPx1 knockdown exert their respective effects on the TNFα-NFκB response, through their effects on ROS levels.

It is possible, indeed likely, that Se depletion decreases the expression of multiple antioxidant selenoproteins, leading to an impaired redox system, increased ROS levels, enhanced redox-signalling and elevated NFκB signalling in response to TNFα stimulation. On the other hand, GPx1 knockdown decreases only GPx1 expression and the expression of other antioxidant selenoproteins is little affected (or possibly a compensatory increase), so following this treatment there is only slight stress to the redox system and ROS levels are unaffected. Thus in turn, this leads to unaffected or decreased redox-signalling (following compensation by the other antioxidant selenoprotein), and thus decreased NFκB signalling following TNFα activation.

In the present study the comparison between Se depletion and GPx1 knockdown at the cellular ROS level only provides indirect information for understanding their different effects in relation to the TNFα-NFκB response. Further investigations, such

as the double knockdown of two antioxidant selenoproteins, would be required to specifically test the hypotheses. On the other hand, it is still possible that some other untested selenoprotein, expression of which is also affected in the Se- cells, might be responsible for the elevated TNFα-NFκB response observed in the Se depletion experiments. Therefore, the exact roles of antioxidant selenoproteins in the Se depletion-caused elevation of TNFα-NFκB response still remain to be elucidated.

Selenoproteins modulate the biosynthesis of eicosanoids, such as the leukotrienes through the 5-LOX metabolism pathway and prostaglandins through the COX1 and COX2 pathways (details reviewed in Section 1.3a), and some of these eicosanoids are capable of participating in the NFκB signalling system. For example, leukotriene B4 (LTB4), known to be inhibited by GPx1 and GPx4, is an NFκB activator in monocytes (Huang et al., 2004). In contrast, a subtype of prostaglandin, the 15-deoxy-Delta12,14-prostaglandin J2 (15d-PGJ2) was elevated by Se supplementation and inhibited NFκB activation (Vunta et al., 2007). Although the interaction between the LOX/COX pathways and the NFκB pathways was beyond the remit of the present study, these eicosaniods, as potential positive and negative NFκB regulators, may also play a role in the regulation of the NFκB signalling pathways by Se depletion and selenoprotein knockdown.

Most of the studies of GPx1 (Li et al., 2001, de Haan et al., 2004, Li and Engelhardt, 2006) and GPx4 (Wenk et al., 2004, Brigelius-Flohe et al., 1997) in relation to the NFκB signalling pathways have suggested that these antioxidant selenoproteins exert negative regulatory effects. The present study found that in Caco-2 cells GPx1 and GPx4 knockdown were associated with a decreased TNFα-NFκB response (Figure 22

(B) and 23 (B)) and flagellin-NFκB response (see Chapter 6 and Figure 32 (B) and 34 (B)), respectively, therefore appearing to contradict the earlier findings. It is notable that in the present study, both the findings in relation to GPx1 knockdown and GPx4 knockdown are consistent when the NFκB signalling pathways were studied using the NFκB-luciferase reporter model and the measurement of IL8 mRNA expression. Therefore, it is unlikely that these results were false-positive. The previous publications suggested that the NFκB signalling pathways are negatively regulated by antioxidants because the antioxidants can repress the cellular production of ROS which mediates the NFκB activation (Li et al., 2001, Li and Engelhardt, 2006). This proposed involvement of ROS is consistent with the findings of the present Se depletion studies, which resulted in both elevated ROS level and TNFα-NFκB response. However, ROS levels were unchanged in Caco-2 cells following GPx1 knockdown (Figure 25 (B)), and this is partially consistent with the decrease in TNFα-NFκB response. Therefore, the present data indicates that mechanisms such as the compensatory control of ROS by antioxidants occur in the cells and also participate in regulating NFκB inflammatory response. In addition, since human colonic epithelial Caco-2 cells are a new cell model for research into effects of Se on NFκB signalling pathways, and NFκB signalling pathways are highly cell-type and inducer-type dependent (reviewed in Section 1.2 and 1.3), it is feasible that the regulatory mechanisms identified in the TNFα- and flagellin-induced NFκB responses in Caco-2 cells are distinct from those observed in breast cancer and liver cells.

Overall, combining the findings of both the Se depletion and selenoprotein knockdown experiments, the present study indicates that in a human gut epithelial cell line, Se supply exerts regulatory effects on the TNFα-activated NFκB signalling

pathway but has no obvious effects on the flagellin-activated NFκB signalling pathway. Se depletion was associated with elevated TNFα-induced NFκB signalling in parallel with elevated cellular ROS level. At the level of individual selenoproteins, GPx1 knockdown exerted regulatory effects on the TNFα-activated NFκB signalling pathway in parallel with unchanged cellular ROS level, whereas GPx4 knockdown exerted regulatory effects on the flagellin-activated NFκB signalling pathway. These findings suggest that the TNFα-NFκB and the flagellin-NFκB signalling pathways are regulated differentially by Se and selenoproteins. The findings of the GPx4 knockdown experiments suggested a novel regulatory role for GPx4 in the flagellin-NFκB pathway, a pathway which has not been previously identified to be affected by Se depletion. Taking together the findings of the GPx1 and GPx4 knockdown experiments, it appears that different antioxidant selenoproteins might exert regulatory effects on different NFκB signalling pathways. Clearly, further investigation in future, provided more selenoproteins, such as TrxR1, TrxR2 and GPx2, could be included in studies of this area, would better expand the current knowledge that which selenoprotein(s) are the key player(s) in the regulation of which NFκB inflammatory signalling pathways.

TNFα is an inflammatory cytokine produced by mammalian cells. A large group of other cytokines, for example, IL1β, TNFβ and IL12, can also activate the NFκB signalling in an endogenous pathway (Gilmore, 2008). As mentioned earlier, these cytokines bind to various membrane receptors such as TNFR1 and are used to transfer inflammatory signals from cell to cell (Li and Lin, 2008). Generally, these cytokines, together with their receptors, are ubiquitously expressed in all eukaryotic cells. In comparison, flagellin together with the other bacterial components, such as LPS and

Triacyl/Diacyl lipopeptide, are produced by bacterial cells and they are capable of activating NFκB signalling through an exogenous pathway (Gilmore, 2008, Arancibia et al., 2007). These bacterial components bind to various TLR receptors and serve as direct inflammatory stimuli from bacteria to host cells (Arancibia et al., 2007). In addition, human gut epithelial cells can differentiate between pathogenic and commensal bacterial antigens so that only the former cause an inflammatory response (Gewirtz et al., 2001, Cario et al., 2002). For example, TLR5 is expressed on the basolateral surface of polarized intestinal cells and only the flagellin of the pathogenic bacteria, but not those of the commensal bacteria, can be transported to the basolateral cell membrane to activate the TLR5 pathway (Gewirtz et al., 2001). Another Toll-like receptor, TLR4, is expressed selectively in some gut epithelial cell-types, such as T84 cells (Cario et al., 2002), but not the others, such as Caco-2 cells (data not shown). Therefore, it is likely that the exogenous bacterial stimuli, together with their receptors, can be differentiated and selectively controlled by the gut epithelial cells.

On the basis of the type of NFκB inducer, i.e. cytokines and bacterial antigens, the results of the present studies suggests a model in which the endogenous and exogenous NFκB signalling pathways are differentially regulated by Se and selenoproteins to control against excessive inflammation in the gut epithelium. This is summarized below and illustrated in Figure 35.

At the beginning of a bacterial challenge, except following extreme changes such as GPx4 knockdown, Se supply does not appear to influence the NFκB inflammatory signalling in response to exogenous bacterial stimuli in the gut epithelial cells. This step probably allows the epithelial cells and/or immune cells to differentiate between

the pathogenic and commensal bacterial types and allows the immune cells to kill the invasive bacteria. Thus, the system allows the host to regulate the inflammatory response. However, Se supply seems to play a role in controlling the NFκB response to endogenous, i.e. host, stimuli. Moreover, this control appears to be accomplished by the different antioxidant proteins compensating for each other. These controls help to repress any excessive inflammation in the epithelial cells and protect cells from damage. This model can help to explain the link between insufficient Se intake and the increased risk of colonic cancer (Whanger, 2004), on the basis that there is increased inflammation resulting in cell damage and cancer. In addition, Se supplementation can ease the symptoms of inflammatory bowel disease (Halliwell et al., 2000, Tirosh et al., 2007) due to the ability of Se to inhibit inflammation in response to the endogenous cytokines. The GPx1 -/- and GPx2 -/- double knockout mice acquire repeated colitis (Esworthy et al., 2003, Lee et al., 2006) due to the additional stresses on the antioxidant system that normally would repress inflammation.

Finally, it is important to consider questions and hypotheses that would have been investigated if time had allowed. Here, Se depletion and GPx1 knockdown in relation to the selenoprotein expression had been studied using semi-quantitative RT-PCR addressing the mRNA level of selenoproteins GPx1, GPx4, SelW, SelH and GPx2 (Figure 26). Additional investigations addressing the mRNA level of these selenoproteins using real-time PCRs, or addressing their protein level using Western blots or protein activity level using GPx1, GPx4 and TrxR1 activity assays, would have been useful to further define how these selenoproteins are differently affected by Se depletion and GPx1 knockdown. Also of interest would be whether, if so, and how

the proposed compensation in combined antioxidant protein expression contributed to ROS clearance. Moreover, the present investigations (Figure 26) did not measure the expression of TrxR1 and TrxR2 and additional information in regard to their mRNA and/or protein expression in response to Se depletion and GPx1 knockdown would be valuable.

A further strategy to elucidate whether and how antioxidant selenoproteins co-operate to control NFκB inflammatory signalling would be to perform double knock-down experiments using two siRNAs in a combination to decrease the expression of both selenoproteins, such as GPx1 + GPx2, or GPx1 + GPx4. The comparison of double knock-down models with the results from Se depletion and/or GPx1/GPx4 knockdown on NFκB response would complement the current knowledge based on knockdown experiments of single selenoproteins. In addition, the Se depletion experiments of the present study relied on the comparison of two cell culture conditions, i.e. Se depletion (0nM) and Se-supplementation (7ng/ml, equivalent to an optimal Se concentration of 40nM), and a dynamic study using a range of Se concentration (0-40nM) might better describe how Se status affects the regulation of NFκB response from severe Se deficiency to optimal Se sufficiency.

In the research area of NFκB inflammatory signalling, to provide more support for the hypothesized NFκB-regulation model (Figure 35), additional NFκB signalling pathways, such as the endogenous IL1β-ILR (interleukin receptor) pathway and exogenous LPS-TLR4 pathway, need to be studied in relation to Se depletion and/or selenoprotein knockdown to test if these pathways are also differentially regulated by Se. Meanwhile, the present study investigated NFκB activation using a

NFκB-luciferase reporter model and IL8 mRNA measurement, but additional methodologies, such as IL8 protein expression (in parallel with the IL8 mRNA expression data by the present study), the expression of more NFκB target genes (a range of genes could be measured using commercial PCR-array approach), NFκB DNA-binding affinity (using EMSA) and IκB degradation (Western blot to measure IκB level), could be used to further strengthen the current conclusions.

The present study used the Carboxy-H_2DCFDA method to measure the total ROS production in cells (Shimizu et al., 2004), but this method could not differentiate between water-soluble ROS, such as H_2O_2, and oxidative fatty acids, such as R-OOH, during the TNFα-induced NFκB activation and/or following Se depletion and GPx1 knockdown. This needs to be addressed. In addition, it has been recently found that the NAPDH oxidase 2 (Nox2) complex and its derivative H_2O_2 play a key role in the TNFR1-NFκB pathway (Li et al., 2009, Yazdanpanah et al., 2009). Therefore, alternative methodologies, such as assessment of Nox2 expression and activities, are needed to provide more precise information in order to further understand the effects of Se depletion and GPx1 knockdown on ROS levels and NFκB signalling activation.

Despite the possible link between Se intake, gut inflammation and colorectal cancer risk, the biochemical and cellular mechanisms that link Se intake, gut epithelial cell function and carcinogenesis are poorly understood. Most previous studies investigating the influence of Se supplementation or selenoprotein overexpression on inflammatory signalling mechanisms such eicosanoid synthesis or NFκB signalling were not carried out on GI epithelial cells. The present research work is the first to study the effects of Se depletion on NFκB activation in response to TNFα or

flagellin in a colonic epithelial cell line (Caco-2 cells) and then to systematically analyze the different roles of depleted Se supply and down-regulated expression of selenoproteins GPx1, GPx4, SelW and SelH in NFκB regulation. Se depletion was found to result in elevated NFκB response to TNFα, but not flagellin. This indicates that Se deficiency, may influence a particular NFκB response rather than acting as a global modulator of these pathways. Further analyses using siRNA knockdown mimicked the down-regulation of GPx1, GPx4, SelW and SelH in Se depletion and revealed that altered expression of none of the tested selenoproteins exerted an effect on the TNFα-NFκB response that mimicked Se depletion. In addition, Se depletion increased cellular ROS levels, whereas GPx1 knockdown did not apparently change the ROS levels. These results indicate that Se, possibly through incorporation into multiple selenoproteins, acts as a unique control factor in NFκB regulation and has greater effects on the redox-system and redox-sensitive signalling pathways than any individual antioxidant selenoproteins. Moreover, GPx1 knockdown was also found to decrease the TNFα-NFκB response, suggesting the existence of functional compensation of antioxidants and co-regulation of NFκB activation by antioxidants in the redox-system.

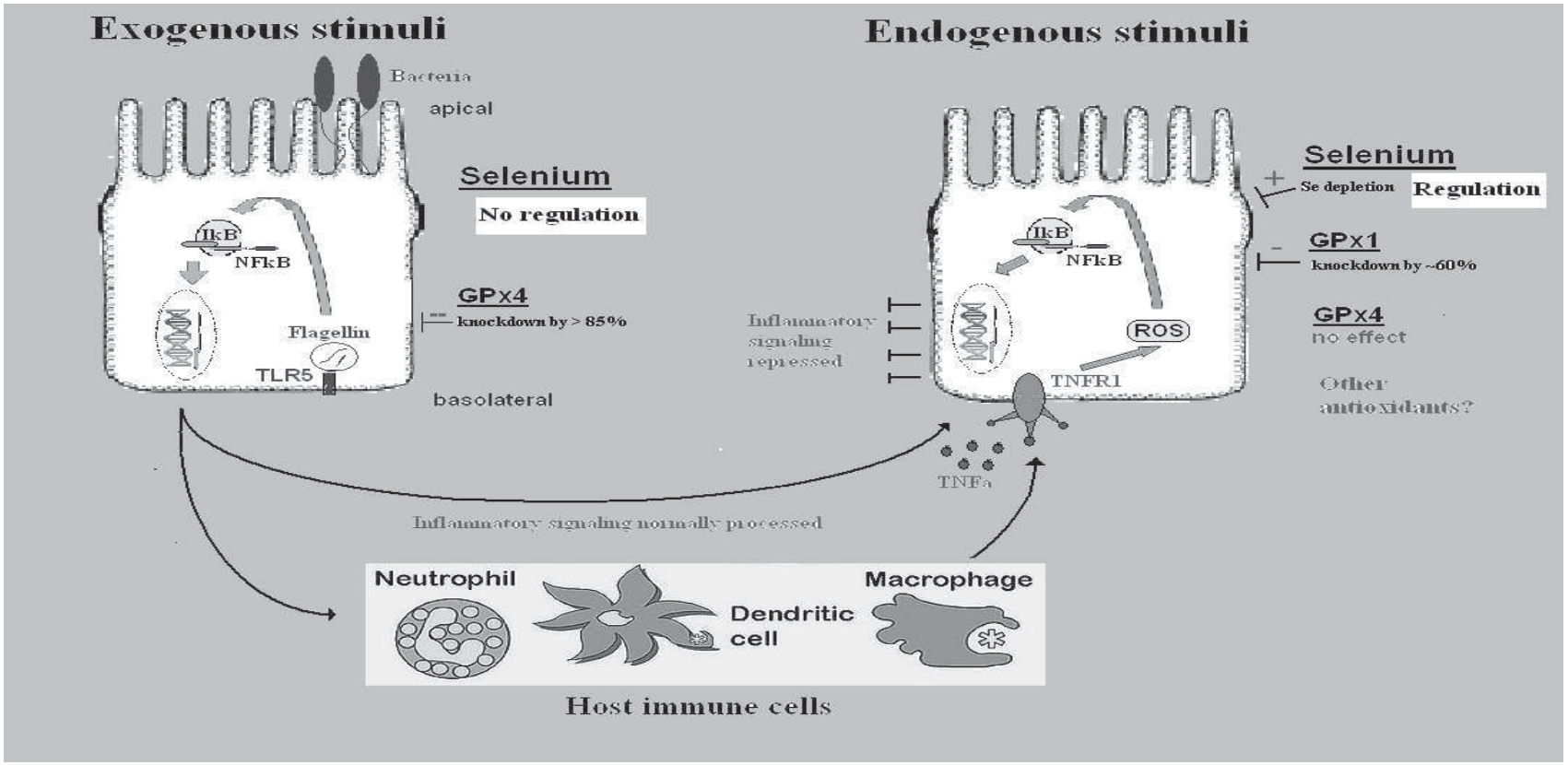

Figure 35: A hypothetical model of regulation of exogenous & endogenous NFκB responses by Se in gut epithelial cells

This hypothesized model is based on the findings described in this thesis. In the model, the exogenous NFκB signalling pathways activated by the bacterial components such as flagellin are not influenced by Se. As a result, the inflammatory signalling can be normally processed and passed to the host immune cells and the other epithelial cells. In contrast, when the inflammatory signalling is fed back through the inflammatory cytokines such as TNFα, the endogenous NFκB signalling pathways are repressed by Se. As a result, the excessive inflammation in the gut epithelial cells can be inhibited so as to avoid any unnecessary injuries to the gut epithelium.

Reference:

ADHIKARI, A., XU, M. & CHEN, Z. J. (2007) Ubiquitin-mediated activation of TAK1 and IKK. *Oncogene,* 26**,** 3214-26.

ANDERSEN-NISSEN, E., SMITH, K. D., BONNEAU, R., STRONG, R. K. & ADEREM, A. (2007) A conserved surface on Toll-like receptor 5 recognizes bacterial flagellin. *Journal of Experimental Medicine,* 204**,** 393-403.

ARAI, M., IMAI, H., SUMI, D., IMANAKA, T., TAKANO, T., CHIBA, N. & NAKAGAWA, Y. (1996) Import into mitochondria of phospholipid hydroperoxide glutathione peroxidase requires a leader sequence. *Biochemical & Biophysical Research Communications,* 227**,** 433-9.

ARAKAWA, T., NAKAMURA, M., YOSHIMOTO, T. & YAMAMOTO, S. (1995) The transcriptional regulation of human arachidonate 12-lipoxygenase gene by NF kappa B/Rel. *FEBS Letters,* 363**,** 105-10.

ARANCIBIA, S. A., BELTRAN, C. J., AGUIRRE, I. M., SILVA, P., PERALTA, A. L., MALINARICH, F. & HERMOSO, M. A. (2007) Toll-like receptors are key participants in innate immune responses. *Biological Research,* 40**,** 97-112.

ARBOGAST, S. & FERREIRO, A. (2010) Selenoproteins and protection against oxidative stress: selenoprotein N as a novel player at the crossroads of redox signaling and calcium homeostasis. *Antioxidants & Redox Signaling,* 12**,** 893-904.

ARTHUR, J. R. (2000) The glutathione peroxidases. *Cellular & Molecular Life Sciences,* 57**,** 1825-35.

ARTHUR, J. R. & BOYNE, R. (1985) Superoxide dismutase and glutathione peroxidase activities in neutrophils from selenium deficient and copper deficient cattle. *Life Sciences,* 36**,** 1569-75.

ATKINSON, G. P., NOZELL, S. E., HARRISON, D. K., STONECYPHER, M. S., CHEN, D. & BENVENISTE, E. N. (2009) The prolyl isomerase Pin1 regulates the NF-kappaB signaling pathway and interleukin-8 expression in glioblastoma. *Oncogene,* 28**,** 3735-45.

AUMANN, K. D., BEDORF, N., BRIGELIUS-FLOHE, R., SCHOMBURG, D. & FLOHE, L. (1997) Glutathione peroxidase revisited--simulation of the catalytic cycle by computer-assisted molecular modelling. *Biomedical & Environmental Sciences,* 10**,** 136-55.

AVISSAR, N., ORNT, D. B., YAGIL, Y., HOROWITZ, S., WATKINS, R. H., KERL, E. A., TAKAHASHI, K., PALMER, I. S. & COHEN, H. J. (1994) Human kidney proximal tubules are the main source of plasma glutathione peroxidase. *American Journal of Physiology,* 266**,** C367-75.

BAJT, M. L., HO, Y.-S., VONDERFECHT, S. L. & JAESCHKE, H. (2002) Reactive oxygen as modulator of TNF and fas receptor-mediated apoptosis in vivo: studies with glutathione peroxidase-deficient mice. *Antioxidants & Redox Signaling,* 4**,** 733-40.

BANNING, A. & BRIGELIUS-FLOHE, R. (2005) NF-kappaB, Nrf2, and HO-1 interplay in redox-regulated VCAM-1 expression. *Antioxidants & Redox Signaling,* 7**,** 889-99.

BANNING, A., FLORIAN, S., DEUBEL, S., THALMANN, S., MULLER-SCHMEHL, K., JACOBASCH, G. & BRIGELIUS-FLOHE, R. (2008a) GPx2 counteracts PGE2 production by dampening COX-2 and

mPGES-1 expression in human colon cancer cells. *Antioxidants & Redox Signaling,* 10**,** 1491-500.

BANNING, A., KIPP, A., SCHMITMEIER, S., LOWINGER, M., FLORIAN, S., KREHL, S., THALMANN, S., THIERBACH, R., STEINBERG, P. & BRIGELIUS-FLOHE, R. (2008b) Glutathione Peroxidase 2 Inhibits Cyclooxygenase-2-Mediated Migration and Invasion of HT-29 Adenocarcinoma Cells but Supports Their Growth as Tumors in Nude Mice. *Cancer Research,* 68**,** 9746-53.

BANNING, A., SCHNURR, K., BOL, G. F., KUPPER, D., MULLER-SCHMEHL, K., VIITA, H., YLA-HERTTUALA, S. & BRIGELIUS-FLOHE, R. (2004) Inhibition of basal and interleukin-1-induced VCAM-1 expression by phospholipid hydroperoxide glutathione peroxidase and 15-lipoxygenase in rabbit aortic smooth muscle cells. *Free Radical Biology & Medicine,* 36**,** 135-44.

BAO, Y., JEMTH, P., MANNERVIK, B. & WILLIAMSON, G. (1997) Reduction of thymine hydroperoxide by phospholipid hydroperoxide glutathione peroxidase and glutathione transferases. *FEBS Letters,* 410**,** 210-2.

BARRIERE, G., RABINOVITCH-CHABLE, H., COOK-MOREAU, J., FAUCHER, K., RIGAUD, M. & STURTZ, F. (2004) PHGPx overexpression induces an increase in COX-2 activity in colon carcinoma cells. *Anticancer Research,* 24**,** 1387-92.

BAUM, M. K., SHOR-POSNER, G., LAI, S., ZHANG, G., LAI, H., FLETCHER, M. A., SAUBERLICH, H. & PAGE, J. B. (1997) High risk of HIV-related mortality is associated with selenium deficiency. *Journal of Acquired Immune Deficiency Syndromes & Human Retrovirology,* 15**,** 370-4.

BECK, M. A. (1997) Increased virulence of coxsackievirus B3 in mice due to vitamin E or selenium deficiency. *Journal of Nutrition,* 127**,** 966S-970S.

BECK, M. A. (1999) Selenium and host defence towards viruses. *Proceedings of the Nutrition Society,* 58**,** 707-11.

BECK, M. A., ESWORTHY, R. S., HO, Y. S. & CHU, F. F. (1998) Glutathione peroxidase protects mice from viral-induced myocarditis. *FASEB Journal,* 12**,** 1143-9.

BECK, M. A., NELSON, H. K., SHI, Q., VAN DAEL, P., SCHIFFRIN, E. J., BLUM, S., BARCLAY, D. & LEVANDER, O. A. (2001) Selenium deficiency increases the pathology of an influenza virus infection. *FASEB Journal,* 15**,** 1481-3.

BECK, M. A., SHI, Q., MORRIS, V. C. & LEVANDER, O. A. (1995) Rapid genomic evolution of a non-virulent coxsackievirus B3 in selenium-deficient mice results in selection of identical virulent isolates. *Nature Medicine,* 1**,** 433-6.

BELLINGER, F. P., RAMAN, A. V., REEVES, M. A. & BERRY, M. J. (2009) Regulation and function of selenoproteins in human disease. *Biochemical Journal,* 422**,** 11-22.

BELLINGHAM, J., GREGORY-EVANS, K., FOX, M. F. & GREGORY-EVANS, C. Y. (2003) Gene structure and tissue expression of human selenoprotein W, SEPW1, and identification of a retroprocessed pseudogene, SEPW1P. *Biochimica et Biophysica Acta,* 1627**,** 140-6.

BEN JILANI, K. E., PANEE, J., HE, Q., BERRY, M. J. & LI, P.-A. (2007) Overexpression of selenoprotein H reduces Ht22 neuronal cell death after

UVB irradiation by preventing superoxide formation. *International Journal of Biological Sciences [Electronic Resource],* 3**,** 198-204.

BERMANO, G., ARTHUR, J. R. & HESKETH, J. E. (1996a) Role of the 3' untranslated region in the regulation of cytosolic glutathione peroxidase and phospholipid-hydroperoxide glutathione peroxidase gene expression by selenium supply. *Biochemical Journal,* 320**,** 891-5.

BERMANO, G., ARTHUR, J. R. & HESKETH, J. E. (1996b) Selective control of cytosolic glutathione peroxidase and phospholipid hydroperoxide glutathione peroxidase mRNA stability by selenium supply. *FEBS Letters,* 387**,** 157-60.

BERMANO, G., NICOL, F., DYER, J. A., SUNDE, R. A., BECKETT, G. J., ARTHUR, J. R. & HESKETH, J. E. (1995) Tissue-specific regulation of selenoenzyme gene expression during selenium deficiency in rats. *Biochemical Journal,* 311**,** 425-30.

BERRY, M. J. (2005) Insights into the hierarchy of selenium incorporation. *Nature Genetics,* 37**,** 1162-3.

BHATTACHARYYA, S., DUDEJA, P. K. & TOBACMAN, J. K. (2008) Lipopolysaccharide activates NF-kappaB by TLR4-Bcl10-dependent and independent pathways in colonic epithelial cells. *American Journal of Physiology - Gastrointestinal & Liver Physiology,* 295**,** G784-90.

BJORNSTEDT, M., XUE, J., HUANG, W., AKESSON, B. & HOLMGREN, A. (1994) The thioredoxin and glutaredoxin systems are efficient electron donors to human plasma glutathione peroxidase. *Journal of Biological Chemistry,* 269**,** 29382-4.

BLONSKA, M., SHAMBHARKAR, P. B., KOBAYASHI, M., ZHANG, D., SAKURAI, H., SU, B. & LIN, X. (2005) TAK1 is recruited to the tumor necrosis factor-alpha (TNF-alpha) receptor 1 complex in a receptor-interacting protein (RIP)-dependent manner and cooperates with MEKK3 leading to NF-kappaB activation. *Journal of Biological Chemistry,* 280**,** 43056-63.

BLONSKA, M., YOU, Y., GELEZIUNAS, R. & LIN, X. (2004) Restoration of NF-kappaB activation by tumor necrosis factor alpha receptor complex-targeted MEKK3 in receptor-interacting protein-deficient cells. *Molecular & Cellular Biology,* 24**,** 10757-65.

BOL, G.-F., JURRMANN, N. & BRIGELIUS-FLOHE, R. (2003) Recruitment of the interleukin-1 receptor (IL-1RI)-associated kinase IRAK to the IL-1RI is redox regulated. *Biological Chemistry,* 384**,** 609-17.

BOLDIN, M. P., METT, I. L., VARFOLOMEEV, E. E., CHUMAKOV, I., SHEMER-AVNI, Y., CAMONIS, J. H. & WALLACH, D. (1995) Self-association of the "death domains" of the p55 tumor necrosis factor (TNF) receptor and Fas/APO1 prompts signaling for TNF and Fas/APO1 effects. *Journal of Biological Chemistry,* 270**,** 387-91.

BOSL, M. R., TAKAKU, K., OSHIMA, M., NISHIMURA, S. & TAKETO, M. M. (1997) Early embryonic lethality caused by targeted disruption of the mouse selenocysteine tRNA gene (Trsp). *Proceedings of the National Academy of Sciences of the United States of America,* 94**,** 5531-4.

BOSSCHAERTS, T., GUILLIAMS, M., NOEL, W., X00E, RIN, M., BURK, R. F., HILL, K. E., BRYS, L., RAES, G., GHASSABEH, G. H., DE BAETSELIER, P. & BESCHIN, A. (2008) Alternatively activated myeloid cells limit pathogenicity associated with African trypanosomiasis through the IL-10 inducible gene selenoprotein P. *Journal of Immunology,* 180**,** 6168-75.

BOYNE, R. & ARTHUR, J. R. (1979) Alterations of neutrophil function in selenium-deficient cattle. *Journal of Comparative Pathology,* 89**,** 151-8.

BRIGELIUS-FLOHE, R. (1999) Tissue-specific functions of individual glutathione peroxidases. *Free Radical Biology & Medicine,* 27**,** 951-65.

BRIGELIUS-FLOHE, R. (2006) Glutathione peroxidases and redox-regulated transcription factors. *Biological Chemistry,* 387**,** 1329-35.

BRIGELIUS-FLOHE, R. (2008) Selenium compounds and selenoproteins in cancer. *Chemistry & Biodiversity,* 5**,** 389-95.

BRIGELIUS-FLOHE, R., BANNING, A., KNY, M. & BOL, G.-F. (2004) Redox events in interleukin-1 signaling. *Archives of Biochemistry & Biophysics,* 423**,** 66-73.

BRIGELIUS-FLOHE, R., FRIEDRICHS, B., MAURER, S., SCHULTZ, M. & STREICHER, R. (1997) Interleukin-1-induced nuclear factor kappa B activation is inhibited by overexpression of phospholipid hydroperoxide glutathione peroxidase in a human endothelial cell line. *Biochemical Journal,* 328**,** 199-203.

BRIGELIUS-FLOHE, R. & KIPP, A. (2009) Glutathione peroxidases in different stages of carcinogenesis. *Biochimica et Biophysica Acta,* 1790**,** 1555-68.

BRIGELIUS-FLOHE, R., MAURER, S., LOTZER, K., BOL, G., KALLIONPAA, H., LEHTOLAINEN, P., VIITA, H. & YLA-HERTTUALA, S. (2000) Overexpression of PHGPx inhibits hydroperoxide-induced oxidation, NFkappaB activation and apoptosis and affects oxLDL-mediated proliferation of rabbit aortic smooth muscle cells. *Atherosclerosis,* 152**,** 307-16.

BROWN, K. M. & ARTHUR, J. R. (2001) Selenium, selenoproteins and human health: a review. *Public Health Nutrition,* 4**,** 593-9.

BURK, R. F. & HILL, K. E. (2009) Selenoprotein P-expression, functions, and roles in mammals. *Biochimica et Biophysica Acta,* 1790**,** 1441-7.

CAMPA, A., SHOR-POSNER, G., INDACOCHEA, F., ZHANG, G., LAI, H., ASTHANA, D., SCOTT, G. B. & BAUM, M. K. (1999) Mortality risk in selenium-deficient HIV-positive children. *Journal of Acquired Immune Deficiency Syndromes & Human Retrovirology,* 20**,** 508-13.

CAMPBELL, L., HOWIE, F., ARTHUR, J. R., NICOL, F. & BECKETT, G. (2007) Selenium and sulforaphane modify the expression of selenoenzymes in the human endothelial cell line EAhy926 and protect cells from oxidative damage.[Erratum appears in Nutrition. 2007 Apr;23(4):378]. *Nutrition,* 23**,** 138-44.

CARIO, E., BROWN, D., MCKEE, M., LYNCH-DEVANEY, K., GERKEN, G. & PODOLSKY, D. K. (2002) Commensal-associated molecular patterns induce selective toll-like receptor-trafficking from apical membrane to cytoplasmic compartments in polarized intestinal epithelium. *American Journal of Pathology,* 160**,** 165-73.

CARLOTTI, F., DOWER, S. K. & QWARNSTROM, E. E. (2000) Dynamic shuttling of nuclear factor kappa B between the nucleus and cytoplasm as a consequence of inhibitor dissociation. *Journal of Biological Chemistry,* 275**,** 41028-34.

CARLSEN, H., MOSKAUG, J. O., FROMM, S. H. & BLOMHOFF, R. (2002) In vivo imaging of NF-kappa B activity. *Journal of Immunology,* 168**,** 1441-6.

CARMODY, R. J. & CHEN, Y. H. (2007) Nuclear factor-kappaB: activation and regulation during toll-like receptor signaling. *Cellular & Molecular Immunology,* 4**,** 31-41.

CATZ, S. D. & JOHNSON, J. L. (2001) Transcriptional regulation of bcl-2 by nuclear factor kappa B and its significance in prostate cancer. *Oncogene,* 20**,** 7342-51.

CHAN, D. W., LIU, V. W. S., TSAO, G. S. W., YAO, K.-M., FURUKAWA, T., CHAN, K. K. L. & NGAN, H. Y. S. (2008) Loss of MKP3 mediated by oxidative stress enhances tumorigenicity and chemoresistance of ovarian cancer cells. *Carcinogenesis,* 29**,** 1742-50.

CHEN, C.-J., HUANG, H.-S. & CHANG, W.-C. (2002) Inhibition of arachidonate metabolism in human epidermoid carcinoma a431 cells overexpressing phospholipid hydroperoxide glutathione peroxidase. *Journal of Biomedical Science,* 9**,** 453-9.

CHEN, C.-J., HUANG, H.-S. & CHANG, W.-C. (2003) Depletion of phospholipid hydroperoxide glutathione peroxidase up-regulates arachidonate metabolism by 12S-lipoxygenase and cyclooxygenase 1 in human epidermoid carcinoma A431 cells. *FASEB Journal,* 17**,** 1694-6.

CHEN, C. J., HUANG, H. S., LIN, S. B. & CHANG, W. C. (2000) Regulation of cyclooxygenase and 12-lipoxygenase catalysis by phospholipid hydroperoxide glutathione peroxidase in A431 cells. *Prostaglandins Leukotrienes & Essential Fatty Acids,* 62**,** 261-8.

CHEN, G. & GOEDDEL, D. V. (2002) TNF-R1 signaling: a beautiful pathway. *Science,* 296**,** 1634-5.

CHEN, K.-M., SPRATT, T. E., STANLEY, B. A., DE COTIIS, D. A., BEWLEY, M. C., FLANAGAN, J. M., DESAI, D., DAS, A., FIALA, E. S., AMIN, S. & EL-BAYOUMY, K. (2007) Inhibition of nuclear factor-kappaB DNA binding by organoselenocyanates through covalent modification of the p50 subunit. *Cancer Research,* 67**,** 10475-83.

CHENG, H., ADDONA, T., KESHISHIAN, H., DAHLSTRAND, E., LU, C., DORSCH, M., LI, Z., WANG, A., OCAIN, T. D., LI, P., PARSONS, T. F., JAFFEE, B. & XU, Y. (2007) Regulation of IRAK-4 kinase activity via autophosphorylation within its activation loop. *Biochemical & Biophysical Research Communications,* 352**,** 609-16.

CHEUNG, P. C. F., CAMPBELL, D. G., NEBREDA, A. R. & COHEN, P. (2003) Feedback control of the protein kinase TAK1 by SAPK2a/p38alpha. *EMBO Journal,* 22**,** 5793-805.

CHOMCZYNSKI, P. & SACCHI, N. (1987) Single-step method of RNA isolation by acid guanidinium thiocyanate-phenol-chloroform extraction. *Analytical Biochemistry,* 162**,** 156-9.

CHOPRA, A., FERREIRA-ALVES, D. L., SIROIS, P. & THIRION, J. P. (1992) Cloning of the guinea pig 5-lipoxygenase gene and nucleotide sequence of its promoter. *Biochemical & Biophysical Research Communications,* 185**,** 489-95.

CHRISTENSEN, M. J., NARTEY, E. T., HADA, A. L., LEGG, R. L. & BARZEE, B. R. (2007) High selenium reduces NF-kappaB-regulated gene expression in uninduced human prostate cancer cells. *Nutrition & Cancer,* 58**,** 197-204.

CHU, F. F., DOROSHOW, J. H. & ESWORTHY, R. S. (1993) Expression, characterization, and tissue distribution of a new cellular selenium-dependent glutathione peroxidase, GSHPx-GI. *Journal of Biological Chemistry,* 268**,** 2571-6.

CHUNG, Y. W., JEONG, D., NOH, O. J., PARK, Y. H., KANG, S. I., LEE, M. G., LEE, T.-H., YIM, M. B. & KIM, I. Y. (2009) Antioxidative role of

selenoprotein W in oxidant-induced mouse embryonic neuronal cell death. *Molecules & Cells,* 27**,** 609-13.

CLARK, L. C., COMBS, G. F., JR., TURNBULL, B. W., SLATE, E. H., CHALKER, D. K., CHOW, J., DAVIS, L. S., GLOVER, R. A., GRAHAM, G. F., GROSS, E. G., KRONGRAD, A., LESHER, J. L., JR., PARK, H. K., SANDERS, B. B., JR., SMITH, C. L. & TAYLOR, J. R. (1996) Effects of selenium supplementation for cancer prevention in patients with carcinoma of the skin. A randomized controlled trial. Nutritional Prevention of Cancer Study Group.[Erratum appears in JAMA 1997 May 21;277(19):1520]. *JAMA,* 276**,** 1957-63.

COIRAS, M., LOPEZ-HUERTAS, M. R., RULLAS, J., MITTELBRUNN, M. & ALCAMI, J. (2007) Basal shuttle of NF-kappaB/I kappaB alpha in resting T lymphocytes regulates HIV-1 LTR dependent expression. *Retrovirology,* 4**,** 56.

COMBS, G. F., JR. (2000) Food system-based approaches to improving micronutrient nutrition: the case for selenium. *Biofactors,* 12**,** 39-43.

CONRAD, M. (2009) Transgenic mouse models for the vital selenoenzymes cytosolic thioredoxin reductase, mitochondrial thioredoxin reductase and glutathione peroxidase 4. *Biochimica et Biophysica Acta,* 1790**,** 1575-85.

COPELAND, P. R., FLETCHER, J. E., CARLSON, B. A., HATFIELD, D. L. & DRISCOLL, D. M. (2000) A novel RNA binding protein, SBP2, is required for the translation of mammalian selenoprotein mRNAs. *EMBO Journal,* 19**,** 306-14.

CRACK, P. J., TAYLOR, J. M., ALI, U., MANSELL, A. & HERTZOG, P. J. (2006) Potential contribution of NF-kappaB in neuronal cell death in the glutathione peroxidase-1 knockout mouse in response to ischemia-reperfusion injury. *Stroke,* 37**,** 1533-8.

CRANE, M. S., HOWIE, A. F., ARTHUR, J. R., NICOL, F., CROSLEY, L. K. & BECKETT, G. J. (2009) Modulation of thioredoxin reductase-2 expression in EAhy926 cells: implications for endothelial selenoprotein hierarchy. *Biochimica et Biophysica Acta,* 1790**,** 1191-7.

CROSLEY, L. K., MEPLAN, C., NICOL, F., RUNDLOF, A. K., ARNER, E. S. J., HESKETH, J. E. & ARTHUR, J. R. (2007) Differential regulation of expression of cytosolic and mitochondrial thioredoxin reductase in rat liver and kidney. *Archives of Biochemistry & Biophysics,* 459**,** 178-88.

CURRAN, J. E., JOWETT, J. B. M., ELLIOTT, K. S., GAO, Y., GLUSCHENKO, K., WANG, J., ABEL AZIM, D. M., CAI, G., MAHANEY, M. C., COMUZZIE, A. G., DYER, T. D., WALDER, K. R., ZIMMET, P., MACCLUER, J. W., COLLIER, G. R., KISSEBAH, A. H. & BLANGERO, J. (2005) Genetic variation in selenoprotein S influences inflammatory response. *Nature Genetics,* 37**,** 1234-41.

DAMAS, P., REUTER, A., GYSEN, P., DEMONTY, J., LAMY, M. & FRANCHIMONT, P. (1989) Tumor necrosis factor and interleukin-1 serum levels during severe sepsis in humans. *Critical Care Medicine,* 17**,** 975-8.

DE HAAN, J. B., BLADIER, C., LOTFI-MIRI, M., TAYLOR, J., HUTCHINSON, P., CRACK, P. J., HERTZOG, P. & KOLA, I. (2004) Fibroblasts derived from Gpx1 knockout mice display senescent-like features and are susceptible to H2O2-mediated cell death. *Free Radical Biology & Medicine,* 36**,** 53-64.

DENG, L., WANG, C., SPENCER, E., YANG, L., BRAUN, A., YOU, J., SLAUGHTER, C., PICKART, C. & CHEN, Z. J. (2000) Activation of the

IkappaB kinase complex by TRAF6 requires a dimeric ubiquitin-conjugating enzyme complex and a unique polyubiquitin chain. *Cell,* 103**,** 351-61.

DEVIN, A., COOK, A., LIN, Y., RODRIGUEZ, Y., KELLIHER, M. & LIU, Z. (2000) The distinct roles of TRAF2 and RIP in IKK activation by TNF-R1: TRAF2 recruits IKK to TNF-R1 while RIP mediates IKK activation. *Immunity,* 12**,** 419-29.

DEY, I., GIEMBYCZ, M. A. & CHADEE, K. (2009) Prostaglandin E(2) couples through EP(4) prostanoid receptors to induce IL-8 production in human colonic epithelial cell lines. *British Journal of Pharmacology,* 156**,** 475-85.

DIKIY, A., NOVOSELOV, S. V., FOMENKO, D. E., SENGUPTA, A., CARLSON, B. A., CERNY, R. L., GINALSKI, K., GRISHIN, N. V., HATFIELD, D. L. & GLADYSHEV, V. N. (2007) SelT, SelW, SelH, and Rdx12: genomics and molecular insights into the functions of selenoproteins of a novel thioredoxin-like family. *Biochemistry,* 46**,** 6871-82.

DOBRZANSKI, P., RYSECK, R. P. & BRAVO, R. (1995) Specific inhibition of RelB/p52 transcriptional activity by the C-terminal domain of p100. *Oncogene,* 10**,** 1003-7.

DREHER, I., SCHMUTZLER, C., JAKOB, F., X00F & HRLE, J. (1997) Expression of selenoproteins in various rat and human tissues and cell lines. *Journal of Trace Elements in Medicine & Biology,* 11**,** 83-91.

DROGE, W. (2002) Free radicals in the physiological control of cell function. *Physiological Reviews,* 82**,** 47-95.

DUERKOP, B. A., VAISHNAVA, S. & HOOPER, L. V. (2009) Immune responses to the microbiota at the intestinal mucosal surface. *Immunity,* 31**,** 368-76.

DUFFIELD-LILLICO, A. J., REID, M. E., TURNBULL, B. W., COMBS, G. F., JR., SLATE, E. H., FISCHBACH, L. A., MARSHALL, J. R. & CLARK, L. C. (2002) Baseline characteristics and the effect of selenium supplementation on cancer incidence in a randomized clinical trial: a summary report of the Nutritional Prevention of Cancer Trial.[see comment]. *Cancer Epidemiology, Biomarkers & Prevention,* 11**,** 630-9.

EA, C.-K., DENG, L., XIA, Z.-P., PINEDA, G. & CHEN, Z. J. (2006) Activation of IKK by TNFalpha requires site-specific ubiquitination of RIP1 and polyubiquitin binding by NEMO. *Molecular Cell,* 22**,** 245-57.

EISINGER, A. L., PRESCOTT, S. M., JONES, D. A. & STAFFORINI, D. M. (2007) The role of cyclooxygenase-2 and prostaglandins in colon cancer. *Prostaglandins & Other Lipid Mediators,* 82**,** 147-54.

ESWORTHY, R. S., BINDER, S. W., DOROSHOW, J. H. & CHU, F.-F. (2003) Microflora trigger colitis in mice deficient in selenium-dependent glutathione peroxidase and induce Gpx2 gene expression. *Biological Chemistry,* 384**,** 597-607.

FAN, C., LI, Q., ROSS, D. & ENGELHARDT, J. F. (2003) Tyrosine phosphorylation of I kappa B alpha activates NF kappa B through a redox-regulated and c-Src-dependent mechanism following hypoxia/reoxygenation. *Journal of Biological Chemistry,* 278**,** 2072-80.

FAROOQ, A. & ZHOU, M.-M. (2004) Structure and regulation of MAPK phosphatases. *Cellular Signalling,* 16**,** 769-79.

FAWZI, W., MSAMANGA, G., SPIEGELMAN, D. & HUNTER, D. J. (2005) Studies of vitamins and minerals and HIV transmission and disease progression. *Journal of Nutrition,* 135**,** 938-44.

FLORIAN, S., KREHL, S., LOEWINGER, M., KIPP, A., BANNING, A., ESWORTHY, S., CHU, F. & BRIGELIUS-FLOHÉ, R. (2010) Loss of GPx2 increases apoptosis, mitosis, and GPx1 expression in the intestine of mice. *Free Radic Biol Med,* 49**,** 1694-702.

FORSTROM, J. W., STULTS, F. H. & TAPPEL, A. L. (1979) Rat liver cytosolic glutathione peroxidase: reactivity with linoleic acid hydroperoxide and cumene hydroperoxide. *Archives of Biochemistry & Biophysics,* 193**,** 51-5.

FURST, R., SCHROEDER, T., EILKEN, H. M., BUBIK, M. F., KIEMER, A. K., ZAHLER, S. & VOLLMAR, A. M. (2007) MAPK phosphatase-1 represents a novel anti-inflammatory target of glucocorticoids in the human endothelium. *FASEB Journal,* 21**,** 74-80.

GANTHER, H. E. (1999) Selenium metabolism, selenoproteins and mechanisms of cancer prevention: complexities with thioredoxin reductase. *Carcinogenesis,* 20**,** 1657-66.

GAO, J., XIONG, Y., HO, Y.-S., LIU, X., CHUA, C. C., XU, X., WANG, H., HAMDY, R. & CHUA, B. H. L. (2008) Glutathione peroxidase 1-deficient mice are more susceptible to doxorubicin-induced cardiotoxicity. *Biochimica et Biophysica Acta,* 1783**,** 2020-9.

GASPARIAN, A. V., YAO, Y. J., LU, J., YEMELYANOV, A. Y., LYAKH, L. A., SLAGA, T. J. & BUDUNOVA, I. V. (2002) Selenium compounds inhibit I kappa B kinase (IKK) and nuclear factor-kappa B (NF-kappa B) in prostate cancer cells. *Molecular Cancer Therapeutics,* 1**,** 1079-87.

GAUTAM, D. K., MISRO, M. M., CHAKI, S. P. & SEHGAL, N. (2006) H2O2 at physiological concentrations modulates Leydig cell function inducing oxidative stress and apoptosis. *Apoptosis,* 11**,** 39-46.

GEERLING, B. J., BADART-SMOOK, A., STOCKBRUGGER, R. W. & BRUMMER, R. J. (2000) Comprehensive nutritional status in recently diagnosed patients with inflammatory bowel disease compared with population controls. *European Journal of Clinical Nutrition,* 54**,** 514-21.

GEWIRTZ, A. T., NAVAS, T. A., LYONS, S., GODOWSKI, P. J. & MADARA, J. L. (2001) Cutting edge: bacterial flagellin activates basolaterally expressed TLR5 to induce epithelial proinflammatory gene expression. *Journal of Immunology,* 167**,** 1882-5.

GILMORE, T. D. (2008) nf-kb.org.

GLINEUR, C., DAVIOUD-CHARVET, E. & VANDENBUNDER, B. (2000) The conserved redox-sensitive cysteine residue of the DNA-binding region in the c-Rel protein is involved in the regulation of the phosphorylation of the protein. *Biochemical Journal,* 352 Pt 2**,** 583-91.

GLOIRE, G., LEGRAND-POELS, S. & PIETTE, J. (2006) NF-kappaB activation by reactive oxygen species: fifteen years later. *Biochemical Pharmacology,* 72**,** 1493-505.

GLOIRE, G. & PIETTE, J. (2009) Redox regulation of nuclear post-translational modifications during NF-kappaB activation. *Antioxidants & Redox Signaling,* 11**,** 2209-22.

GRANDVAUX, N., SOUCY-FAULKNER, A. & FINK, K. (2007) Innate host defense: Nox and Duox on phox's tail. *Biochimie,* 89**,** 1113-22.

GROSSMANN, A. & WENDEL, A. (1983) Non-reactivity of the selenoenzyme glutathione peroxidase with enzymatically hydroperoxidized phospholipids. *European Journal of Biochemistry,* 135**,** 549-52.

GRUNE, T., REINHECKEL, T. & DAVIES, K. J. (1997) Degradation of oxidized proteins in mammalian cells. *FASEB Journal,* 11**,** 526-34.

HADDAD, J. J. (2002) Oxygen-sensitive pro-inflammatory cytokines, apoptosis signaling and redox-responsive transcription factors in development and pathophysiology. *Cytokines, Cellular & Molecular Therapy,* 7**,** 1-14.

HAHN, M. A., HAHN, T., LEE, D.-H., ESWORTHY, R. S., KIM, B.-W., RIGGS, A. D., CHU, F.-F. & PFEIFER, G. P. (2008) Methylation of polycomb target genes in intestinal cancer is mediated by inflammation. *Cancer Research,* 68**,** 10280-9.

HALLIWELL, B., ZHAO, K. & WHITEMAN, M. (2000) The gastrointestinal tract: a major site of antioxidant action? *Free Radical Research,* 33**,** 819-30.

HARRISON, L. M., RALLABHANDI, P., MICHALSKI, J., ZHOU, X., STEYERT, S. R., VOGEL, S. N. & KAPER, J. B. (2008) Vibrio cholerae flagellins induce Toll-like receptor 5-mediated interleukin-8 production through mitogen-activated protein kinase and NF-kappaB activation. *Infection & Immunity,* 76**,** 5524-34.

HATTORI, H., IMAI, H., HANAMOTO, A., FURUHAMA, K. & NAKAGAWA, Y. (2005) Up-regulation of phospholipid hydroperoxide glutathione peroxidase in rat casein-induced polymorphonuclear neutrophils.[Erratum appears in Biochem J. 2005 Aug 1;389(Pt 3):920]. *Biochemical Journal,* 389**,** 279-87.

HAYASHI, F., SMITH, K. D., OZINSKY, A., HAWN, T. R., YI, E. C., GOODLETT, D. R., ENG, J. K., AKIRA, S., UNDERHILL, D. M. & ADEREM, A. (2001) The innate immune response to bacterial flagellin is mediated by Toll-like receptor 5. *Nature,* 410**,** 1099-103.

HAYASHI, T., UENO, Y. & OKAMOTO, T. (1993) Oxidoreductive regulation of nuclear factor kappa B. Involvement of a cellular reducing catalyst thioredoxin. *Journal of Biological Chemistry,* 268**,** 11380-8.

HAYDEN, M. S. & GHOSH, S. (2008) Shared principles in NF-kappaB signaling. *Cell,* 132**,** 344-62.

HEIRMAN, I., GINNEBERGE, D., BRIGELIUS-FLOHE, R., HENDRICKX, N., AGOSTINIS, P., BROUCKAERT, P., ROTTIERS, P. & GROOTEN, J. (2006) Blocking tumor cell eicosanoid synthesis by GP x 4 impedes tumor growth and malignancy. *Free Radical Biology & Medicine,* 40**,** 285-94.

HENDERSON, W. R., JR. (1994) The role of leukotrienes in inflammation. *Annals of Internal Medicine,* 121**,** 684-97.

HILL, K. E., ZHOU, J., MCMAHAN, W. J., MOTLEY, A. K., ATKINS, J. F., GESTELAND, R. F. & BURK, R. F. (2003) Deletion of selenoprotein P alters distribution of selenium in the mouse. *Journal of Biological Chemistry,* 278**,** 13640-6.

HISAMATSU, T., OGATA, H. & HIBI, T. (2008) Innate immunity in inflammatory bowel disease: state of the art. *Current Opinion in Gastroenterology,* 24**,** 448-54.

HO, Y. S., MAGNENAT, J. L., BRONSON, R. T., CAO, J., GARGANO, M., SUGAWARA, M. & FUNK, C. D. (1997) Mice deficient in cellular glutathione peroxidase develop normally and show no increased sensitivity to hyperoxia. *Journal of Biological Chemistry,* 272**,** 16644-51.

HOFFMANN, A., LEVCHENKO, A., SCOTT, M. L. & BALTIMORE, D. (2002a) The IkappaB-NF-kappaB signaling module: temporal control and selective gene activation. *Science,* 298**,** 1241-5.

HOFFMANN, E., DITTRICH-BREIHOLZ, O., HOLTMANN, H. & KRACHT, M. (2002b) Multiple control of interleukin-8 gene expression. *Journal of Leukocyte Biology,* 72**,** 847-55.

HORNG, T., BARTON, G. M., FLAVELL, R. A. & MEDZHITOV, R. (2002) The adaptor molecule TIRAP provides signalling specificity for Toll-like receptors. *Nature,* 420**,** 329-33.

HOU, N., TORII, S., SAITO, N., HOSAKA, M. & TAKEUCHI, T. (2008) Reactive oxygen species-mediated pancreatic beta-cell death is regulated by interactions between stress-activated protein kinases, p38 and c-Jun N-terminal kinase, and mitogen-activated protein kinase phosphatases. *Endocrinology,* 149**,** 1654-65.

HSU, H., SHU, H. B., PAN, M. G. & GOEDDEL, D. V. (1996) TRADD-TRAF2 and TRADD-FADD interactions define two distinct TNF receptor 1 signal transduction pathways. *Cell,* 84**,** 299-308.

HUANG, H. S., CHEN, C. J., LU, H. S. & CHANG, W. C. (1998) Identification of a lipoxygenase inhibitor in A431 cells as a phospholipid hydroperoxide glutathione peroxidase. *FEBS Letters,* 424**,** 22-6.

HUANG, H. S., CHEN, C. J., SUZUKI, H., YAMAMOTO, S. & CHANG, W. C. (1999) Inhibitory effect of phospholipid hydroperoxide glutathione peroxidase on the activity of lipoxygenases and cyclooxygenases. *Prostaglandins & Other Lipid Mediators,* 58**,** 65-75.

HUANG, L., ZHAO, A., WONG, F., AYALA, J. M., STRUTHERS, M., UJJAINWALLA, F., WRIGHT, S. D., SPRINGER, M. S., EVANS, J. & CUI, J. (2004) Leukotriene B4 strongly increases monocyte chemoattractant protein-1 in human monocytes. *Arteriosclerosis, Thrombosis & Vascular Biology,* 24**,** 1783-8.

HUGOT, J. P., CHAMAILLARD, M., ZOUALI, H., LESAGE, S., CEZARD, J. P., BELAICHE, J., ALMER, S., TYSK, C., O'MORAIN, C. A., GASSULL, M., BINDER, V., FINKEL, Y., CORTOT, A., MODIGLIANI, R., LAURENT-PUIG, P., GOWER-ROUSSEAU, C., MACRY, J., COLOMBEL, J. F., SAHBATOU, M. & THOMAS, G. (2001) Association of NOD2 leucine-rich repeat variants with susceptibility to Crohn's disease. *Nature,* 411**,** 599-603.

HYDE, C. A. C. & MISSAILIDIS, S. (2009) Inhibition of arachidonic acid metabolism and its implication on cell proliferation and tumour-angiogenesis. *International Immunopharmacology,* 9**,** 701-15.

IM, J., JEON, J. H., CHO, M. K., WOO, S. S., KANG, S.-S., YUN, C.-H., LEE, K., CHUNG, D. K. & HAN, S. H. (2009) Induction of IL-8 expression by bacterial flagellin is mediated through lipid raft formation and intracellular TLR5 activation in A549 cells. *Molecular Immunology,* 47**,** 614-22.

IMAI, H., HIRAO, F., SAKAMOTO, T., SEKINE, K., MIZUKURA, Y., SAITO, M., KITAMOTO, T., HAYASAKA, M., HANAOKA, K. & NAKAGAWA, Y. (2003a) Early embryonic lethality caused by targeted disruption of the mouse PHGPx gene. *Biochemical & Biophysical Research Communications,* 305**,** 278-86.

IMAI, H., KOUMURA, T., NAKAJIMA, R., NOMURA, K. & NAKAGAWA, Y. (2003b) Protection from inactivation of the adenine nucleotide translocator during hypoglycaemia-induced apoptosis by mitochondrial phospholipid hydroperoxide glutathione peroxidase. *Biochemical Journal,* 371**,** 799-809.

IMAI, H. & NAKAGAWA, Y. (2003) Biological significance of phospholipid hydroperoxide glutathione peroxidase (PHGPx, GPx4) in mammalian cells. *Free Radical Biology & Medicine,* 34**,** 145-69.

IMAI, H., NARASHIMA, K., ARAI, M., SAKAMOTO, H., CHIBA, N. & NAKAGAWA, Y. (1998) Suppression of leukotriene formation in RBL-2H3 cells that overexpressed phospholipid hydroperoxide glutathione peroxidase. *Journal of Biological Chemistry,* 273**,** 1990-7.

IMAI, H., SUMI, D., HANAMOTO, A., ARAI, M. & SUGIYAMA, A. (1995) Molecular cloning and functional expression of a cDNA for rat phospholipid hydroperoxide glutathione peroxidase: 3'-untranslated region of the gene is necessary for functional expression. *Journal of Biochemistry,* 118**,** 1061-7.

ISHIBASHI, N., WEISBROT-LEFKOWITZ, M., REUHL, K., INOUYE, M. & MIROCHNITCHENKO, O. (1999) Modulation of chemokine expression during ischemia/reperfusion in transgenic mice overproducing human glutathione peroxidases. *Journal of Immunology,* 163**,** 5666-77.

JABLONSKA, E., GROMADZINSKA, J., SOBALA, W., RESZKA, E. & WASOWICZ, W. (2008) Lung cancer risk associated with selenium status is modified in smoking individuals by Sep15 polymorphism. *European Journal of Nutrition,* 47**,** 47-54.

JAMALUDDIN, M., WANG, S., BOLDOGH, I., TIAN, B. & BRASIER, A. R. (2007) TNF-alpha-induced NF-kappaB/RelA Ser(276) phosphorylation and enhanceosome formation is mediated by an ROS-dependent PKAc pathway. *Cellular Signalling,* 19**,** 1419-33.

JANG, B.-C., PAIK, J.-H., KIM, S.-P., BAE, J.-H., MUN, K.-C., SONG, D.-K., CHO, C.-H., SHIN, D.-H., KWON, T. K., PARK, J.-W., PARK, J.-G., BAEK, W.-K., SUH, M.-H., LEE, S. H., BAEK, S.-H., LEE, I.-S. & SUH, S.-I. (2004) Catalase induces the expression of inducible nitric oxide synthase through activation of NF-kappaB and PI3K signaling pathway in Raw 264.7 cells. *Biochemical Pharmacology,* 68**,** 2167-76.

JASPERS, I., ZHANG, W., BRIGHTON, L. E., CARSON, J. L., STYBLO, M. & BECK, M. A. (2007) Selenium deficiency alters epithelial cell morphology and responses to influenza. *Free Radical Biology & Medicine,* 42**,** 1826-37.

JEONG, D.-W., YOO, M.-H., KIM, T. S., KIM, J.-H. & KIM, I. Y. (2002a) Protection of mice from allergen-induced asthma by selenite: prevention of eosinophil infiltration by inhibition of NF-kappa B activation. *Journal of Biological Chemistry,* 277**,** 17871-6.

JEONG, D. W., KIM, T. S., CHUNG, Y. W., LEE, B. J. & KIM, I. Y. (2002b) Selenoprotein W is a glutathione-dependent antioxidant in vivo. *FEBS Letters,* 517**,** 225-8.

JIANG, Y., WORONICZ, J. D., LIU, W. & GOEDDEL, D. V. (1999) Prevention of constitutive TNF receptor 1 signaling by silencer of death domains.[Erratum appears in Science 1999 Mar 19;283(5409):1852]. *Science,* 283**,** 543-6.

KALANTARI, P., NARAYAN, V., NATARAJAN, S. K., MURALIDHAR, K., GANDHI, U. H., VUNTA, H., HENDERSON, A. J. & PRABHU, K. S. (2008) Thioredoxin reductase-1 negatively regulates HIV-1 transactivating protein Tat-dependent transcription in human macrophages. *Journal of Biological Chemistry,* 283**,** 33183-90.

KALTSCHMIDT, B., LINKER, R., DENG, J. & KALTSCHMIDT, C. (2002) Cyclooxygenase-2 is a neuronal target gene of NF-kB. *BMC Molecular Biology,* 3**,** 16.

KAMATA, H., HONDA, S.-I., MAEDA, S., CHANG, L., HIRATA, H. & KARIN, M. (2005) Reactive oxygen species promote TNFalpha-induced death and sustained JNK activation by inhibiting MAP kinase phosphatases. *Cell,* 120**,** 649-61.

KANDOUZ, M., NIE, D., PIDGEON, G. P., KRISHNAMOORTHY, S., MADDIPATI, K. R. & HONN, K. V. (2003) Platelet-type 12-lipoxygenase activates NF-kappaB in prostate cancer cells. *Prostaglandins & Other Lipid Mediators,* 71**,** 189-204.

KANG, S. M., TRAN, A. C., GRILLI, M. & LENARDO, M. J. (1992) NF-kappa B subunit regulation in nontransformed CD4+ T lymphocytes. *Science,* 256**,** 1452-6.

KARIN, M. & BEN-NERIAH, Y. (2000) Phosphorylation meets ubiquitination: the control of NF-[kappa]B activity. *Annual Review of Immunology,* 18**,** 621-63.

KARIN, M. & GRETEN, F. R. (2005) NF-kappaB: linking inflammation and immunity to cancer development and progression. *Nature Reviews,* Immunology. 5**,** 749-59.

KARP, S. M. & KOCH, T. R. (2006) Micronutrient supplements in inflammatory bowel disease. *Disease-A-Month,* 52**,** 211-20.

KATO, T., READ, R., ROZGA, J. & BURK, R. F. (1992) Evidence for intestinal release of absorbed selenium in a form with high hepatic extraction. *American Journal of Physiology,* 262**,** G854-8.

KAWAHARA, T., KUWANO, Y., TESHIMA-KONDO, S., TAKEYA, R., SUMIMOTO, H., KISHI, K., TSUNAWAKI, S., HIRAYAMA, T. & ROKUTAN, K. (2004) Role of nicotinamide adenine dinucleotide phosphate oxidase 1 in oxidative burst response to Toll-like receptor 5 signaling in large intestinal epithelial cells. *Journal of Immunology,* 172**,** 3051-8.

KAWAI, T. & AKIRA, S. (2006) TLR signaling. *Cell Death & Differentiation,* 13**,** 816-25.

KELLY, D., CAMPBELL, J. I., KING, T. P., GRANT, G., JANSSON, E. A., COUTTS, A. G. P., PETTERSSON, S. & CONWAY, S. (2004) Commensal anaerobic gut bacteria attenuate inflammation by regulating nuclear-cytoplasmic shuttling of PPAR-gamma and RelA. *Nature Immunology,* 5**,** 104-12.

KIM, J.-H., NA, H.-J., KIM, C.-K., KIM, J.-Y., HA, K.-S., LEE, H., CHUNG, H.-T., KWON, H. J., KWON, Y.-G. & KIM, Y.-M. (2008) The non-provitamin A carotenoid, lutein, inhibits NF-kappaB-dependent gene expression through redox-based regulation of the phosphatidylinositol 3-kinase/PTEN/Akt and NF-kappaB-inducing kinase pathways: role of H(2)O(2) in NF-kappaB activation. *Free Radical Biology & Medicine,* 45**,** 885-96.

KIM, S. H., JOHNSON, V. J., SHIN, T.-Y. & SHARMA, R. P. (2004) Selenium attenuates lipopolysaccharide-induced oxidative stress responses through modulation of p38 MAPK and NF-kappaB signaling pathways. *Experimental Biology & Medicine,* 229**,** 203-13.

KIM, Y.-J., CHAI, Y.-G. & RYU, J.-C. (2005) Selenoprotein W as molecular target of methylmercury in human neuronal cells is down-regulated by GSH depletion. *Biochemical & Biophysical Research Communications,* 330**,** 1095-102.

KIM, Y.-S., MORGAN, M. J., CHOKSI, S. & LIU, Z.-G. (2007) TNF-induced activation of the Nox1 NADPH oxidase and its role in the induction of necrotic cell death. *Molecular Cell,* 26**,** 675-87.

KING, E. M., HOLDEN, N. S., GONG, W., RIDER, C. F. & NEWTON, R. (2009) Inhibition of NF-kappaB-dependent transcription by MKP-1: transcriptional repression by glucocorticoids occurring via p38 MAPK. *Journal of Biological Chemistry,* 284**,** 26803-15.

KIPP, A., BANNING, A., VAN SCHOTHORST, E. M., MEPLAN, C., SCHOMBURG, L., EVELO, C., COORT, S., GAJ, S., KEIJER, J., HESKETH, J. & BRIGELIUS-FLOHE, R. (2009) Four selenoproteins, protein biosynthesis, and Wnt signalling are particularly sensitive to limited selenium intake in mouse colon. *Molecular Nutrition & Food Research,* 53**,** 1561-72.

KIRILLOV, A., KISTLER, B., MOSTOSLAVSKY, R., CEDAR, H., WIRTH, T. & BERGMAN, Y. (1996) A role for nuclear NF-kappaB in B-cell-specific demethylation of the Igkappa locus. *Nature Genetics,* 13**,** 435-41.

KOHRLE, J. (2000) The deiodinase family: selenoenzymes regulating thyroid hormone availability and action. *Cellular & Molecular Life Sciences,* 57**,** 1853-63.

KOLLEWE, C., MACKENSEN, A.-C., NEUMANN, D., KNOP, J., CAO, P., LI, S., WESCHE, H. & MARTIN, M. U. (2004) Sequential autophosphorylation steps in the interleukin-1 receptor-associated kinase-1 regulate its availability as an adapter in interleukin-1 signaling. *Journal of Biological Chemistry,* 279**,** 5227-36.

KRETZ-REMY, C. & ARRIGO, A. P. (2001) Selenium: a key element that controls NF-kappa B activation and I kappa B alpha half life. *Biofactors,* 14**,** 117-25.

KRETZ-REMY, C., BATES, E. E. & ARRIGO, A. P. (1998) Amino acid analogs activate NF-kappaB through redox-dependent IkappaB-alpha degradation by the proteasome without apparent IkappaB-alpha phosphorylation. Consequence on HIV-1 long terminal repeat activation. *Journal of Biological Chemistry,* 273**,** 3180-91.

KRETZ-REMY, C., MEHLEN, P., MIRAULT, M. E. & ARRIGO, A. P. (1996) Inhibition of I kappa B-alpha phosphorylation and degradation and subsequent NF-kappa B activation by glutathione peroxidase overexpression. *Journal of Cell Biology,* 133**,** 1083-93.

KREUZ, S., SIEGMUND, D., SCHEURICH, P. & WAJANT, H. (2001) NF-kappaB inducers upregulate cFLIP, a cycloheximide-sensitive inhibitor of death receptor signaling. *Molecular & Cellular Biology,* 21**,** 3964-73.

KRYUKOV, G. V., CASTELLANO, S., NOVOSELOV, S. V., LOBANOV, A. V., ZEHTAB, O., GUIGO, R. & GLADYSHEV, V. N. (2003) Characterization of mammalian selenoproteomes. *Science,* 300**,** 1439-43.

KUCHARZIK, T. & WILLIAMS, I. R. (2002) Neutrophil migration across the intestinal epithelial barrier--summary of in vitro data and description of a new transgenic mouse model with doxycycline-inducible interleukin-8 expression in intestinal epithelial cells. *Pathobiology,* 70**,** 143-9.

KUMARASWAMY, E., MALYKH, A., KOROTKOV, K. V., KOZYAVKIN, S., HU, Y., KWON, S. Y., MOUSTAFA, M. E., CARLSON, B. A., BERRY, M. J., LEE, B. J., HATFIELD, D. L., DIAMOND, A. M. & GLADYSHEV, V. N. (2000) Structure-expression relationships of the 15-kDa selenoprotein gene. Possible role of the protein in cancer etiology. *Journal of Biological Chemistry,* 275**,** 35540-7.

LABUNSKYY, V. M., YOO, M.-H., HATFIELD, D. L. & GLADYSHEV, V. N. (2009) Sep15, a thioredoxin-like selenoprotein, is involved in the unfolded

protein response and differentially regulated by adaptive and acute ER stresses. *Biochemistry,* 48**,** 8458-65.

LAMOTHE, B., BESSE, A., CAMPOS, A. D., WEBSTER, W. K., WU, H. & DARNAY, B. G. (2007) Site-specific Lys-63-linked tumor necrosis factor receptor-associated factor 6 auto-ubiquitination is a critical determinant of I kappa B kinase activation. *Journal of Biological Chemistry,* 282**,** 4102-12.

LANIADO-SCHWARTZMAN, M., LAVROVSKY, Y., STOLTZ, R. A., CONNERS, M. S., FALCK, J. R., CHAUHAN, K. & ABRAHAM, N. G. (1994) Activation of nuclear factor kappa B and oncogene expression by 12(R)-hydroxyeicosatrienoic acid, an angiogenic factor in microvessel endothelial cells. *Journal of Biological Chemistry,* 269**,** 24321-7.

LEE, C.-K., LEE, E. Y., KIM, Y. G., MUN, S. H., MOON, H.-B. & YOO, B. (2008) Alpha-lipoic acid inhibits TNF-alpha induced NF-kappa B activation through blocking of MEKK1-MKK4-IKK signaling cascades. *International Immunopharmacology,* 8**,** 362-70.

LEE, D.-H., ESWORTHY, R. S., CHU, C., PFEIFER, G. P. & CHU, F.-F. (2006) Mutation accumulation in the intestine and colon of mice deficient in two intracellular glutathione peroxidases. *Cancer Research,* 66**,** 9845-51.

LEE, M. & KOH, W. S. (2003) Raf-independent and MEKK1-dependent activation of NF-kappaB by hydrogen peroxide in 70Z/3 pre-B lymphocyte tumor cells. *Journal of Cellular Biochemistry,* 88**,** 545-56.

LI, H. & LIN, X. (2008) Positive and negative signaling components involved in TNFalpha-induced NF-kappaB activation. *Cytokine,* 41**,** 1-8.

LI, Q. & ENGELHARDT, J. F. (2006) Interleukin-1beta induction of NFkappaB is partially regulated by H2O2-mediated activation of NFkappaB-inducing kinase. *Journal of Biological Chemistry,* 281**,** 1495-505.

LI, Q., SANLIOGLU, S., LI, S., RITCHIE, T., OBERLEY, L. & ENGELHARDT, J. F. (2001) GPx-1 gene delivery modulates NFkappaB activation following diverse environmental injuries through a specific subunit of the IKK complex. *Antioxidants & Redox Signaling,* 3**,** 415-32.

LI, Q., SPENCER, N. Y., OAKLEY, F. D., BUETTNER, G. R. & ENGELHARDT, J. F. (2009) Endosomal Nox2 facilitates redox-dependent induction of NF-kappaB by TNF-alpha. *Antioxidants & Redox Signaling,* 11**,** 1249-63.

LI, S., STRELOW, A., FONTANA, E. J. & WESCHE, H. (2002) IRAK-4: a novel member of the IRAK family with the properties of an IRAK-kinase. *Proceedings of the National Academy of Sciences of the United States of America,* 99**,** 5567-72.

LIANG, H., VAN REMMEN, H., FROHLICH, V., LECHLEITER, J., RICHARDSON, A. & RAN, Q. (2007) Gpx4 protects mitochondrial ATP generation against oxidative damage. *Biochemical & Biophysical Research Communications,* 356**,** 893-8.

LING, L., CAO, Z. & GOEDDEL, D. V. (1998) NF-kappaB-inducing kinase activates IKK-alpha by phosphorylation of Ser-176. *Proceedings of the National Academy of Sciences of the United States of America,* 95**,** 3792-7.

LIOU, H. C., NOLAN, G. P., GHOSH, S., FUJITA, T. & BALTIMORE, D. (1992) The NF-kappa B p50 precursor, p105, contains an internal I kappa B-like inhibitor that preferentially inhibits p50. *EMBO Journal,* 11**,** 3003-9.

LOFLIN, J., LOPEZ, N., WHANGER, P. D. & KIOUSSI, C. (2006) Selenoprotein W during development and oxidative stress. *Journal of Inorganic Biochemistry,* 100**,** 1679-84.

LOH, K., DENG, H., FUKUSHIMA, A., CAI, X., BOIVIN, B., GALIC, S., BRUCE, C., SHIELDS, B. J., SKIBA, B., OOMS, L. M., STEPTO, N., WU, B., MITCHELL, C. A., TONKS, N. K., WATT, M. J., FEBBRAIO, M. A., CRACK, P. J., ANDRIKOPOULOS, S. & TIGANIS, T. (2009) Reactive oxygen species enhance insulin sensitivity. *Cell Metabolism,* 10**,** 260-72.

LU, J., BERNDT, C. & HOLMGREN, A. (2009) Metabolism of selenium compounds catalyzed by the mammalian selenoprotein thioredoxin reductase. *Biochimica et Biophysica Acta,* 1790**,** 1513-9.

LU, J. & HOLMGREN, A. (2009) Selenoproteins. *Journal of Biological Chemistry,* 284**,** 723-7.

MAIER, H. J., MARIENFELD, R., WIRTH, T. & BAUMANN, B. (2003) Critical role of RelB serine 368 for dimerization and p100 stabilization. *Journal of Biological Chemistry,* 278**,** 39242-50.

MAIORINO, M., CHU, F. F., URSINI, F., DAVIES, K. J., DOROSHOW, J. H. & ESWORTHY, R. S. (1991) Phospholipid hydroperoxide glutathione peroxidase is the 18-kDa selenoprotein expressed in human tumor cell lines. *Journal of Biological Chemistry,* 266**,** 7728-32.

MAITI, B., ARBOGAST, S., ALLAMAND, V., MOYLE, M. W., ANDERSON, C. B., RICHARD, P., GUICHENEY, P., FERREIRO, A., FLANIGAN, K. M. & HOWARD, M. T. (2009) A mutation in the SEPN1 selenocysteine redefinition element (SRE) reduces selenocysteine incorporation and leads to SEPN1-related myopathy. *Human Mutation,* 30**,** 411-6.

MANDAL, P. K., SEILER, A., PERISIC, T., KOLLE, P., BANJAC CANAK, A., FORSTER, H., WEISS, N., KREMMER, E., LIEBERMAN, M. W., BANNAI, S., KUHLENCORDT, P., SATO, H., BORNKAMM, G. W. & CONRAD, M. (2010) System x(c)- and thioredoxin reductase 1 cooperatively rescue glutathione deficiency. *Journal of Biological Chemistry,* 285**,** 22244-53.

MARTEAU, P., LEPAGE, P., MANGIN, I., SUAU, A., DORE, J., POCHART, P. & SEKSIK, P. (2004) Review article: gut flora and inflammatory bowel disease. *Alimentary Pharmacology & Therapeutics,* 20 Suppl 4**,** 18-23.

MENDELEV, N., WITHERSPOON, S. & LI, P. A. (2009) Overexpression of human selenoprotein H in neuronal cells ameliorates ultraviolet irradiation-induced damage by modulating cell signaling pathways. *Experimental Neurology,* 220**,** 328-34.

MEPLAN, C., CROSLEY, L. K., NICOL, F., BECKETT, G. J., HOWIE, A. F., HILL, K. E., HORGAN, G., MATHERS, J. C., ARTHUR, J. R. & HESKETH, J. E. (2007) Genetic polymorphisms in the human selenoprotein P gene determine the response of selenoprotein markers to selenium supplementation in a gender-specific manner (the SELGEN study). *FASEB Journal,* 21**,** 3063-74.

MEPLAN, C., PAGMANTIDIS, V. & HESKETH, J. (Eds.) (2006) *Advances in selenoprotein expression: patterns and individual variations,* Weinheim, Wiley-Vch Press

MOGHADASZADEH, B. & BEGGS, A. H. (2006) Selenoproteins and their impact on human health through diverse physiological pathways. *Physiology,* 21**,** 307-15.

MORGAN, M. J., KIM, Y.-S. & LIU, Z.-G. (2008) TNFalpha and reactive oxygen species in necrotic cell death. *Cell Research,* 18**,** 343-9.

MORIOKA, S., OMORI, E., KAJINO, T., KAJINO-SAKAMOTO, R., MATSUMOTO, K. & NINOMIYA-TSUJI, J. (2009) TAK1 kinase determines

TRAIL sensitivity by modulating reactive oxygen species and cIAP. *Oncogene,* 28**,** 2257-65.

MULLENBACH, G. T., TABRIZI, A., IRVINE, B. D., BELL, G. I., TAINER, J. A. & HALLEWELL, R. A. (1988) Selenocysteine's mechanism of incorporation and evolution revealed in cDNAs of three glutathione peroxidases. *Protein Engineering,* 2**,** 239-46.

NAKANO, H., NAKAJIMA, A., SAKON-KOMAZAWA, S., PIAO, J. H., XUE, X. & OKUMURA, K. (2006) Reactive oxygen species mediate crosstalk between NF-kappaB and JNK. *Cell Death & Differentiation,* 13**,** 730-7.

NEURATH, M. F., BECKER, C. & BARBULESCU, K. (1998) Role of NF-kappaB in immune and inflammatory responses in the gut. *Gut,* 43**,** 856-60.

NOMURA, K., IMAI, H., KOUMURA, T., ARAI, M. & NAKAGAWA, Y. (1999) Mitochondrial phospholipid hydroperoxide glutathione peroxidase suppresses apoptosis mediated by a mitochondrial death pathway. *Journal of Biological Chemistry,* 274**,** 29294-302.

NOVOSELOV, S. V., KRYUKOV, G. V., XU, X.-M., CARLSON, B. A., HATFIELD, D. L. & GLADYSHEV, V. N. (2007) Selenoprotein H is a nucleolar thioredoxin-like protein with a unique expression pattern. *Journal of Biological Chemistry,* 282**,** 11960-8.

OHKUSA, T., YOSHIDA, T., SATO, N., WATANABE, S., TAJIRI, H. & OKAYASU, I. (2009) Commensal bacteria can enter colonic epithelial cells and induce proinflammatory cytokine secretion: a possible pathogenic mechanism of ulcerative colitis. *Journal of Medical Microbiology,* 58**,** 535-45.

OMORI, E., MORIOKA, S., MATSUMOTO, K. & NINOMIYA-TSUJI, J. (2008) TAK1 regulates reactive oxygen species and cell death in keratinocytes, which is essential for skin integrity. *Journal of Biological Chemistry,* 283**,** 26161-8.

PACQUELET, S., JOHNSON, J. L., ELLIS, B. A., BRZEZINSKA, A. A., LANE, W. S., MUNAFO, D. B. & CATZ, S. D. (2007) Cross-talk between IRAK-4 and the NADPH oxidase. *Biochemical Journal,* 403**,** 451-61.

PAGMANTIDIS, V., BERMANO, G., VILLETTE, S., BROOM, I., ARTHUR, J. & HESKETH, J. (2005) Effects of Se-depletion on glutathione peroxidase and selenoprotein W gene expression in the colon. *FEBS Letters,* 579**,** 792-6.

PAHL, H. L. (1999) Activators and target genes of Rel/NF-kappaB transcription factors. *Oncogene,* 18**,** 6853-66.

PANEE, J., STOYTCHEVA, Z. R., LIU, W. & BERRY, M. J. (2007) Selenoprotein H is a redox-sensing high mobility group family DNA-binding protein that up-regulates genes involved in glutathione synthesis and phase II detoxification. *Journal of Biological Chemistry,* 282**,** 23759-65.

PARK, H. S., CHUN, J. N., JUNG, H. Y., CHOI, C. & BAE, Y. S. (2006) Role of NADPH oxidase 4 in lipopolysaccharide-induced proinflammatory responses by human aortic endothelial cells. *Cardiovascular Research,* 72**,** 447-55.

PFEIFER, H., CONRAD, M., ROETHLEIN, D., KYRIAKOPOULOS, A., BRIELMEIER, M., BORNKAMM, G. W. & BEHNE, D. (2001) Identification of a specific sperm nuclei selenoenzyme necessary for protamine thiol cross-linking during sperm maturation. *FASEB Journal,* 15**,** 1236-8.

PRABHU, K. S., ZAMAMIRI-DAVIS, F., STEWART, J. B., THOMPSON, J. T., SORDILLO, L. M. & REDDY, C. C. (2002) Selenium deficiency increases the expression of inducible nitric oxide synthase in RAW 264.7 macrophages:

role of nuclear factor-kappaB in up-regulation. *Biochemical Journal,* 366**,** 203-9.

RAMAKERS, J. D., MENSINK, R. P., SCHAART, G. & PLAT, J. (2007) Arachidonic acid but not eicosapentaenoic acid (EPA) and oleic acid activates NF-kappaB and elevates ICAM-1 expression in Caco-2 cells. *Lipids,* 42**,** 687-98.

RAN, Q., LIANG, H., GU, M., QI, W., WALTER, C. A., ROBERTS, L. J., 2ND, HERMAN, B., RICHARDSON, A. & VAN REMMEN, H. (2004) Transgenic mice overexpressing glutathione peroxidase 4 are protected against oxidative stress-induced apoptosis. *Journal of Biological Chemistry,* 279**,** 55137-46.

RAN, Q., VAN REMMEN, H., GU, M., QI, W., ROBERTS, L. J., 2ND, PROLLA, T. & RICHARDSON, A. (2003) Embryonic fibroblasts from Gpx4+/- mice: a novel model for studying the role of membrane peroxidation in biological processes. *Free Radical Biology & Medicine,* 35**,** 1101-9.

RENKO, K., WERNER, M., RENNER, M., X00FC, LLER, I., COOPER, T. G., YEUNG, C. H., HOLLENBACH, B., SCHARPF, M., X00F, HRLE, J., SCHOMBURG, L. & SCHWEIZER, U. (2008) Hepatic selenoprotein P (SePP) expression restores selenium transport and prevents infertility and motor-incoordination in Sepp-knockout mice. *Biochemical Journal,* 409**,** 741-9.

REYNOLDS, A., LEAKE, D., BOESE, Q., SCARINGE, S., MARSHALL, W. S. & KHVOROVA, A. (2004) Rational siRNA design for RNA interference. *Nature Biotechnology,* 22**,** 326-30.

RHEE, S. H., IM, E. & POTHOULAKIS, C. (2008) Toll-like receptor 5 engagement modulates tumor development and growth in a mouse xenograft model of human colon cancer.[see comment]. *Gastroenterology,* 135**,** 518-28.

ROEBUCK, K. A. (1999a) Oxidant stress regulation of IL-8 and ICAM-1 gene expression: differential activation and binding of the transcription factors AP-1 and NF-kappaB (Review). *International Journal of Molecular Medicine,* 4**,** 223-30.

ROEBUCK, K. A. (1999b) Regulation of interleukin-8 gene expression. *Journal of Interferon & Cytokine Research,* 19**,** 429-38.

ROUZER, C. A. & SAMUELSSON, B. (1986) The importance of hydroperoxide activation for the detection and assay of mammalian 5-lipoxygenase. *FEBS Letters,* 204**,** 293-6.

RUSSO, M. W., MURRAY, S. C., WURZELMANN, J. I., WOOSLEY, J. T. & SANDLER, R. S. (1997) Plasma selenium levels and the risk of colorectal adenomas. *Nutrition & Cancer,* 28**,** 125-9.

SAKAMOTO, H., IMAI, H. & NAKAGAWA, Y. (2000) Involvement of phospholipid hydroperoxide glutathione peroxidase in the modulation of prostaglandin D2 synthesis. *Journal of Biological Chemistry,* 275**,** 40028-35.

SAKURAI, A., YUASA, K., SHOJI, Y., HIMENO, S., TSUJIMOTO, M., KUNIMOTO, M., IMURA, N. & HARA, S. (2004) Overexpression of thioredoxin reductase 1 regulates NF-kappa B activation. *Journal of Cellular Physiology,* 198**,** 22-30.

SAMBUCETTI, L. C., CHERRINGTON, J. M., WILKINSON, G. W. & MOCARSKI, E. S. (1989) NF-kappa B activation of the cytomegalovirus enhancer is mediated by a viral transactivator and by T cell stimulation. *EMBO Journal,* 8**,** 4251-8.

SANCHEZ-DUFFHUES, G., CALZADO, M. A., DE VINUESA, A. G., APPENDINO, G., FIEBICH, B. L., LOOCK, U., LEFARTH-RISSE, A., KROHN, K. & MUNOZ, E. (2009) Denbinobin inhibits nuclear factor-kappaB and induces apoptosis via reactive oxygen species generation in human leukemic cells. *Biochemical Pharmacology,* 77**,** 1401-9.

SANLIOGLU, S., WILLIAMS, C. M., SAMAVATI, L., BUTLER, N. S., WANG, G., MCCRAY, P. B., JR., RITCHIE, T. C., HUNNINGHAKE, G. W., ZANDI, E. & ENGELHARDT, J. F. (2001) Lipopolysaccharide induces Rac1-dependent reactive oxygen species formation and coordinates tumor necrosis factor-alpha secretion through IKK regulation of NF-kappa B. *Journal of Biological Chemistry,* 276**,** 30188-98.

SATO, S., SANJO, H., TAKEDA, K., NINOMIYA-TSUJI, J., YAMAMOTO, M., KAWAI, T., MATSUMOTO, K., TAKEUCHI, O. & AKIRA, S. (2005) Essential function for the kinase TAK1 in innate and adaptive immune responses. *Nature Immunology,* 6**,** 1087-95.

SCHENK, H., KLEIN, M., ERDBRUGGER, W., DROGE, W. & SCHULZE-OSTHOFF, K. (1994) Distinct effects of thioredoxin and antioxidants on the activation of transcription factors NF-kappa B and AP-1. *Proceedings of the National Academy of Sciences of the United States of America,* 91**,** 1672-6.

SCHLABACH, M. R., HU, J. K., LI, M. & ELLEDGE, S. J. (2010) Synthetic design of strong promoters. *Proceedings of the National Academy of Sciences of the United States of America,* 107**,** 2538-43.

SCHNEIDER, P., THOME, M., BURNS, K., BODMER, J. L., HOFMANN, K., KATAOKA, T., HOLLER, N. & TSCHOPP, J. (1997) TRAIL receptors 1 (DR4) and 2 (DR5) signal FADD-dependent apoptosis and activate NF-kappaB. *Immunity,* 7**,** 831-6.

SCHNURR, K., BELKNER, J., URSINI, F., SCHEWE, T. & KUHN, H. (1996) The selenoenzyme phospholipid hydroperoxide glutathione peroxidase controls the activity of the 15-lipoxygenase with complex substrates and preserves the specificity of the oxygenation products. *Journal of Biological Chemistry,* 271**,** 4653-8.

SCHOMBURG, L., SCHWEIZER, U., HOLTMANN, B., FLOH, X00E, LEOPOLD, SENDTNER, M., X00F & HRLE, J. (2003) Gene disruption discloses role of selenoprotein P in selenium delivery to target tissues. *Biochemical Journal,* 370**,** 397-402.

SCHOONBROODT, S., FERREIRA, V., BEST-BELPOMME, M., BOELAERT, J. R., LEGRAND-POELS, S., KORNER, M. & PIETTE, J. (2000) Crucial role of the amino-terminal tyrosine residue 42 and the carboxyl-terminal PEST domain of I kappa B alpha in NF-kappa B activation by an oxidative stress. *Journal of Immunology,* 164**,** 4292-300.

SCHRECK, R., RIEBER, P. & BAEUERLE, P. A. (1991) Reactive oxygen intermediates as apparently widely used messengers in the activation of the NF-kappa B transcription factor and HIV-1. *EMBO Journal,* 10**,** 2247-58.

SEILER, A., SCHNEIDER, M., FORSTER, H., ROTH, S., WIRTH, E. K., CULMSEE, C., PLESNILA, N., KREMMER, E., RADMARK, O., WURST, W., BORNKAMM, G. W., SCHWEIZER, U. & CONRAD, M. (2008) Glutathione peroxidase 4 senses and translates oxidative stress into 12/15-lipoxygenase dependent- and AIF-mediated cell death.[see comment]. *Cell Metabolism,* 8**,** 237-48.

SHCHEDRINA, V. A., ZHANG, Y., LABUNSKYY, V. M., HATFIELD, D. L. & GLADYSHEV, V. N. (2010) Structure-function relations, physiological roles, and evolution of mammalian ER-resident selenoproteins. *Antioxidants & Redox Signaling,* 12**,** 839-49.

SHEN, Y., LUCHE, R., WEI, B., GORDON, M. L., DILTZ, C. D. & TONKS, N. K. (2001) Activation of the Jnk signaling pathway by a dual-specificity phosphatase, JSP-1. *Proceedings of the National Academy of Sciences of the United States of America,* 98**,** 13613-8.

SHIM, J.-H., XIAO, C., PASCHAL, A. E., BAILEY, S. T., RAO, P., HAYDEN, M. S., LEE, K.-Y., BUSSEY, C., STECKEL, M., TANAKA, N., YAMADA, G., AKIRA, S., MATSUMOTO, K. & GHOSH, S. (2005) TAK1, but not TAB1 or TAB2, plays an essential role in multiple signaling pathways in vivo. *Genes & Development,* 19**,** 2668-81.

SHIMIZU, T., NUMATA, T. & OKADA, Y. (2004) A role of reactive oxygen species in apoptotic activation of volume-sensitive Cl(-) channel. *Proceedings of the National Academy of Sciences of the United States of America,* 101**,** 6770-3.

SHIN, K.-M., SHEN, L., PARK, S. J., JEONG, J.-H. & LEE, K.-T. (2009) Bis-(3-hydroxyphenyl) diselenide inhibits LPS-stimulated iNOS and COX-2 expression in RAW 264.7 macrophage cells through the NF-kappaB inactivation. *Journal of Pharmacy & Pharmacology,* 61**,** 479-86.

SHUREIQI, I., WU, Y., CHEN, D., YANG, X. L., GUAN, B., MORRIS, J. S., YANG, P., NEWMAN, R. A., BROADDUS, R., HAMILTON, S. R., LYNCH, P., LEVIN, B., FISCHER, S. M. & LIPPMAN, S. M. (2005) The critical role of 15-lipoxygenase-1 in colorectal epithelial cell terminal differentiation and tumorigenesis. *Cancer Research,* 65**,** 11486-92.

SIMON, R. & SAMUEL, C. E. (2007) Activation of NF-kappaB-dependent gene expression by Salmonella flagellins FliC and FljB. *Biochemical & Biophysical Research Communications,* 355**,** 280-5.

SORDILLO, L. M., STREICHER, K. L., MULLARKY, I. K., GANDY, J. C., TRIGONA, W. & CORL, C. M. (2008) Selenium inhibits 15-hydroperoxyoctadecadienoic acid-induced intracellular adhesion molecule expression in aortic endothelial cells. *Free Radical Biology & Medicine,* 44**,** 34-43.

STOLL, M., CORNELIUSSEN, B., COSTELLO, C. M., WAETZIG, G. H., MELLGARD, B., KOCH, W. A., ROSENSTIEL, P., ALBRECHT, M., CROUCHER, P. J. P., SEEGERT, D., NIKOLAUS, S., HAMPE, J., LENGAUER, T., PIERROU, S., FOELSCH, U. R., MATHEW, C. G., LAGERSTROM-FERMER, M. & SCHREIBER, S. (2004) Genetic variation in DLG5 is associated with inflammatory bowel disease. *Nature Genetics,* 36**,** 476-80.

STRAIF, D., WERZ, O., KELLNER, R., BAHR, U. & STEINHILBER, D. (2000) Glutathione peroxidase-1 but not -4 is involved in the regulation of cellular 5-lipoxygenase activity in monocytic cells. *Biochemical Journal,* 349**,** 455-61.

SUBRAMANIAN, S., RHODES, J. M., HART, C. A., TAM, B., ROBERTS, C. L., SMITH, S. L., CORKILL, J. E., WINSTANLEY, C., VIRJI, M. & CAMPBELL, B. J. (2008) Characterization of epithelial IL-8 response to inflammatory bowel disease mucosal E. coli and its inhibition by mesalamine. *Inflammatory Bowel Diseases,* 14**,** 162-75.

SUNDE, R. A., RAINES, A. M., BARNES, K. M. & EVENSON, J. K. (2009) Selenium status highly regulates selenoprotein mRNA levels for only a subset of the selenoproteins in the selenoproteome. *Bioscience Reports,* 29**,** 329-38.

SUTHERLAND, M., SHANKARANARAYANAN, P., SCHEWE, T. & NIGAM, S. (2001) Evidence for the presence of phospholipid hydroperoxide glutathione peroxidase in human platelets: implications for its involvement in the regulatory network of the 12-lipoxygenase pathway of arachidonic acid metabolism. *Biochemical Journal,* 353**,** 91-100.

SUZUKI, N., SUZUKI, S., DUNCAN, G. S., MILLAR, D. G., WADA, T., MIRTSOS, C., TAKADA, H., WAKEHAM, A., ITIE, A., LI, S., PENNINGER, J. M., WESCHE, H., OHASHI, P. S., MAK, T. W. & YEH, W.-C. (2002) Severe impairment of interleukin-1 and Toll-like receptor signalling in mice lacking IRAK-4. *Nature,* 416**,** 750-6.

TAKAESU, G., NINOMIYA-TSUJI, J., KISHIDA, S., LI, X., STARK, G. R. & MATSUMOTO, K. (2001) Interleukin-1 (IL-1) receptor-associated kinase leads to activation of TAK1 by inducing TAB2 translocation in the IL-1 signaling pathway. *Molecular & Cellular Biology,* 21**,** 2475-84.

TAKASE, O., MARUMO, T., HISHIKAWA, K., FUJITA, T., QUIGG, R. J. & HAYASHI, M. (2008) NF-kappaB-dependent genes induced by proteinuria and identified using DNA microarrays. *Clinical & Experimental Nephrology,* 12**,** 181-8.

TALLANT, T., DEB, A., KAR, N., LUPICA, J., DE VEER, M. J. & DIDONATO, J. A. (2004) Flagellin acting via TLR5 is the major activator of key signaling pathways leading to NF-kappa B and proinflammatory gene program activation in intestinal epithelial cells. *BMC Microbiology,* 4**,** 33.

TANG, W., WANG, W., ZHANG, Y., LIU, S., LIU, Y. & ZHENG, D. (2009) TRAIL receptor mediates inflammatory cytokine release in an NF-kappaB-dependent manner. *Cell Research,* 19**,** 758-67.

TAYLOR, J. M., CRACK, P. J., GOULD, J. A., ALI, U., HERTZOG, P. J. & IANNELLO, R. C. (2004) Akt phosphorylation and NFkappaB activation are counterregulated under conditions of oxidative stress. *Experimental Cell Research,* 300**,** 463-75.

THIERRY-MIEG, D. & THIERRY-MIEG, J. (2006) AceView: a comprehensive cDNA-supported gene and transcripts annotation. *Genome Biology,* 7 Suppl 1**,** S12.1-14.

THOMAS, J. P., MAIORINO, M., URSINI, F. & GIROTTI, A. W. (1990) Protective action of phospholipid hydroperoxide glutathione peroxidase against membrane-damaging lipid peroxidation. In situ reduction of phospholipid and cholesterol hydroperoxides. *Journal of Biological Chemistry,* 265**,** 454-61.

TING, A. T., PIMENTEL-MUINOS, F. X. & SEED, B. (1996) RIP mediates tumor necrosis factor receptor 1 activation of NF-kappaB but not Fas/APO-1-initiated apoptosis. *EMBO Journal,* 15**,** 6189-96.

TIROSH, O., LEVY, E. & REIFEN, R. (2007) High selenium diet protects against TNBS-induced acute inflammation, mitochondrial dysfunction, and secondary necrosis in rat colon. *Nutrition,* 23**,** 878-86.

TURANOV, A. A., KEHR, S., MARINO, S. M., YOO, M.-H., CARLSON, B. A., HATFIELD, D. L. & GLADYSHEV, V. N. (2010) Mammalian thioredoxin reductase 1: roles in redox homoeostasis and characterization of cellular targets. *Biochemical Journal,* 430**,** 285-93.

TURNER, D. A., PASZEK, P., WOODCOCK, D. J., NELSON, D. E., HORTON, C. A., WANG, Y., SPILLER, D. G., RAND, D. A., WHITE, M. R. H. & HARPER, C. V. (2010) Physiological levels of TNFalpha stimulation induce stochastic dynamics of NF-kappaB responses in single living cells. *Journal of Cell Science,* 123**,** 2834-43.

UI-TEI, K., NAITO, Y., TAKAHASHI, F., HARAGUCHI, T., OHKI-HAMAZAKI, H., JUNI, A., UEDA, R. & SAIGO, K. (2004) Guidelines for the selection of highly effective siRNA sequences for mammalian and chick RNA interference. *Nucleic Acids Research,* 32**,** 936-48.

URSINI, F., MAIORINO, M. & GREGOLIN, C. (1985) The selenoenzyme phospholipid hydroperoxide glutathione peroxidase. *Biochimica et Biophysica Acta,* 839**,** 62-70.

VALLABHAPURAPU, S. & KARIN, M. (2009) Regulation and function of NF-kappaB transcription factors in the immune system. *Annual Review of Immunology,* 27**,** 693-733.

VILLETTE, S., KYLE, J. A. M., BROWN, K. M., PICKARD, K., MILNE, J. S., NICOL, F., ARTHUR, J. R. & HESKETH, J. E. (2002) A novel single nucleotide polymorphism in the 3' untranslated region of human glutathione peroxidase 4 influences lipoxygenase metabolism. *Blood Cells Molecules & Diseases,* 29**,** 174-8.

VOUDOURI, A. E., CHADIO, S. E., MENEGATOS, J. G., ZERVAS, G. P., NICOL, F. & ARTHUR, J. R. (2003) Selenoenzyme activities in selenium- and iodine-deficient sheep. *Biological Trace Element Research,* 94**,** 213-24.

VUNTA, H., DAVIS, F., PALEMPALLI, U. D., BHAT, D., ARNER, R. J., THOMPSON, J. T., PETERSON, D. G., REDDY, C. C. & PRABHU, K. S. (2007) The anti-inflammatory effects of selenium are mediated through 15-deoxy-Delta12,14-prostaglandin J2 in macrophages. *Journal of Biological Chemistry,* 282**,** 17964-73.

VYKHOVANETS, E. V., SHUKLA, S., MACLENNAN, G. T., RESNICK, M. I., CARLSEN, H., BLOMHOFF, R. & GUPTA, S. (2008) Molecular imaging of NF-kappaB in prostate tissue after systemic administration of IL-1 beta. *Prostate,* 68**,** 34-41.

WALSHE, J., SEREWKO-AURET, M. M., TEAKLE, N., CAMERON, S., MINTO, K., SMITH, L., BURCHAM, P. C., RUSSELL, T., STRUTTON, G., GRIFFIN, A., CHU, F.-F., ESWORTHY, S., REEVE, V. & SAUNDERS, N. A. (2007) Inactivation of glutathione peroxidase activity contributes to UV-induced squamous cell carcinoma formation. *Cancer Research,* 67**,** 4751-8.

WEN, Z. & FIOCCHI, C. (2004) Inflammatory bowel disease: autoimmune or immune-mediated pathogenesis? *Clinical & Developmental Immunology,* 11**,** 195-204.

WENK, J., SCHULLER, J., HINRICHS, C., SYROVETS, T., AZOITEI, N., PODDA, M., WLASCHEK, M., BRENNEISEN, P., SCHNEIDER, L.-A., SABIWALSKY, A., PETERS, T., SULYOK, S., DISSEMOND, J., SCHAUEN, M., KRIEG, T., WIRTH, T., SIMMET, T. & SCHARFFETTER-KOCHANEK, K. (2004) Overexpression of phospholipid-hydroperoxide glutathione peroxidase in human dermal fibroblasts abrogates UVA irradiation-induced expression of interstitial collagenase/matrix metalloproteinase-1 by suppression of phosphatidylcholine

hydroperoxide-mediated NFkappaB activation and interleukin-6 release. *Journal of Biological Chemistry,* 279**,** 45634-42.

WHANGER, P. D. (2004) Selenium and its relationship to cancer: an update. *British Journal of Nutrition,* 91**,** 11-28.

WHANGER, P. D. (2009) Selenoprotein expression and function-selenoprotein W. *Biochimica et Biophysica Acta,* 1790**,** 1448-52.

WILLETT, W. C., POLK, B. F., MORRIS, J. S., STAMPFER, M. J., PRESSEL, S., ROSNER, B., TAYLOR, J. O., SCHNEIDER, K. & HAMES, C. G. (1983) Prediagnostic serum selenium and risk of cancer. *Lancet,* 2**,** 130-4.

WONG, E. T. & TERGAONKAR, V. (2009) Roles of NF-kappaB in health and disease: mechanisms and therapeutic potential. *Clinical Science,* 116**,** 451-65.

WU, C.-J., CONZE, D. B., LI, T., SRINIVASULA, S. M. & ASHWELL, J. D. (2006) Sensing of Lys 63-linked polyubiquitination by NEMO is a key event in NF-kappaB activation [corrected].[Erratum appears in Nat Cell Biol. 2006 Apr;8(4):424]. *Nature Cell Biology,* 8**,** 398-406.

XU, X.-M., CARLSON, B. A., IRONS, R., MIX, H., ZHONG, N., GLADYSHEV, V. N. & HATFIELD, D. L. (2007) Selenophosphate synthetase 2 is essential for selenoprotein biosynthesis. *Biochemical Journal,* 404**,** 115-20.

YAMAMOTO, M., SATO, S., HEMMI, H., UEMATSU, S., HOSHINO, K., KAISHO, T., TAKEUCHI, O., TAKEDA, K. & AKIRA, S. (2003) TRAM is specifically involved in the Toll-like receptor 4-mediated MyD88-independent signaling pathway. *Nature Immunology,* 4**,** 1144-50.

YANG, J., LIN, Y., GUO, Z., CHENG, J., HUANG, J., DENG, L., LIAO, W., CHEN, Z., LIU, Z. & SU, B. (2001) The essential role of MEKK3 in TNF-induced NF-kappaB activation. *Nature Immunology,* 2**,** 620-4.

YANT, L. J., RAN, Q., RAO, L., VAN REMMEN, H., SHIBATANI, T., BELTER, J. G., MOTTA, L., RICHARDSON, A. & PROLLA, T. A. (2003) The selenoprotein GPX4 is essential for mouse development and protects from radiation and oxidative damage insults. *Free Radical Biology & Medicine,* 34**,** 496-502.

YAZDANPANAH, B., WIEGMANN, K., TCHIKOV, V., KRUT, O., PONGRATZ, C., SCHRAMM, M., KLEINRIDDERS, A., WUNDERLICH, T., KASHKAR, H., UTERMOHLEN, O., BRUNING, J. C., SCHUTZE, S. & KRONKE, M. (2009) Riboflavin kinase couples TNF receptor 1 to NADPH oxidase. *Nature,* 460**,** 1159-63.

YE, Y., SHIBATA, Y., YUN, C., RON, D. & RAPOPORT, T. A. (2004) A membrane protein complex mediates retro-translocation from the ER lumen into the cytosol. *Nature,* 429**,** 841-7.

YU, Y., ZENG, H., LYONS, S., CARLSON, A., MERLIN, D., NEISH, A. S. & GEWIRTZ, A. T. (2003) TLR5-mediated activation of p38 MAPK regulates epithelial IL-8 expression via posttranscriptional mechanism. *American Journal of Physiology - Gastrointestinal & Liver Physiology,* 285**,** G282-90.

YUN, C.-H., YANG, J. S., KANG, S.-S., YANG, Y., CHO, J. H., SON, C. G. & HAN, S. H. (2007) NF-kappaB signaling pathway, not IFN-beta/STAT1, is responsible for the selenium suppression of LPS-induced nitric oxide production. *International Immunopharmacology,* 7**,** 1192-8.

ZAFIRIOU, M. P., DEVA, R., CICCOLI, R., SIAFAKA-KAPADAI, A. & NIGAM, S. (2007) Biological role of hepoxilins: upregulation of phospholipid hydroperoxide glutathione peroxidase as a cellular response to oxidative stress? *Prostaglandins Leukotrienes & Essential Fatty Acids,* 77**,** 209-15.

ZAMAMIRI-DAVIS, F., LU, Y., THOMPSON, J. T., PRABHU, K. S., REDDY, P. V., SORDILLO, L. M. & REDDY, C. C. (2002) Nuclear factor-kappaB mediates over-expression of cyclooxygenase-2 during activation of RAW 264.7 macrophages in selenium deficiency. *Free Radical Biology & Medicine,* 32**,** 890-7.

ZENG, H., WU, H., SLOANE, V., JONES, R., YU, Y., LIN, P., GEWIRTZ, A. T. & NEISH, A. S. (2006) Flagellin/TLR5 responses in epithelia reveal intertwined activation of inflammatory and apoptotic pathways. *American Journal of Physiology - Gastrointestinal & Liver Physiology,* 290**,** G96-G108.

ZHANG, F., YU, W., HARGROVE, J. L., GREENSPAN, P., DEAN, R. G., TAYLOR, E. W. & HARTLE, D. K. (2002) Inhibition of TNF-alpha induced ICAM-1, VCAM-1 and E-selectin expression by selenium. *Atherosclerosis,* 161**,** 381-6.

ZHONG, H., MAY, M. J., JIMI, E. & GHOSH, S. (2002) The phosphorylation status of nuclear NF-kappa B determines its association with CBP/p300 or HDAC-1. *Molecular Cell,* 9**,** 625-36.